

**Novel Formulation Strategies
to Overcome Poorly Water Soluble Compounds**

by

Kelly Etherson

A thesis submitted to the Strathclyde Institute of Pharmacy and
Biomedical Sciences, University of Strathclyde, in fulfilment of the
requirement for degree of Doctor of Philosophy

2016

Declaration of authenticity and author's rights

'This thesis is the result of the author's original research. It has been composed by the author and has not been previously submitted for examination which has led to the award of a degree.'

'The copyright of this thesis belongs to the author under the terms of the United Kingdom Copyright Acts as qualified by University of Strathclyde Regulation 3.50. Due acknowledgement must always be made of the use of any material contained in, or derived from, this thesis.'

Signed:

Date:

Acknowledgments

I would like to thank the following people for their assistance in the completion of this thesis. Firstly, I thank Professor Gavin Halbert for his continued support, advice and encouragement throughout my PhD and for giving me this opportunity. I would also like to thank Dr Moira Elliott for her advice and insight during the course of my PhD. I send my gratitude to Dr Elke Prasad who assisted me during the commencement of my laboratory work and getting to know and understand the equipment I would be using. On that note I would also like to thank Dr Karl Box and Dr Robert Taylor from Sirius Analytical for further T3 training. I would also like to thank Dr Blair Johnston for his assistance with the molecular dynamics aspect of my thesis. I would like to thank Dr Michelle Armstrong for her help with rheology and Dr Steve Ford for HPLC training. I am also very grateful to Dr Ibrahim Khadra for his help with HPLC. To all the staff in the formulation unit, thank you for your help.

To the friends I have made throughout the course of my PhD; Lisa, Jen, Shonagh, Gemma, Stewart, Ian, Joe, Gracie, Ruairidh, Walid, Rachel, Monica, David K and David M, thank you for the good times we have shared. I would also like to send huge thanks to my family for supporting me throughout. To my mum, thank you I could not have done this without you. Thank you for everything you have done for me. I would also like to send thanks to my sister Dr Michelle Etherson, to Tom and to Samuel for helping me stay focused and encouraging me to stick at it during the writing of my thesis.

Table of Contents

Declaration.....	i
Acknowledgements.....	ii
Table of Contents.....	iii
List of Tables.....	xi
List of Figures.....	xiii
List of Equations.....	xix
Abstract.....	xxiii
1 Chapter 1: Introduction	1
1.1 Introduction.....	1
1.2 Biopharmaceutics Classification System	2
1.3 Different Types of Solubility	5
1.4 Predicting Solubility.....	6
1.5 Measuring Solubility	8
1.5.1 Shake-Flask Method.....	8
1.5.2 CheqSol Method.....	9
1.5.3 Curve-Fitting Method.....	10
1.6 Methods for Improving Solubility	13
1.6.1 Salt Formation	14
1.6.2 Prodrug Formation.....	15
1.6.3 Solvents and Cosolvents	17

1.6.4	Micelles and Emulsions	19
1.6.5	Liposomes	21
1.6.6	Nanosuspensions	23
1.6.7	Complexation	24
1.6.8	Other Methods.....	26
1.6.9	Combinations	27
1.7	Reducing Solubility	28
1.8	Phase-Solubility Diagrams	28
1.9	Project background	31
1.10	Aims	32
2	Chapter 2 – Solubility Determination Using CheqSol	34
2.1	Introduction.....	34
2.1.1	pK _a	34
2.1.2	CheqSol.....	35
2.1.3	Cyclodextrins.....	47
2.1.4	Poloxamers.....	49
2.1.5	Cholic Acid	52
2.2	Aims	52
2.3	Materials.....	53
2.4	Methods	54

2.4.1	Determination of Excipient Water Content	55
2.4.2	Preparation of Study Solutions	56
2.4.3	Potentiometric Determination of pK_a	57
2.4.4	Potentiometric Determination of Solubility	58
2.4.5	Shake-Flask Solubility Determination of Propranolol	59
2.4.6	Cholic Acid as an Excipient	64
2.4.7	Analysis of Results	65
2.5	Results	66
2.5.1	Excipient Water Content	66
2.5.2	Potentiometric Determination of pK_a	66
2.5.3	Potentiometric Determination of Solubility Using CheqSol	71
2.5.4	Shake-Flask Solubility Determination of Propranolol	89
2.5.5	Cholic Acid as an Excipient	93
2.6	Discussion	94
2.6.1	pK_a Results.....	94
2.6.2	Intrinsic Solubility Results	96
2.6.3	Kinetic Solubility Results	100
2.6.4	CheqSol versus Shake-Flask	105
2.6.5	Complexation and Micellisation of Compounds with Excipients.....	106
2.6.6	CheqSol.....	110

2.6.7	Other Observations from CheqSol Studies	110
2.6.8	Cholic Acid as an Excipient	111
2.7	Conclusions.....	112
2.8	Limitations	112
3	Chapter 3: Dissolution and Precipitation Rates.....	114
3.1	Introduction.....	114
3.1.1	Dissolution.....	115
3.1.2	Thermodynamics of Dissolution	116
3.1.3	Factors affecting Compound Dissolution.....	117
3.1.4	Precipitation	117
3.1.5	Spring and Parachute Effect.....	119
3.1.6	T3 Determinations of Dissolution and Precipitation Rates.....	120
3.2	Aim.....	121
3.3	Materials.....	121
3.4	CheqSol Data Methods.....	122
3.4.1	Data Extraction.....	122
3.4.2	Data Analysis	122
3.5	Experimental Methods	124
3.5.1	Solution Preparation	124
3.5.2	Molar Extinction Coefficient Determination.....	125

3.5.3	Experimental Disc Dissolution Assays	126
3.5.4	Excipient Solution Viscosity.....	127
3.6	Results	128
3.6.1	Precipitation Rates from CheqSol Assays	128
3.6.2	Dissolution Rates from CheqSol Assays	134
3.6.3	Disc Dissolution Assays	140
3.6.4	Excipient Gain Factor	142
3.6.5	Excipient Solution Viscosity.....	145
3.7	Discussion	148
3.7.1	Precipitation Rates: CheqSol.....	148
3.7.2	Dissolution Rates: CheqSol versus Disc Dissolution Assays.....	152
3.7.3	CheqSol versus Disc Dissolution.....	162
3.7.4	Excipient Gain Factor	163
3.7.5	Measuring ‘Spring and Parachute’ Effects Using T3	165
3.8	Conclusions.....	166
4	Chapter 4 – Association Constants	167
4.1	Introduction.....	167
4.1.1	Determination of Association Constants	169
4.1.2	Complexation Association Constants Determination	173
4.1.3	Other Methods for Complexation Constant Determination	178

4.1.4	Micelle Association Constant Determination	181
4.1.5	Calculating K_a^c	182
4.2	Aims	182
4.3	Methods	183
4.3.1	Complexation Association Constants.....	183
4.3.2	Micelle Association Constants	184
4.4	Results	184
4.4.1	Complexation Association Constants.....	184
4.4.2	Micelle Association Constants	190
4.5	Discussion	197
4.5.1	Complexation Association Constants.....	197
4.5.2	Micelle Association Constants	204
4.5.3	General Discussion	206
4.6	Conclusions.....	208
5	Chapter 5 – Molecule Design.....	210
5.1	Introduction.....	210
5.1.1	Common self-assemblies	211
5.1.2	Nature’s self-assembly	212
5.1.3	Polymers.....	213
5.1.4	Small molecules.....	213

5.1.5	Molecular Field Point Descriptors.....	214
5.2	Aims.....	215
5.3	Methods.....	216
5.3.1	Literature Review.....	216
5.3.2	Molecule design.....	216
5.4	Results.....	216
5.4.1	Literature Review.....	216
5.4.2	Molecule Design.....	217
5.5	Discussion.....	220
5.5.1	Molecule Design.....	220
5.5.2	Selected Molecules.....	222
5.5.3	Other Molecules.....	228
6	Chapter 6 – Molecular Dynamics Simulations.....	229
6.1	Introduction.....	229
6.1.1	Force Fields.....	229
6.1.2	Cohesive energy density.....	230
6.2	Aims.....	231
6.3	Methods.....	231
6.4	Results.....	233
6.4.1	Ibuprofen and Gliclazide Solubility.....	233

6.4.2	Excipient Self-Assembly	238
6.5	Discussion	240
6.5.1	Ibuprofen and Gliclazide Solubility	240
6.5.2	Excipient Self-Assembly	247
6.5.3	Simulation Conditions Choice	248
6.6	Conclusions.....	249
7	Chapter 7 - Conclusions and Future Work.....	250
7.1	Conclusions.....	250
7.1.1	Experimental Results.....	250
7.1.2	Computational Results	251
7.2	Future Work	251
7.2.1	Experimental	251
7.2.2	Computational.....	252
8	References	254
	Appendix1 - Abbreviations.....	284
	Appendix 2 - Table of the total volumes and pH recordings for each vial for Shake-Flask Solubility Studies.....	287
	Appendix 3 - Table detailing the 3D - and 2D- structures of the designed molecules.....	291
	Appendix 4 - Abstracts for publications and posters.....	303

List of Tables

Table 1.1. Solubility definitions as defined by the British Pharmacopeia (4)	3
Table 1.2. Classification of drugs according to the BCS system (11).	3
Table 2.1. CheqSol values versus literature or shake-flask.....	35
Table 2.2. Structure and physicochemical data of the four test compounds used. .	43
Table 2.3. Structures of the excipients used during experiments.	45
Table 2.4. Six HP- β -CD concentrations used in assays with volumes of buffer and stock solutions used.....	62
Table 2.5. Standard solutions used for HPLC calibration curve.....	64
Table 2.6. Regression analysis of intrinsic solubility results for the four drugs in the presence of Poloxamer 407	78
Table 2.7. Regression analysis of kinetic solubility results for the four drugs in the presence of Poloxamer 407	78
Table 2.8. Regression analysis results for intrinsic solubility of the four drugs in the presence of Poloxamer 188.	84
Table 2.9. Regression analysis results for kinetic solubility of the four drugs in the presence of Poloxamer 188.	84
Table 2.10. Solubility results for cholic acid in a starting volume of 1.5 mL ISA water.	93
Table 3.1. Viscosity of excipient solutions used during disc dissolution assays.	145
Table 3.2. Flow behaviour index of excipient solutions used during disc dissolution assays.	146

Table 4.1. K_{11a} values from CheqSol studies of the four compounds with HP- β -CD	185
Table 4.2. K_{11} values from shake-flask solubility studies of propranolol in the presence of HP- β -CD at the two wavelengths studied and both forms.....	188
Table 4.3. Association constants, as K_{11a}/N and adjusted to K_{11a} when $N = 9$, of the four drugs in the presence of P407.	191
Table 4.4. Association constants, as K_{11a}/N and adjusted to K_{11a} when $N = 15$, of the four drugs in the presence of P188.....	194
Table 4.5. Table showing the average number of molecules per micelle.	197
Table 4.6. Comparison of association constants with excluded data.....	201
Table 5.1. Predicted physicochemical properties of molecule 1.	223
Table 5.2. Predicted physicochemical properties of molecule 2.	224
Table 5.3. Predicted physicochemical properties of molecule 3.	225
Table 5.4. Predicted physicochemical properties of molecule 4.	226
Table 5.5. Predicted physicochemical properties of molecule 5.	227
Table 6.1. Mean (standard deviation) solubility parameters (cal/cc) ^{1/2} for ibuprofen. All simulations run in 1000 water molecules, $n = 1001$	236
Table 6.2. Mean (standard deviation) solubility parameters (cal/cc) ^{1/2} for gliclazide. All simulations run in 1000 water molecules, $n = 1001$	237

List of Figures

Figure 1.1. Bjerrum curves for solutions and in the presence of precipitation	12
Figure 1.2. Diagrams representing the two types of phase solubility diagram	30
Figure 2.1. Example neutral species concentration plot, showing titrant addition during the assay	37
Figure 2.2. An example of the crossover plot produced by the software running the instrument.....	41
Figure 2.3. Suggested orientation of poloxamer molecules within micelle	50
Figure 2.4. The equipment set-up of the T3 during an assay in a 4 mL vial, height 12mm	54
Figure 2.5. Scatterplot and regression line for the effect that HP- β -CD has on the pK_a of the four drugs	68
Figure 2.6. Scatterplot and regression line for the effect that a) poloxamer 407 and b) poloxamer 188 have on the pK_a of the four drugs	70
Figure 2.7. Scatterplots and regression lines of solubility of propranolol in the presence of HP- β -CD for a) intrinsic solubility, and b) kinetic solubility	73
Figure 2.8. Scatterplots and regression lines of solubility of gliclazide in the presence of HP- β -CD for a) intrinsic solubility, and b) kinetic solubility	74
Figure 2.9. Scatterplots and regression lines of solubility of atenolol in the presence of HP- β -CD for a) intrinsic solubility, and b) kinetic solubility	75
Figure 2.10. Scatterplots and regression lines of solubility of ibuprofen in the presence of HP- β -CD for a) intrinsic solubility, and b) kinetic solubility	76

Figure 2.11. Scatterplots and regression lines of solubility of propranolol in the presence of P407 for a) intrinsic solubility, and b) kinetic solubility.....	79
Figure 2.12. Scatterplots and regression lines of solubility of atenolol in the presence of P407 for a) intrinsic solubility, and b) kinetic solubility.....	80
Figure 2.13. Scatterplots and regression lines of solubility of gliclazide in the presence of P407 for a) intrinsic solubility, and b) kinetic solubility.....	81
Figure 2.14. Scatterplots and regression lines of solubility of ibuprofen in the presence of P407 for a) intrinsic solubility, and b) kinetic solubility.....	82
Figure 2.15. Scatterplots and regression lines of solubility of propranolol in the presence of P188 for a) intrinsic solubility, and b) kinetic solubility.....	85
Figure 2.16. Scatterplots and regression lines of solubility of atenolol in the presence of P188 for a) intrinsic solubility, and b) kinetic solubility.....	86
Figure 2.17. Scatterplots and regression lines of solubility of gliclazide in the presence of P188 for a) intrinsic solubility, and b) kinetic solubility.....	87
Figure 2.18. Scatterplots and regression lines of solubility of ibuprofen in the presence of P188 for a) intrinsic solubility, and b) kinetic solubility.....	88
Figure 2.19. Calibration curves at 254 nm and 280 nm wavelengths.....	89
Figure 2.20. Scatterplot of unionised propranolol concentration versus HP- β -CD concentration at pH 12	91
Figure 2.21. Scatterplot of ionised propranolol concentration versus HP- β -CD concentration at pH 5.5	92
Figure 2.22. Scatterplot showing the effect that the amount of drug used has on the kinetic solubility in the presence of HP- β -CD at the varying ratios	102

Figure 2.23. Scatterplot showing the effect that the amount of drug used has on the kinetic solubility in the presence of Poloxamer 407 at the varying concentrations.	103
Figure 2.24. Scatterplot showing the effect that the amount of drug used has on the kinetic solubility in the presence of Poloxamer 188 at the varying concentrations.	104
Figure 2.25. Scatterplots showing the regression analysis for intrinsic propranolol solubility and HP- β -CD cocentration with both CheqSol and Shake-Flask phase solubility studies.....	106
Figure 3.1. Diagram representing the areas used during the EGF determination.	124
Figure 3.2. Setup of die used during tablet preparation.....	127
Figure 3.3. Scatterplot showing the mean propranolol precipitation rates obtained during CheqSol assays with increasing concentrations of a) HP- β -CD, b) P407, and c) P188.....	130
Figure 3.4. Scatterplot showing the mean gliclazide precipitation rates obtained during CheqSol assays with increasing concentrations of a) HP- β -CD, b) P407, and c) P188.....	131
Figure 3.5. Scatterplot showing the mean ibuprofen precipitation rates obtained during CheqSol assays with increasing concentrations of a) HP- β -CD, b) P407, and c) P188.....	132

Figure 3.6. Scatterplot showing the mean atenolol precipitation rates obtained during CheqSol assays with increasing concentrations of a) HP- β -CD, b) P407, and c) P188.....	133
Figure 3.7. Scatterplot showing the mean propranolol dissolution rates obtained during CheqSol assays with increasing concentrations of a) HP- β -CD, b) P407, and c) P188.....	136
Figure 3.8. Scatterplot showing the mean gliclazide dissolution rates obtained during CheqSol assays with increasing concentrations of a) HP- β -CD, b) P407, and c) P188	137
Figure 3.9. Scatterplot showing the mean ibuprofen dissolution rates obtained during CheqSol assays with increasing concentrations of a) HP- β -CD, b) P407, and c) P188	138
Figure 3.10. Scatterplot showing the mean atenolol dissolution rates obtained during CheqSol assays with increasing concentrations of a) HP- β -CD, b) P407, and c) P188	139
Figure 3.11. Mean dissolution rates of four drug compounds in different media \pm SD.	141
Figure 3.12. The EGF of a) propranolol and b) atenolol in HP- β -CD, P407 and P188	143
Figure 3.13. The EGF of a) gliclazide and b) ibuprofen in HP- β -CD, P407 and P188	144
Figure 3.14. Example plot of τ (Pa) vs $\dot{\gamma}$ (s^{-1}).....	147

Figure 3.15. Scatterplot showing the mean τ (Pa) vs $\dot{\gamma}$ (s^{-1}) for all solvents investigated	148
Figure 3.16. Corrected absorbance spectra of excipients	162
Figure 4.1. Scatterplot of Iga <i>et al.</i> method to determine K_{11a} and K_{12a} of gliclazide following phase-solubility results.	186
Figure 4.2. Scatterplot of Iga <i>et al.</i> method to determine K_{11a} and K_{12a} of ibuprofen following phase-solubility results	187
Figure 4.3. Double reciprocal plots of acidic drugs. a) gliclazide and b) ibuprofen.	189
Figure 4.4. Double reciprocal plots of basic drugs. a) propranolol and b) atenolol.	190
Figure 4.5. Scatterplots of $\frac{([St] - [Sw])}{[Sw]}$ versus $([C_t] - CMC)$ for a) gliclazide and b) ibuprofen in the presence of P407	192
Figure 4.6. Scatterplots of $\frac{([St] - [Sw])}{[Sw]}$ versus $([C_t] - CMC)$ for a) propranolol and b) atenolol in the presence of P407	193
Figure 4.7. Scatterplots of $\frac{([St] - [Sw])}{[Sw]}$ versus $([C_t] - CMC)$ for a) gliclazide and b) ibuprofen in the presence of P188	195
Figure 4.8. Scatterplots of $\frac{([St] - [Sw])}{[Sw]}$ versus $([C_t] - CMC)$ for a) propranolol and b) atenolol in the presence of P188	196
Figure 4.9. Double reciprocal plots of acidic drugs with negative HP- β -CD concentrations excluded. a) gliclazide and b) ibuprofen	202
Figure 4.10. Double reciprocal plots of basic drugs with negative HP- β -CD concentrations excluded. a) propranolol and b) atenolol	203

Figure 4.11. Mean % ionised of all drugs in the presence and absence of excipients during CheqSol crossing points	208
Figure 5.1. Structure of a) trimesic acid and b) and example of a trigonal rigid triphenol.....	214
Figure 5.2. Molecule designs (1-34) which were drawn using FieldView 2.0.2 Revision 14848.....	220
Figure 6.1. Bar chart of the difference between $\Delta\delta_{\text{water}}$ and $\Delta\delta_{\text{excipient}}$	235
Figure 6.2. Screenshots of dynamics simulations of five novel excipients in water.	239
Figure 6.3. Screenshots of the dynamics simulations between a) ibuprofen and HP- β -CD at 1:1 ratio, b) ibuprofen and HP- β -CD at 1:2 ratio, c) gliclazide and HP- β -CD at 1:1 ratio, d) gliclazide and HP- β -CD at 1:2 ratio.....	241
Figure 6.4. Screenshots of dynamics simulations of ibuprofen with the five novel excipients	245
Figure 6.5. Screenshots of dynamics simulations of gliclazide with the five novel excipients	247

List of Equations

$\ln \phi_B = -A + B - D - F + O - OH$	Equation 1.1	6
$\Delta H_{\text{sub}} = -E_{\text{latt}} - 2RT$	Equation 1.2	7
$B_j = H^+ H^+ + K_a$	Equation 1.3	10
$B_j = S_o H^+ X_{\text{total}} K_a$	Equation 1.4	11
$B_j = H^+ H^+ K_a^{-1}$	Equation 1.5	11
$B_j = 1 - S_o K_a X_{\text{total}} [H^+]$	Equation 1.6	11
$\log S_m = f_c \log S_c + f_w \log S_w$	Equation 1.7	17
$K_a = H^+ A^- / HA$	Equation 2.1	34
$K_a = H^+ B B H^+$	Equation 2.2	34
$H^+ = 10^{-\text{pH}}$	Equation 2.3	39
$OH^- = K_w H^+$	Equation 2.4	39
$v_t = v_w + v_a + v_b$	Equation 2.5	39
$K^+ = v_b c_b + m_s z_{s^+} / f_w v_t$	Equation 2.6	39
$Cl^- = v_a c_a + m_s z_{s^-} / f_w v_t$	Equation 2.7	39
$[A^-] = [H^+] - [OH^-] + [K^+] - [Cl^-]$	Equation 2.8	39
$[BH^+] = [OH^-] - [H^+] + [Cl^-] - [K^+]$	Equation 2.9	39
$HA = A^- H^+ 10^{-\text{p}K_a}$	Equation 2.10	40
$B = 10^{-\text{p}K_a} B H^+ H^+$	Equation 2.11	40
$0.001 * \mu\text{g waterweight 1 - weight 2} = \text{Result 1}$	Equation 2.12	55
$\text{weight B} + \text{weight 0} = \text{Result 2}$	Equation 2.13	55
$\text{weight A} * \text{weight B} = \text{Result 3}$	Equation 2.14	56

Result 1 * Result 2 * 1000 - Result 310000= % water content	Equation 2.15	56
$J = P \times C$	Equation 3.1.....	114
$dxdt = CS - x$	Equation 3.2.....	115
$dCdt = DSVh \times C_s - C_b$	Equation 3.3	115
$\Delta G_{d,2} = \Delta H_{d,2} - T\Delta S_{d,2}$	Equation 3.4.....	116
$H_{dissolution} = H_{melt} + H_{mix}$	Equation 3.5	116
$\Delta G = \Delta G_s + \Delta G_v$	Equation 3.6	118
$J = A \exp(-\Delta G^* / kT)$	Equation 3.7.....	119
Precipitation Rate M/min= -dpHdt x Blaverage molecular charge	Equation 3.8	121
$EGF = \text{Area A} + \text{Area B} + \text{Area C}$	Equation 3.9.....	123
$\tau = K \dot{\gamma}^n$	Equation 3.10.....	128
$K_a = H^+ A^- HA$	Equation 4.1.....	170
$K_a^c = H^+ AL^- HAL$	Equation 4.2.....	170
$K_{11a} = HALHAL$	Equation 4.3	170
$K_{11b} = AL^- A^- L$	Equation 4.4	170
$K_a = H^+ BBH^+$	Equation 4.5.....	170
$K_a^c = H^+ BLBHL^+$	Equation 4.6.....	170
$K_{11a} = BLBL$	Equation 4.7.....	170
$K_{11b} = BHL^+ BH^+ L$	Equation 4.8.....	170
$K_{12a} = HAL_2HALL \text{ or } BL_2BLL$	Equation 4.9	172
$K_{12b} = AL_2^- AL^- L \text{ or } BHL_2^+ BHL^+ L$	Equation 4.10.....	172
$K_{mn} = D_m L_n D^m L^n$	Equation 4.11.....	172
$K_{12} = G : HP - \beta - CD_2 GHP - \beta - CD^2$	Equation 4.12	173

$\Delta pK_a = pK_a' - pK_a$	Equation 4.13	174
$C = 1 + K_{11a}L + K_{11b}L = 10\Delta pK_a$	Equation 4.14	174
$[L_t] = L^*(1 + K_{11a} + K_{11b} \cdot C[A_t] + C + K_{11a} + K_{11b} \cdot CL)$	Equation 4.15	174
$C = 1 + K_{11a}L + K_{11a}K_{12a}L^2 + K_{11b}L + K_{11b}K_{12b}L^2$	Equation 4.16	175
$L_t = L + S_t[M2A + N2B]$	Equation 4.17	175
$K_a K_a' - K_a = 1K_{11b} - K_{11a}L + K_{11a}K_{11b} - K_{11a}$	Equation 4.18	175
$K_{11a} = \text{intercept/slope}$	Equation 4.19	176
$K_{11b} = 1 + \text{intercept/slope}$	Equation 4.20	176
$pK_b = 14 - pK_a$	Equation 4.21	176
$K_{11a} = \text{slope}S_o - \text{slope}$	Equation 4.22	177
$K_{11a} = S_t - S_oS_oL_t - S_t + S_o$	Equation 4.23	177
$S_t - S_oL = K_{11a}S_o + K_{11a}K_{12a}S_o[L]$	Equation 4.24	177
$S_t - S_oL_t - 2S_t - S_o = \alpha + \beta(L_t - 2S_t - S_o)$	Equation 4.25	178
$\alpha = K_{11a}S_o - K_{11a}S_o$	Equation 4.26	178
$\beta = K_{11a}K_{12a}S_o - K_{11a}S_o^2$	Equation 4.27	178
$FF_o = 1 + k_{11a}k_S K_{11a}L + K_{11a}L + k_L k_S [L]$	Equation 4.28	179
$FF_o = 1 + k_{11a}k_S K_{11a}L + K_{11a}L$	Equation 4.29	179
$1\Delta\delta = 1K_{11a} \Delta\delta_{\max}H_o + 1\Delta\delta_{\max}$	Equation 4.30	179
$\Delta G = -RT \ln K = \Delta H - T\Delta S$	Equation 4.31	180
$Q = nL_t \Delta H_b V_o^2 (1 + D_t n L_t + 1n K_{11} L_t - 1 + D_t n L_t + 1n K_{11} L_t^2 - 4D_t n L_t^2)$	Equation 4.32	181
$S_t - S_w S_w = K_{11a} N (C_t - CMC)$	Equation 4.33	181
$S^M = S_t - S_w M_t = K_{11a} [S_w]$	Equation 4.34	182
$K_a K_a^c = K_{11a} K_{11b}$	Equation 4.35	182

$\Delta S = -k(\ln\phi_N - N\ln\phi_{free})$	Equation 5.1.....	211
$\delta = CED$	Equation 6.1.....	230
$CED = \Delta H - RTV_m$	Equation 6.2.....	230

Abstract

Drug solubility plays an important role during formulation development; it affects drug delivery and, as many new drug candidates developed have poor water solubility, it is necessary to increase their aqueous solubility for administration. The solubility increases, achieved by prodrugs or salt formation for example, are traditionally measured using the shake-flask method. This thesis investigated the advantages of the CheqSol method for phase-solubility studies. This method, using small pH changes, brings a compound close to its intrinsic solubility then alternates the system between sub- and supersaturated states. It also looked at *in silico* design and molecular dynamics simulations to investigate the solubilising properties of novel molecules. CheqSol studies were carried out on four compounds, two basic (propranolol HCl and atenolol) and two acidic (gliclazide and ibuprofen), in water and in the presence of HP- β -CD and two poloxamers using the Sirius T3. All three non-ionising excipients used during CheqSol assays were found to increase the solubility of the four example drugs. It was concluded that this method was suitable for phase-solubility studies using non-ionizing excipients. Molecular dynamics were carried out using Materials Studio 5.5. Five novel molecules were investigated to determine if they are predicted to increase the solubility of gliclazide and ibuprofen. The solubility enhancements were compared to HP- β -CD simulations conducted using the software. All five molecules were less effective than HP- β -CD at improving the calculated solubility parameters. Further studies would need to be conducted with excipients, with known solubility effects, for conclusions about the molecular dynamics technique to be drawn.

1 Chapter 1: Introduction

1.1 Introduction

Aqueous solubility is an important characteristic assessed during drug development in order to determine the drug-likeness of the compound as it plays an important role during drug delivery (1). The pharmaceutical industry is constantly striving to develop new and improved drugs for the treatment of disease. Unfortunately many drug candidates discovered today (estimated to be 40% to 70%) display poor water solubility (2). Li *et al.* expressed that it is common for new drug candidates to have an intrinsic solubility less than 100 µg/mL (3), and classified as practically insoluble according to the definitions in the British Pharmacopoeia 2015 (4) (Table 1.1). The term 'water insoluble drug' can be associated with compounds which require more than 100 mL of water for the dissolution of 1 gram of solute (5).

Poor solubility is a problem for drug administration. The issues between oral and parenteral formulations differ. For absorption following oral administration, compounds need to be in solution before absorption. Drugs which, in water, have a solubility of 'slightly soluble' or lower can have problems with absorption and bioavailability, especially if the permeability and/or potency is/are low (6). When administered as a solid dosage form, dissolution must occur before absorption. For parenteral formulations, the compound is usually already in a liquid form. While the volume of dose to be administered should be considered for all liquid formulations, this is especially true for subcutaneous and intramuscular injections, where only

small volumes can be administered (7, 8). The drug has to be sufficiently soluble to allow the dose to be formulated in a small enough volume for the route of administration. Volume is less of an issue for intravenous administration. However, some excipients available to improve solubility can cause effects such as pain and inflammation following injection which can limit suitability for intravenous use (9). For example, propylene glycol, a commonly used cosolvent, can induce haemolysis in 50% of human blood cells at a concentration of 5.7% (9). Both propylene glycol (20% v/v) and polyethylene glycol (50% v/v) have been shown to cause muscle damage following intramuscular injection (10). Toxicity is not limited to parenteral administration; sucrose palmitate when administered orally at doses above 30 mg/kg can cause diarrhoea (11). Care therefore needs to be taken to ensure that excipients in the formulation are not damaging or toxic, especially when being administered parenterally.

1.2 Biopharmaceutics Classification System

For orally administered compounds solubility is not the only factor which needs to be taken into consideration. The drugs must also be absorbed from the gastrointestinal tract (GIT) following administration. The Biopharmaceutics Classification System (BCS) is a system developed to correlate *in vitro* solubility and *in vivo* bioavailability with drugs grouped into one of four categories (Table 1.2) depending on their aqueous solubility and GIT permeability (12).

Table 1.1. Solubility definitions as defined by the British Pharmacopeia (4)

Term	Approximate volume of solvent to dissolve 1g of solute (mL)
Very Soluble	Less than 1
Freely Soluble	Between 1 and 10
Soluble	Between 10 and 30
Sparingly Soluble	Between 30 and 100
Slightly Soluble	Between 100 and 1000
Very Slightly Soluble	Between 1000 and 10,000
Practically Insoluble	More than 10,000

Table 1.2. Classification of drugs according to the BCS system (12).

	High Permeability	Low Permeability
High Solubility	Class I	Class III
Low Solubility	Class II	Class IV

For a drug to be classed as having high solubility, the maximum dose is required to dissolve in up to 250 mL of aqueous media over the pH range of the GIT (pH 1 – 7.5) at body temperature (37°C) (13, 14). If more than 90% of an administered dose is absorbed in humans then a drug is classed as having high permeability (14).

For drugs belonging to classes II and IV, the low solubility can reduce the oral bioavailability, and for class II drugs, dissolution is the rate limiting factor in absorption (12). The BCS was developed for oral drugs; however drug solubility is important for drugs that are administered by other routes. For example, drugs given intravenously, although not absorbed, are required to be administered in a liquid form and the solubility of the drug in water needs to be considered.

During the formulation of drugs for oral administration, improving the BCS classification is achieved by improving solubility and/or permeability; this would ideally be to class I compound. Improvements in solubility and/or permeability can also be used to affect drug delivery by parenteral and other routes of delivery. This work will concentrate on methods used to affect drug solubility.

As described by Liu, poor solubility problems are encountered often (5). It is therefore good to know the predicted or actual solubility of a substance under investigation (chapters 1.4 and 1.5), and if poor solubility is a problem then further work can be carried out to solve this issue as discussed below (chapter **Error! eference source not found.**). As well as the solubility figure that has been measured

or predicted, it is also important to know the type of solubility that this result represents.

1.3 Different Types of Solubility

There are different types of solubility depending on the methods and conditions for determination. If these conditions are changed, for example temperature, solvent or pH, then the solubility results will change. Intrinsic solubility is the solubility of the un-ionised form of the compound under investigation (15). For ionisable compounds this is measured at a pH where ionisation is suppressed. Kinetic solubility is the concentration of the compound present at the point of precipitation (15). Kinetic solubility can be obtained from supersaturated states, which can be formed by various methods such as changes in temperature or solvent, use of amorphous forms or changes in pH. Thermodynamic solubility is the concentration of the compound in its most stable crystalline form at equilibrium; it can be composed of a mix of the ionised and unionised species depending on the conditions of the system (16). For the mentioned solubility types, both solid and liquid are present in the system, and under equilibrium in the case of intrinsic and thermodynamic solubility.

The extent of compound dissolution and solubility in any given solvent will be affected by a number of factors.

- The compound's structure is important. The presence of certain functional groups will mediate the interaction of the compound with water molecules. These functional groups include hydroxyls, amides, amines, carboxylic acids and

esters (17). These functional groups, which can be classed as hydrogen donors or acceptors, would need to be able to interact with the water molecules so the conformation of the molecule is important (6). Some of the functional groups listed are ionisable; the ionisation state of these functional groups can be changed by variation of the pH. The amines will gain a positive charge at pHs below their pK_a and carboxylic acids will be negatively charged at pHs above their pK_a .

- Bonding within the solid compound will affect dissolution (17). The solid can be crystalline or amorphous, with the bonds within amorphous solids being easier to break. To allow dissolution to occur these intermolecular bonds must be broken.

1.4 Predicting Solubility

A number of models have been developed to predict the solubility of compounds (ϕ_B). Ruelle *et al.* (18) developed a model based on the thermodynamics of mobile disorder which includes the enthalpy of fusion and the effect entropy has on the system.

$$\ln \phi_B = -A + B - D - F + O - OH \quad \text{Equation 1.1}$$

Ruelle and colleague's equation, Equation 1.1, takes account of fluidisation (A), the corrected entropy of mixing (B), the enthalpy change of solution (D), hydrophobic effects (F), hydrogen bonding between drug and hydrogen donor solvents (O) and hydrogen bonding between drug and hydrogen acceptor solvent (OH) (18, 19).

Other models based on the use of the molecular structure to estimate aqueous solubility of drugs have been developed. Klopman *et al.* developed a model using the functional groups present in organic compounds and calculated their contribution to aqueous solubility (17). Huuskonen also produced a model for estimating solubility based on molecular structure. This model used the topological indices described by Kier and Hall to develop the parameters followed by multiple linear regression and artificial neural network models (20).

The solubility of a compound will be affected by crystal lattice interactions (21). Salahinejad *et al.* have described a model for predicting solubility which utilises the descriptors for these crystal lattice interactions and enthalpies of sublimation (21). Crystal lattice energy (E_{latt}) was determined from measured energies of sublimation (ΔH_{sub}) by the relationship expressed in Equation 1.2, where R is the gas constant and T is the temperature in Kelvin. The model also used other descriptors including hydrogen bond acceptors and donors, hydrophobic and hydrophilic regions, polar intermolecular interactions and logP (21).

$$\Delta H_{sub} \text{ (kJ/mol)} = -E_{latt} - 2RT \quad \text{Equation 1.2}$$

In silico solubility prediction utilises a training set of compounds with intrinsic solubility data, the properties used for prediction include: molecular weight, logP, hydrogen bond donors and acceptors, the presence and number of rings and aromatic rings, atoms, fragments and rotating bonds (16).

The accuracy of solubility prediction is dependent on the training set of compounds used; therefore accuracy of prediction is likely to be poor if predicting solubility for a structure which does not have similar properties to training set of molecules (16). If possible determination of the solubility should be carried out.

1.5 Measuring Solubility

Determining the solubility of a compound is an important step during the development stage and more than one technique exists to derive the solubility. However, the compound solubility can be difficult to determine accurately since a number of factors during the process can alter the result. The solubility can be affected by pH of the solvent, the temperature that the assay is carried out at, the purity of the solute and solvent, the presence of any co-solutes, equilibration conditions (length of time and degree of agitation), how the excess solid is separated from the saturated solution and how the concentration of the solution is analysed (22-24).

1.5.1 Shake-Flask Method

The determination of a compound's equilibrium solubility can be carried out using the conventional shake-flask method (25). In this method, an excess of the solid compound is allowed to dissolve in the solvent, such as water, this stage can last up to seven days (26). During the dissolution stage, temperature and stirring can be controlled to standardise the results. Following dissolution the remaining saturated

solution is removed from the excess solid by sedimentation for up to 24 hours (25), centrifugation and/or filtration. The concentration of the compound in solution can be determined by comparing UV spectrophotometry or mass spectrometry results, preceded by HPLC separation, against a standard of known concentration (25-27). If the process is carried out at a pH where the drug is fully unionised then the equilibrium solubility can be referred to as the intrinsic solubility (15).

This method, if performed well, is accurate and is the technique to which other methods are compared (25, 28). It is however a relatively slow method and the solubility results obtained can be affected by the conditions of the assay. For example, time to equilibrate, time to settle and temperature (25).

1.5.2 CheqSol Method

Another method for solubility determination that can be used is the potentiometric method **Chasing Equilibrium Solubility (CheqSol)**. CheqSol is a method which utilises pH changes to determine a compound's intrinsic solubility. This method can be used to determine the solubility of ionisable compounds which can form supersaturated solutions (15). This method utilises pH changes to determine the solubility of the unionised form of the compound. Compounds where pH can have measurable effects on dissolution and precipitation suitable for this method are called **chasers** (15) as they can be found to chase equilibrium, i.e. they precipitate dissolve slowly and the solution can be switched between sub- and supersaturated states with small changes in pH (15).

1.5.3 Curve-Fitting Method

The Curve-Fitting Method is another potentiometric technique which can be used when a compound precipitates from solution quickly and does not form a supersaturated solution. The kinetic solubility is found to be close to the intrinsic solubility and these compounds can be referred to as **non-chasers** as they cannot be switched between sub- and supersaturated states (15). At the point of precipitation, equilibrium between solid and solution is quickly established and the concentration calculation (see chapter 2.1) result is the equilibrium solubility of the compound.

From the results of these assays Bjerrum (B_j) curves can be plotted and from examination of these curves it can be seen that before precipitation all data points fit on the solution curve. There is a difference between chasers and non-chasers after precipitation. For chasers, the B_j value at the point of precipitation lies between the solution and precipitation curves (Figure 1.1a), and this differs from non-chasers as after precipitation occurs, the B_j value data points lie on or close to the precipitation curve (Figure 1.1b). B_j is the proportion of molecules which have a proton bound to them, for acids this is the unionised form and for bases this is the ionised form. A greater distance between the solution and precipitation curves corresponds to a lower solubility (15). The curves can be defined by Equations 1.3 to 1.6 (15, 26).

Monoprotic base solution Bjerrum curve

$$B_j = \frac{[H^+]}{[H^+] + K_a} \quad \text{Equation 1.3}$$

Monoprotic base precipitation Bjerrum curve

$$B_j = \frac{S_o[H^+]}{[X_{total}]K_a} \quad \text{Equation 1.4}$$

Monoprotic acid solution Bjerrum curve

$$B_j = \left(\frac{[H^+]}{[H^+]K_a} \right) - 1 \quad \text{Equation 1.5}$$

Monoprotic acid precipitation Bjerrum curve

$$B_j = 1 - \frac{S_oK_a}{[X_{total}][H^+]} \quad \text{Equation 1.6}$$

For the solution curves the B_j value is calculated from $[H^+]$ and the K_a . This is compared to the precipitation curve which also takes account of the intrinsic solubility (S_o) of the compound and the total concentration in solution ($[X_{total}]$). As with the CheqSol method, this technique is only suitable for ionisable compounds.

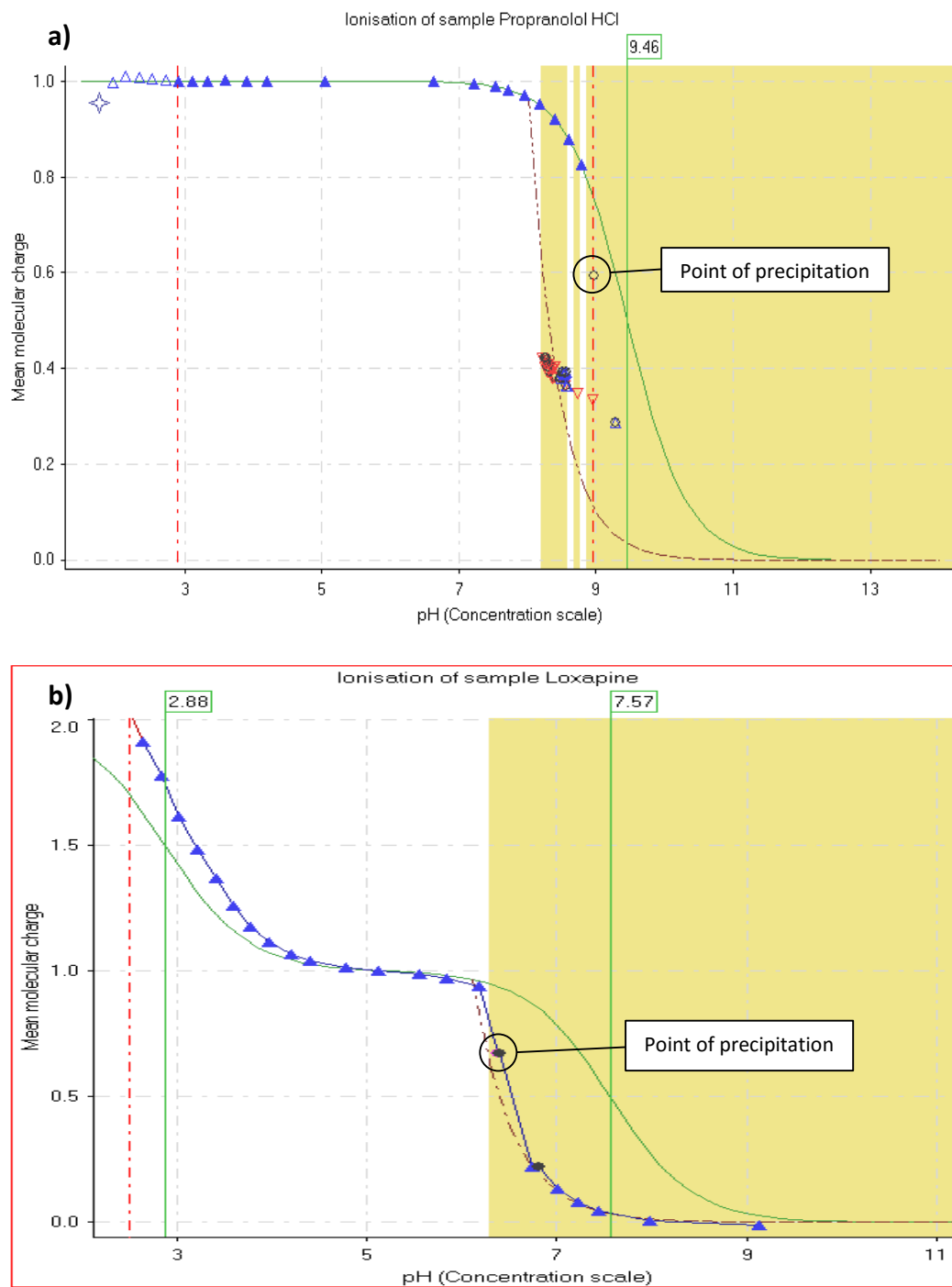


Figure 1.1. Bjerrum curves for solutions (solid green line) and in the presence of precipitation (purple dotted line). a) Example Bjerrum curves for a base which chases equilibrium (propranolol HCl). b) Example Bjerrum curves for a non-chasing base (loxapine). Points of precipitation are marked.

1.6 Methods for Improving Solubility

The challenge facing the pharmaceutical industry during the development of poorly-water soluble or water-insoluble compounds is therefore to formulate the compounds to have an improved solubility. A number of approaches have been developed for both oral and parenteral preparations. Improvement of solubility can be achieved by either increasing the free energy of the solid or through decreasing the chemical potential of the molecule in solution (9). Chemical potential is the change in Gibb's free energy associated with a change in the number of molecules of the solute; when in equilibrium, the free energy and potential energy of the system are equal (29).

If the chemical potential of the molecule in solution is reduced then a higher concentration of molecules will be required to reach equilibrium. The free energy of the solid is increased by, for example, altering the salt used or reducing the particle size, the addition of excipients such as co-solvents, surfactants or complexing agents can reduce the chemical potential of the system (9).

These approaches include making changes to the parent drug through salt or prodrug formation or with the choice of excipients used (30). The technique used to improve solubility should take into consideration a number of factors including the drug structure and route of administration. The techniques described below are examples

of some methods developed for both orally and parenterally administered compounds. The advantages and disadvantages of the techniques will be discussed.

1.6.1 Salt Formation

Salt formation is the most common method for increasing the solubility of ionisable compounds (24). Different salts of compounds have different properties, such as solubility, dissolution rate, toxicity and hygroscopicity (31, 32). For example, the sodium, potassium, calcium and zinc salts of experimental compound BMS-180431 were found to be more hygroscopic than the arginine, lysine and magnesium salts of the same compound (33). The reviews by Berge *et al.* and Verbeeck *et al.* can be referred to for more information (31, 32). It is therefore necessary to evaluate the different salts produced to maximise the solubility, whilst taking into consideration the other characteristics such as safety and stability (34). There are a large variety of salts that can be utilised to optimise the physicochemical properties of drugs. These include inorganic (sodium and hydrochloride) and organic (mesylate and succinic acids) salts (34).

Advantages and disadvantages

Different salt forms differ not only in their solubility but some salts may be able to reduce the toxicity of the drug (34). It has also been shown that salts can have improved thermal stability when compared to the parent drug (34) which may be desirable if manufacturing or storage conditions could increase the risk of degradation. Although salts can increase the solubility of compounds, the compound

may not have sufficient solubility and another method to improve solubility may be required (24). The common-ion effect must also be considered during the development of a salt. When a salt has a relatively low solubility, an excess of the counter-ion in the medium can reduce the solubility of the salt (24). For suitable salts the pH of the solution needs to be controlled since altering the pH affects the proportion of ionised to unionised forms of the compound (24). The chemical and physical stability of different salts needs to be assessed since the salt formed may change to another less stable/soluble salt in the presence of other ions/buffers (34). Salt formation is not a suitable method for improving the solubility of compounds which are not ionisable.

Examples for solubility improvement

Salt formation has been successfully utilised to improve the solubility for oral and parenteral formulations with up to 50% of drugs on the market presented as a salt (35). Of these salts nearly 43% of basic drugs are hydrochloride salts and nearly 62% of acidic compounds are sodium salts (31).

1.6.2 Prodrug Formation

Another strategy to improve drug solubility is through the formation of prodrugs. Prodrugs are biologically inactive compounds with an inactive moiety covalently linked to the active drug (36). These compounds are utilised to overcome a number of poor drug-like parameters such as poor aqueous solubility and chemical instability (37).

Advantages and disadvantages

The prodrug approach has successfully been used to increase the solubility of drugs. Prodrugs also have the advantage that as well as increasing the drugs' solubility, the inactive moiety added can also be used for targeted therapy, for example, in cancer treatment. Leu *et al.* developed a prodrug of 9-aminocamptothecin which improved solubility and could also be targeted to tumours with β -glucuronidase conjugated antibodies (38). However, since prodrugs require conversion to the active drug following administration or absorption, some patients may have issues converting the prodrug to the active drug, especially if enzymatic processes are involved. This could be due to genetic differences, or changes in the enzymes present by, for example, hepatic failure. Not all drugs may be suitable for prodrug formation. The active compound would have to possess at least one functional group amenable to prodrug formation. These functional groups include carboxylic acid, hydroxyl, amine or ketone (37).

Examples for solubility improvement

A number of prodrugs are available on the market, these include fosamprenavir. Amprenavir is a protease inhibitor used in the treatment of HIV in combination with ritonavir (39). The parent drug, amprenavir, has low aqueous solubility; the addition of a phosphate to the molecule increases the water solubility (40). Fosamprenavir is formulated and administered as the calcium salt of the prodrug (39).

1.6.3 Solvents and Cosolvents

In some instances a compound which is insoluble in water, may have sufficient solubility in another solvent, in which it can be formulated. The solvent can be used alone or in conjunction with one or more miscible solvents i.e. cosolvents. Cosolvent formulations can contain an aqueous solvent and a miscible organic solvent (30). The addition of the cosolvent increases solubility by reducing the hydrophilic forces between water molecules and reduces their ability to keep out more hydrophobic compounds (41). The increase in solubility varies depending on the solubility of the compound in water, the solubility in the cosolvent and the fraction of the cosolvent in the system (9, 23). This increase is exponential and can be expressed according to Equation 1.7.

$$\log S_m = f_c \log S_c + f_w \log S_w \quad \text{Equation 1.7}$$

Where f is the volume fraction and S is the solubility in the water-cosolvent mixture (m), pure water (w) and cosolvent (c) (23).

Cosolvents commonly used include ethanol, propylene glycol, polyethylene glycols (PEG), dimethylacetamide (DMA) and dimethylsulfoxide (DMSO) (42). Other solvents commonly used in pharmaceutical products include triglycerides, beeswax, oleic acid, vitamin E and oils (including peanut, corn and soybean) (9).

Advantages and disadvantages

An advantage with the use of organic solvents is that poorly water soluble compounds are likely to be soluble in organic solvents, which allows the use of single solvents for administration. When a cosolvent is added to water, the solubility of the compound increases. However, deviations from the log-linear model have been observed. These deviations result in either increased or decreased compound solubility than predicted. This can be due to interactions between water and the cosolvent or between the compound and the water-cosolvent system (23). Deviations from predicted have been shown with a number of mixes including water-alcohol, water-DMSO and water-PEG mixtures with the drugs phenytoin, benzocaine and diazepam (42). Formulations involving organic solvents can induce pain and inflammation at the site of injection, and there is a risk of precipitation of poorly water soluble compounds after injection (9, 41).

Examples for solubility improvement

The vitamin D metabolite, calcitriol, has been manufactured with the use of triglycerides as the solvent and contained within a soft gelatin capsule (9, 43). Cosolvents are also used in pharmaceutical products on the market. Paricalcitol has been formulated with propylene glycol and ethanol to produce a 0.005 mg/mL for administration intravenously (44).

1.6.4 Micelles and Emulsions

Surfactants can also be added to a formulation to improve solubility. Surfactants are compounds with both hydrophilic and hydrophobic moieties and are found at the interfaces between polar and non-polar regions (45). Surfactants can aggregate to form micelles; in an aqueous formulation the core of the micelle is hydrophobic. The hydrophobic tails of the surfactant molecules are found within the core and the hydrophilic heads form the shell (46). Micelles form spontaneously after the concentration of the surfactant(s) reaches the critical micelle concentration (CMC). Micelles improve solubility as the water insoluble compound is found within the core of the micelle (9, 46). Surfactants are not the only type of molecule to form micelles. Amphiphilic polymers can also form micelles, these molecules may have an advantage over classic surfactants in that the CMC for these substances is lower and the size of the micelles produced is more easily controlled (46).

Cosurfactants such as short-chain alcohols can be included in the system. Their role is to improve stability of the system by dispersing between the surfactant molecules (30, 47). Surfactants can also be used to stabilise emulsions by reducing the surface tension at the polar/non-polar interfaces (45). Formulations containing a polar phase, a non-polar phase, a surfactant with/without the presence of a cosurfactant can self-emulsify with mild agitation; these formulations are called Self-Emulsifying Drug Delivery Systems (SEDDS) (48). The increase in stability of emulsions offered by the presence of surfactants allows stable formulations of drugs to be produced (30).

Examples of surfactants include non-ionic (polyoxyl 35 castor oil, polyoxyl 40 hydrogenated castor oil, polysorbates, PEGs, fatty alcohol), cationic (cetyltrimethylammonium bromide (CTAB)), anionic (soaps) and zwitterionic (phosphatidylcholines) surfactants, the classification depending on the charge of the hydrophilic heads of the molecules (9, 45).

Advantages and disadvantages

The ability of formulations to self-emulsify or form micelles with little/no energy input (30) could improve the ease of administration or reconstitution. Surfactants and their ability to form micelles can increase the solubility of many drug compounds with poor aqueous solubility. Although the presence of surfactants improves stability, emulsions can be thermodynamically unstable with the droplet size of the dispersed phase increasing over time; this gradual move to splitting of the emulsion needs to be controlled (49). Factors affecting the stability of an emulsion include surfactant type and concentration used, storage temperature and the compatibility of the drug and other excipients in the formulation (49). When a micelle approach is used to improve solubility, the CMC following administration should be maintained to prevent precipitation of the compound. If for example, following intravenous administration the micelle concentration falls below the CMC there is a risk that the drug could precipitate out of solution (46). This could pose a problem not only due to lack of biological activity, and therefore lack of efficacy, but also due to the presence of particles. Surfactants can pose issues relating to toxicity. The adverse effects produced can be related to an interaction with molecules and structures

within the body, including cell membranes. Disruption of cell membranes and macromolecules can affect the normal functioning of the cellular processes (45). Polyoxyl 35 castor oil (Cremophor EL), for example, has been implicated in the high incidence of hypersensitivity reactions to paclitaxel (50).

Examples for solubility improvement

Ciclosporin has been successfully formulated as a 100 mg/mL microemulsion oral solution and soft gelatin capsules with excipients including vitamin E (DL- α -tocopherol), alcohol, propylene glycol, corn oil glycerides and polyoxyl 40 hydrogenated castor oil (9, 51). Licensed micelle formulations also exist. An example is the intravenously administered vitamin K₁ (phytomenadione) preparation Konakion MM, where the micelles are formed from the glycocholic acid and lecithin present in the formulation (52).

1.6.5 Liposomes

Liposomes are formed by phospholipids in an aqueous environment. The phospholipids form bilayers as observed in the bilayer of cell membranes. The spherical vesicles formed have an aqueous (polar) core and the hydrophobic tails are protected from the aqueous environment by the hydrophilic heads (53). An increase in solubility is observed when the poorly water soluble compound is incorporated into the bilayer (9). Sterols, like cholesterol, can also be incorporated into the formulation. The addition of sterols to the formulation acts to improve the stability of the liposomes (54).

Advantages and disadvantages

Liposomes may have an advantage over other methods to improve solubility due to the lower incidence of adverse effects (53). This is due to them being composed of phospholipids (and cholesterol) which are naturally occurring compounds within the body. Due to their structure, liposomes have the ability to incorporate both hydrophobic and hydrophilic compounds into the vesicles. Liposomes have also been shown to alter pharmacokinetics and toxicity of drugs. For example, the antifungal agent amphotericin B has a number of formulations including a liposome preparation (AmBisome®). When administered in the liposome formulation, amphotericin B has reduced nephrotoxicity and an increased *in vivo* half-life. The liposome formulation also increases the solubility 50-fold (9). Although high lipid-drug ratios can be observed in the formulation the actual concentration of the drug in the product may be relatively low (46), which may limit the drug loading of this method.

Examples for solubility improvement

As well as AmBisome®, other liposomal formulations are licenced. Liposome preparations have also been developed for doxorubicin, cisplatin and oxaliplatin (55, 56). These preparations were developed to reduce the toxicity associated with the medication (55, 56).

1.6.6 Nanosuspensions

Although the drug is not in solution, the use of nanosuspensions is another method which has been developed for poorly soluble drug delivery. In these suspensions nanocrystals or nanoparticles with a diameter less than 1 μm are suspended as the solid state in solution (30). To prevent aggregation of the particles/crystals the suspension may need to be stabilised, through the addition of surfactants, lipophilic compounds or polymeric stabilisers (30, 46). Nanosuspensions are produced using either 'top-down' or 'bottom-up' methods. 'Top-down' methods involve breaking larger particles into smaller particles through a number of techniques, including milling and high-pressure homogenisation (57). 'Bottom-up' technologies involve precipitation of the drug into nanoparticles from solution (57). Nanosuspensions can improve the bioavailability of orally administered drugs by improving the rate of dissolution of the compound (57). Nanosuspensions can also be administered by intravenous injection/infusion.

Advantages and disadvantages

Nanosuspensions are a suitable formulation for a number of poorly aqueous and non-aqueous soluble drugs (58). It is also possible that nanosuspension formulations may have improved stability over other formulations (46). Although nanosuspensions may be effective for a wide variety of drug candidates, they have their disadvantages. For 'bottom-up' techniques the compound must be soluble in at least one solvent to allow precipitation from solution (57). Control of particle size and/or aggregation of particles during the precipitation process would also be required (46). In 'top-down'

technologies there is the possibility of contamination of the crystals with the milling media metal ions from the homogeniser (58). The process can also be time consuming and may take days for the particles to be reduced to the appropriate size (58). Some techniques also require the use of large quantities of surfactants or other stabilisers to produce a stable preparation (58).

Examples for solubility improvement

Marketing authorisations for nanosuspension formulations have been granted. These include Abraxane, a nanoparticulate formulation of paclitaxel, which is reconstituted before use (46, 59). Nanotechnology is also used in oral preparations. Rapamune®, active ingredient sirolimus, is an oral preparation using nanotechnology (60).

1.6.7 Complexation

Another method for improving the solubility of a drug compound is through association with another water-soluble molecule, called complexation (30, 46). The bonds holding the complex together include hydrogen bonds, hydrophobic interactions, Van der Waals forces and electrostatic bonds (30, 46). The drug agent should interact with the complexing agent in such a way that covalent bonds are not formed (61). Complexation can be either via stacking or inclusion.

Cyclodextrins and cucurbit[n]urils are two groups of molecules which form inclusion complexes. Cyclodextrins form roughly cylindrical structures, likened to a truncated

cone (62), with a hydrophobic core (63). The most common cyclodextrins used consist of 6 to 8 glucose subunits in the pyranose form (9, 61). The cores vary in size, and the ability of the drug to fit within the core will determine whether or not an inclusion complex will form (63). Cucurbit[n]urils are a group of molecules composed of glycoluril monomer units (64, 65). Cucurbit[6]uril was the first of these to be produced in 1905. Lagona *et al.* state that Behrend and colleagues synthesised the oligomer by condensing of glycoluril with formaldehyde in concentrated solutions of hydrochloric acid (64).

Stacking of planar molecules is another method of complexation which can increase solubility (46). The mechanism by which the stacking of hydrophobic aromatic rings improves solubility is thought to be due to the reduction in the exposure of the hydrophobic regions to water (66). Stacking complexation has not been exploited to the same extent as inclusion complexation in the pharmaceutical industry (46).

Dendritic polymers are also being investigated as solubility enhancers via complexation. These dendrimers are composed of a core group with 2 – 4 scaffolding units attached. Extension of the structure is through interaction of the scaffolding moieties of more than one subunit. The solubility enhancement of the drug is through entrapment in the branched scaffolding units (46).

Advantages and disadvantages

The solubility of a compound has been increased by as much as 10^5 times with the use of cyclodextrins (9). Complexing agents can be modified or designed to target specific tissues or cells (46). Issues with solubility and toxicity can be improved through the use of derivatives (46). An advantage of cyclodextrins is that they can reduce the toxicity of the drugs they are used to solubilise. This reduction could be due to reduced doses or to reduced irritation at point of injection (62, 67).

Examples for solubility improvement

Licensed preparations which incorporate a cyclodextrin in the formulation include itraconazole oral solution (Sporanox) (68), aripiprazole injection (Abilify) (69) and voriconazole infusion (VFEND) (70).

1.6.8 Other Methods

Other techniques used to improve the solubility of drug compounds exist. These may be based on other techniques used and include:

- **Cochleates.** These are structures based on the theory behind liposomes. In contrast to liposomes, the lipid bilayer formed by the phospholipids, is not spherical but cylindrical. The phospholipid bilayers form sheets which then coil to form the structure. They can be used to deliver both hydrophilic and hydrophobic drug compounds (46). A cochleate preparation of amphotericin B has been developed and is under investigation (71).

- Liquid crystal nanoparticles. Liquid crystals are matter which are neither liquid nor solid but have properties in between the two (72). Drug formulations utilising this technology are made up of lipids. Improvement in solubility is mediated by the incorporation of the drug into these nanoparticles (46).
- Hydrotropes. The addition of a hydrotrope in sufficiently large quantities to a formulation has been shown to increase the solubility of some poorly water soluble drug compounds (73, 74). The mechanism by which these compounds improve solubility is unknown (74). Some theories for the ability to increase solubility include complexation, self-aggregation, stacking complexation or the hydrotrope may act as a cosolvent (73, 74).

1.6.9 Combinations

While the above techniques have been considered individually, it is common for more than one excipient and/or method to be used to improve the solubility of the compound. For example, Chaudhari *et al.* utilised a cosolvent (PEG-400) and cyclodextrin system to increase the solubility of valdecoxib (41). Another example is the necessity to utilise more than one method to formulate the prodrug of the anti-angiogenesis agent, SU5416. The prodrug has improved solubility over the parent compound, but has poor stability (75). Sistla *et al.* developed a lyophilised formulation of the SU5416 prodrug which involved complexation with cyclodextrin and adjusting the pH, while minimising surfactant and co-solvent content (75).

Combinations could be advantageous as they can maximise the solubility enhancement of the drug molecule while minimising the concentration of potentially toxic excipients. The use of more than one technique to improve solubility increases the complexity of the formulation. While the use of more than one excipient can have a synergistic effect on solubility, it is also possible that the excipients interact with each other, reducing drug solubility and/or stability (41).

1.7 Reducing Solubility

While the main aspect of this thesis introduction has looked at increasing solubility, attention is drawn to the fact that some of the methods described above can also be used to reduce the solubility. These can be utilised in modified-release preparations such as benzathine benzylpenicillin. The benzathine salt reduces the aqueous solubility of the penicillin, compared to the sodium salt, from very soluble to very slightly soluble (76). This results in a slow release following intramuscular injection and prolonged duration of action over benzylpenicillin sodium (77).

1.8 Phase-Solubility Diagrams

When excipients are used in the formulation the increase in solubility can be concentration dependant. When the solubility of the drug is plotted against the concentration of excipient added a phase-solubility diagram is produced. These have been described by Higuchi and Connors (78). The two main groups of plots are A and B type diagrams. In type A diagrams the drug and excipient form soluble complexes,

whereas in type B diagrams insoluble complexes are formed. These can be further subdivided (78).

In type A diagrams there is an increase in solubility with increasing excipient concentration. This can be a linear relationship (A_L), or a curved line which has a positive (A_P) or negative (A_N) gradient (Figure 1.2a). Type B diagrams can be divided into B_S and B_I (Figure 1.2b). Type B_S diagrams show an initial increase in drug solubility (following a type A diagram), at a threshold there is no further increase in solubility as the complex solubility has been reached. Addition of more drug can lead to precipitation of the complex and a decrease in solubility (marked at point b in Figure 1.2b). B_I diagrams differ to B_S diagrams in that no increase in drug solubility is observed (78).

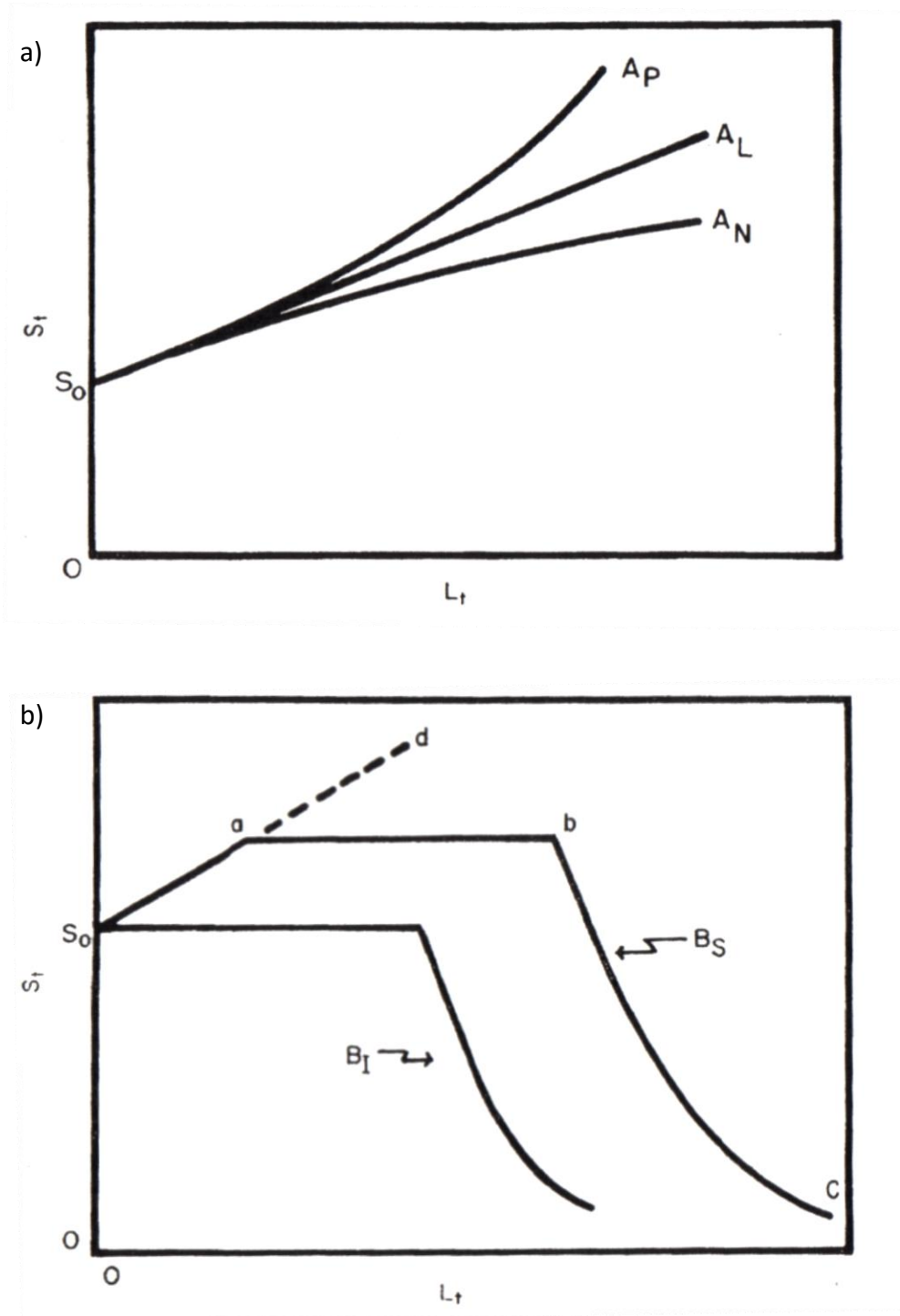


Figure 1.2. Diagrams representing the two types of phase solubility diagram. They represent the increase of solubility of a drug/compound (S_t) versus the increase in ligand concentration in the system (L_t). a) Type A Diagrams, b) Type B Diagrams. Taken from Higuchi and Connors, 1965 (78).

1.9 Project background

Measuring the solubility of a compound can be time consuming with the shake-flask method being the most commonly used technique. During the formulation development stage it might be possible to assist the screening of excipients and to decrease the time required for investigating the solubility enhancements offered by excipients.

The methods described above have been effective in increasing the solubility of compounds for administration. However, these formulations have to be specifically developed and tested for the individual drugs. While a number of techniques can be used to enhance the solubility of a wide variety of compounds, the excipients used and the formulation technique has to be optimised for each drug candidate. There is therefore the potential for a single agent or formulation to be developed which can increase the solubility of a wide variety of poorly water soluble compounds.

The possible advantages of a new solubilising agent over other methods to improve solubility are that it could save time and money during the drug development process. The new solubilising agent will be used with intravenous drugs. Drugs for intravenous administration have to meet certain criteria. In the UK these requirements can be found in the British Pharmacopeia. These criteria are (76):

- Sterile; preparations should be manufactured so that micro-organisms are not present and cannot grow, and to minimise contamination.

- Pyrogen free; it is important that intravenous formulations do not contain bacterial endotoxins or pyrogens.
- Virtually particle free; formulations for intravenous injection (infusion or bolus) should be examined for particles to ensure they meet the requirements.
- The pH of the formulation should be maintained within range 2-12 (9).

1.10 Aims

The project will have two main sections for investigation. The aims of the first section will be to investigate if phase-solubility studies can be carried out using the CheqSol method. The aims of the second section will be to design and examine *in silico* a novel low molecular weight molecule, solubilising agent that can be used as a solvent for multiple, poorly water soluble compounds. Ideally the properties of this agent should meet the requirements detailed above for intravenous formulations, but also include:

- Provide good solubilisation of compounds.
- Not pharmacologically active.
- Degradable in the body following administration.
- Neither the compound nor any metabolites should be toxic.
- Excretion not affected by renal or hepatic impairment.
- Stable in storage.
- Compatible with a large number of drugs.
- Miscible with water.
- Liquid at room temperature.
- Should not alter the drug so that it is no longer active.

- Spontaneously self-assemble.

2 Chapter 2 – Solubility Determination Using CheqSol

2.1 Introduction

The work carried out in this chapter used potentiometric pK_a studies and phase-solubility studies using the CheqSol technique to determine the effect of excipients on the solubility of compounds.

2.1.1 pK_a

One of the properties of ionisable groups in a structure is the point at which 50% of the groups are present in the ionised form and the other 50% are unionised. This ionisation constant can be explained by Equations 2.1 and 2.2 below for acidic and basic groups respectively:

$$K_a = \frac{[H^+][A^-]}{[HA]} \quad \text{Equation 2.1}$$

$$K_a = \frac{[H^+][B]}{[BH^+]} \quad \text{Equation 2.2}$$

The acid dissociation constants are usually referred to as the $-\log_{10}(K_a)$ or pK_a. The pK_a marks the pH at which the 50% ionisation occurs. Potentiometric determination of the pK_a can be carried out by an automated system like the T3 instrument used here used here. Determination of pK_a is carried out by titrating the sample from high to low pH or vice versa. At the point where 50% is unionised an inflection of the

titration curve is observed. Subtracting the blank titration curve and plotting the mean molecular charge versus the pH gives the pK_a (79, 80).

2.1.2 CheqSol

This technique for solubility determination utilises pH changes to determine a compound's intrinsic and kinetic solubility (see chapter 1.3). CheqSol has previously been shown to produce results comparable to literature and shake-flask values (26, 27). Examples of experimental CheqSol values can be found in Table 2.1.

Table 2.1. CheqSol values versus literature or shake-flask. a – thermodynamic values determined at pH 7.4, b – literature value, c – shake-flask value.

Drug	Solubility Type ^a	CheqSol Value	Literature or Shake-Flask Value	Ref.
Diclofenac	Intrinsic	0.9 $\mu\text{g}/\text{mL}$	0.8 $\mu\text{g}/\text{mL}^{\text{b}}$	(26)
Lidocaine	Intrinsic	3500 $\mu\text{g}/\text{mL}$	3810 $\mu\text{g}/\text{mL}^{\text{b}}$	(26)
Glipizide	Thermodynamic	0.0270 g/100mL	0.0260 g/100mL ^c	(27)
Amlodipine	Thermodynamic	3.39 g/100mL	3.25 g/100mL ^c	(27)

The method involves dissolving a compound at a pH where solubility is at its greatest, which, unless the compound is amphoteric, is the pH at which it is fully ionised. For weak bases, the compound is dissolved in acidic conditions, and vice versa. The

amount of drug used in experiments requires being in excess of the intrinsic solubility, but less than the solubility of the ionised form. The pH of the solution is then slowly titrated towards the unionised form of the compound. As compound ionisation decreases during pH titration, the compound will begin to precipitate out of solution. Precipitation is detected by an increase in absorbance of UV/Vis light due to the presence of solid particles within the assay vial. The wavelength for detection is set out with the range where the compounds absorb light, with default detection in the visible range at 650 nm. To determine the solubility alternating aliquots of acid and base are then added to the solution and the pH changes monitored. This process brings the solution close to equilibrium, and the addition of small aliquots of acid and base flips the solution between super- and sub-saturated states. For example, when a basic drug is being investigated, it is dissolved in acid; base is then added to the vial slowly until the drug begins to precipitate. Once precipitation is detected, more base is added to increase precipitation before acid is titrated into the solution. Acid is added until the drug starts to dissolve again i.e. the solution is sub-saturated. Base titrant is then added, switching to a super-saturated solution and restarting the precipitation process (Figure 2.1).

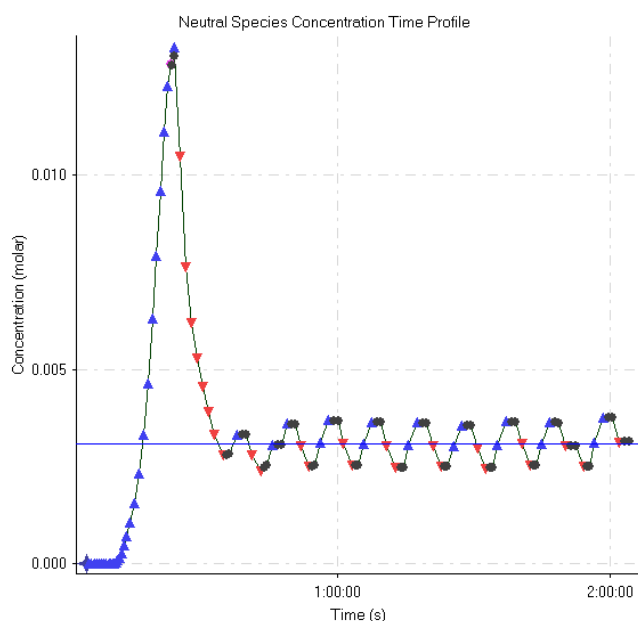


Figure 2.1. Example neutral species concentration plot, showing titrant addition during the assay. Assay is an example Propranolol HCl in the presence of cyclodextrin. The drug was dissolved in acid, following complete dissolution: base addition represented by ▲, and acid addition represented by ▼. X-axis label quotes units of time in seconds instead of hours, this graph is produced by the software with the incorrect units.

Dissolution/precipitation is detected by monitoring the pH changes. The pH changes observed are in the opposite direction than expected. This is exemplified by the addition of acid to the above system in near equilibrium conditions, during weak base dissolution, which demonstrates an increase in pH due to the removal of free H^+ ions as the ionised base dissolves. The opposite is true if base is added to the system, and decreases pH, the precipitating unionised base releases H^+ into solution. From this, it can be observed that at the point where dissolution and precipitation are complete,

i.e. where there is no further change in pH, is the intrinsic solubility. In order to determine the solubility, the pH of the system is recorded to determine the slope of the pH change over time; these are then extrapolated to where $\Delta\text{pH}/\Delta t$ is zero (crossing point). At each crossing point, the extrapolated pH can be used to determine compound concentration. Each cycle of dissolution/precipitation is referred to as a crossing point. Multiple crossings are carried out close to the equilibrium point of the compound to produce a mean and increase confidence in the result.

The concentration of the solution is calculated from a series of equations, which require other parameters in addition to the crossing point pH. These are: molecular or formula weight of the drug (accounting for the presence of salts or hydrates); weight of drug used; the drug's pK_a value(s) and whether they are acidic or basic groups; volume of the solution; and volume and concentration factors for the acid and base for each data point (15, 26).

Details of the eight calculations involved in solubility determination can be found in Stuart and Box, 'Chasing Equilibrium: Measuring the Intrinsic Solubility of Weak Acids and Bases' (26).

The concentration of hydrogen ions is calculated from the pH of the system at each data point (Equation 2.3). From this, the hydroxide ion concentration is calculated (Equation 2.4), where K_w is the ionic product of water (taken to be $1 \times 10^{-14} \text{ M}^2$). The total volume of the system (v_t) is calculated from the total volume of water (v_w), base

(v_b) and acid (v_a) added to the system (Equation 2.5). The total concentration of free positive and negative ions (Equations 2.6 and 2.7), where c_b and c_a are the base and acid titrant concentration factors respectively, m_s is the weight of compound, f_w is the formula weight and z_{s+} and z_{s-} are the charges of any positive or negative counterions (in salt samples) respectively.

$$[H^+] (M) = 10^{-pH} \quad \text{Equation 2.3}$$

$$[OH^-] (M) = \frac{K_w}{[H^+]} \quad \text{Equation 2.4}$$

$$v_t (L) = v_w + v_a + v_b \quad \text{Equation 2.5}$$

$$[K^+] (M) = \frac{v_b c_b + m_s z_{s+} / f_w}{v_t} \quad \text{Equation 2.6}$$

$$[Cl^-] (M) = \frac{v_a c_a + m_s z_{s-} / f_w}{v_t} \quad \text{Equation 2.7}$$

The above equations allow the calculation of the concentration of the ionised form of the drug using the appropriate charge balance equation. For a monoprotic acid this is:

$$[A^-] (M) = [H^+] - [OH^-] + [K^+] - [Cl^-] \quad \text{Equation 2.8}$$

And for a monoprotic base:

$$[BH^+] (M) = [OH^-] - [H^+] + [Cl^-] - [K^+] \quad \text{Equation 2.9}$$

Therefore, the concentration of unionised species is calculated from Equations 2.10 and 2.11 for monoprotic acids and bases respectively.

$$[\text{HA}] (\text{M}) = \frac{[\text{A}^-][\text{H}^+]}{10^{-\text{pK}_a}} \quad \text{Equation 2.10}$$

$$[\text{B}] (\text{M}) = \frac{(10^{-\text{pK}_a})[\text{BH}^+]}{[\text{H}^+]} \quad \text{Equation 2.11}$$

The solubility is taken to be the concentration of unionised drug at the crossing points. The mean concentration/intrinsic solubility is calculated from all crossing points included. The software calculates the coefficient of variation. Graphical representation of the variation can be observed in the Equilibrium Chasing Crossover Plot of change in pH over time versus concentration (Figure 2.2). The crossing points where $\Delta\text{pH}/\Delta t$ is zero are represented.

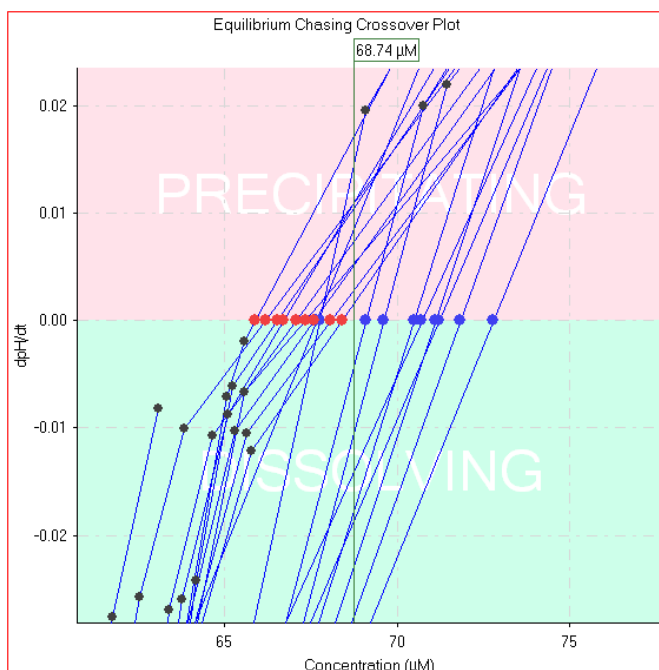
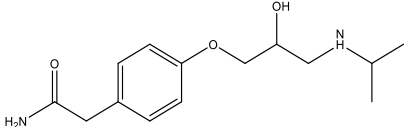
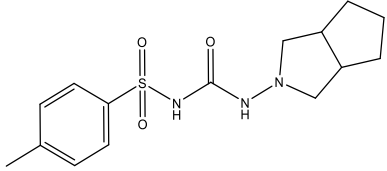
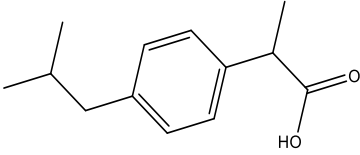


Figure 2.2. An example of the crossover plot produced by the software running the instrument. When the change in pH over time is equal to zero the calculated concentration at this point is the intrinsic solubility. Twenty crossovers are carried out and a mean calculated to improve confidence in the results. The crossover plot is from a gliclazide CheqSol assay. The red and blue dots represent the extrapolated crossover points following acid and base addition respectively. Black dots represent the experimental data used to extrapolate to zero.

This method can be used to determine the solubility of ionisable compounds which can form supersaturated solutions and where the kinetic solubility is greater than the intrinsic solubility, which is a disadvantage of the technique (15). Another disadvantage of this technique is that it is not suitable for acids with a pK_a greater than 11, or bases with a pK_a less than 3 (28).

Since the CheqSol method is largely aimed for the development stage, there is little information regarding the use of excipients in CheqSol assays. Studying excipient solubility effects on four drugs will provide information regarding the suitability of the method for formulation development and will provide information on excipients used in CheqSol phase-solubility studies. The two classes of excipients added during the investigation are complexing agents and surfactants. As excipients can have ionisable groups with pK_as within the range, non-ionisable excipients were chosen. The solubility improvement that hydroxypropyl-β-cyclodextrin (HP-β-CD) and two poloxamers (P407 and P188) have on four drugs was investigated. The effect of the ionisable cholic acid was also investigated on ibuprofen and propranolol HCl. The structures for the compounds investigated can be found in Table 2.2 and 2.3.

Table 2.2. Structure and physicochemical data of the four test compounds used.

Name	Structure	Molecular weight	Literature pKa	Literature Solubility	References
Atenolol		266.3	9.48	62.1 mM	(27)
Gliclazide		323.4	5.54	0.092 mM	(27) (81)
Ibuprofen		206.3	4.35	0.242 mM	(26)

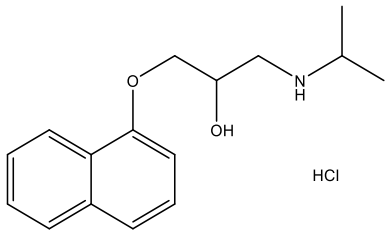
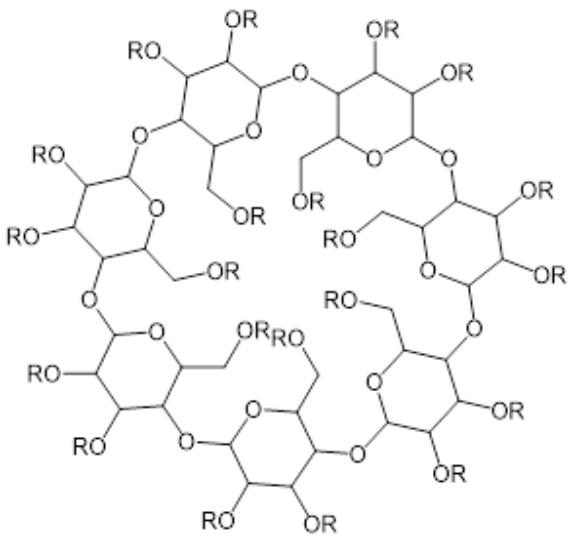
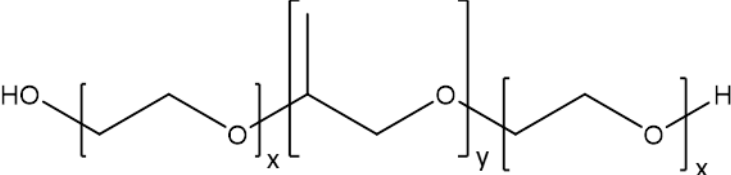
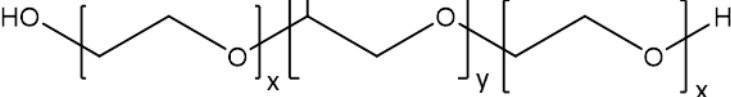
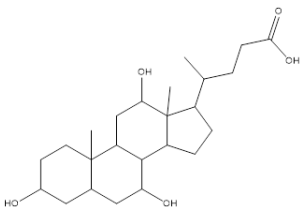
Propranolol HCl	 <chem>CC(C)NCC(O)COc1ccc2ccccc12.[Cl-]</chem>	259.3 (MW) 295.8 (FW)	9.54	0.312 mM	(26)
--------------------	--	--------------------------	------	----------	------

Table 2.3. Structures of the excipients used during experiments. For HP- β -CD, R can be either $-H$ or $-\text{CH}_2\text{CH}(\text{OH})\text{CH}_3$, with 5-8 substitutions per molecule. For poloxamers x and y vary depending on the poloxamer used. Average values for P407 are x = 98 and y = 67, and for P188 are x = 75 and y = 30 (82).

Name	Structure	Average Molecular Weight
HP- β -CD	 <p>The image shows the chemical structure of hydroxypropyl-beta-cyclodextrin (HP-beta-CD). It consists of a cyclodextrin ring, which is a cyclic oligomer of D-glucopyranose units linked by alpha-1,4-glycosidic bonds. The structure is shown with several hydroxypropyl groups (OR) attached to the glucose units, representing the hydroxypropylation modification.</p>	1454

P407		12600 (83)
P188		8350 (84)
Cholic Acid		408.57

2.1.3 Cyclodextrins

Cyclodextrins are (α -1,4)-linked α -D-glucopyranose units (61) and form a roughly cylindrical molecule, with a narrow and wide opening. The internal core of the molecule is hydrophobic and the shell is hydrophilic (85). The most common natural cyclodextrin molecules have 6 (α -), 7 (β -) or 8 (γ -) subunits (86), with core size dependent on the number of subunits. The diameters of α -, β - and γ -cyclodextrins are 4.7-5.3 Å, 6.0-6.5 Å and 7.5-8.3 Å respectively (87). Cyclodextrins form inclusion complexes whereby the poorly water soluble molecule, in whole or in part, is found within the core (30, 46). The size of the core can influence inclusion complex formation as the molecule or part of the molecule must fit within the core (63). The hydrophobic core of the molecule can interact with non-polar molecules, the hydroxyl groups on the exterior of the molecule can form hydrogen bonds, with a preference to bond with anionic molecules (88).

The natural cyclodextrins have limited water solubility, with β -cyclodextrin's (β -CD) solubility being just 1.85 g/100mL (63, 67). They have also been shown to have adverse effects such as renal problems due to precipitation following glomerular filtration (46). Derivatives of these cyclodextrins have been developed which improve the physicochemical and toxicological properties of the natural cyclodextrins including: HP- β -CD and sulfobutylether- β -cyclodextrin (SBE- β -CD) which show solubilities of greater than 60 g/100mL and 50 g/100mL respectively (46, 62, 63). Cyclodextrins have the ability to greatly increase the solubility of compounds and increases by a factor of 10^5 (9) have been reported. Another advantage of

cyclodextrins is that they can reduce the toxicity of the drugs that complex within them. For example, Weisz *et al.* have reported the ability of β -CD to reduce the haemolysis caused by chlorpromazine *in vitro*, the polysulphated β -CD was also observed to reduce the haemolysis of other non-sulphated β -CDs (89). Cyclodextrins, when complexed with piroxicam, have also been shown to reduce gastrointestinal lesions compared to the non-complexed formulation following oral administration (90). The addition of complexing agents into parenteral formulations can have benefits such as reduced doses or reduced irritation at the point of injection (62, 67). Further formulation techniques might be required for intravenous products such as liposome formation if precipitation in the glomerular filtrate is still an issue (46, 62).

Cyclodextrins have been shown to have a good toxicity profile when administered orally due to the limited absorption from the GIT (91). Side effects of HP- β -CD include diarrhoea which was observed when human subjects received between 16 and 24 g of HP- β -CD daily for two weeks (91). The low toxicity profile following oral administration is due to poor absorption from the GIT. The cyclodextrins are not metabolised easily until entering the colon, where the microflora present have been found to have the capability of degrading cyclodextrins (91). Following parenteral administration, cyclodextrins have a volume of distribution nearly equivalent to the volume of the extracellular fluid suggesting that there is little or no distribution (91). HP- β -CD is excreted renally and in humans was found to have a clearance rate of 110 – 130 mL/min, which is similar to the glomerular filtration rate of 125 mL/min (92).

HP- β -CD has been shown to have a good toxicity profile following intravenous use with no detrimental effect on kidney function (93).

2.1.4 Poloxamers

The poloxamers are non-ionic block copolymer surfactants. The general structure of poloxamers is polyoxyethylene-polyoxypropylene-polyoxyethylene at varying quantities and ratios (94, 95). The properties of the poloxamers vary considerably depending on the quantities of the hydrophilic polyoxyethylene (POE) and the hydrophobic polyoxypropylene (POP) present in the copolymer. Poloxamers are found as liquids, solids or pastes, the characteristics again dependent on the hydrophilic and hydrophobic proportions. For example, poloxamers with a higher percentage of oxyethylene in the molecule show higher water solubility and a higher oxypropylene content reduces water solubility (96) which is not unexpected.

Poloxamers can form micelles. The process and structure of micellisation has been studied to determine the aggregation number of poloxamers, however literature values for the number of molecules per micelle are varied. Smolka has quoted that the aggregation number is between two and eight (96). However, more recent studies have found the aggregation number for P407 to be nine for a 10% w/w solution in water at 25°C (97). Cespi *et al.* have also shown that the concentration of the poloxamer solution may affect the aggregation number of the micelles with a 25% w/w solution having a slightly larger N of ten (97). Wulff-Pérez *et al.* have shown that the aggregation number for P188 is larger than that for P407 at 15 molecules per

micelle (98). Each molecule is oriented in a horseshoe shape (Figure 2.3) with the hydrophobic polyoxypropylene block in the centre protected from aqueous environment by the hydrophilic tails (96). Sasaki and Shah determined the CMC of poloxamer 188 to be 0.1% w/v at approximately 25°C (99). Poloxamer 188 CMC used was quoted as 0.04 mM (0.03% w/v) from the supplier (84). The CMC of poloxamer 407 at 25.5°C was found to be 0.1% w/v (100), and with the supplier quoted CMC being 950 – 1000 ppm (101), which is equivalent to 0.095 to 0.1%. Poloxamer micelles form due to dehydration of the oxypropylene subunits.

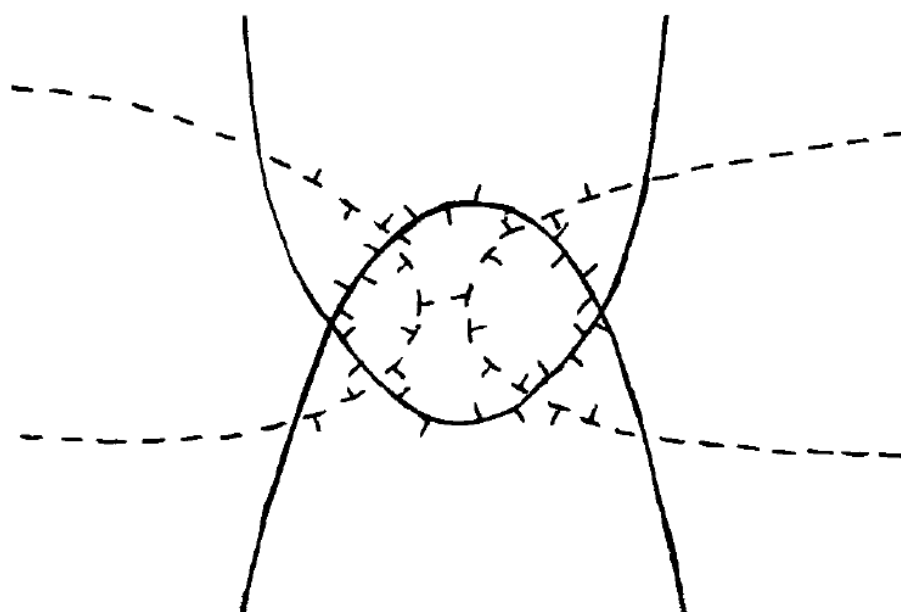


Figure 2.3. Suggested orientation of poloxamer molecules within micelle. The poloxamer molecules form a horseshoe shape with the hydrophobic POP block protected from water by the hydrophilic POE blocks. Taken from Smolka, 1977 figure 7 (96).

The nomenclature of the surfactants gives details on the proportions of hydrophobic and hydrophilic subunits. The last digit of the name multiplied by ten gives the percentage polyoxyethylene, and the first two digits multiplied by 100 gives the approximate weight of polyoxypropylene in the molecule (102).

The pharmaceutical uses of poloxamers, in addition to the ability to form micelles and increase solubility, include reducing drug resistance in cancer chemotherapy. Zhang *et al.* demonstrated that paclitaxel/P188 nanoparticles significantly increase the toxicity to resistant human breast cancer cells (103).

The toxicity profiles of poloxamers have been investigated with varying results about adverse effects. P407 has been shown to affect the lipid profile of mice following administration twice weekly for a period of one month (104). While P188 was found to be beneficial in a model for haemorrhagic shock compared to no intervention (105). Other studies administering P188 to human volunteers have found that the poloxamer can cause side effects. Following intravenous infusion, Jewell *et al.* showed that P188 can cause pain, nausea and problems at the injection site (106). Other adverse effects included reversible proteinuria and increased hepatic enzymes (106). Grindel *et al.* also reported pain as a side-effect of P188 infusion over 48 hours and also reported lethargy and frequent urination (107).

Poloxamer 188 is excreted renally with over 70% of the surfactant excreted unchanged in the urine during the study, which collected urine up to 36 hours after

the infusion was completed (106). Li *et al.* have shown that following intraperitoneal injection in rats, excretion of P407 in the urine is around 25% after 24 hours (108). The limited renal excretion was said to be due to kidney damage allowing some of the P407 to be excreted in the urine despite limited glomerular filtration (108). Li *et al.* also reported that 5% of the P407 accumulated in the liver, which could result in the lipid effects observed following administration of P407 (108).

2.1.5 Cholic Acid

The bile acid, cholic acid, is a self-associating molecule that can form micelles. The CMC for cholic acid has been reported as between 7.6 and 8 mM (109). The molecule has a convex, hydrophobic face and a concave hydrophilic face (110). The micellisation of bile acids involves aggregation of small numbers of molecules with both hydrophobic and hydrogen bonding (110). The micelles formed have the ability of solubilising compounds, including self-solubilisation (111).

2.2 Aims

The aims of this section are to look at the effect that excipients have on four model compounds, two of which are basic (propranolol HCl and atenolol) and two acidic drugs (gliclazide and ibuprofen). The effects to be examined are pK_a changes and any increases in solubility. As assays carried out on the equipment require knowledge of the pK_a this must first be calculated for the four drugs compounds alone and in the presence of the excipients under examination. The CheqSol technique can be used to determine the solubility of ionisable compounds; however, it is used mainly in the

absence of excipients. One aim of the experiment is to determine if it is possible to use excipients with this technique, such as the solubilising compounds (HP- β -CD, poloxamer 188 and poloxamer 407) described above. Another aim of this experiment is to determine if the excipients can improve the solubility of the four drugs. The excipients described are all non-ionisable; another study will investigate whether the ionisable cholic acid is a suitable excipient for study using the T3.

2.3 Materials

All experiments were carried out using the Sirius T3 titrator (Sirius Analytical Instruments Ltd, East Sussex, UK). Ionic strength adjusted (ISA) water contains 0.15M potassium chloride, obtained from VWR (Leuven, Belgium), in HPLC grade water. Propranolol HCl, atenolol, ibuprofen, gliclazide, poloxamer 407 (Pluronic[®] F-127), poloxamer 188 (Pluronic[®] F-68) and cholic acid were obtained from Sigma-Aldrich Company Ltd (Dorset, UK). HP- β -CD (Cavitron 82004) was obtained from Cargill (Cedar Rapids, Iowa, USA). 0.5M Potassium hydroxide (KOH) (Fisher Scientific, Loughborough, Leicestershire, UK) was prepared from 1 mole vial of KOH diluted to 2 L with HPLC grade water. 0.5M Hydrochloric acid (HCl) (Fisher Scientific, Loughborough, Leicestershire, UK) was used as purchased. HPLC grade water was obtained using an Elga UHQ2 system (Marlow, Buckinghamshire, UK).

The T3 set-up (Figure 2.4) includes a Ag/AgCl double junction reference pH electrode, a Peltier temperature control device, with thermocouple temperature probe, an overhead stirrer (variable speed, computer controlled). The spectrophotometer was

a MMS UV–VIS Carl Zeiss Microimaging spectrophotometer with an ultra-mini immersion probe attached (Welwyn Garden City, Hertfordshire, UK).

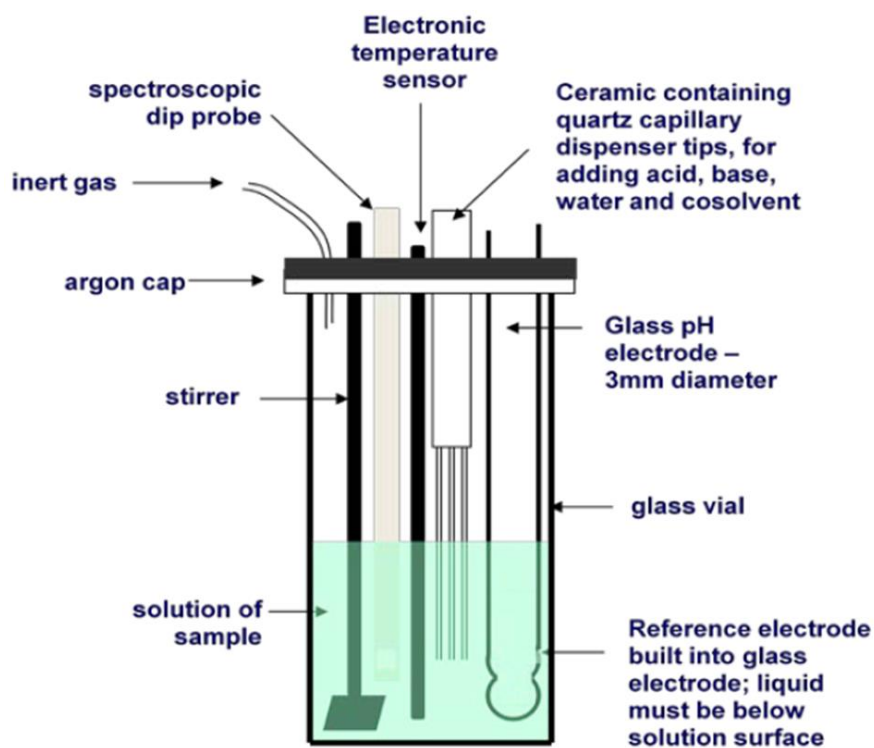


Figure 2.4. The equipment set-up of the T3 during an assay in a 4 mL vial, height 12mm. Image taken from T3 instruction manual (80).

2.4 Methods

Experiments were conducted at a temperature of $25^{\circ}\text{C} \pm 0.5^{\circ}\text{C}$ in an argon atmosphere. The apparatus was connected to and run from Sirius software on a Dell desktop. Except where stated the settings for each assay used were the default settings on the software.

2.4.1 Determination of Excipient Water Content

Excipients were dissolved in methanol at a concentration of 100 mg/mL to be analysed on a Mettler Toledo DL37 KF Coulometer. For water content of methanol the system was set up to run method 2, calculation number 2. Water content of excipient solutions was calculated using method 1, calculation number 3. Determination of water content was carried out on 100 µL aliquots of sample. Details entered for blank titrations were weight of syringe before methanol injection (weight 1) and weight of syringe after injection (weight 2). Method 1 requires the input of weight 1 and weight 2 as before and in addition weight 0 (the weight of excipient used to make up solution) and weight B (the weight of methanol used to make up the solution). This method also requires the weight of water in methanol determined during blank titrations (weight A in ppm). The output for excipient assays was weight of water (µg converted to %). Mean water content was calculated using the apparatus. Results are quoted as mean ± standard deviation.

The water content in ppm of methanol was determined by the amount of water present divided by the total amount of solvent put into the system.

The calculations for excipient solutions were as defined in Equations 2.12 to 2.15.

$$\frac{0.001 * \mu\text{g water}}{\text{weight 1} - \text{weight 2}} = \text{Result 1} \quad \text{Equation 2.12}$$

$$\frac{\text{weight B} + \text{weight 0}}{\text{weight 0}} = \text{Result 2} \quad \text{Equation 2.13}$$

$$\frac{\text{weight A} * \text{weight B}}{\text{weight 0}} = \text{Result 3} \quad \text{Equation 2.14}$$

$$\frac{(\text{Result 1} * \text{Result 2} * 1000) - \text{Result 3}}{10000} = \% \text{ water content} \quad \text{Equation 2.15}$$

2.4.2 Preparation of Study Solutions

The T3 apparatus requires ISA water in experiments and all cosolvent solutions and poloxamer solutions used in the study were prepared using ISA water. The 80% methanol cosolvent solution was prepared by dissolving 2.795 g KCl in 50 mL HPLC grade water and made up to 250 mL with methanol (80). Poloxamer solutions were prepared as needed in ISA water. The required mass of poloxamer was weighed out and this was made up to 100 mL with refrigerated ISA water according to the directions of Shin and Cho (95).

The concentrations of poloxamers used were selected to be comparable to each other and to cover as big a range as possible without risking gelation of poloxamer 407. A lower maximum concentration was selected as compounds can affect the gelation properties in either direction. For example, diclofenac and ethanol can increase the temperature at which gelation occurs, while sodium chloride and carbopol reduce transition temperature from solution to gel (112-114).

For pK_a and CheqSol assays, solutions of HP-β-CD were not prepared in advance. The mass of cyclodextrin was calculated and weighed into the assay vial along with the sample compound and dissolved together.

2.4.3 Potentiometric Determination of pK_a

The pK_a s of four compounds (two acids and two bases) were determined. For each pK_a determination, the titration was run from a pH where the compound is fully ionised to a pH where the compound is fully un-ionised. The pK_a was determined for the drugs on their own and in the presence of HP- β -CD and poloxamers.

For propranolol HCl, gliclazide and atenolol the assay used was the pH-metric pK_a assay, each with three titrations per assay. The overall pK_a was calculated by fitting the best Bjerrum plot to all three titrations. The pK_a result reported is therefore not equivalent to the mean pK_a , which can be calculated from the three individual pK_a results. The T3 was set up with 0.4 mg to 1.2 mg of active compound, which was dissolved in 1.5 mL to 1.75 mL of ISA water. The pH titrations were carried out using 0.5M potassium hydroxide (KOH) and 0.5M hydrochloric acid (HCl). Due to the low aqueous solubility of ibuprofen potentiometric pK_a determination could not be carried out as above. A cosolvent was required to ensure the drug did not precipitate during the assay. An initial solvent volume of 1.5 mL was used. The software was used to calculate the volume of 80% methanol and ISA water required for each stage of the titration. The first titration was carried out with approximately 50% methanol, the second with 40% methanol and the third with 30% methanol. The pK_a s in the presence of methanol (p_sK_a) were then extrapolated to 0% methanol to achieve the pK_a for ibuprofen using the Yasuda-Shedlovsky method (115, 116).

For titrations involving HP- β -CD the mass added to the drug before dissolution was calculated based on a molecular weight of 1454 g/mole and adjusted for the water content in the powder. The five ratios of HP- β -CD used for all four drugs were 1:0.1, 1:0.5, 1:1, 1:1.5 and 1:2. In addition, the pK_a at the following ratios were determined for propranolol HCl (1:2.5 and 1:5), gliclazide (1:5 and 1:10), atenolol (1:0.05, 1:0.15 and 1:0.2) and ibuprofen (1:0.75). For titrations using poloxamers, solutions of 0.5% w/v, 1% w/v, 2% w/v, 5% w/v and 10% w/v of both poloxamers were made up as described. The assays were run with 1.5 mL to 1.75 mL of the poloxamer added manually. The determined pK_a results were used as model entry parameters in the assays to determine solubility.

Ibuprofen pK_as in the presence of cyclodextrin and poloxamer was carried out as before. For poloxamer solutions, an 80% methanol, x% w/v poloxamer and 0.15M KCl was prepared by dissolving the required quantity of poloxamer in 2 mL of the 80% methanol cosolvent mixture described earlier. The quantities of poloxamer/cosolvent and ISA water were added manually before each titration.

2.4.4 Potentiometric Determination of Solubility

As with pK_a determination, the solubility experiments were run on T3 equipment using the solubility CheqSol assay. This technique requires the drug to precipitate out of solution during the titration therefore enough active drug was weighed out into an assay vial that exceeded the expected intrinsic solubility, and lower than the solubility of the fully ionised form. ISA water was added to the vial (1.5 mL for

propranolol HCl, gliclazide and ibuprofen, 1 mL for atenolol) before the pH was adjusted. The titrations were carried out using KOH (0.5 M) and HCl (0.5 M), from a pH where the compound was fully ionised, until precipitation was detected. After precipitation detection, more titrant was added to increase precipitation before the alternating aliquots of acid and base were added. Twenty crossing points in total were used and the mean concentration of the points was calculated to determine the solubility. As for pK_a determination, the solubility was determined for the drug alone and in the presence of HP-β-CD and poloxamer. For propranolol HCl, the HP-β-CD ratios used were 1:0.1, 1:0.5, 1:1, 1:1.5, 1:2 and 1:2.5. The ratios used for the determination of gliclazide solubility increases were 1:0.1, 1:0.5, 1:1, 1:1.5, 1:2 and 1:5. The solubility of atenolol in the presence of HP-β-CD at ratios of 1:0.05, 1:0.1, 1:0.15 and 1:0.2 was determined and for ibuprofen the ratios used were 1:0.1, 1:0.5, 1:0.75 and 1:1. The concentrations of poloxamer used were the same as described for pK_a determination (0.5% w/v, 1% w/v, 2% w/v, 5% w/v and 10% w/v).

2.4.5 Shake-Flask Solubility Determination of Propranolol

To compare the phase-solubility results achieved with CheqSol, a shake-flask study on the solubility improvement that HP-β-CD has on propranolol was carried out. The study was conducted in two buffers, one at pH 5.5 and one at pH 12 where propranolol is ionised and unionised respectively. Buffer solution recipes were obtained from (117).

- pH 12 - 50 mL 0.2 M KCl (0.74557 g/50 mL), 12 mL of 0.2 M NaOH (1.2 mL of 2 M NaOH) and diluted to 200 mL with HPLC grade water.
- pH 5.5 – 100 mL 0.1 M potassium hydrogen phthalate (2.04221 g/100mL), 73.2 mL of 0.1 M NaOH (3.66 mL of 2 M NaOH) and diluted to 200 mL with HPLC grade water.

Two 50 mL stock solutions of 0.01393 M HP- β -CD were prepared, one at pH 5.5 (1080.78 mg HP- β -CD) and one at pH 12 (1080.72 mg HP- β -CD). The phase-solubility study was carried out with propranolol HCl alone and with five target concentrations of HP- β -CD (0.697 mM to 13.930 mM). From the stock solutions, different concentrations were prepared according to Table 2.4. The actual concentration of HP- β -CD in the vial was corrected for the inclusion of titrants to adjust pH. For unionised solubility assays at pH 12, approximately 3 mg of propranolol HCl was added to the vial and 1.5 mL of buffer alone or buffer and cyclodextrin solution (Table 2.4). An excess of approximately 300 mg of propranolol HCl was added to vials for the assays at pH 5.5, with the buffer/cyclodextrin solutions as before. The pH values of the vials were checked and adjusted if necessary, for pH 12 assays the pH had to be at least 12 ± 0.1 to ensure the pH remains 2 units above the pK_a for propranolol. Since the ionised assay pH was 5.5, a greater range of 5.5 ± 0.3 for the pH was used due to the greater difference between pH and pK_a . Any pH adjustments were carried out with 0.5 M HCl and 0.5 M KOH, and the volume added recorded for accurate HP- β -CD concentration. For the total volumes and pH recordings for each vial see appendix 2.

The vials were shaken at 320 motions/min on an orbital shaker, in a 25°C constant temperature room for 24 hours. After shaking the pH was checked again, if the pH was within the $pK_a \pm 2$ then the pH was readjusted and if required more propranolol HCl was added and shaken for a further 24 hours at 25°C. Following the first period of shaking, none of the vials were found to have a pH within $pK_a \pm 2$, and all had excess undissolved powder remaining within the vials. After shaking was complete, the contents of the vials were transferred to centrifuge tubes and left to settle for 48 hours. After settling, the tubes were centrifuged at 13000 rpm (on a Mikro 20 centrifuge) for five minutes. One mL of the supernatant was carefully removed and transferred to another tube. The tubes were stored at 25°C until HPLC was run.

Table 2.4. Six HP- β -CD concentrations used in assays with volumes of buffer and stock solutions used.

HP- β -CD Concentration (mM)	Buffer Volume (mL)	HP- β -CD Stock Volume (mL)
0	1.5	0
0.697	1.425	0.075
3.483	1.125	0.375
6.965	0.75	0.75
10.448	0.375	1.125
13.930	0	1.5

The HPLC method used was developed based on an existing method detailed by Basci *et al.* (118). The mobile phase was 70% phosphate buffer (10 mM, pH 3.0) and 30% acetonitrile. The column used was a Luna C18 column (5 μ m, 150mm x 4.6 mm i.d.). The instrument settings were flow rate 1 mL/min, 20 μ L injection volume and absorbance detection at 254 nm and 280 nm. The mobile phase was prepared by weighing 2.28 g of potassium phosphate dibasic trihydrate (MW 228.22) per litre of HPLC grade water. The pH was then adjusted to pH 3.0 with 2 M HCl before filling to the volume mark. The phosphate solution was then filtered before mixing with acetonitrile (analytical grade). The mobile phase was altered from the Basci *et al.*

method to reduce the retention time of propranolol in the column, at proportions of acetonitrile greater than 70% in the mobile phase, the void volume peak and propranolol peak merged.

Calibration curve for propranolol was carried out from a 1073 $\mu\text{g}/\text{mL}$ stock solution of propranolol HCl in mobile phase (Table 2.5). The standard solutions were then diluted 1:1 with mobile phase as during test runs high concentrations reached the absorbance threshold. Before HPLC, the sample vials were diluted with mobile phase (either 1 in 2, 1 in 4 or 1 in 1000) to ensure the concentration was within the standard curve range. Each assay was run in triplicate.

Blank assays were also run with buffer alone and cyclodextrin at both pHs to ensure there were no effects on results due to buffer/cyclodextrin, these were run following a 1:1 dilution with mobile phase and in triplicate.

Table 2.5. Standard solutions used for HPLC calibration curve.

Propranolol HCl Concentration ($\mu\text{g}/\text{mL}$)	Stock Solution Volume (mL)	Mobile Phase Volume (mL)
1073	1	0
804.8	0.75	0.25
536.5	0.5	0.5
268.3	0.25	0.75
107.3	0.1	0.9
53.65	0.05	0.95

2.4.6 Cholic Acid as an Excipient

Work was carried out to determine whether solubility enhancements of ionisable excipients can be investigated using the CheqSol method. As cholic acid is ionisable within the range pH 2-12, cholic acid p_sK_a determination was carried out. Solubility studies for cholic acid using the CheqSol method on the T3 apparatus, as described above, were carried out. For the effect on ibuprofen pK_a , approximately 1 mg of cholic acid was added to 3 vials containing ibuprofen. For these vials different volumes of ISA water and methanol were mixed together. The volume of 80% methanol to give total methanol content roughly equal to 50%, 40% and 30% were 1.15 mL, 1.00 mL and 0.85 mL respectively. The volume was made up to 1.50 mL with

ISA water. To examine effect on ibuprofen solubility, approximately 1 mg of cholic acid was added to a vial containing ibuprofen and a CheqSol assay was run.

As ibuprofen is a weakly acidic compound, cholic acid was investigated with propranolol HCl. Assays were run from pH 7 to pH 12, where cholic acid would be fully ionised, to try to prevent precipitation. A stock solution of 7.24 mM cholic acid at pH 7 was prepared for propranolol HCl assays. CheqSol and pH-metric assays were run as above, with 1 mL of 7.24 mM cholic acid solution and 0.5 mL ISA water.

2.4.7 Analysis of Results

To determine if the excipients had any effect on pK_a , the regression line between the molar HP- β -CD concentration and the mean pK_a or extrapolated pK_a was calculated. Mean solubility results at each HP- β -CD molar ratio or poloxamer concentration were recorded and the regression line calculated. The mean kinetic solubility results were recorded and plotted and the regression line determined.

Shake-flask results were analysed following linear regression of the calibration curve (area under the curve (AUC) versus propranolol concentration), and the concentration calculated. The concentrations were then treated with linear regression of concentration versus cyclodextrin concentration. Comparison of regression equations was carried out using the General Linear Model function in Minitab™ 16.

Mean values are quoted \pm one standard deviation, error bars in graphs. Slope confidence intervals are quoted $\pm t(5\%, \text{degrees of freedom}) \times \text{standard error}$. All statistical analysis was carried out using Minitab™ 16, and the scatterplots were plotted using Microsoft® Excel 2010, errors bars represent the result \pm one standard deviation.

2.5 Results

2.5.1 Excipient Water Content

Following Karl Fischer, the water content of the three excipients was determined as:

- HP- β -CD had a water content of 6.3%, so HP- β -CD weights were adjusted by 0.937 to account for the water present.
- P407 had a water content of 0.1714%, the weight of P407 was not adjusted due to the small percentage of water within the solid.
- P188 had a water content of -0.1429, as with P407, P188 weights were not adjusted.

2.5.2 Potentiometric Determination of pK_a

It was necessary to examine if the presence of HP- β -CD or poloxamer in the solution altered the pK_a of the drugs. This information is required as concentration/intrinsic solubility results calculated from Equations 2.10 and 2.11 are affected by the pK_a of the compound. The pK_a at each molar ratio of drug:HP- β -CD and poloxamer concentration was determined for model entry during the assay design stage for CheqSol.

Hydroxypropyl- β -cyclodextrin

The cyclodextrin only affected the pK_a of ibuprofen (Figure 2.5). The pK_a for ibuprofen appears to increase as the molar ratio to cyclodextrin increases (p -value = 0.013) with a R^2 value = 74.1%. The pK_a increases by 0.110 ± 0.0748 for every millimolar increase in HP- β -CD concentration. The regression equation was determined to be:

- $pK_a = 4.36 + 0.110 \times \text{HP-}\beta\text{-CD Concentration (mM)}$.

The standard deviation for the pK_a constant 4.36 is 0.0805 and the standard deviation for the slope 0.0110 is 0.0291. There is no significant variation in the pK_a for propranolol, gliclazide or atenolol (p -value > 0.05).

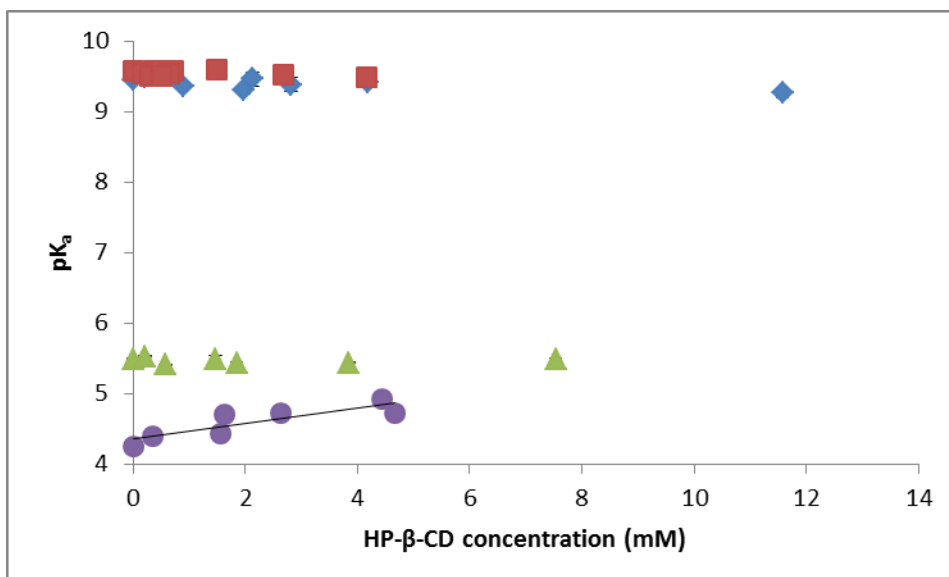


Figure 2.5. Scatterplot and regression line for the effect that HP-β-CD has on the pK_a of the four drugs. For propranolol (◆), atenolol (■) and gliclazide (▲), the points represent the mean pK_a determined from three titrations. The data points plotted for ibuprofen (●) are extrapolated pK_a values from three titrations. HP-β-CD concentration is the concentration in the vial before titrant addition. Error bars represent standard deviation and where they are not visible their size does not exceed that of the symbol used.

Poloxamer 407

Poloxamer 407 affected the pK_a of all four drugs examined up to 5% ^w/_v P407. For the bases propranolol and atenolol, the pK_a decreased with increasing poloxamer concentration. The opposite effect was observed for the acids gliclazide and ibuprofen, with a positive slope equating to increasing pK_as (Figure 2.6a). The regression equations for the drugs are as follows:

- Propranolol pK_a = 9.40 - 0.131 x P407 concentration (%^w/_v).

- Atenolol $pK_a = 9.56 - 0.0390 \times \text{P407 concentration (\%W/V)}$.
- Gliclazide $pK_a = 5.45 + 0.111 \times \text{P407 concentration (\%W/V)}$.
- Ibuprofen $pK_a = 4.39 + 0.103 \times \text{P407 concentration (\%W/V)}$.

With R^2 values greater than 85%.

Poloxamer 188

Like poloxamer 407, poloxamer 188 affected the pK_a of propranolol, atenolol, gliclazide and ibuprofen. For the bases propranolol and atenolol, the pK_a also decreased with increasing poloxamer concentration. As for P407, the opposite effect was observed for the acids gliclazide and ibuprofen, with a positive slope equating to increasing pK_a s (Figure 2.6b). The regression equations for the drugs are as follows:

- Propranolol $pK_a = 9.44 - 0.0435 \times \text{P188 concentration (\%W/V)}$.
- Atenolol $pK_a = 9.57 - 0.0256 \times \text{P188 concentration (\%W/V)}$.
- Gliclazide $pK_a = 5.45 + 0.0725 \times \text{P188 concentration (\%W/V)}$.
- Ibuprofen $pK_a = 4.40 + 0.0417 \times \text{P188 concentration (\%W/V)}$.

With R^2 values greater than 80%.

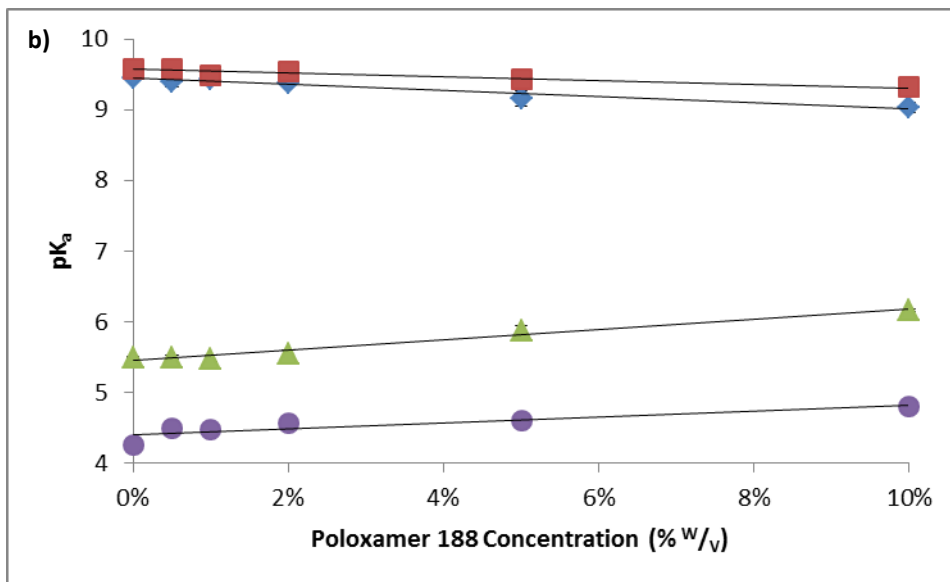
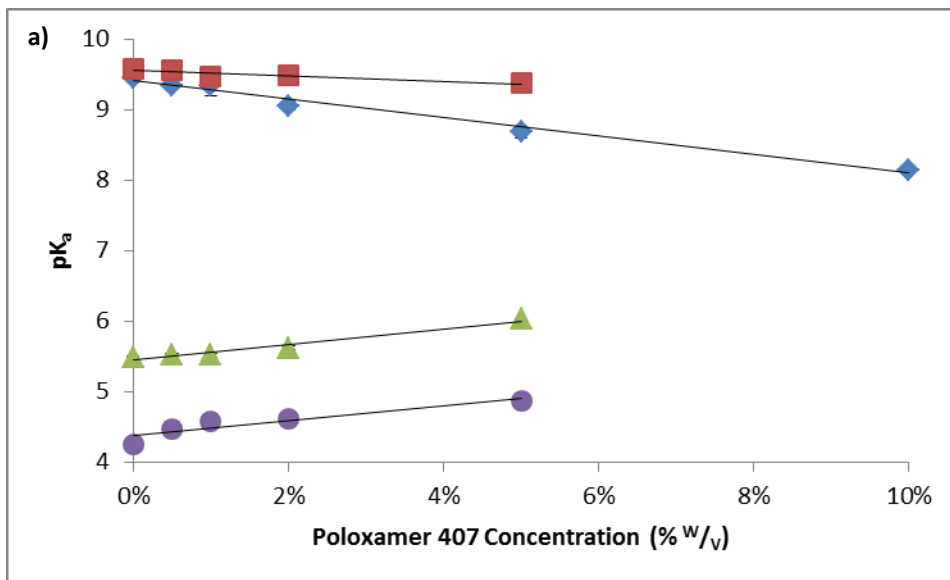


Figure 2.6. Scatterplot and regression line for the effect that a) poloxamer 407 and b) poloxamer 188 have on the pK_as of the four drugs. For propranolol (◆), atenolol (■) and glyclazide (▲), the points represent the mean pK_a determined from three titrations. The data points plotted for ibuprofen (●) are extrapolated pK_a values, from three titrations. Poloxamer concentration is the concentration in the vial before titrant addition. Error bars represent standard deviation and where they are not visible their size does not exceed that of the symbol used.

2.5.3 Potentiometric Determination of Solubility Using CheqSol

Following on from the pK_a determinations, solubility was investigated. The experiments were designed to determine if the presence of HP- β -CD or poloxamer in the assay improved the solubility of the drugs at varying concentrations and molar ratios.

Hydroxypropyl- β -Cyclodextrin

As can be seen for propranolol (Figure 2.7), increasing the concentration of HP- β -CD increases the solubility of propranolol. The regression equation of the intrinsic solubility results was found to be:

- Intrinsic Solubility (mM) = $0.344 + 0.0757 \times \text{HP-}\beta\text{-CD (mM)}$, with $R^2 = 99.4\%$.

The kinetic solubility results appear to follow a linear relationship up to molar ratio of 1:2 propranolol:HP- β -CD. At the highest molar ratio used, there was a decrease in kinetic solubility, and the linear relationship no longer holds.

The results for the effect of HP- β -CD on gliclazide solubility can be found in Figure 2.8. As with propranolol, the presence of the cyclodextrin increases the concentration of gliclazide in the system. The solubility of gliclazide in the presence of HP- β -CD was found to follow the regression equation:

- Intrinsic Solubility (mM) = $0.0730 + 0.0127 \times \text{HP-}\beta\text{-CD (mM)}$, with $R^2 = 98.1\%$.

The kinetic solubility results can be seen to decrease at the 1:0.1 molar ratio before increasing in a HP- β -CD dependent manner, with a regression equation of:

- Kinetic Solubility (mM) = $2.01 + 0.188 \times \text{HP-}\beta\text{-CD (mM)}$, with $R^2 = 97.9\%$.

Atenolol solubility in the presence of lower molar ratios of HP- β -CD, increased with a regression equation of (Figure 2.9):

- Intrinsic Solubility (mM) = $54.4 + 0.392 \times \text{HP-}\beta\text{-CD (mM)}$, with $R^2 = 91.6\%$.

The kinetic solubility of atenolol does not follow a linear relationship, with increases in HP- β -CD not corresponding to an increase in atenolol present.

At the cyclodextrin concentrations used the intrinsic solubility of atenolol, gliclazide and propranolol followed A_L type curves i.e. the increase was linear (see chapter 1.8). The curve of ibuprofen solubility is an A_P type curve (Figure 2.10), with a large increase in solubility associated with the 1:1 molar ratio (drug:HP- β -CD). The regression results were determined as:

- Intrinsic Solubility (mM) = $0.0247 + 0.146 \times \text{HP-}\beta\text{-CD (mM)}$, with $R^2 = 95.9\%$ up to molar ratios of 1:0.75.

The kinetic solubility for ibuprofen also follows an A_P type curve. When regression analysis was carried out on the data up to an including HP- β -CD molar ratios of 0.75, the regression equation was found to be:

- Ibuprofen Solubility (mM) = $0.276 + 0.393 \times \text{HP-}\beta\text{-CD (mM)}$, with $R^2 = 94.4\%$ up to molar ratios of 1:0.75.

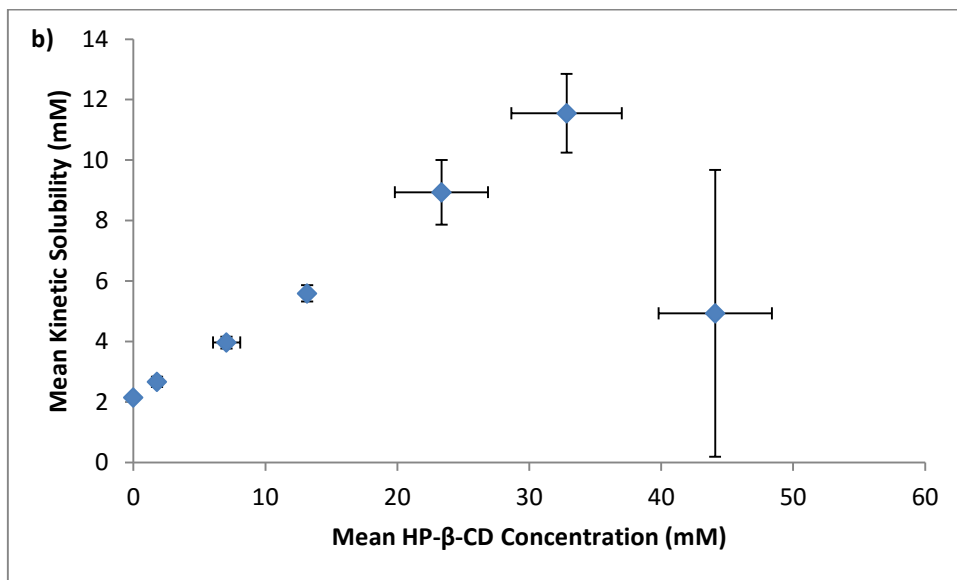
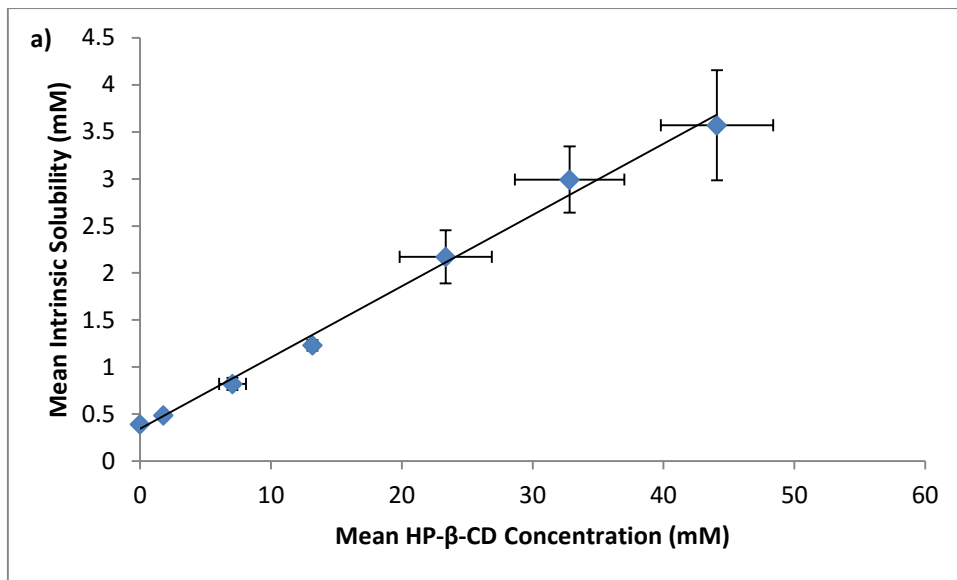


Figure 2.7. Scatterplots and regression lines of solubility of propranolol in the presence of HP-β-CD for a) intrinsic solubility, and b) kinetic solubility. The results are grouped according to the molar ratio of HP-β-CD used. The molar ratios used are 1:0, 1:0.1, 1:0.5, 1:1, 1:1.5, 1:2 and 1:2.5. $n \geq 3$. Error bars represent standard deviation and where they are not visible their size does not exceed that of the symbol used.

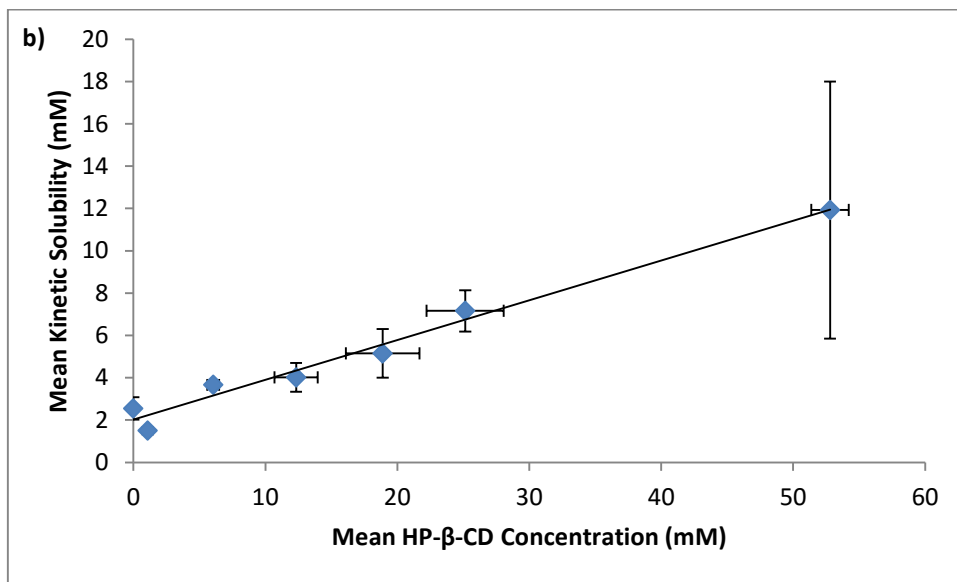
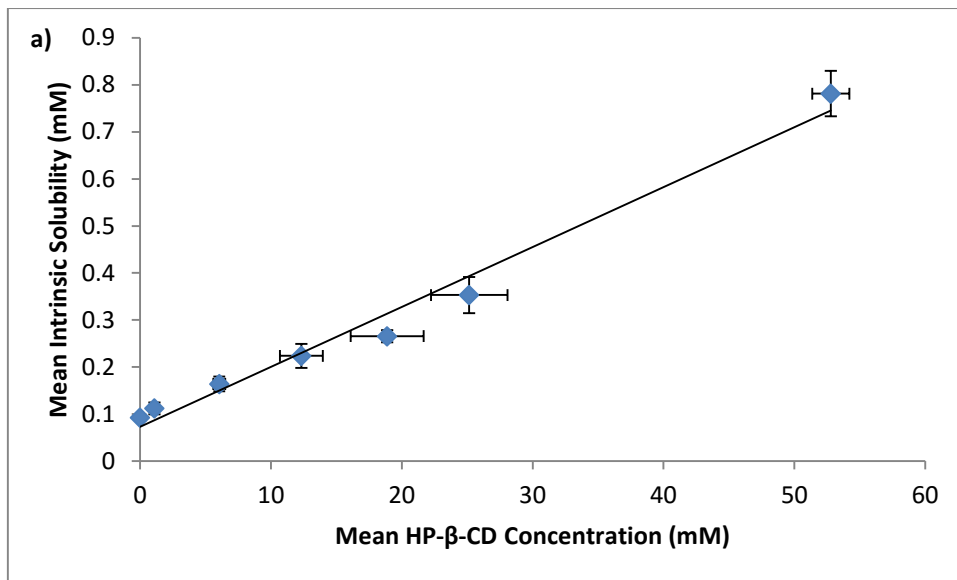


Figure 2.8. Scatterplots and regression lines of solubility of gliclazide in the presence of HP-β-CD for a) intrinsic solubility, and b) kinetic solubility. The results are grouped according to the molar ratio of HP-β-CD used. The molar ratios used are 1:0, 1:0.1, 1:0.5, 1:1, 1:1.5, 1:2 and 1:5. $n \geq 3$. Error bars represent standard deviation and where they are not visible their size does not exceed that of the symbol used.

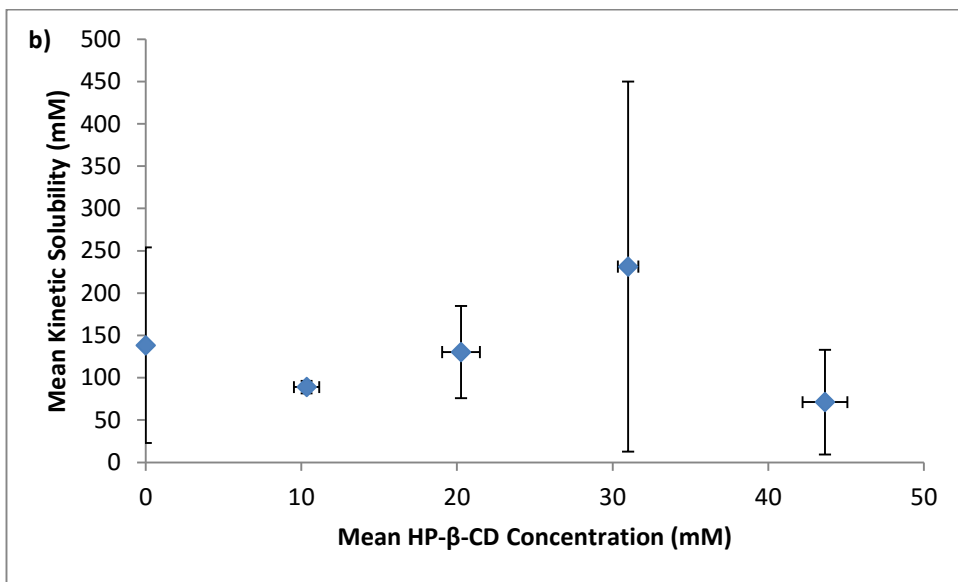
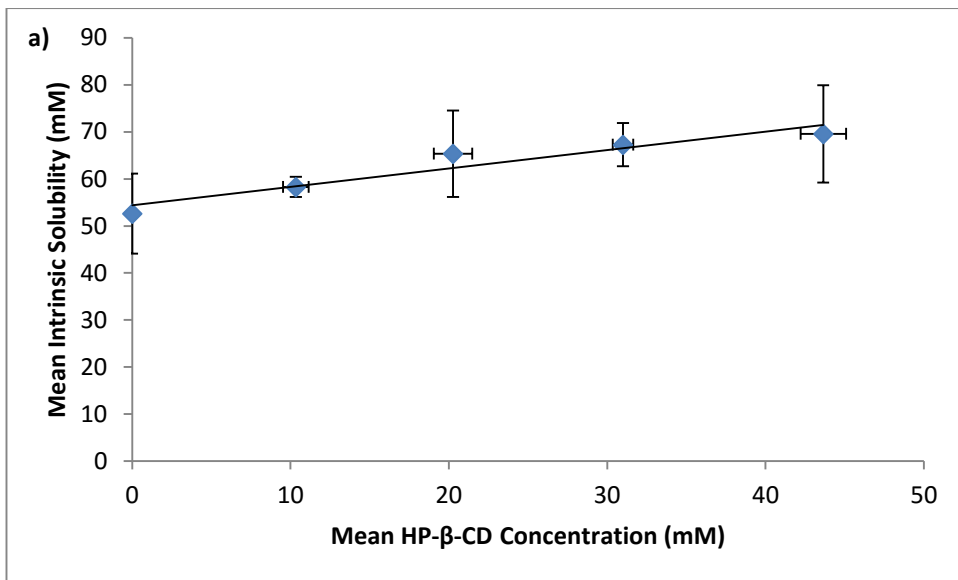


Figure 2.9. Scatterplots and regression lines of solubility of atenolol in the presence of HP-β-CD for a) intrinsic solubility, and b) kinetic solubility. The results are grouped according to the molar ratio of HP-β-CD used. The molar ratios used are 1:0, 1:0.05, 1:0.1, 1:0.15 and 1:0.2. $n \geq 3$. Error bars represent standard deviation and where they are not visible their size does not exceed that of the symbol used.

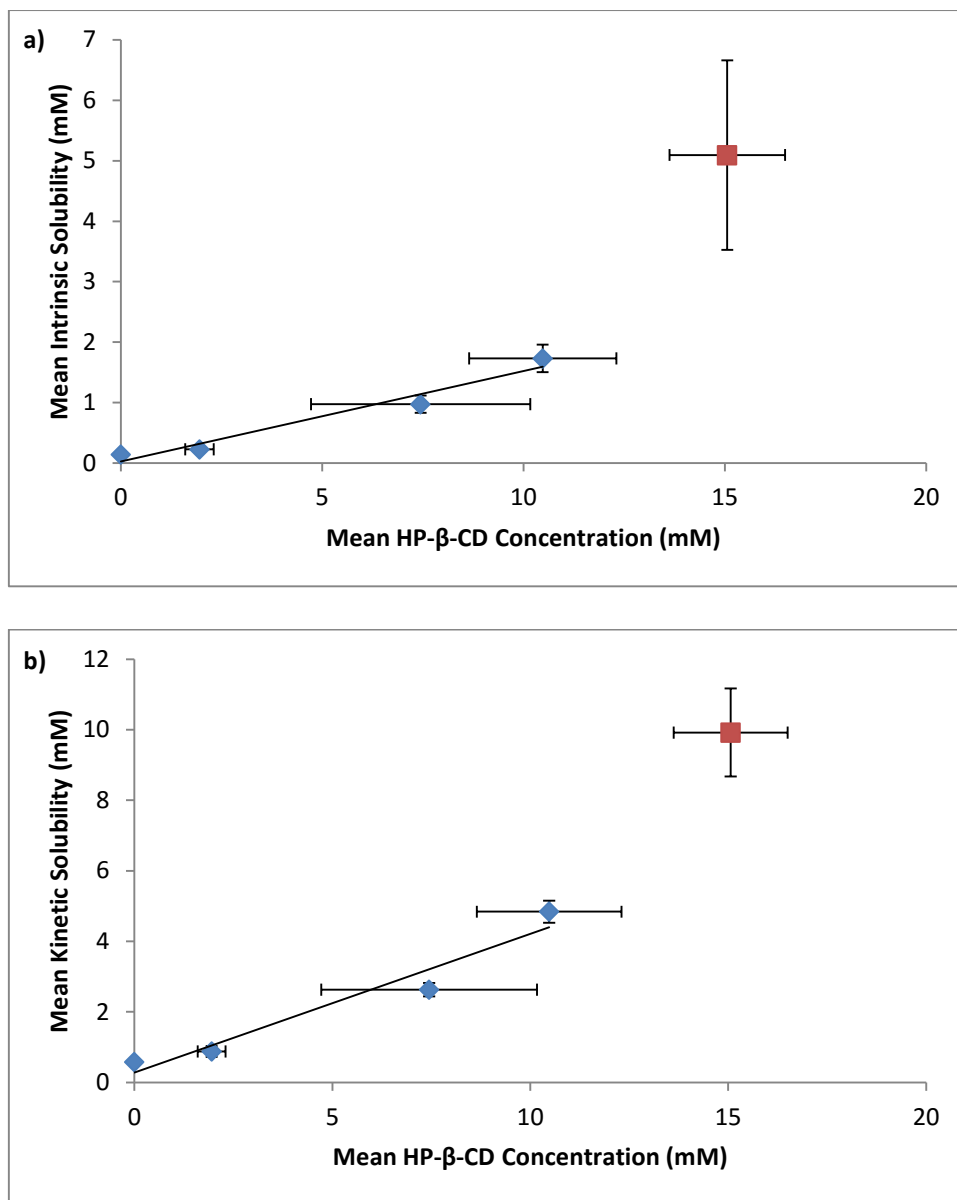


Figure 2.10. Scatterplots and regression lines of solubility of ibuprofen in the presence of HP-β-CD for a) intrinsic solubility, and b) kinetic solubility. The results are grouped according to the molar ratio of HP-β-CD used. The molar ratios used are 1:0, 1:0.1, 1:0.5, 1:0.75 and 1:1. $n \geq 3$. Error bars represent standard deviation and where they are not visible their size does not exceed that of the symbol used. The data points for ibuprofen also contain the points not included in the linear regression analysis (red).

Poloxamer 407

The intrinsic solubility of the four compounds investigated increased in the presence of P407 (Figure 2.11a, Figure 2.12a, Figure 2.13a and Figure 2.14a). The solubility improvement is concentration dependent with the highest P407 concentrations increasing compound solubility the greatest. The positive relationship between the compound solubility and poloxamer concentration holds for all points with the exception of atenolol in the presence of 2% w/v P407. Positive linear relationships for propranolol, gliclazide and ibuprofen were observed (Table 2.6). The relationship for atenolol was not found to be linear following regression analysis. However, following ANOVA, the presence of 1% w/v and 5% w/v P407 resulted in increased solubility compared to atenolol alone.

Kinetic solubility for all four drugs also increased in the presence of P407 (Figure 2.11b, Figure 2.12b, Figure 2.13b and Figure 2.14b). The relationship between P407 concentration and propranolol kinetic solubility is not linear, at the 5% w/v level the kinetic solubility was recorded as 0 mM. The relationship for the other three drugs was found to be linear with a minimum R^2 value of 86.5%. The slope of the kinetic solubility regression lines was larger for all four drugs than the intrinsic solubility lines, and the kinetic solubility (y-intercept) from regression lines was greater than the intrinsic solubility (y-intercept) for propranolol, gliclazide and atenolol. The kinetic solubility value of ibuprofen was negative following regression analysis (Table 2.7).

Table 2.6. Regression analysis of intrinsic solubility results for the four drugs in the presence of Poloxamer 407

Drug	Regression Equation	R ² Value
Propranolol	Solubility (mM) = 0.403 + 0.663 x P407 (% w/v)	99.7%
Gliclazide	Solubility (mM) = 0.0859 + 0.0467 x P407 (% w/v)	96.3%
Atenolol	Solubility (mM) = 60.1 + 3.26 x P407 (% w/v)	62.1%
Ibuprofen	Solubility (mM) = 0.892 + 3.93 x P407 (% w/v)	99.5%

Table 2.7. Regression analysis of kinetic solubility results for the four drugs in the presence of Poloxamer 407

Drug	Regression Equation	R ² Value
Propranolol	Solubility (mM) = 1.12 + 2.33 x P407 (% w/v)	65.5%
Gliclazide	Solubility (mM) = 2.10 + 0.488 x P407 (% w/v)	86.5%
Atenolol	Solubility (mM) = 139 + 13.5 x P407 (% w/v)	97.1%
Ibuprofen	Solubility (mM) = -24.5 + 50.3 x P407 (% w/v)	99.5%

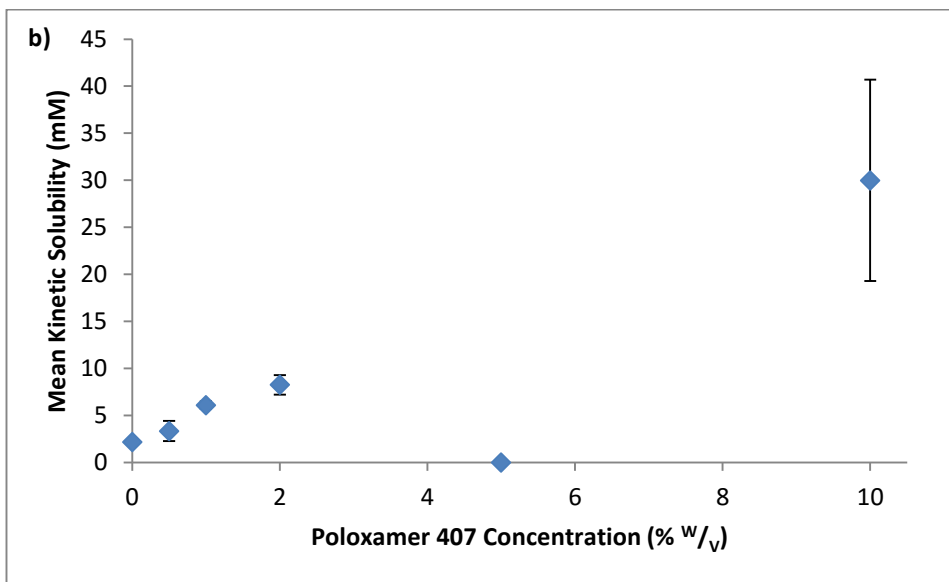
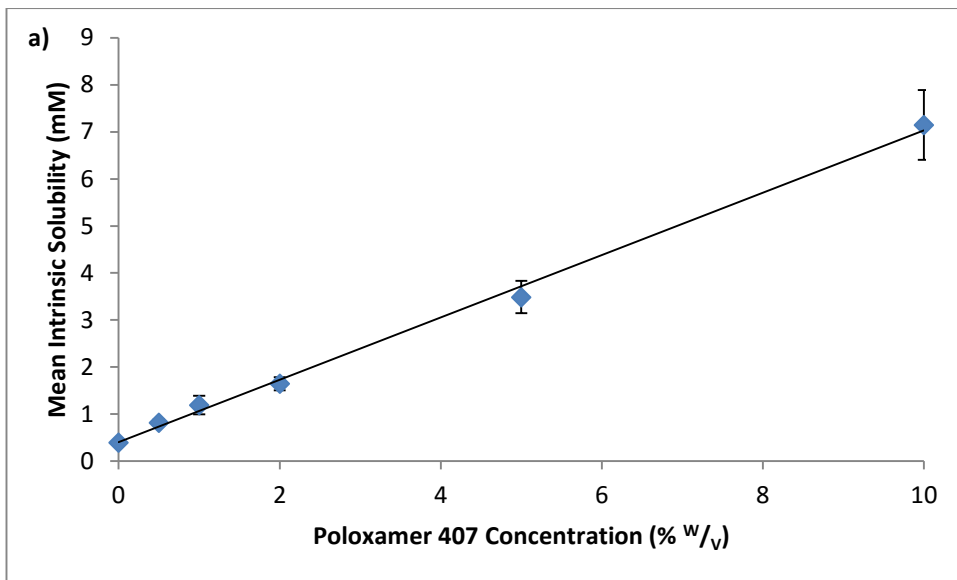


Figure 2.11. Scatterplots and regression lines of solubility of propranolol in the presence of P407 for a) intrinsic solubility, and b) kinetic solubility. $n \geq 3$. Error bars represent standard deviation and where they are not visible their size does not exceed that of the symbol used.

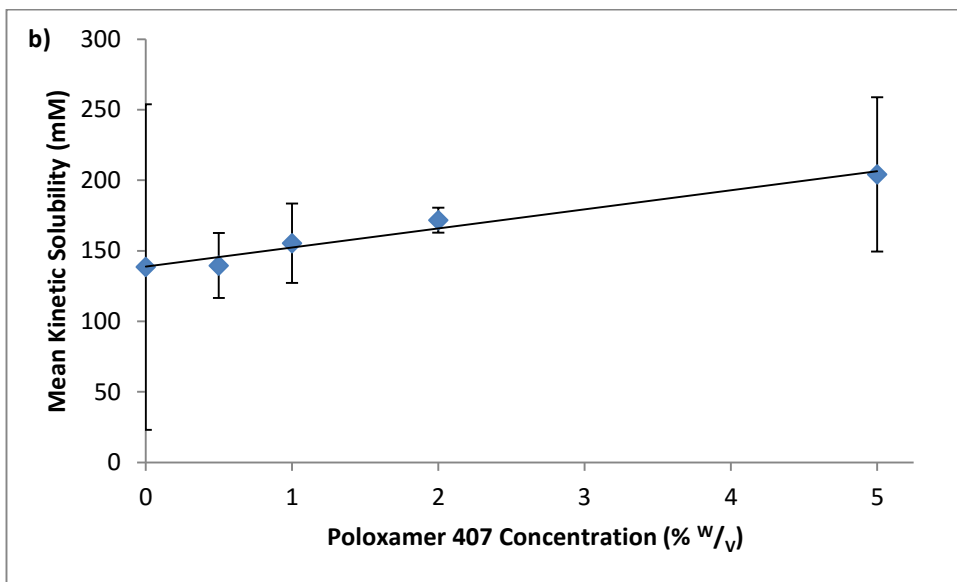
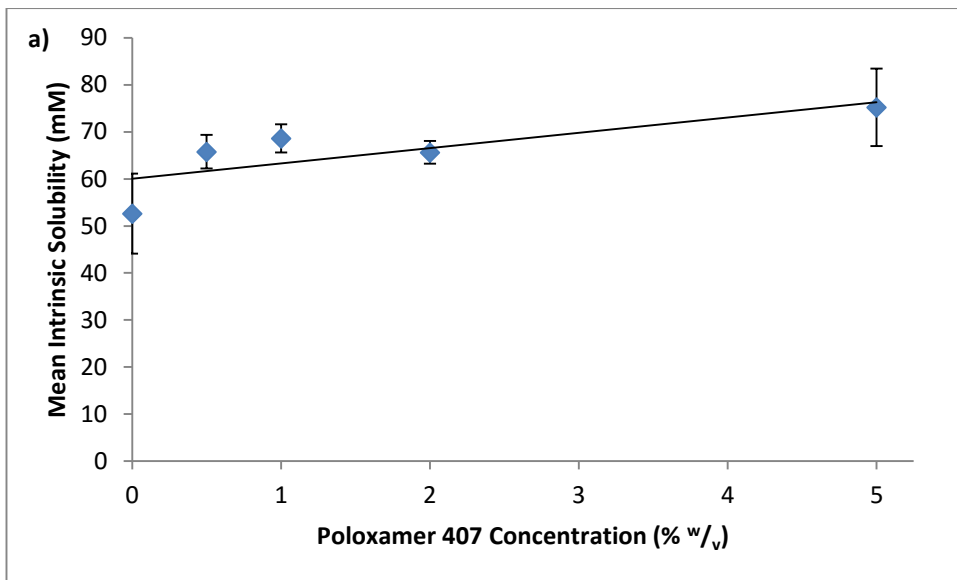


Figure 2.12. Scatterplots and regression lines of solubility of atenolol in the presence of P407 for a) intrinsic solubility, and b) kinetic solubility. $n \geq 3$. Error bars represent standard deviation and where they are not visible their size does not exceed that of the symbol used.

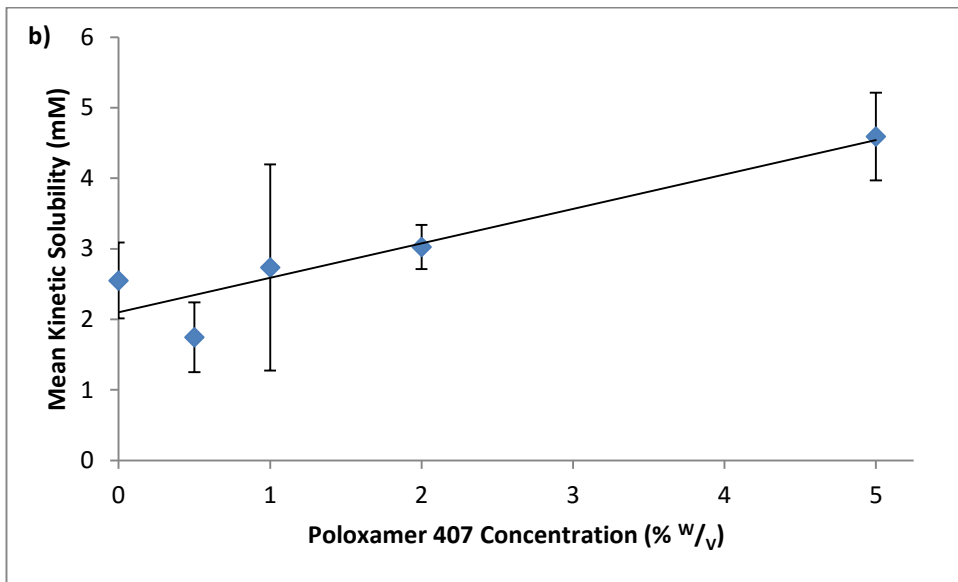
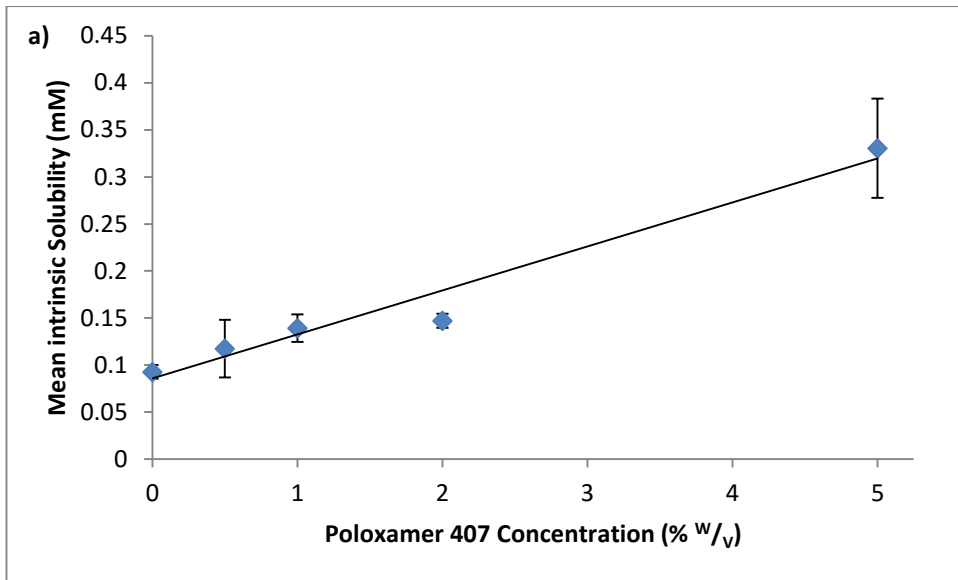


Figure 2.13. Scatterplots and regression lines of solubility of gliclazide in the presence of P407 for a) intrinsic solubility, and b) kinetic solubility. $n \geq 3$. Error bars represent standard deviation and where they are not visible their size does not exceed that of the symbol used.

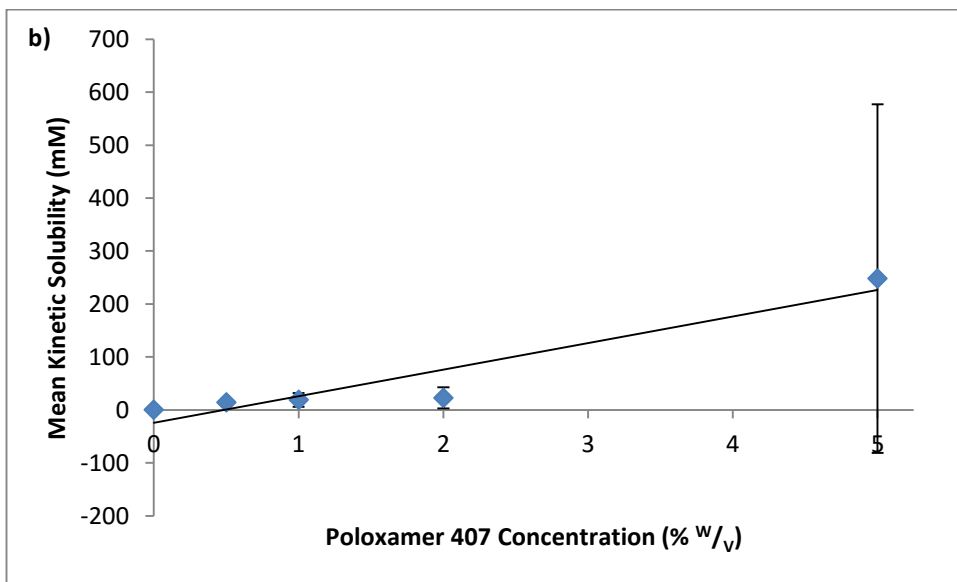
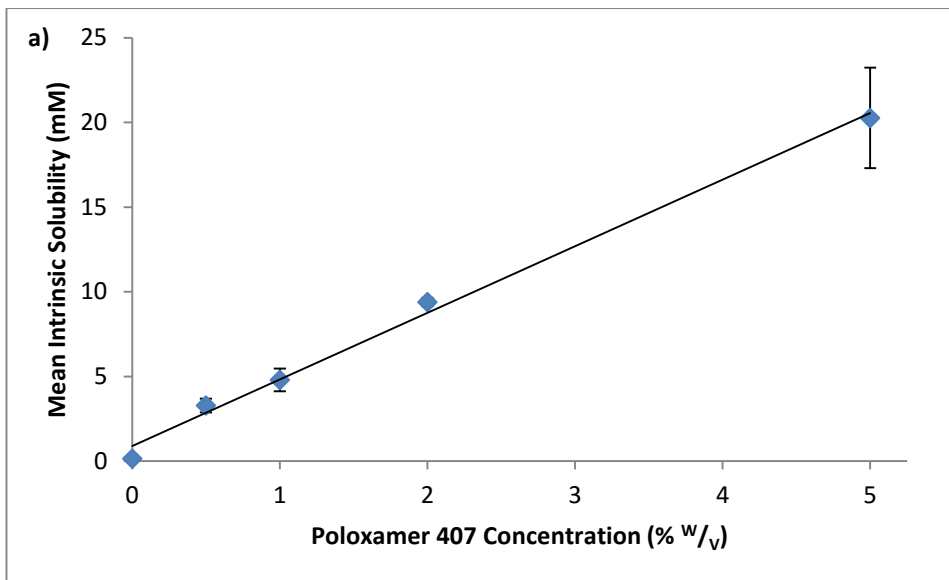


Figure 2.14. Scatterplots and regression lines of solubility of ibuprofen in the presence of P407 for a) intrinsic solubility, and b) kinetic solubility. $n \geq 3$. Error bars represent standard deviation and where they are not visible their size does not exceed that of the symbol used.

Poloxamer 188

Poloxamer 188 increased the solubility of all four drugs investigated (Figure 2.15a, Figure 2.16a, Figure 2.17a and Figure 2.18a). There is a positive relationship between the compound solubility and the concentration of P188 in the system, with the exception of gliclazide in the presence of 2% w/v P188 and propranolol in the presence of 0.5% w/v P188. Regression analysis gave equations with a minimum R^2 value of 92.3% (Table 2.8).

Looking at the kinetic solubility of the drugs, the presence of P188 in increasing concentrations showed a linear relationship for ibuprofen, atenolol and propranolol (Figure 2.15b, Figure 2.16b and Figure 2.18b). Gliclazide kinetic solubility did not show a linear relationship to P188 concentration (Figure 2.17b). As observed with P407 the slope of the regression lines was greater for kinetic solubility results than intrinsic solubility results (Table 2.9). As expected, the kinetic solubilities taken from the regression lines (y-intercepts) are greater for all four drugs than the intrinsic solubilities determined from the regression lines (y-intercepts).

Table 2.8. Regression analysis results for intrinsic solubility of the four drugs in the presence of Poloxamer 188.

Drug	Regression Equation	R ² Value
Propranolol	Solubility (mM) = 0.289 + 0.166 x P188 (% w/v)	98.6%
Gliclazide	Solubility (mM) = 0.115 + 0.0183 x P188 (% w/v)	92.4%
Atenolol	Solubility (mM) = 56.0 + 2.04 x P188 (% w/v)	92.3%
Ibuprofen	Solubility (mM) = 0.727 + 0.658 x P188 (% w/v)	97.8%

Table 2.9. Regression analysis results for kinetic solubility of the four drugs in the presence of Poloxamer 188.

Drug	Regression Equation	R ² Value
Propranolol	Solubility (mM) = 1.45 + 1.15 x P188 (% w/v)	98.5%
Gliclazide	Solubility (mM) = 2.44 + 0.0818 x P188 (% w/v)	52.4%
Atenolol	Solubility (mM) = 111 + 7.36 x P188 (% w/v)	77.8%
Ibuprofen	Solubility (mM) = 2.79 + 1.65 x P188 (% w/v)	95.1%

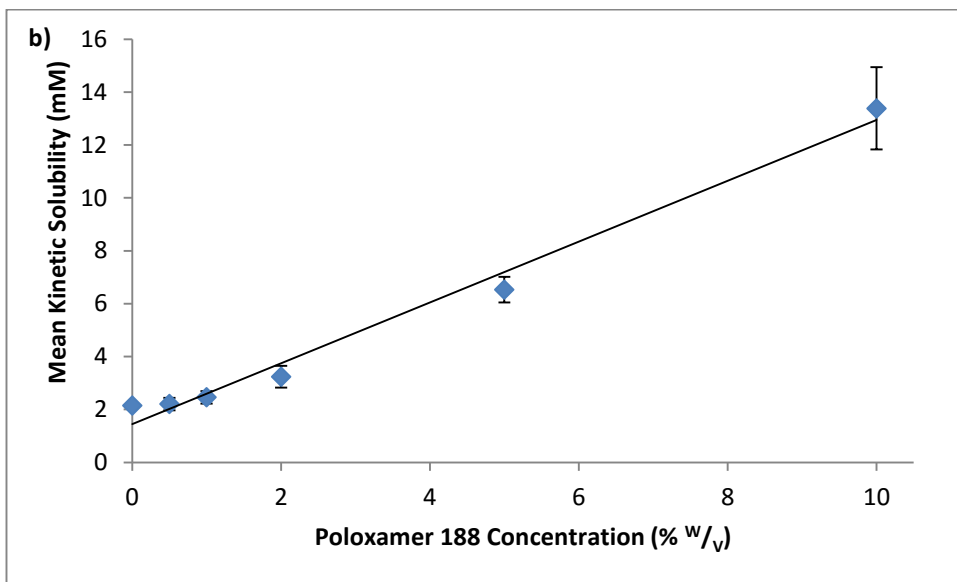
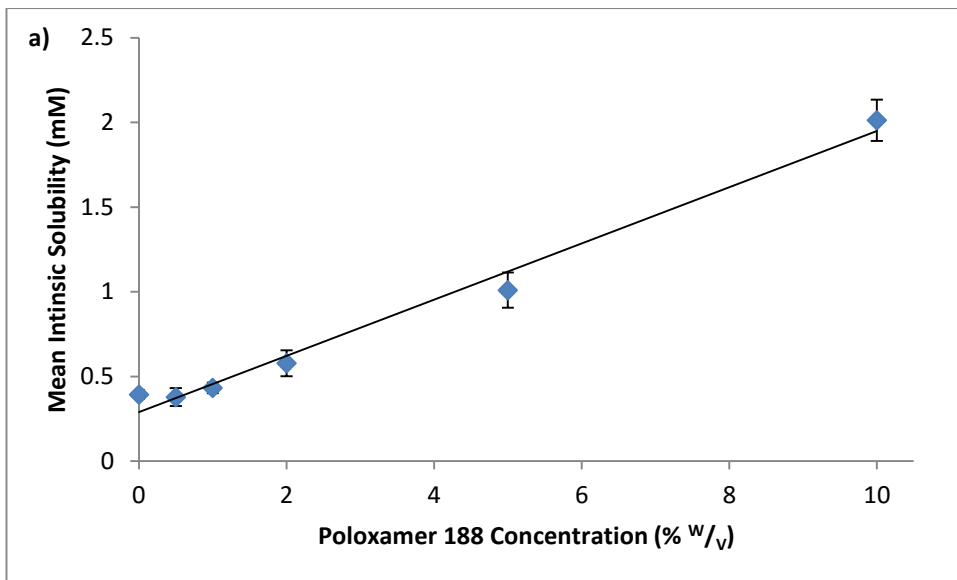


Figure 2.15. Scatterplots and regression lines of solubility of propranolol in the presence of P188 for a) intrinsic solubility, and b) kinetic solubility. $n \geq 3$. Error bars represent standard deviation and where they are not visible their size does not exceed that of the symbol used.

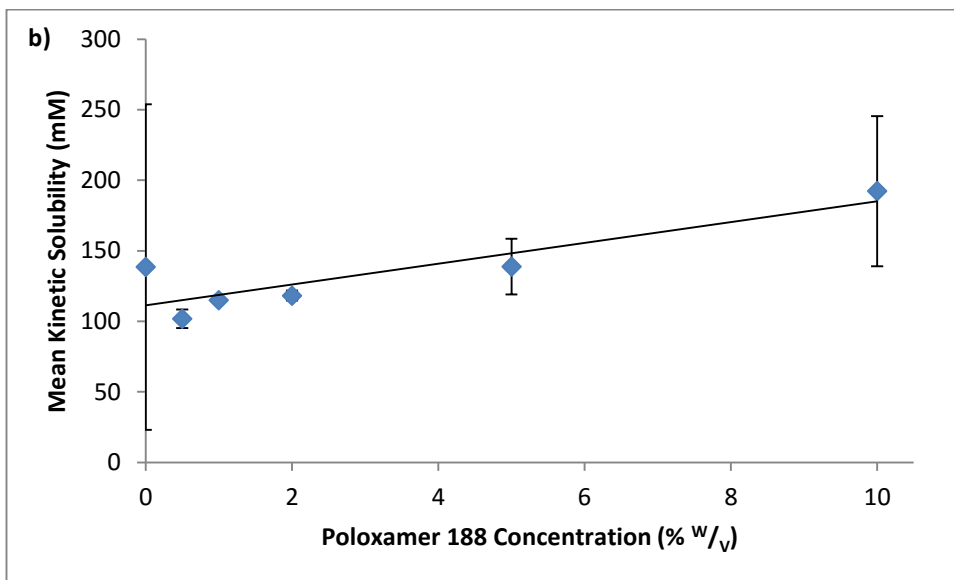
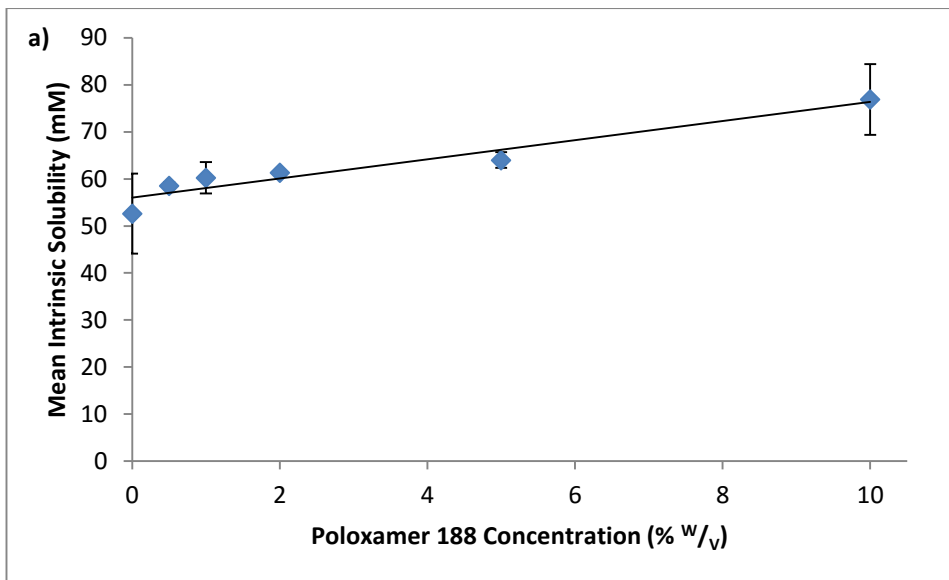


Figure 2.16. Scatterplots and regression lines of solubility of atenolol in the presence of P188 for a) intrinsic solubility, and b) kinetic solubility. $n \geq 3$. Error bars represent standard deviation and where they are not visible their size does not exceed that of the symbol used.

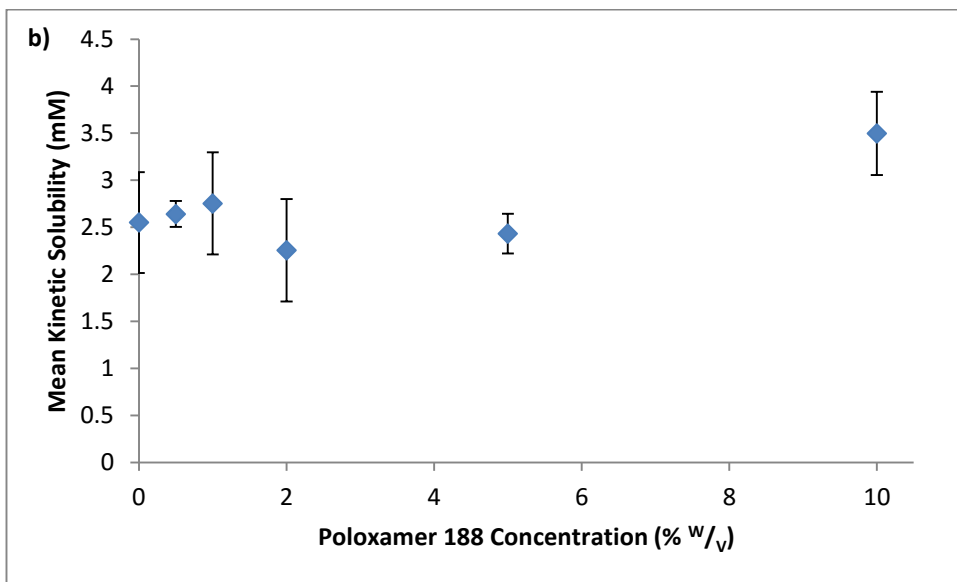
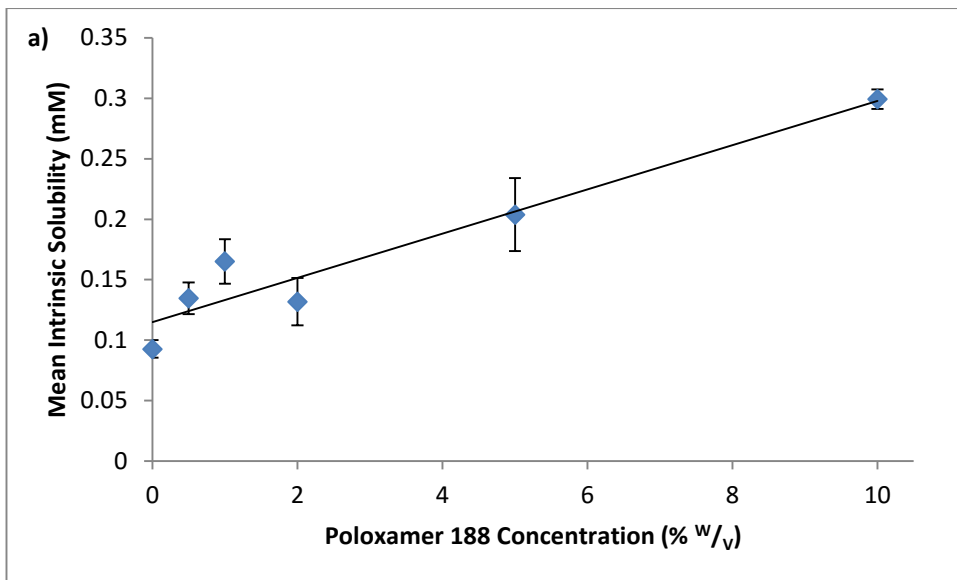


Figure 2.17. Scatterplots and regression lines of solubility of gliclazide in the presence of P188 for a) intrinsic solubility, and b) kinetic solubility. $n \geq 3$. Error bars represent standard deviation and where they are not visible their size does not exceed that of the symbol used.

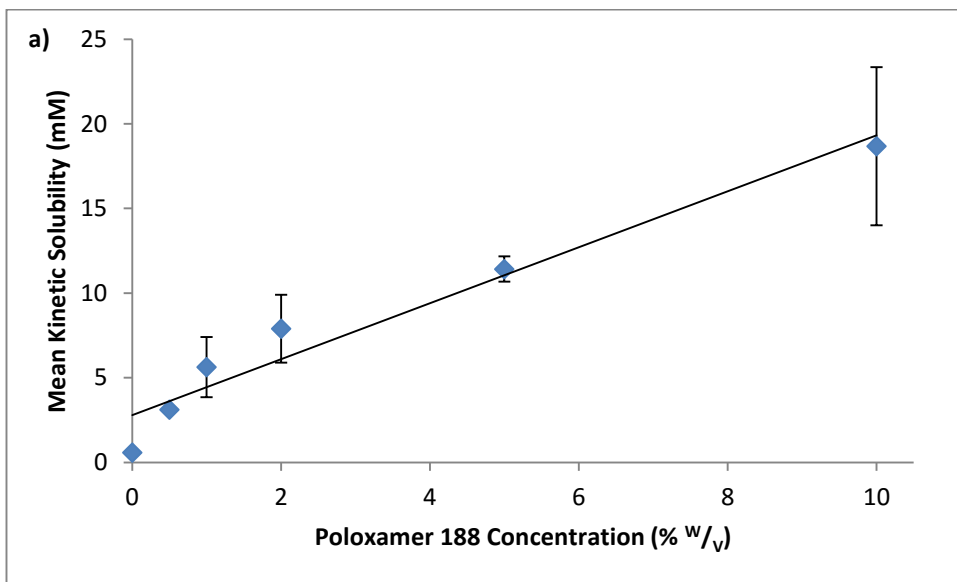
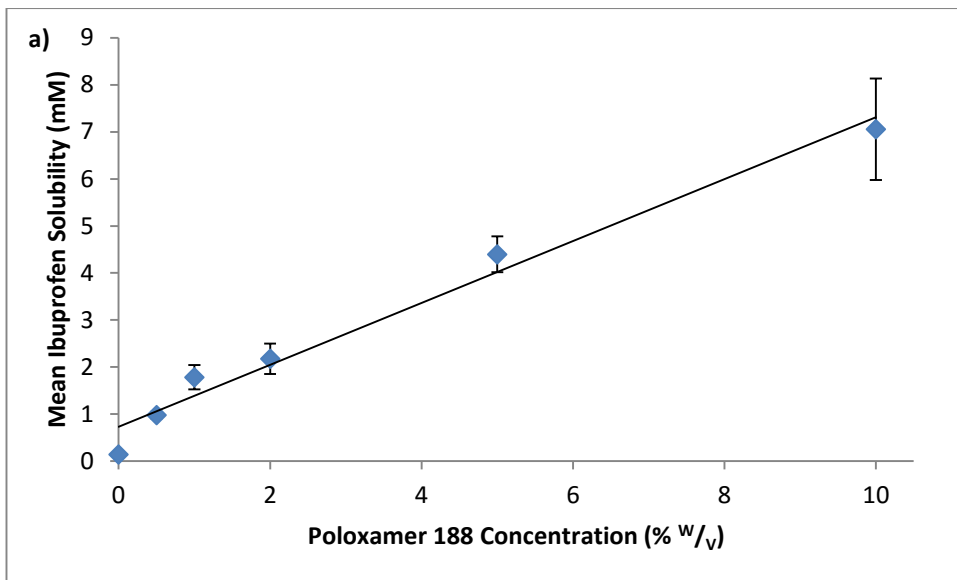


Figure 2.18. Scatterplots and regression lines of solubility of ibuprofen in the presence of P188 for a) intrinsic solubility, and b) kinetic solubility. $n \geq 3$. Error bars represent standard deviation and where they are not visible their size does not exceed that of the symbol used.

2.5.4 Shake-Flask Solubility Determination of Propranolol

CheqSol has previously been shown to produce comparable solubility results to shake-flask. However, due to the lack of data on phase-solubility studies using this technique a traditional shake-flask experiment with propranolol HCl and HP- β -CD was carried out. The calibration curves produced at 254 nm and 280 nm UV detection wavelengths can be found in Figure 2.19. The relationship between AUC (mAU/min) and propranolol concentration (mM) was found to be:

- $\text{AUC (mAU/min)} = 92760 + 6664533 \times \text{Propranolol Concentration (mM)}$ at 254 nm ($R^2 = 100\%$)
- $\text{AUC (mAU/min)} = 1557833 + 24294410 \times \text{Propranolol Concentration (mM)}$ at 280 nm ($R^2 = 99.4\%$)

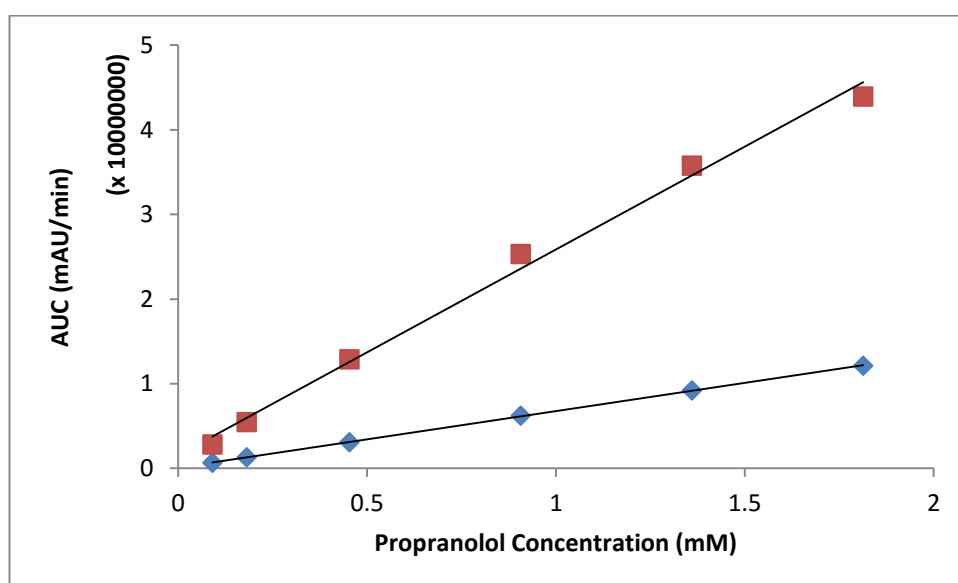


Figure 2.19. Calibration curves at 254 nm (\blacklozenge) and 280 nm (\blacksquare) wavelengths. $n=3$ for all data points. Error bars represent standard deviation; the error bars are smaller than the symbols.

In pH 12 buffer, HP- β -CD was shown to increase the solubility of propranolol in a linear concentration dependent manner (Figure 2.20). The concentrations were calculated using the regression equations obtained from the calibration curves and then multiplying by the dilution factor to get the final concentration in the vial. The concentrations calculated at 254 nm were not the same as 280 nm. The variation at 280 nm wavelength was greater with the highest CV equal to 12.0 %, whereas for 254 nm wavelength the highest CV was calculated as 4.79 %. At 254 nm, the regression equation was determined to be:

- Propranolol Solubility (mM) = $0.356 + 0.0843 \times \text{HP-}\beta\text{-CD (mM)}$, with $R^2 = 99.2\%$.

At 280 nm, the regression equation has a lower constant and a higher slope:

- Propranolol Solubility (mM) = $0.279 + 0.0900 \times \text{HP-}\beta\text{-CD (mM)}$, with $R^2 = 99.6\%$.

The results described above are for the unionised form of propranolol. Assays were also run at pH 5.5 to determine if there was an effect on ionised propranolol concentration in the presence of HP- β -CD. The presence of increasing concentrations of HP- β -CD decreased the concentration of ionised propranolol in the system (Figure 2.21). The regression equations were:

- Ionised Propranolol Solubility (mM) = $1210 - 9.14 \times \text{HP-}\beta\text{-CD (mM)}$, at 254 nm ($R^2 = 69.6\%$).
- Ionised Propranolol Solubility (mM) = $1250 - 8.39 \times \text{HP-}\beta\text{-CD (mM)}$, at 280 nm ($R^2 = 72.6\%$).

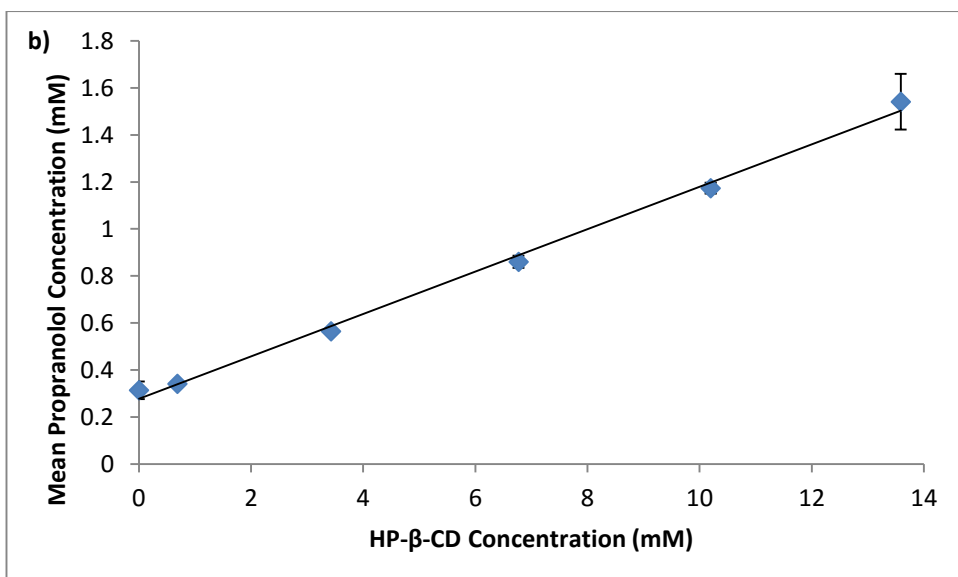
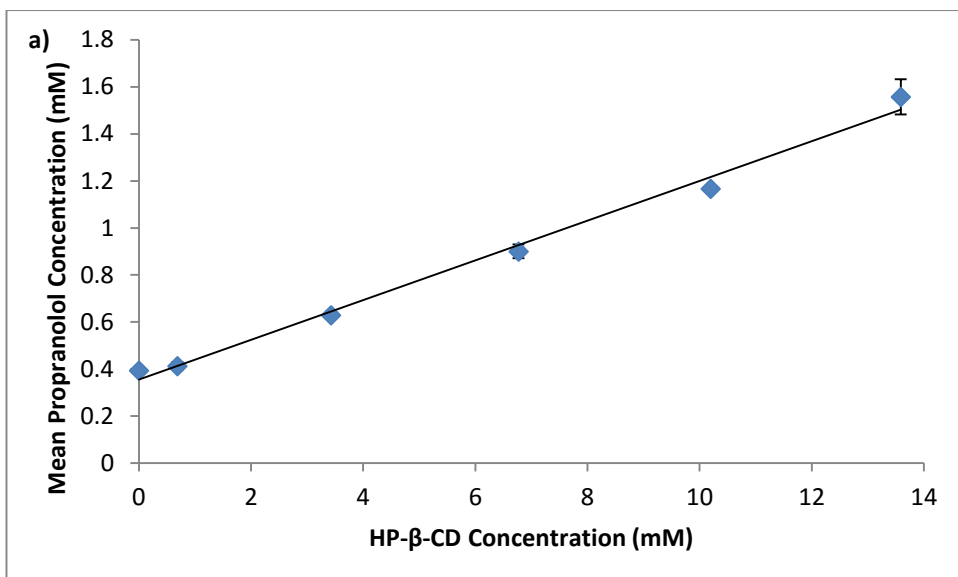


Figure 2.20. Scatterplot of unionised propranolol concentration versus HP-β-CD concentration at pH 12, measured from AUC at a) 254 nm and b) 280 nm. The mean concentration (mM) was calculated from duplicate runs, each run in triplicate. Error bars represent standard deviation and where they are not visible their size does not exceed that of the symbol used.

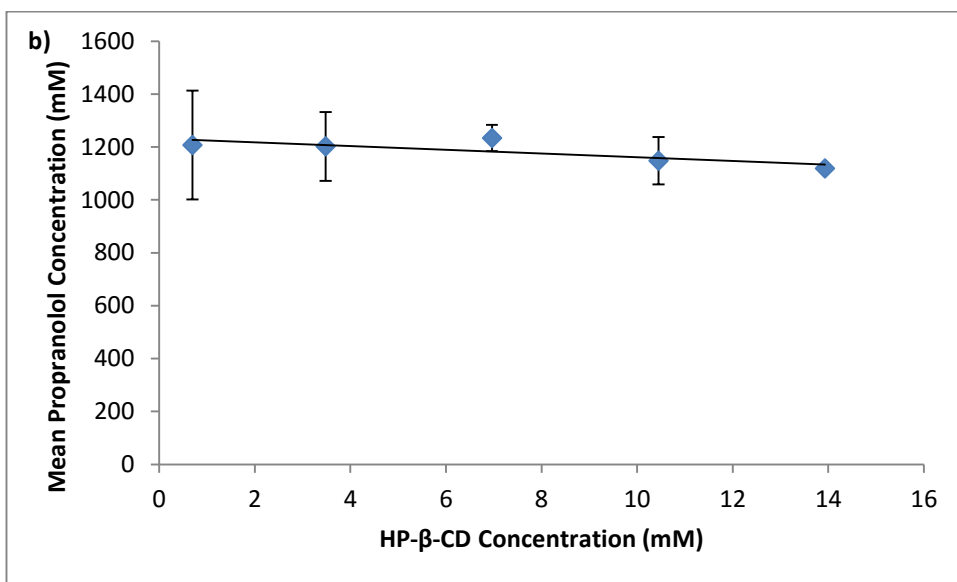
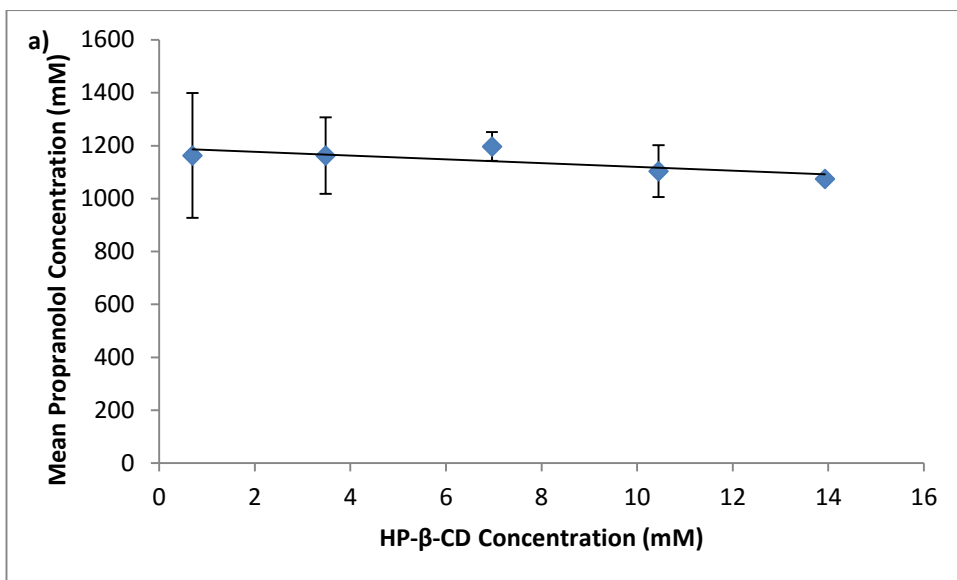


Figure 2.21. Scatterplot of ionised propranolol concentration versus HP-β-CD concentration at pH 5.5, measured from AUC at a) 254 nm and b) 280 nm. The mean concentration (mM) was calculated from duplicate runs, each run in triplicate. Error bars represent standard deviation and where they are not visible their size does not exceed that of the symbol used.

2.5.5 Cholic Acid as an Excipient

In order to investigate whether ionisable excipients can be used with the CheqSol method, the effects of cholic acid on ibuprofen and propranolol HCl were investigated. The pK_a of cholic acid was determined to be 4.73 using p_sK_a method described for ibuprofen. Precipitation was observed during pK_a assays without methanol present in the system. Solubility studies on cholic acid were not able to provide reliable results. Cholic acid failed to chase during assays but curve-fitting method gave results which had high variation, and in two out of the three assays, gave a higher concentration than the concentration added to the system. The solubility of cholic acid using the curve-fitting results from assays can be found in Table 2.10.

Table 2.10. Solubility results for cholic acid in a starting volume of 1.5 mL ISA water.

Assay Number	Solubility (mg/mL)	Total in Vial (mg)
1	1.15	3.08
2	3.30	1.18
3	8.93	1.29

With cholic acid, the pK_a of ibuprofen was found to be 5.19, with an R^2 value of 63.3%.

The solubility of ibuprofen was found to be 36.6 $\mu\text{g/mL}$ or 0.177 mM. The pK_a of

propranolol could not be determined as there was precipitation in the system during the pH-metric assay. The solubility of propranolol was 182 µg/mL or 0.702 mM.

2.6 Discussion

2.6.1 pK_a Results

HP-β-CD

From the pK_a results it can be seen that the presence of HP-β-CD affects the pK_a of ibuprofen. The pK_a results for all four drugs in both the absence and presence of HP-β-CD were within the literature range for the drugs alone (27, 119-121). However, the cyclodextrin may be affecting the pK_a of ibuprofen since regression analysis shows a statistically significant linear relationship between HP-β-CD concentration and pK_a. In the presence of a large excess of β-CD (35 x molar concentration), it has been shown that β-CD increased the pK_a of ibuprofen by 0.54 units (122), agreeing with the results observed here. The R² values reveal that another factor(s), in addition to the concentration of cyclodextrin, may be affecting the pK_a of ibuprofen. This is expected as variations in pK_a results are common, as can be seen by the literature ranges. One factor, which may partly explain the lower R² value, is the molar ratio of ibuprofen to HP-β-CD. After examining the pK_a changes versus the molar ratio, a positive relationship was observed giving a regression equation of:

- $pK_a = 4.35 + 0.301 \times \text{Molar Ratio}$ (R² value 86.4%).

Taking both variables into consideration a multiple regression relationship of:

- $pK_a = 4.36 - 0.0830 \times \text{HP-}\beta\text{-CD Concentration (mM)} + 0.498 \times \text{Molar Ratio}$ (88.9%).

The pK_a for gliclazide (acid) in the presence of high concentrations of HP- β -CD does not appear to be affected, with variations in pK_a ranging from 5.53 to 5.63, in a non HP- β -CD concentration dependent manner. Previous findings have reported that β -CD does not affect the pK_a of gliclazide (121). HP- β -CD, at a concentration of 0.1 M, has been shown to have no effect on the pK_a of atenolol in the past (123). The results here are in agreement with the previous findings for atenolol. No previous data on the effect of cyclodextrins on the pK_a of propranolol could be found in the literature.

Shifts in pK_a attributed to cyclodextrins have been observed for other compounds. A reduction in pK_a was observed when the basic dyes acridine orange and neutral red were complexed with β -CD of 0.7 and 0.75 units at a concentration of 0.006 M and 0.01 M respectively (65, 124). Cyclodextrins have also been shown to affect the pK_a of acidic groups. Schmidt *et al.* demonstrated that the pK_a of carboxylic acid on L-*p*-boronphenylalanine was increased in the presence of HP- β -CD at equimolar concentrations (125). See chapter 2.6.5 for a discussion on the possible mechanism by which cyclodextrins can alter pK_a s.

Poloxamers

Both poloxamers altered the pK_a of all drugs investigated. The pK_a s of the bases decreased and the pK_a s for the acids increased in the presence of the poloxamers. These effects were statistically significant in all cases. No literature could be found on the pK_a effects induced by poloxamers on the drugs examined. These effects are not unexpected as the micelle core is hydrophobic and would favour the unionised,

less hydrophilic form of the four molecules. This is demonstrated by the fact that the point of 50% ionisation occurs earlier during the titration from the ionised to unionised form.

During solubility assays, the pK_a can also be determined. However, this data is not ideal to use as the pK_a is calculated from data up until the point of precipitation, which may occur before the point where the molecules are fully unionised. The Bjerrum plot would therefore be incomplete. At the point of precipitation the ratio of drug:HP- β -CD no longer holds as the drug precipitates out of solution, with the cyclodextrin remaining in solution, which could alter the observed pK_a s.

2.6.2 Intrinsic Solubility Results

HP- β -CD

The molar ratios used for each drug were increased until precipitation during assays failed. The ratios for atenolol to HP- β -CD used were lower than for the other drugs due to the solubility of atenolol being greater than that of propranolol, gliclazide and ibuprofen. This higher solubility would have resulted in aqueous concentrations of HP- β -CD reaching the maximum solubility for the HP- β -CD which has been quoted as up to 750 mg/mL (126) and/or the assay volume exceeding the maximum volume of 3.75 mL. The solubility of atenolol in the absence of excipient was found to be 14.5 mg/mL (54.4 mM), which is in good agreement with the literature quoted solubility (27).

From the regression equation, the solubility of propranolol HCl in the absence of HP- β -CD is 0.344 mM or 89.2 $\mu\text{g}/\text{mL}$. This is greater than the previous reported results for propranolol HCl solubility using the CheqSol method which have solubility results of 68.31 $\mu\text{g}/\text{mL}$ and 81 $\mu\text{g}/\text{mL}$ (26, 27). After searching the literature, no papers could be identified which measured the solubility increase of propranolol by HP- β -CD. A product information leaflet for HP- β -CD produced by Sigma-Aldrich quoted a 2.4 fold increase in solubility when propranolol HCl is dissolved in a 45% $^w/v$ solution of HP- β -CD (127). These results are, however, not suitable for comparison to the results outlined above. This is due to the quoted intrinsic solubility of propranolol being over 40 fold greater than that determined here, with no methodology to examine the technique used. The R^2 value of 99.4% denotes a good relationship between HP- β -CD concentration and propranolol solubility, as it can be concluded that 99.4% of the variation in solubility can be explained by the concentration of HP- β -CD.

The intrinsic solubility for gliclazide alone is 0.0730 mM, which is equal to 23.6 $\mu\text{g}/\text{mL}$. When compared to the literature the solubility results obtained, the determined solubility is lower than quoted solubilities of 0.092 mM (81) and approximately 0.1mM (128). The reduced solubility observed following regression analysis could be down to an underestimation of the aqueous solubility in the absence of excipient, since the mean solubility obtained from CheqSol studies of gliclazide alone is 30 $\mu\text{g}/\text{mL}$. It should also be noted that when the solubility of gliclazide is calculated from the slope and stability constant quoted by Sharma *et al.*, the value is 0.0700mM (128). On examination of the regression equation, the slope of the regression equation was

determined to be 0.0127. Therefore for every mM increase in HP- β -CD concentration, the solubility of gliclazide increases by 0.0127 mM. This is the same result that Sharma *et al.* achieved of 0.0127 (128). Over 98% of the variation in gliclazide solubility can be accounted for by the molar concentration of HP- β -CD.

Ibuprofen and HP- β -CD produced an A_P type solubility curve. This is in disagreement with Loftsson *et al.* and Mura *et al.* who showed A_L type curves (129, 130) although these were carried out at pH \approx 6, where ibuprofen is not fully ionised, which could alter the results. The studies were also conducted utilising a different method of complexation formation, which can affect the solubility improvement observed, see below (81, 128, 131-133). From the regression equation the p-value of the intercept was found to be greater than 0.05 indicating that in the absence of HP- β -CD the solubility of ibuprofen is not different from 0 μ g/mL. This result is not accurate and the mean solubility determined from the CheqSol assays should be used. The mean solubility in the absence of HP- β -CD was found to be 30.0 μ g/mL \pm 5.25. This is lower than the literature value which has been reported to be 50 μ g/mL following CheqSol determination (26). The solubility data includes ratios up to and including 1:1. At higher ratios (HP- β -CD), ibuprofen was found not to precipitate at the concentrations examined.

Poloxamers

Both poloxamers were found to increase the solubility of all four drugs examined.

In agreement with current findings, P407 has previously been shown to increase the solubility of ibuprofen (134). The solubility of ibuprofen alone differs between both results. Following regression analysis Newa *et al.* found the solubility of ibuprofen to be 0.0325 mM compared to 0.891 mM from regression analysis in this study. The results obtained following regression analysis of the CheqSol results overestimate ibuprofen intrinsic solubility. The mean intrinsic solubility of ibuprofen from CheqSol assays was found to be 0.145 mM. An underestimation of ibuprofen solubility appears to have been found here and reported by Newa *et al.* as other literature values for ibuprofen solubility are around 0.242 mM (26). As the phase-solubility study conducted by Newa *et al.* was carried out at pH 6.8, and ibuprofen would be present in the ionised form, it would be expected that the solubility results would be greater than the results obtained here. The regression analysis for the phase-solubility study of P407 on ibuprofen intrinsic solubility produced a negative intrinsic solubility of the drug alone, this value was obtained due to the influence that 5% w/v P407 had on the regression line. An increase in atenolol solubility in the presence of P407 in microparticles has been shown previously by Albertini *et al.* (135), which agrees with the results found here. No literature could be found on the effect of poloxamers on propranolol and gliclazide. The maximum concentration of P407 used was 5% w/v for the acidic compounds and for atenolol. The higher concentration of 10% w/v P407 was not able to be completed for atenolol, ibuprofen and gliclazide due

to problems with errors in the system. The errors recorded were high levels of carbonate in the system. The carbonate from dissolved carbon dioxide has two pK_a s and is recorded and measured by the system, and the results are therefore a combination of drug and carbonate. Degassing by sonication, carbonate purges and fresh media preparation were tried but failed to produce any beneficial effects on carbonate levels.

2.6.3 Kinetic Solubility Results

The CheqSol method also determines the kinetic solubility of the system. The kinetic solubility is the concentration of unionised drug present in the system at the point of precipitation. The concentration is calculated from the equations described above. The kinetic solubility can be used to give an indication of the degree of supersaturation. The mean measured kinetic solubility in the absence of solubilising excipient for ibuprofen, gliclazide, atenolol and propranolol were 0.579 mM, 2.55 mM, 138 mM, 2.15 mM respectively. These results are in good agreement with literature values (26, 27). As can be seen from the results the kinetic solubility of all four drugs was greater than their intrinsic solubility, thus showing that all undergo supersaturation. The kinetic solubility results obtained had large variation, especially as the concentration of solubilising agent increased. The reason for the large variation is not known, however could be due to the conditions of the individual experiments. One factor could be that the total amount of drug used varied for each assay and therefore supersaturated concentration would have been affected. This could have altered the time required for and the concentration at precipitation. From

Figure 2.22 (in the presence of HP- β -CD) it can be observed that the amount of drug used does not seem to affect the kinetic solubility of the four drugs. In the presence of P407, the amount of drug used appears to increase the kinetic solubility for propranolol, ibuprofen and gliclazide; the kinetic solubility of atenolol appears to be unaffected by the amount of drug used (Figure 2.23). The amount of drug used increases the kinetic solubility of propranolol and ibuprofen in the presence of P188 appears to be similar, neither gliclazide nor atenolol kinetic solubilities are affected (Figure 2.24). From these results however, it cannot be concluded that the amount of drug used is the cause of the variability of the kinetic solubilities. This is due to the higher amounts of drug required for CheqSol studies as a result of the higher intrinsic solubilities measured.

Kinetic solubility increased to a greater extent than the intrinsic solubility for most of the studies. The higher increase could be explained by a delay in precipitation of the drug molecules or 'parachute effect'. Both poloxamers (136) and cyclodextrins (137) have been found to delay precipitation of compounds previously (see chapter 3). It should be noted that following regression analysis of ibuprofen kinetic solubility and P407 concentration (% w/v) the kinetic solubility of ibuprofen was negative. This is likely due to the influence that the results at 5% w/v P407 has on the regression equation.

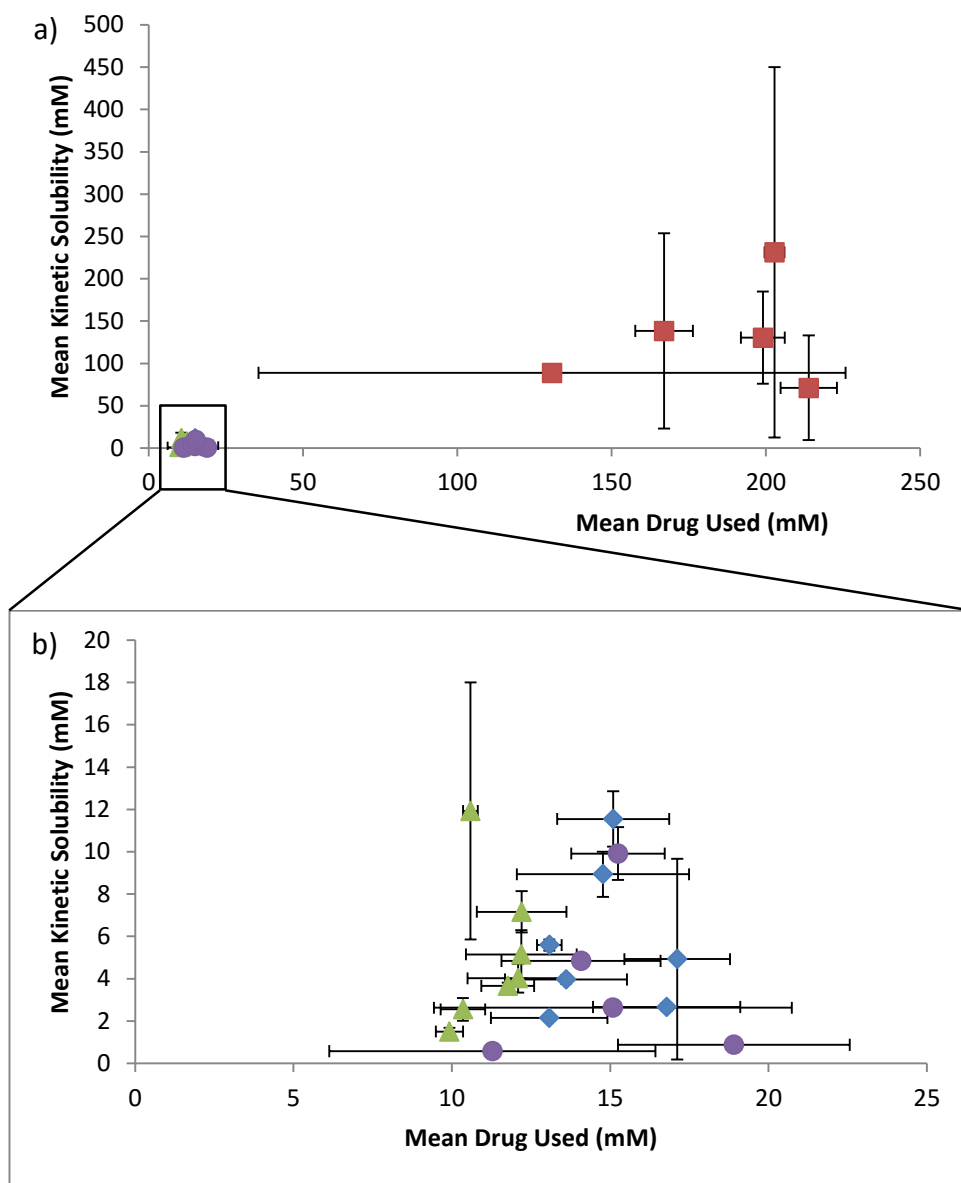


Figure 2.22. Scatterplot showing the effect that the amount of drug used has on the kinetic solubility in the presence of HP- β -CD at the varying ratios. Propranolol (◆), Atenolol (■), Gliclazide (▲) Ibuprofen (●). a) shows all four drugs, b) close up of the lower section for clarity. $n \geq 3$. Error bars represent standard deviation and where they are not visible their size does not exceed that of the symbol used. There is no correlation between the amount of drug used and the mean kinetic solubility.

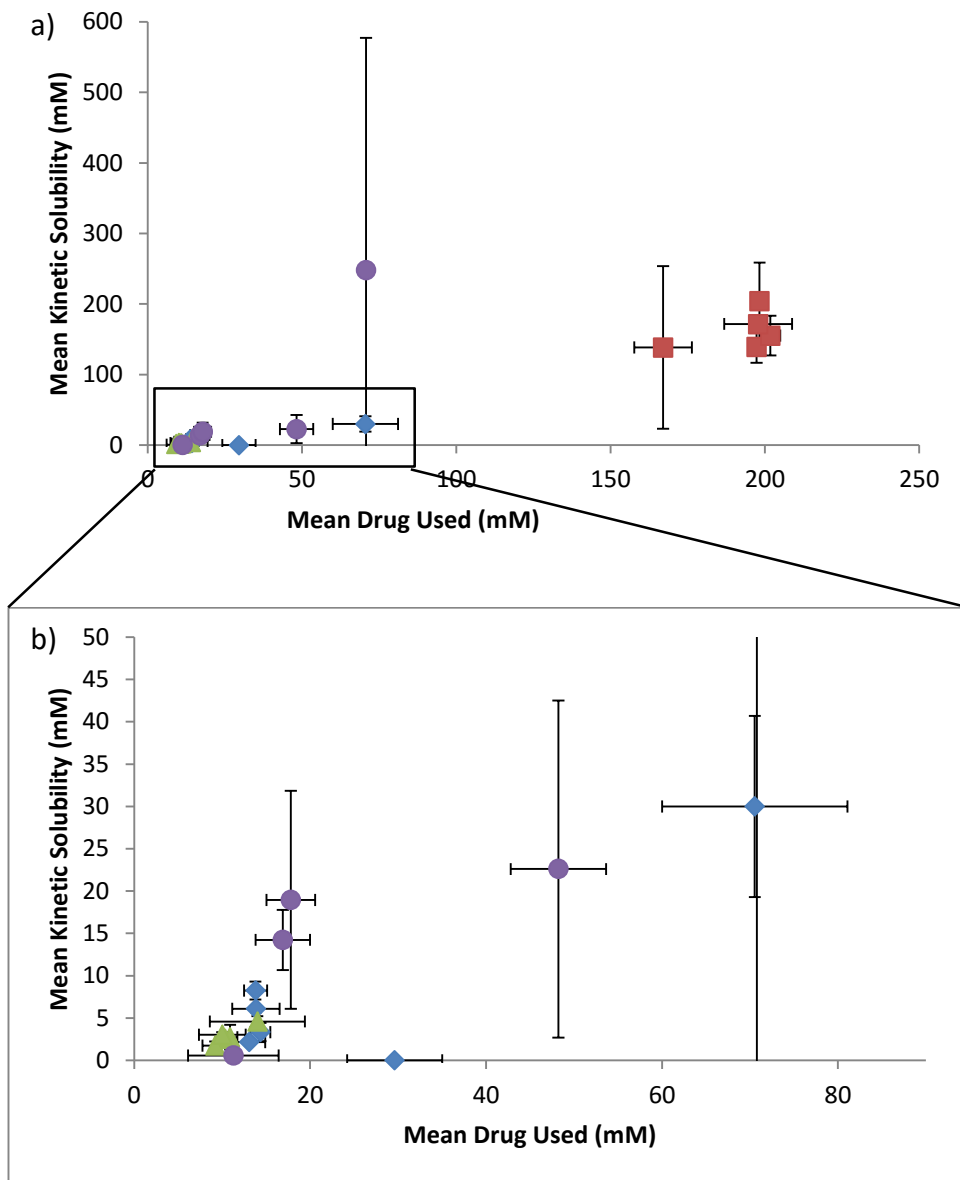


Figure 2.23. Scatterplot showing the effect that the amount of drug used has on the kinetic solubility in the presence of Poloxamer 407 at the varying concentrations. Propranolol (◆), Atenolol (■), Gliclazide (▲) Ibuprofen (●). a) shows all four drugs, b) close up of the lower section for clarity. $n \geq 3$. Error bars represent standard deviation and where they are not visible their size does not exceed that of the symbol used. There is no correlation between the amount of drug used and the mean kinetic solubility.

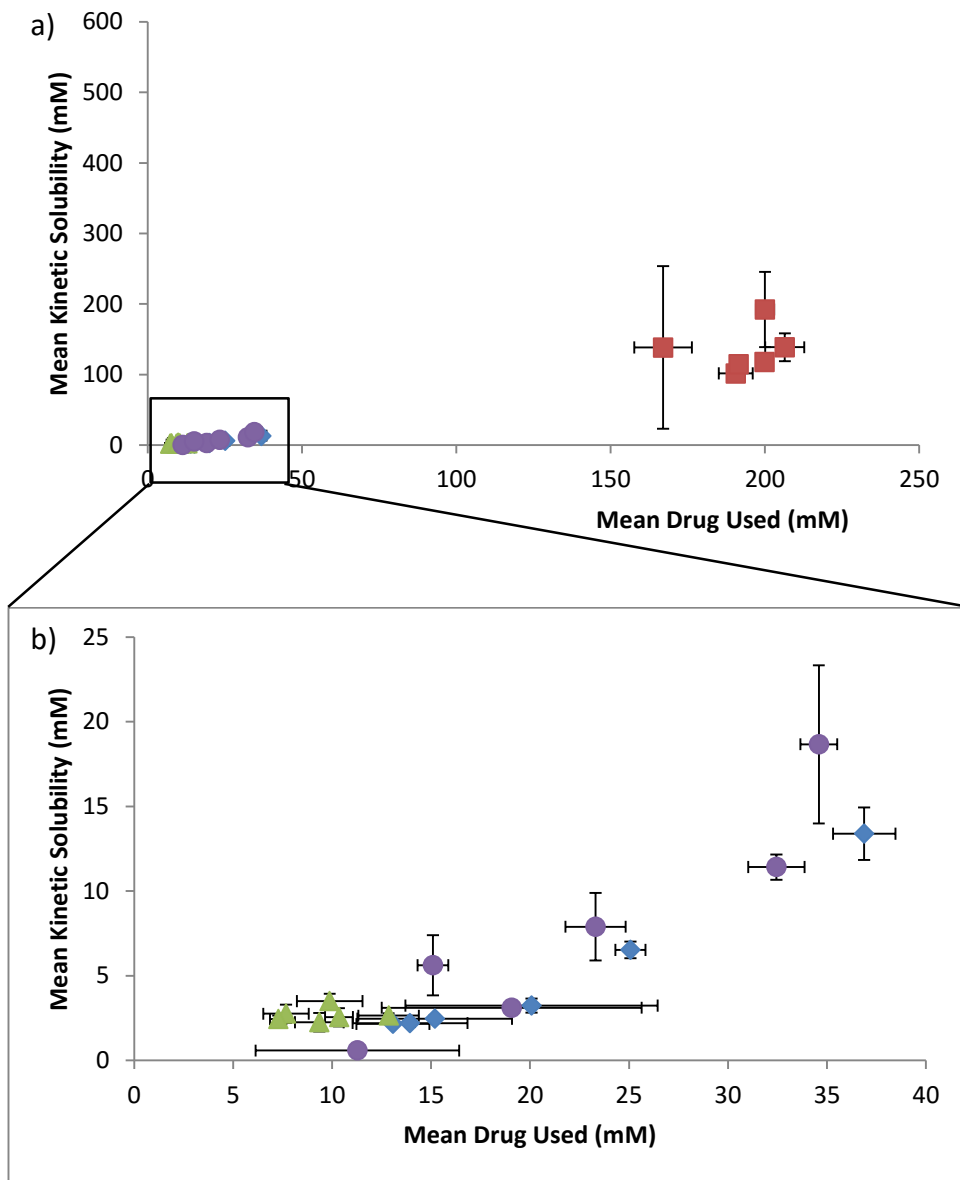


Figure 2.24. Scatterplot showing the effect that the amount of drug used has on the kinetic solubility in the presence of Poloxamer 188 at the varying concentrations. Propranolol (◆), Atenolol (■), Gliclazide (▲) Ibuprofen (●). a) shows all four drugs, b) close up of the lower section for clarity. $n \geq 3$. Error bars represent standard deviation and where they are not visible their size does not exceed that of the symbol used. There is no correlation between the amount of drug used and the mean kinetic solubility.

2.6.4 CheqSol versus Shake-Flask

The regression equations determined during the CheqSol and shake-flask solubility methods (at 254 nm) had constants that were similar. General Linear Model analysis was carried out on the data, with propranolol concentration as the response, CheqSol or Shake-Flask as the factor with HP- β -CD concentration as the covariate. The p-value for the factor was 0.869, therefore the null hypothesis, that there is no difference between the intercepts, is not rejected. The p-value for factor x covariate is 0.285, and again the null hypothesis of equal slopes is accepted. From the statistical analysis, we can conclude that there is no difference between CheqSol and Shake-Flask methods for phase-solubility studies of the intrinsic solubility of propranolol. The solubility results and regression line at 280 nm differs from the results at 254 nm. There was variation in the AUC of repeat runs for individual vials up to 12.0% at this wavelength suggesting that the results are not as reproducible/reliable as those at 254 nm. As the regression equations for the shake-flask and CheqSol are not different from each other, it can be concluded that, for the solubilisation of propranolol by HP- β -CD that both techniques can be used. The usefulness of CheqSol could be further validated, as the effect that HP- β -CD has on gliclazide solubility has already been discussed as having similar regression slopes to literature values (see chapter 2.6.2).

At a pH where propranolol is ionised, the regression equations show a negative relationship between increasing HP- β -CD concentration and propranolol concentration. The presence of the cyclodextrin appears to reduce the solubility of

ionised propranolol in pH 5.5 buffer possibly due to a reduced interaction between the ionised propranolol and solvent molecules (88). The negative slope of the phase-solubility diagram suggests that HP- β -CD does not associate with the ionised form of propranolol.

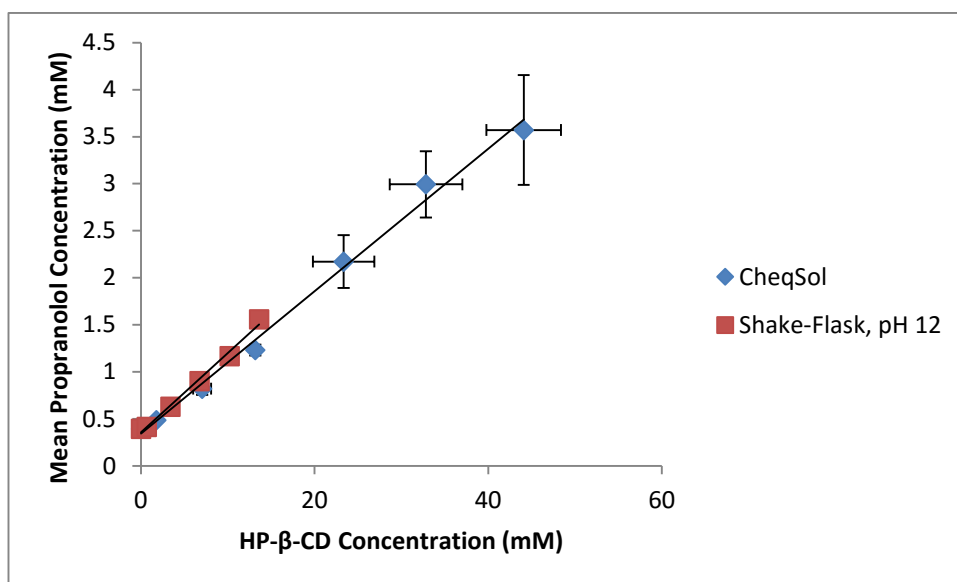


Figure 2.25. Scatterplots showing the regression analysis for intrinsic propranolol solubility and HP- β -CD concentration with both CheqSol (◆- Figure 2.7a) and Shake-Flask (■- Figure 2.20a) phase solubility studies. Shake-Flask studies carried out at pH 12 and 254nm wavelength. Error bars represent standard deviation and where they are not visible their size does not exceed that of the symbol used.

2.6.5 Complexation and Micellisation of Compounds with Excipients

The results show that pK_a for propranolol HCl and atenolol may be reduced in the presence of poloxamers, meaning the point of 50% ionisation occurs at a lower pH than would be expected. The opposite for the acids, gliclazide and ibuprofen, was

observed with an increased pK_a in solutions of P407 and P188. With the cyclodextrin, a similar effect on pK_a was observed with ibuprofen. Cyclodextrins and poloxamers have a hydrophobic core and would likely show preference to the non-ionised species of compounds (65, 85, 96). This could explain why the pK_a s can be affected, if the ionisable portion of the molecule interacts with the excipient molecule.

The ability cyclodextrins have on altering a compound's pK_a (s) could be due to a number of reasons. The preferential binding for the non-ionised, and thus more hydrophobic, species might be able to shift the equilibrium between the protonated and the de-protonated state. The cyclodextrin might also bond with the molecule at the ionisable group or in close proximity to the group. This bonding could affect the electrons around the ionisable group, altering its behaviour (130). The direction of the pK_a shift may indicate that the change is due to preference to the non-ionised form of the compound. No information could be found in the literature about the effect that poloxamers have on pK_a however, the observed changes could be due to the preference to the non-ionised form of the drug.

Another question from these results is whether the solubility increase observed is related to the change (if any) in pK_a . When looking at the data the increase in solubility does not appear to be affected by the degree of pK_a change.

Characterisation of the complex formed between propranolol, gliclazide, ibuprofen and atenolol has been carried out. Propranolol has been shown to form complexes

with β -cyclodextrins. This stoichiometry of the complex is 1:1, with the naphthyl group interacting with the core (138). The slope of the A_L curve of propranolol HCl solubility indicates that one propranolol molecule interacts with one HP- β -CD molecule. The complex formed between gliclazide and β -cyclodextrins has been demonstrated to result in a complex with a 1:2 ratio of gliclazide to cyclodextrin with both the aromatic and aliphatic ring moieties complex within individual cyclodextrin cavities (139). The observation that the phase-solubility results obtained here show a type A_L diagram, indicating that one cyclodextrin molecule is involved in the complex formation (78) is in disagreement with the literature (139). It may be assumed that since the slope of the regression line is less than 1 then the complex formation may be the result of 1:1 complexation, which is in agreement with other literature results (78, 128). The A_P type curve produced by ibuprofen at increasing concentrations of HP- β -CD indicates that there is more than one HP- β -CD molecule involved in the complex formation (78). This contrasts with other results which show that a 1:1 complex between ibuprofen and HP- β -CD is formed (122, 140). Oh *et al.* demonstrated that when ibuprofen complexes with HP- β -CD the aromatic ring is fully within the hydrophobic cavity of HP- β -CD. The side chains of ibuprofen may have reduced rotation when complexed with HP- β -CD (140), and the hydroxyl groups of HP- β -CD may interact with and alter the properties of the ionisable carboxylic acid group of ibuprofen (122). Like ibuprofen, the atenolol/HP- β -CD complex has been shown to be 1:1 ratio, with the molecule entering the cyclodextrin cavity and the aromatic ring interacting with the hydrophobic core (141). The slope of the phase-

solubility study for atenolol was determined to be 0.729, which demonstrates that a 1:1 relationship can be assumed.

A number of methods for the complexation and combining process have been described including physical mixture, kneading, neutralisation, ultrasonication and co-precipitation or re-crystallisation (81, 128, 131-133). These methods are not equivalent, with some techniques affecting dissolution and solubility more than others. Physical mixtures of HP- β -CD and gliclazide (81, 128), prazosin (131), domperidone (132) and ursodeoxycholic acid (133) have been shown to be less effective than other methods for improving solubility and dissolution. Methods which have been shown to increase solubility and dissolution compared to other techniques include neutralisation, ultrasonication and lyophilised complexes for gliclazide, domperidone and ursodeoxycholic acid respectively (81, 132, 133). Here, the complex in each experiment was prepared by dissolving the drug and cyclodextrin together (at pH 2 or pH 12) in one assay vial before slowly bringing the pH closer to the other extreme until the point of precipitation. The CheqSol technique used is similar to the neutralisation method except that the pH is adjusted beyond pH 7 where necessary to the point of precipitation which should provide efficient increases in solubility. It may be interesting to further study the effect of HP- β -CD on solubility by first forming the complex before CheqSol analysis.

For all four drugs, P407 resulted in a greater increase in solubility and change in pK_a per % w/v increase in poloxamer concentration compared to P188. This effect could

be down to the fact that P407 has a lower percentage of hydrophilic subunits compared to P188 (70% instead of 80%). This could result in a greater affinity for molecules with low hydrophilicity.

2.6.6 CheqSol

This technique and the instrument used are largely aimed for the early drug development stage to reduce failure due to poor physicochemical properties (142). Experiments are usually carried out with the drug on its own in the absence of excipients, although co-solvent measurements with alcohols such as methanol or ethanol can be carried out. The experiments carried out here show that the technique could be used as a tool during the formulation stage. It would be possible to determine any effects on pK_a and solubility an excipient has on the drug, as long as the drug is ionisable. Care would also need to be taken during experiments if the excipient is also ionisable which may interfere with measurements.

2.6.7 Other Observations from CheqSol Studies

During examination of the CheqSol data other observations were made on the behaviour of the compounds both alone and in the presence of excipients. The data suggested alterations in the rates of precipitation and dissolution of the compounds when cyclodextrin or poloxamer was present in the system. Further examination of the data to understand these effects will be carried out and discussed in chapter 3.

2.6.8 Cholic Acid as an Excipient

Ekwall *et al.* determined the pK_a of cholic acid to be 4.98, which is higher than the pK_a results from these experiments (111). The authors discuss the effect of concentration on cholic acid pK_a due to the formation of micelles above 0.0140 M. The concentration used in this study was below 0.014 M so the pK_a s would be expected to be similar. The methods used for pK_a determination differed. While both were potentiometric assays, the method used here involved a cosolvent in the system whereas Ekwall *et al.* conducted experiments in an aqueous environment (111), which may have altered the result due to changes in the behaviour of the bile acid. The solubility results are not reliable, with large variation in the data, some results being greater than the amount input into the system. The ability of cholic acid micelles to solubilise monomers of cholic acid could be affecting the solubility measurements.

Conclusions on the effect cholic acid has on ibuprofen cannot be drawn as both substances are likely to have precipitated during the CheqSol assay. The results observed for propranolol show that the presence of cholic acid might increase the solubility of propranolol. However, as precipitation was observed during the pK_a assays, precipitation of cholic acid during the CheqSol assay cannot be excluded, which may have affected the results. The observed precipitation during the pK_a assay may not wholly be due to cholic acid. If the presence of the bile acid affects the metastable zone (i.e. the zone within which it remains in supersaturated state) of propranolol then, some of the precipitation may be propranolol.

2.7 Conclusions

Hydroxypropyl- β -cyclodextrin, P407 and P188 are excipients which can be used to increase the solubility of the four drugs tested. As the experiments were conducted using the potentiometric CheqSol method and obtained results agree with the literature then the instrument can be used to measure solubility improvements with HP- β -CD, P407 and P188. The results show that it may be possible to use CheqSol to determine the solubility changes offered by other excipients used in a pharmaceutical formulation. Therefore, the instrument can be used to measure the solubility increase, if any, by the novel compound(s) produced as detailed in the project aims. For use with ionisable excipients further, studies would have to be conducted before any conclusions could be drawn.

2.8 Limitations

The limitations with the use of the potentiometric technique are that not all drugs developed will be ionisable and therefore not suitable to be tested using the CheqSol or curve-fitting method. It is possible that other formulation excipients could be tested to determine their effect on drug solubility, however if these excipients are ionisable within the pH range of the assay then they may interfere with the readings from the electrode probe. A limitation encountered which would affect any method using the HP- β -CD, was the variation in degree of substitution, the accurate molecular weight of the cyclodextrin was not known. Instead, a value in the middle of the range was chosen to determine the molar ratios and concentrations.

The experiments carried out only looked at drugs which chase equilibrium, and it would be appropriate to repeat the process with drugs which are known to be non-chasers to explore if the results using the Curve-Fitting Method would be the same. It may also be beneficial to investigate the effects observed if an excipient is used which has its own pK_a .

3 Chapter 3: Dissolution and Precipitation Rates

3.1 Introduction

As described earlier many novel drug candidates have poor aqueous solubility and different techniques can be used to improve the water solubility for administration. Excipients added to either the media or a formulation can affect the dissolution and precipitation rates of compounds (136). An understanding of these effects on dissolution and precipitation rates is important. Knowledge of dissolution rate effects allows for the development of formulations with appropriate release rates. Precipitation rate knowledge could be used to develop formulations which can maintain supersaturated solutions for prolonged periods, allowing for an improvement in bioavailability due to increased absorption following oral administration. As the rate of absorption of a drug through the gastrointestinal tract (J) is based on Fick's First Law (Equation 3.1) and is a product of the permeability coefficient (P) and the concentration (C) of the drug in the gastrointestinal fluid (143) then a formulation, which does not affect the absorption of the drug through the GIT wall, can increase the amount of drug absorbed by increasing the concentration in the GIT fluids. Therefore an improvement of the oral bioavailability of a compound following administration can be achieved by both increasing dissolution and decreasing precipitation rate of the drug. This has been referred to as the 'spring and Parachute' effect (136).

$$J \text{ (mol m}^{-2} \text{ s}^{-1}) = P \times C$$

Equation 3.1

3.1.1 Dissolution

The process of dissolution involves the breaking of the intermolecular forces in the solid form and allowing bonds to form with the solvent. The rate of dissolution is represented by the Noyes-Whitney equation. Noyes and Whitney first published their equation in 1897 as:

$$\frac{dx}{dt} (\text{M time}^{-1}) = C(S-x) \quad \text{Equation 3.2}$$

where x is the concentration of the substance at time 't', S is the solubility of the compound under the experimental conditions and C is a constant (144). This equation can be expanded to

$$\frac{dC}{dt} (\text{M time}^{-1}) = \frac{DS}{Vh} \times (C_s - C_b) \quad \text{Equation 3.3}$$

Where $\frac{dC}{dt}$ is the change in the concentration of compound over time, S is the surface area of the solute in contact with the solvent, D is the diffusion coefficient, h is the thickness of the solvent layer in contact with the solute, V is the volume of the bulk medium, and $C_s - C_b$ is the difference between the concentration at saturation or solubility (present at the interface) and the bulk solution concentration (145).

3.1.2 Thermodynamics of Dissolution

The dissolution process is driven by a negative change in Gibb's free energy. When free-energy of the solid is greater than the solution then dissolution will occur until both are equal (9). The equation for the change in free energy brings together the relationship between the change in free energy (ΔG), entropy change (ΔS) and enthalpy change (ΔH), Equation 3.4 (19).

$$\Delta G_{d,2} \text{ (kJ/mol)} = \Delta H_{d,2} - T\Delta S_{d,2} \quad \text{Equation 3.4}$$

Where $_d$ denotes dissolution and $_2$ denotes that the solute is the second component in the solution system and T is the absolute temperature of the dissolution process in Kelvin (19).

The enthalpy of dissolution ($H_{\text{dissolution}}$) is associated with the enthalpy of fusion (H_{melt}) with or without the enthalpy of mixing (H_{mix}), Equation 3.5 (18).

$$H_{\text{dissolution}} \text{ (kJ/mol)} = H_{\text{melt}} + H_{\text{mix}} \quad \text{Equation 3.5}$$

The enthalpy change of dissolution can be positive or negative i.e. endothermic or exothermic respectively. An exothermic process promotes dissolution as it contributes to a negative change in Gibb's free energy. If dissolution is endothermic then dissolution may be inhibited due to the positive influence on Gibb's free energy changes (19). However, a solute with a positive enthalpy change may still dissolve in

the solvent. This is because the entropy change of mixing also influences the free energy change. When a solute is dissolved in a solvent there is an increase in disorder in the system and therefore the entropy of the system increases (17, 146). If the increase in entropy is sufficient to overcome the enthalpy increase and result in a negative $\Delta G_{d,2}$ then dissolution occurs (19).

3.1.3 Factors affecting Compound Dissolution

As observed from Equation 3.3, increasing the surface area of the solute in contact with the solvent will increase dissolution rate, thus smaller particle sizes can be used to increase dissolution rate. Increases in solubility by techniques, including those discussed earlier in chapter **Error! Reference source not found.**, will also enhance dissolution rate by increasing the concentration gradient between the bulk solution and the saturated layer surrounding the solid/liquid interfaces. Decreases in saturated layer thickness, by stirring, can also be used to increase dissolution rate.

3.1.4 Precipitation

Precipitation occurs when a compound is found in a supersaturated solution. As this is thermodynamically unfavourable, the dissolved compound may begin to come out of solution and precipitate. Supersaturated solutions can be found in a metastable state and precipitation may not be observed, unless conditions are altered or the ΔG maximum is reached and surpassed (147). There are two stages to precipitation: nucleation and crystal growth.

Nucleation occurs first and is a random process (148) and involves the aggregation of molecules in solution into clusters (149). The Classical Nucleation Theory suggests that these clusters, when sufficiently large, can form nuclei on which crystal growth can occur (149, 150). Two factors make up the changes to free energy for the formation of clusters (ΔG): the free energy changes associated with the formation of a surface (ΔG_s) and phase transformation (ΔG_v) where (149)

$$\Delta G \text{ (kJ/mol)} = \Delta G_s + \Delta G_v \quad \text{Equation 3.6}$$

Since ΔG_s is positive and proportional to the surface area of the solid/liquid interface, and ΔG_v is negative, the clusters must have enough molecules to allow ΔG_v to overcome ΔG_s , which decreases as surface area decreases (149). Clusters of molecules can be defined as critical (n^*) when their size reaches point where ΔG is a maximum (147, 149). At cluster sizes below this critical value ($n < n^*$) the molecules will dissolve into the medium, clusters which have size $n > n^*$ can be called nuclei, and these clusters will undergo crystal growth (147, 149, 150). The Classical Nucleation Model assumes that the molecules in the nuclei have the same characteristics as the crystal (149). However it has been suggested that there is an intermediary step where nuclei are dense, disordered, liquid-like clusters of the precipitating compound (149).

Nucleation rate, J , defines the number of nuclei formed per cm^3 per second:

$$J \text{ (nuclei cm}^{-3} \text{ s}^{-1}) = A \exp\left(-\frac{\Delta G^*}{kT}\right)$$

Equation 3.7

Where A is the pre-exponential factor estimated to be $10^{30} \text{ cm}^{-3} \text{ s}^{-1}$, k is Boltzmann's Constant, T is temperature in Kelvin, and ΔG^* is the free energy change of the critical nuclei, n^* (149, 151). The equation demonstrates that as the ΔG^* increases at constant temperature, the rate of nucleation will increase.

When administered orally, drugs have to be in solution before absorption can take place, it has been suggested that increasing solubility of some compounds is not as effective as increasing the amount and time of supersaturation for improving bioavailability (152). Precipitation from supersaturated solutions has been shown to be delayed in the presence of excipients.

3.1.5 Spring and Parachute Effect

The spring effect is obtained by developing a formulation from which the active ingredient is rapidly released and dissolves in the media to form a supersaturated solution. Amorphous forms, crystalline salts, co-crystals, cosolvent systems and lipid-based formulations can give rise to supersaturated solutions when dissolved in media (143, 153). Supersaturated solutions have a higher free energy than saturated solutions, thus the compounds are likely to precipitate out of solution to a more stable crystalline form (153). Delaying this precipitation, or creating a 'parachute', to slow down this process prolongs the existence of the supersaturated solution, thus increasing the amount absorbed (Equation 3.1). Excipients have been shown to

prolong the supersaturation of compounds in simulated gastric fluids without affecting the solubility (154).

The parachute can be obtained by kinetic and thermodynamic inhibition of precipitation. An increase of solubility in the media would result in a reduction in the degree of supersaturation present therefore reducing the thermodynamic drive for nucleation and crystal growth (155). Kinetic inhibition of precipitation is achieved by interfering with nucleation and/or crystal growth (155). Although a number of excipients have been shown to inhibit nucleation, the mechanism by which this occurs is unknown (153). The presence of polymers in a system has been shown to reduce nucleation. Both Hydroxypropyl methylcellulose (HPMC) and polyvinylpyrrolidone (PVP) have been shown to increase the level of supersaturation required before nucleation is observed without having an observable effect on solubility (153). Crystal growth may be inhibited by the hydrogen bonding of polymers to the surface of the crystal blocking drug access to the surface preventing growth (156).

3.1.6 T3 Determinations of Dissolution and Precipitation Rates

Precipitation rates are calculated during CheqSol assays using the $\frac{dpH}{dt}$. From this data the precipitation rate in molar units per minute are determined by software from Equation 3.8 (157)

$$\text{Precipitation Rate (M/min)} = \frac{\left(\frac{d\text{pH}}{dt}\right) \times \text{BI}}{\text{average molecular charge}} \quad \text{Equation 3.8}$$

Where BI is the buffer index. The units specified can be sub-molar concentrations e.g. mM/min or $\mu\text{M}/\text{min}$. The software only calculates precipitation rates, negative precipitation rates are taken as dissolution rates.

3.2 Aim

The software calculates the dissolution and precipitation rates measured during the crossing points in a CheqSol assay (see chapter 2). After examination of the graphs produced by the software it was noted that there may be concentration dependent differences between precipitation and dissolution rates in the presence of excipients. The aim of this section was to determine whether the presence of the solubilising excipients significantly affects precipitation and dissolution in near equilibrium conditions of the compounds tested. The system was also used to compare the dissolution of the two of the tested compounds in the absence and presence of the three excipients used.

3.3 Materials

In addition to materials mentioned earlier (chapter 2.3) dipotassium hydrogen phosphate trihydrate and glacial acetic acid, both obtained from Sigma-Aldrich Company Ltd (Dorset, UK), were also used. Rheology was carried out on a Haake MARS III rheometer.

3.4 CheqSol Data Methods

3.4.1 Data Extraction

The software used for refining the assay results allows extraction of the x- and y-axis points from all plots into Microsoft® Excel spreadsheets. Data extraction was carried out for each individual assay. For precipitation and dissolution rate analyses the data was extracted from three plots to provide a complete picture of the rates. The extracted data included:

- From the Precipitation Rate Graph, the concentration and the precipitation rate.
- From the Equilibrium Chasing Crossover Plot concentration and $\frac{d\text{pH}}{dt}$ for the data points and extrapolated points.
- From the plot of $\frac{d\text{pH}}{dt}$ versus pH, the pH points, corresponding to the $\frac{d\text{pH}}{dt}$ points from the Equilibrium Chasing Crossover Plot.

The different plots can be found within the Solubility, pH-metric and Assay Events tabs within the refinement program.

For excipient gain factor (EGF) determination the following was also extracted:

- The concentration and time data from the Neutral Species Concentration Time Profile.

3.4.2 Data Analysis

Following extraction, the data were ordered into precipitation and dissolution sections and crossings were grouped together as defined in the Precipitation Rate

Graph. For each crossover point the mean precipitation rate was calculated. As the software calculates only precipitation rates, negative precipitation rates were regarded as dissolution rates. The mean of these crossover mean precipitation rates was calculated for each ratio of HP- β -CD and poloxamer concentration used.

The EGF was also calculated for each assay, this factor was calculated based on Equation 3.9 using calculated area under the curve (AUC):

$$\text{EGF} = \frac{\text{Area A} + \text{Area B} + \text{Area C}}{\text{Area A} + \text{Area B}} \quad \text{Equation 3.9}$$

Where Area A is the AUC of the intrinsic solubility of the drug in the solvent, Area B is the AUC of the drug in the solvent following supersaturation and precipitation and Area C is the AUC of the supersaturation and precipitation of the drug in the solvent in the presence of the excipient (158). A representation of the AUCs used in the calculation can be found in Figure 3.1.

The AUC was calculated using the trapezoidal method. The first time point from this data was set as zero to allow AUC to be calculated. The mean AUC for the drugs in the absence of excipient was used as the denominator (Area A + Area B) and the numerator was the AUC of each assay in the presence of excipient (Area A + Area B + Area C). The mean of these EGFs were calculated and plotted in a column chart.

The statistical analysis was carried out on the mean data by transferring information into Minitab™ 16 and carrying out one-way analysis of variance (ANOVA). For EGF, the ANOVA was carried out against the control group which is equal to 1.

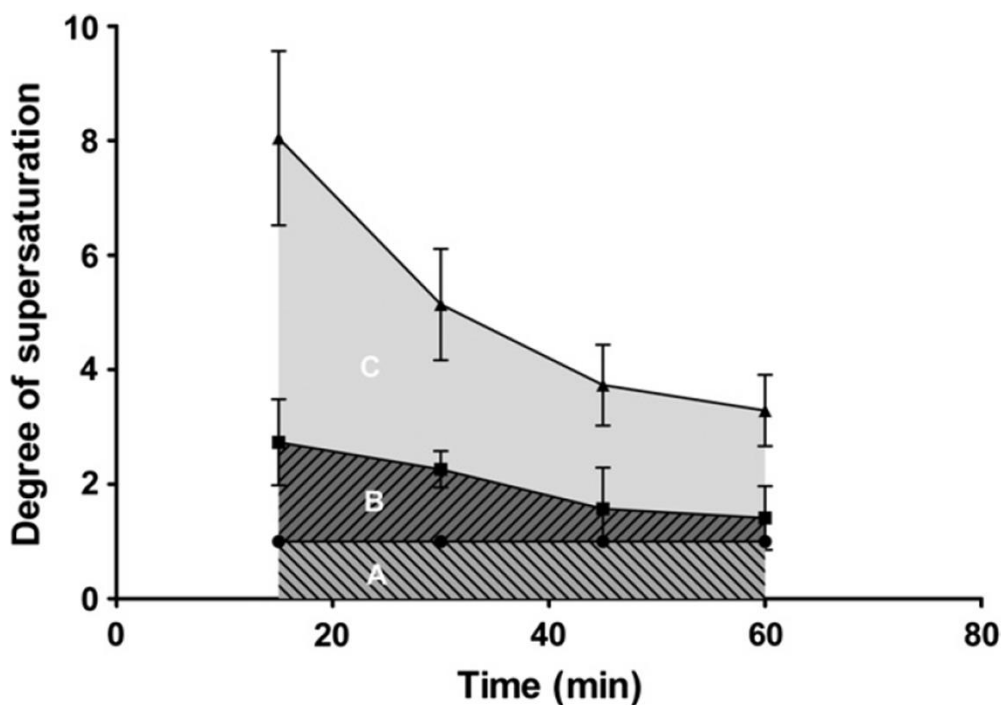


Figure 3.1. Diagram representing the areas used during the EGF determination. Area A is the compound's intrinsic solubility, area B is the compound is the supersaturation of the compound in the solvent and area C is the supersaturation of the compound in the solvent in the presence of excipient. Taken from Bevernage *et al.* 2012 (158).

3.5 Experimental Methods

3.5.1 Solution Preparation

A dissolution buffer was prepared based on the recipe from Sirius Analytical. Sodium dihydrogen phosphate was substituted for dipotassium hydrogen phosphate

trihydrate, due to availability, the mass used was adjusted to maintain the molar phosphate in the buffer. The recipe used was:

- 2.282 g dipotassium hydrogen phosphate trihydrate
- 11.18 g potassium chloride
- 572 μ L glacial acetic acid.
- Made up to 1L with HPLC grade water.

The pH used varied depending on the drug under investigation.

Solutions of HP- β -CD, P407 and P188 were prepared in the buffer recipe above. A 10% $^w/v$ solution of the poloxamers was used to represent the maximum concentration used during CheqSol assays. HP- β -CD concentration which has a molar excess compared to the drug was used. The concentrations prepared ranged from 0.0211 M HP- β -CD to 0.0426 M HP- β -CD.

3.5.2 Molar Extinction Coefficient Determination

In order for amount of drug dissolved in the assay medium to be calculated, the software requires information on the molar extinction coefficients (MEC). The MECs are determined using UV-metric pK_a assays. For each drug a 5 mM solution in DMSO was prepared and at least 10 μ L of this solution was used for the assay. For drugs with low UV absorbance (gliclazide, ibuprofen and atenolol), a higher volume of the DMSO solution was required.

3.5.3 Experimental Disc Dissolution Assays

Tablets of pure drug were prepared by weighing out approximately 5 – 10 mg of powder into the tablet disc, within the locating ring and placed on the compression base. Tablets were formed by compressing the powder to 80 kilogram-force (kgf) four times. Between each compression and final release of pressure the tablets were left for one minute to allow the compression to equilibrate throughout the disc. The tablet disc was removed and placed in the tablet holder for dissolution (Figure 3.2).

Dissolution was set up to study the dissolution rate at one pH over one hour with 120 data points during that time. The pH was chosen based on the pH at which the drug chased equilibrium during CheqSol assays. For propranolol HCl, gliclazide, ibuprofen and atenolol the pH was 8.5, 6.5, 5.5 and 10.5 respectively. Necessary pH adjustments were made in small steps to prevent too much acid or base being added. Assays were carried out at room temperature.

ANOVA was used to determine if any differences between dissolution rates were statistically significant. Dunnett's test was used to compare any differences to the control group of acetate phosphate buffer alone.

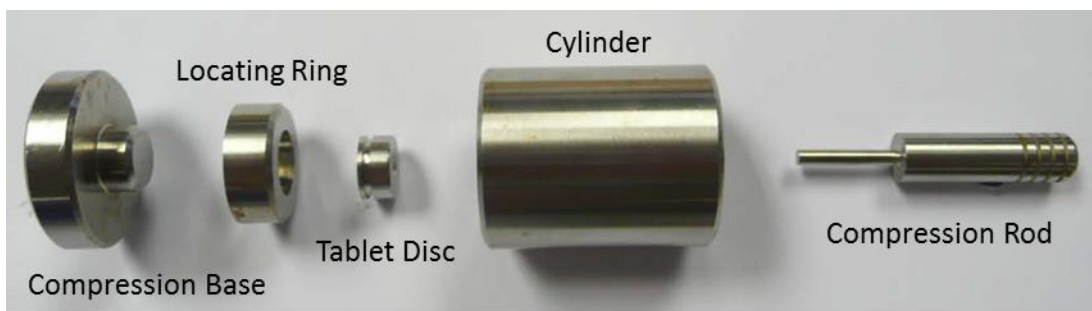


Figure 3.2. Setup of die used during tablet preparation. Image from Sirius Analytical Dissolution Manual for T3 (159).

3.5.4 Excipient Solution Viscosity

To explore whether differences in viscosity could explain changes in dissolution rates measured during disc dissolution assays the viscosity of the acetate phosphate buffer and the three excipient solutions at the highest concentrations were determined. Solutions of P407 and P188 were prepared by dissolving 1 g in 10 mL of the acetate phosphate buffer prepared earlier. The highest concentration of HP- β -CD used was 0.0426 M, so for a 10 mL solution 660.4 mg (weight adjusted for water presence) was dissolved in the buffer.

As the samples had a low viscosity, the measuring geometries used were MPC60 measuring plate with a C60/1° cone. The samples were run from 0 to 100 s⁻¹ for thirty seconds, one measurement every second, for shear effects to be determined. Data were plotted τ (Pa, shear stress) vs $\dot{\gamma}$ (s⁻¹, shear rate) and fit to Ostwald de Waele (Equation 3.10) to provide flow consistency index (K) and flow behaviour index (n). The samples were then held at 100 s⁻¹ and 100 measurements were taken over 30

seconds to determine viscosity. The average of the 100 measurements was calculated and ANOVA with Dunnett's test against buffer alone was carried out.

$$\tau \text{ (Pa)} = K\dot{\gamma}n \quad \text{Equation 3.10}$$

3.6 Results

3.6.1 Precipitation Rates from CheqSol Assays

At propranolol:HP- β -CD molar ratios 1:0.5 to 1:2.5, the precipitation rate was observed to decrease compared to drug on its own. At the 1:0.1 ratio, precipitation rate increased, with a large standard deviation (Figure 3.3a). Both poloxamers were found to increase the precipitation rate observed for propranolol (Figure 3.3b and c).

A reduction in precipitation rate was observed for gliclazide for all ratios of HP- β -CD used. The precipitation rate is lowest at the highest molar ratios (Figure 3.4a). P407 reduced the precipitation rate of gliclazide at concentrations of 1% w/v and above, with 2% w/v and 5% w/v having the greatest effect (Figure 3.4b). After an initial increase in precipitation rate at 0.5% w/v P188, precipitation rates decrease at 5% w/v and 10% w/v P188, 1% w/v and 2% w/v concentrations saw no difference in measured rates (Figure 3.4c).

HP- β -CD results in an increase in ibuprofen precipitation rate at the 1:0.1 drug:cyclodextrin molar ratio, this effect is not observed at higher molar ratios. The precipitation rate was seen to decrease at molar ratios of 1:0.75 and 1:1 (Figure 3.5a).

At the highest poloxamer concentrations both P407 (at 2% w/v and 5% w/v) and P188 (at 5% w/v and 10% w/v) were found to increase precipitation rate. At lower P407 concentrations no change in ibuprofen precipitation rate, however and 0.5% w/v and 1% w/v P188 a reduced precipitation rate is observed (Figure 3.5b and c).

The precipitation rate of atenolol is not affected by HP- β -CD at ratios of 1:0.05 and 1:0.2. There is a significant increase in precipitation rate at 1:0.1 and 1:0.15 molar ratios however these results have large standard deviations (Figure 3.6a). Only 0.5% w/v P407 was shown to reduce the precipitation rate of atenolol, with the higher concentrations having no effect (Figure 3.6b). With the presence of P188 only 2% w/v has an effect on precipitation rate (Figure 3.6c).

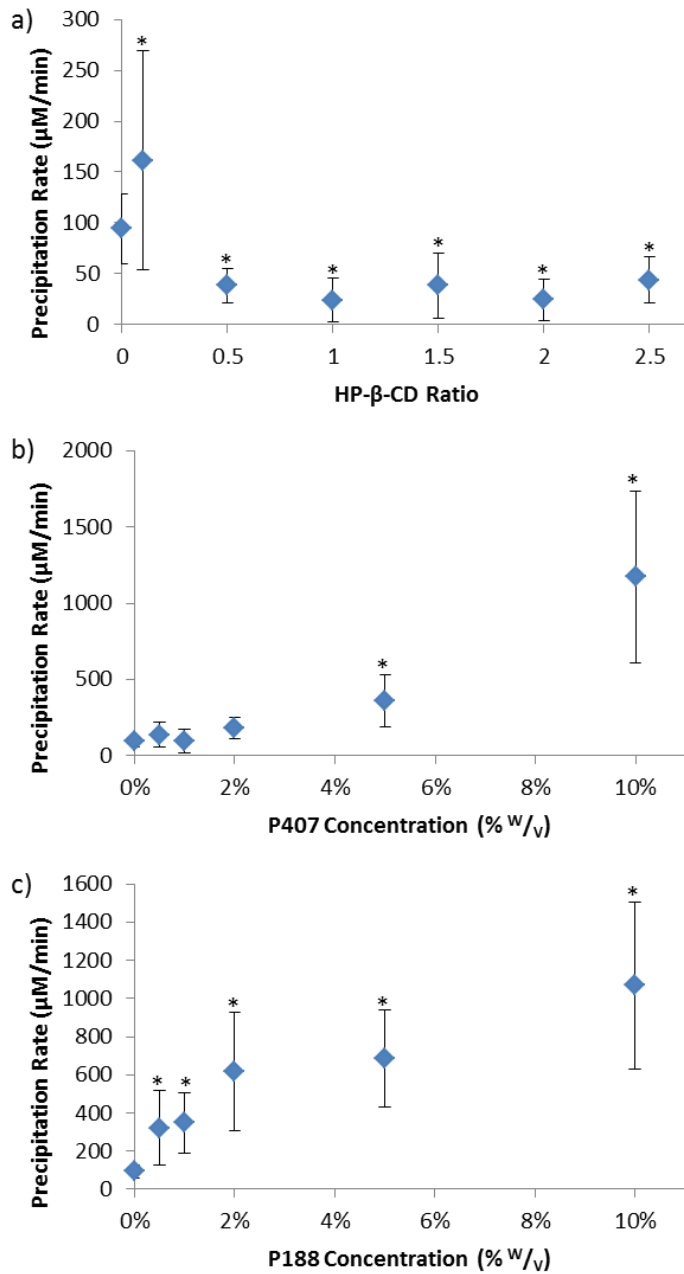


Figure 3.3. Scatterplot showing the mean propranolol precipitation rates obtained during CheqSol assays with increasing concentrations of a) HP-β-CD, b) P407, and c) P188. * Represents statistically significant difference from control group, 0, following ANOVA with Dunnett's test with 0.05 significance level. $n \geq 3$. Error bars represent standard deviation and where they are not visible their size does not exceed that of the symbol used.

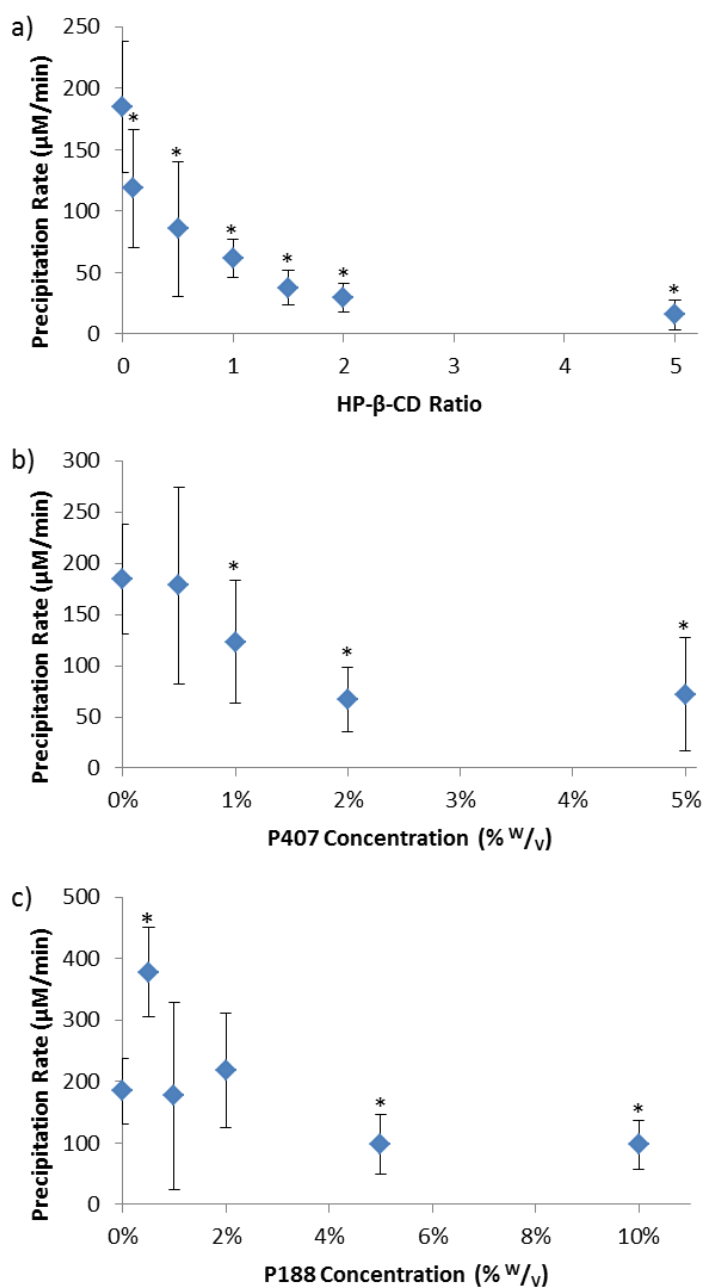


Figure 3.4. Scatterplot showing the mean gliclazide precipitation rates obtained during CheqSol assays with increasing concentrations of a) HP-β-CD, b) P407, and c) P188. * Represents statistically significant difference from control group, 0, following ANOVA with Dunnett's test with 0.05 significance level. $n \geq 3$. Error bars represent standard deviation and where they are not visible their size does not exceed that of the symbol used.

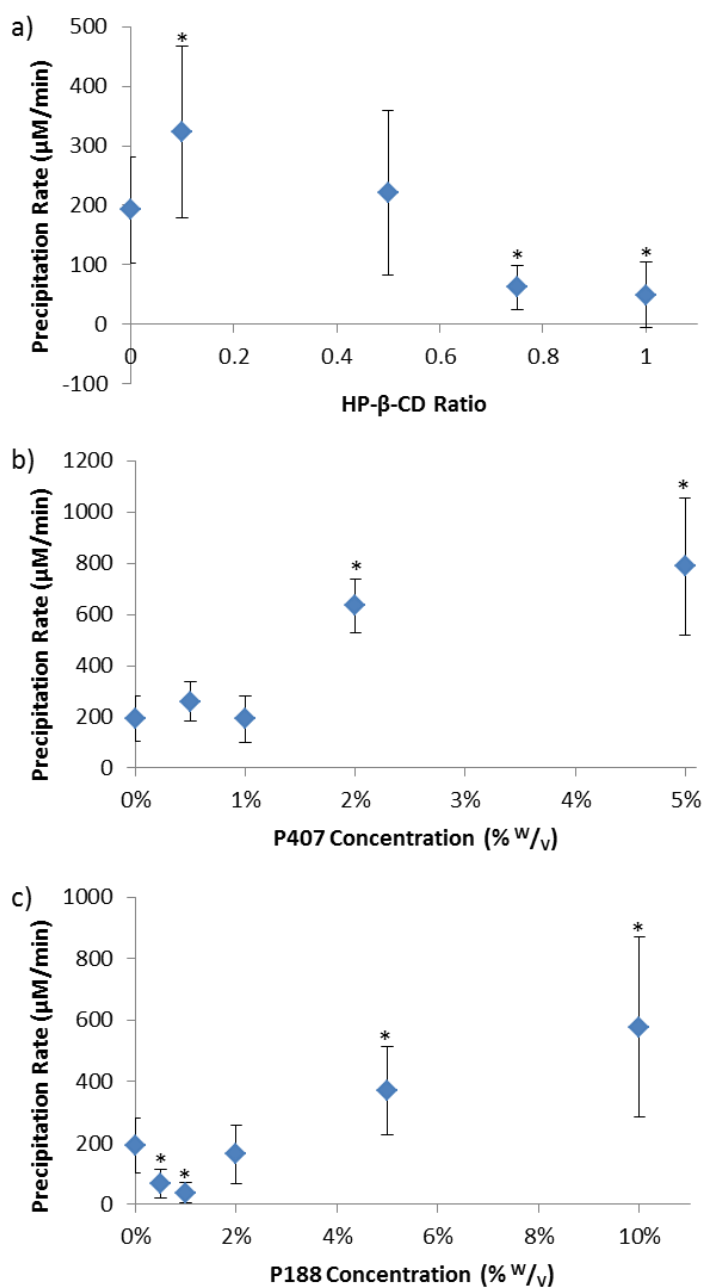


Figure 3.5. Scatterplot showing the mean ibuprofen precipitation rates obtained during CheqSol assays with increasing concentrations of a) HP-β-CD, b) P407, and c) P188. * Represents statistically significant difference from control group, 0, following ANOVA with Dunnett's test with 0.05 significance level. $n \geq 3$. Error bars represent standard deviation and where they are not visible their size does not exceed that of the symbol used.

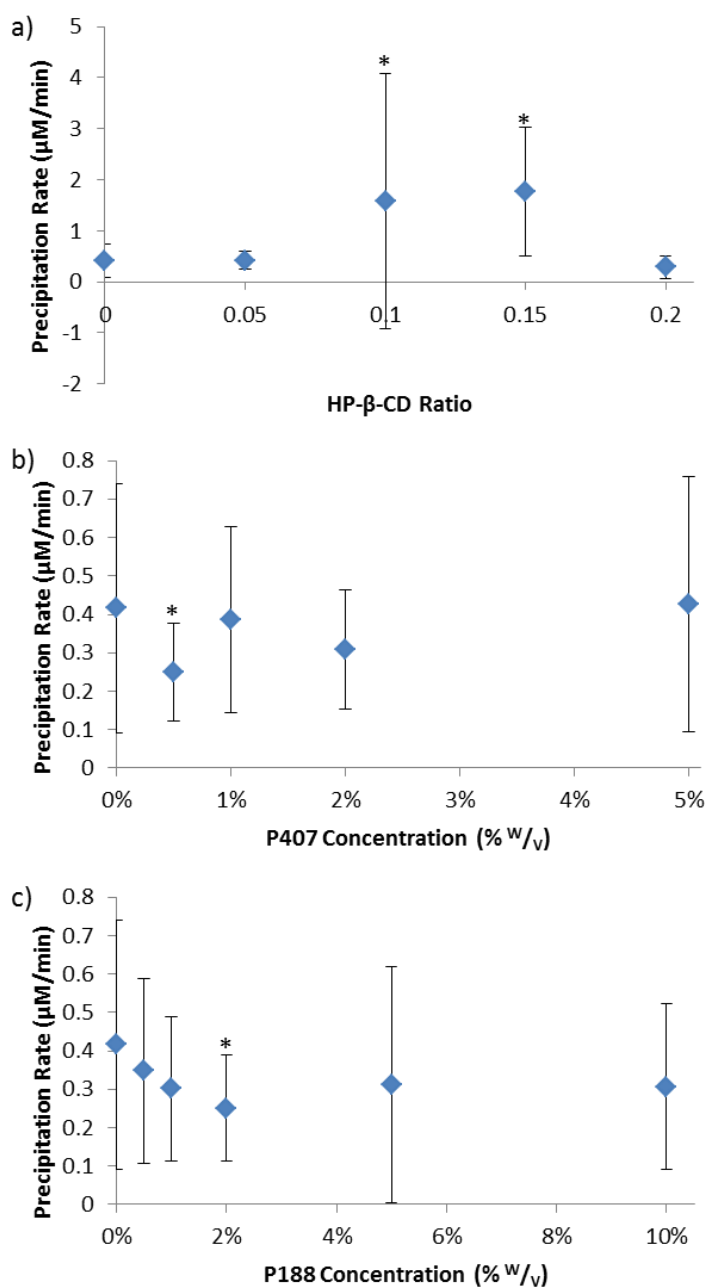


Figure 3.6. Scatterplot showing the mean atenolol precipitation rates obtained during CheqSol assays with increasing concentrations of a) HP-β-CD, b) P407, and c) P188. * Represents statistically significant difference from control group, 0, following ANOVA with Dunnett's test with 0.05 significance level. $n \geq 3$. Error bars represent standard deviation and where they are not visible their size does not exceed that of the symbol used.

3.6.2 Dissolution Rates from CheqSol Assays

Analysis of dissolution rates obtained during CheqSol assays shows that at high concentrations of both HP- β -CD and P407 the dissolution rate of propranolol decreases, whereas the rate in P188 shows an increase in dissolution rate at the highest concentrations (Figure 3.7). The dissolution rate decrease in the presence of P407 is not concentration dependent, with 1% w/v P407 showing the largest decrease in propranolol dissolution rate. The dissolution rate changes for P188 follows a similar pattern for the dissolution rate changes associated with the effect of P407 on propranolol dissolution rate.

Gliclazide dissolution rates appear to be affected slightly by the presence of the excipients. Only at the highest molar drug:HP- β -CD ratio is the dissolution rate significantly different from the control group. However, in the presence of P407, there is an initial increase in dissolution rate at 0.5% w/v, before dissolution rate decreases. No pattern for the effect of P188 on the dissolution rate of gliclazide is easily identifiable from the results (Figure 3.8).

At the lowest ratio of drug:HP- β -CD, ibuprofen dissolution rate increased, and at ratios 1:0.5 to 1:1 the dissolution rate decreased. The dissolution rate of ibuprofen decreased in the presence of concentrations 2% w/v P407 and less. At 5% w/v the dissolution rate of ibuprofen increased. P188 decreased the measured dissolution rate of ibuprofen at 0.5% w/v, 1% w/v, 2% w/v and 10% w/v (Figure 3.9).

HP- β -CD does not appear to affect the dissolution rate of atenolol measured during CheqSol assays although at ratios of 1:0.1 and 1:0.5 the dissolution rate is higher than for the drug alone. From the results obtained P407 does not affect the rate of atenolol dissolution at any concentration, whereas at 1% w/v, 5% w/v and 10% w/v P188 the atenolol dissolution rate measured is less than the dissolution rate in ISA water (Figure 3.10).

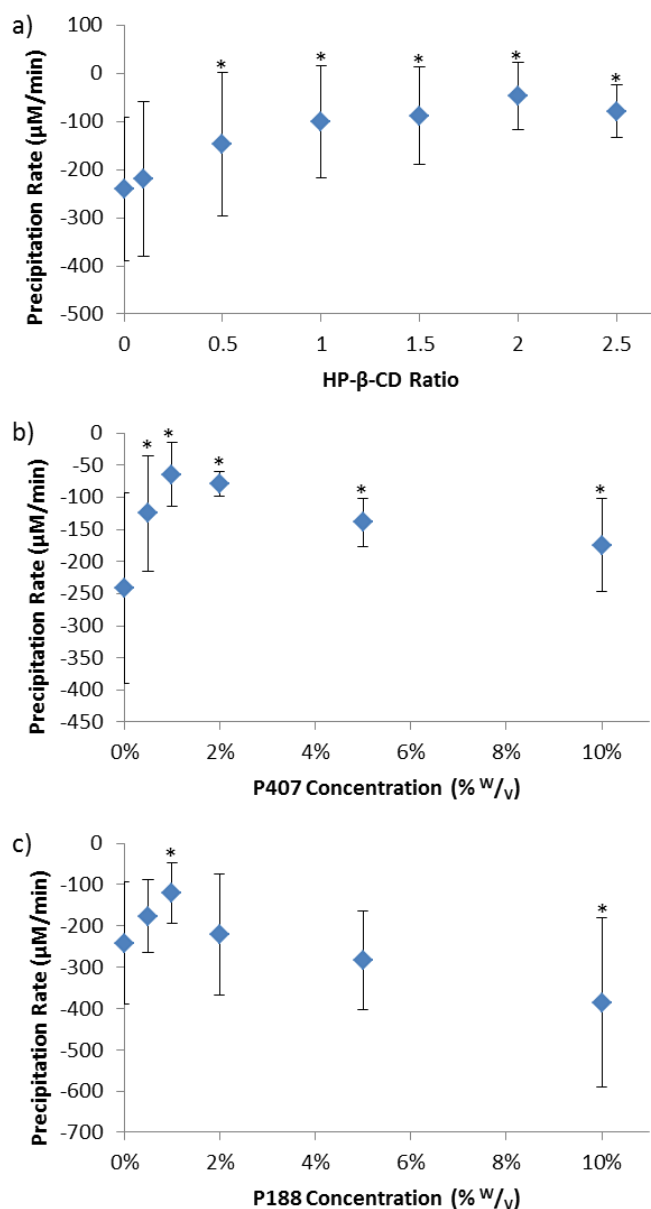


Figure 3.7. Scatterplot showing the mean propranolol dissolution rates (represented as negative precipitation rates) obtained during CheqSol assays with increasing concentrations of a) HP-β-CD, b) P407, and c) P188. * Represents statistically significant difference from control group, 0, following ANOVA with Dunnett's test with 0.05 significance level. $n \geq 3$. Error bars represent standard deviation and where they are not visible their size does not exceed that of the symbol used.

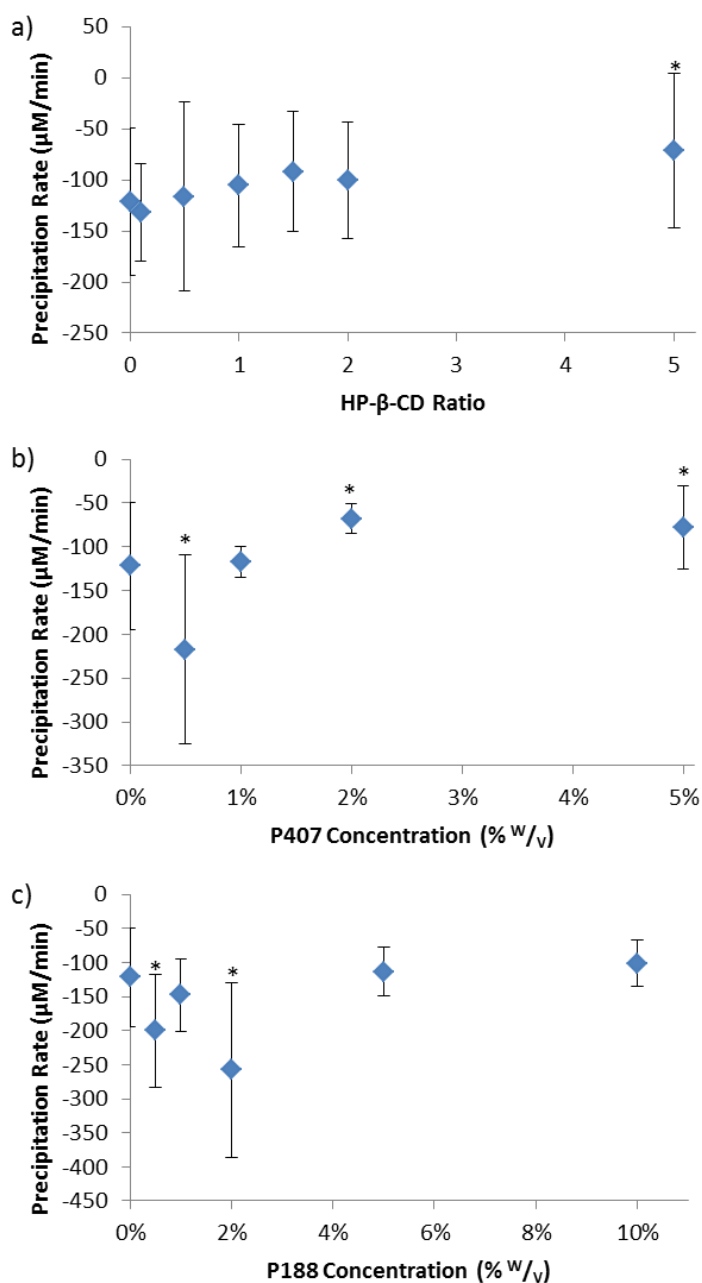


Figure 3.8. Scatterplot showing the mean gliclazide dissolution rates (represented as negative precipitation rates) obtained during CheqSol assays with increasing concentrations of a) HP-β-CD, b) P407, and c) P188. * Represents statistically significant difference from control group, 0, following ANOVA with Dunnett's test with 0.05 significance level. $n \geq 3$. Error bars represent standard deviation and where they are not visible their size does not exceed that of the symbol used.

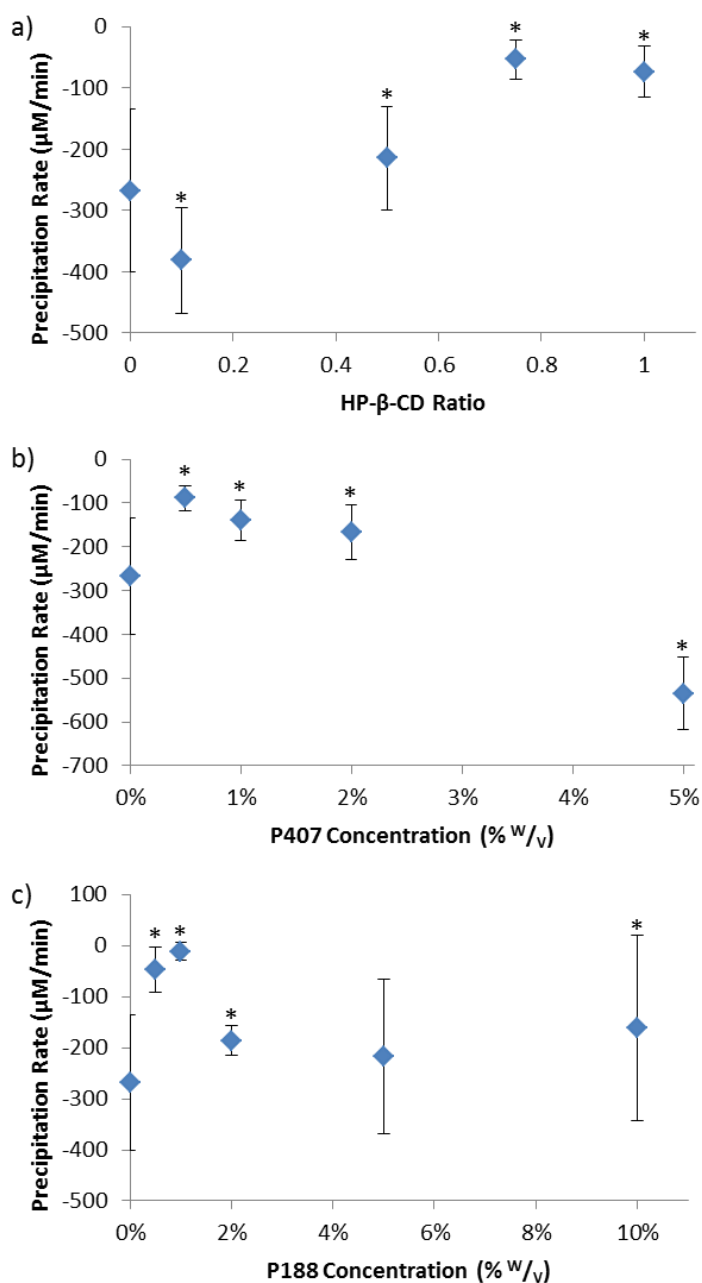


Figure 3.9. Scatterplot showing the mean ibuprofen dissolution rates (represented as negative precipitation rates) obtained during CheqSol assays with increasing concentrations of a) HP-β-CD, b) P407, and c) P188. * Represents statistically significant difference from control group, 0, following ANOVA with Dunnett's test with 0.05 significance level. $n \geq 3$. Error bars represent standard deviation and where they are not visible their size does not exceed that of the symbol used.

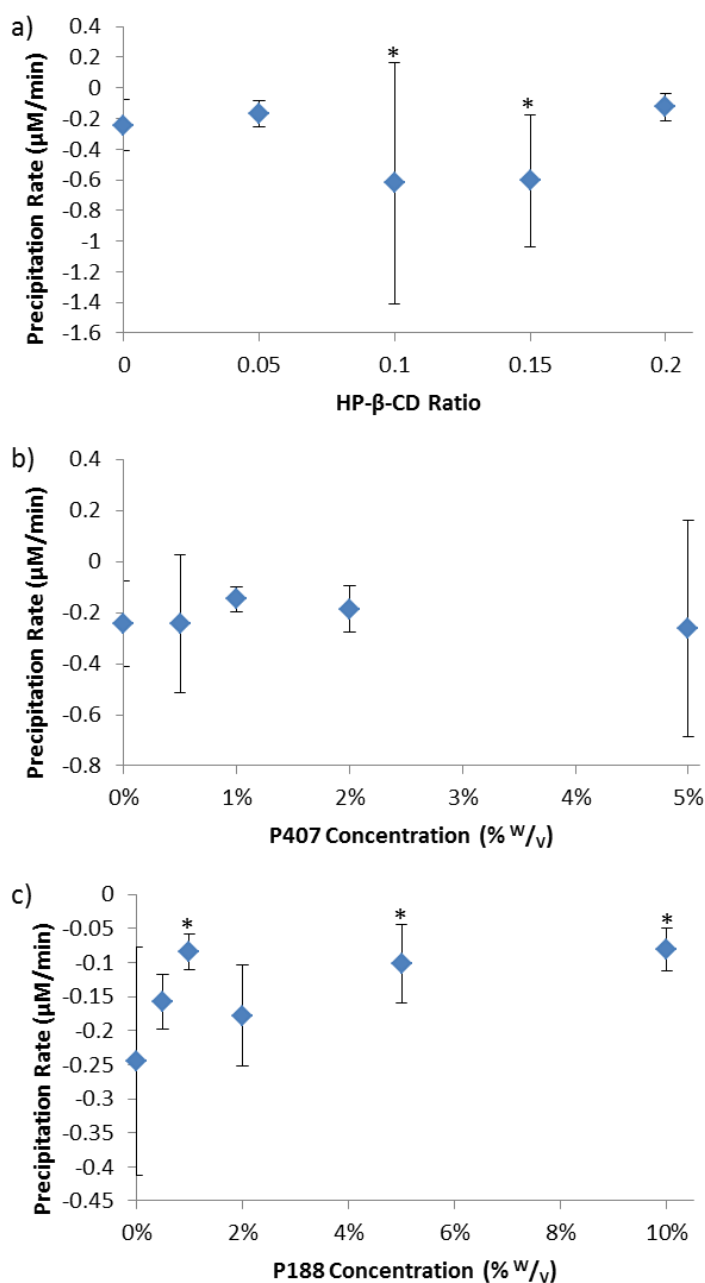


Figure 3.10. Scatterplot showing the mean atenolol dissolution rates (represented as negative precipitation rates) obtained during CheqSol assays with increasing concentrations of a) HP-β-CD, b) P407, and c) P188. * Represents statistically significant difference from control group, 0, following ANOVA with Dunnett's test with 0.05 significance level. $n \geq 3$. Error bars represent standard deviation and where they are not visible their size does not exceed that of the symbol used.

3.6.3 Disc Dissolution Assays

Following MEC determination the pK_as of the four compounds were found to be 9.50 for propranolol, 5.62 for gliclazide, 4.52 for ibuprofen and 9.54 for atenolol.

Propranolol dissolution rates in the presence of all three excipients (0.0412 M HP- β -CD, 10% w/v P407 and 10% w/v P188) were lower than the dissolution rate in acetate phosphate alone. ANOVA analysis had a p-value < 0.0005 (Figure 3.11a). The dissolution rate of gliclazide is only significantly affected by the presence of 0.0426 M HP- β -CD; overall p-value < 0.0005 (Figure 3.11b). The dissolution rate of ibuprofen in the presence of all excipients was significantly different to dissolution in the buffer alone, p-value < 0.0005. Poloxamers reduce the dissolution rate of ibuprofen, whereas the presence of the cyclodextrin results (0.0426 M) in an increase in dissolution rate (Figure 3.11c). Atenolol dissolution rate is decreased in the presence of both poloxamers. HP- β -CD (0.0211 M) was not found to affect the dissolution rate of atenolol, p-value = 0.001 (Figure 3.11d)

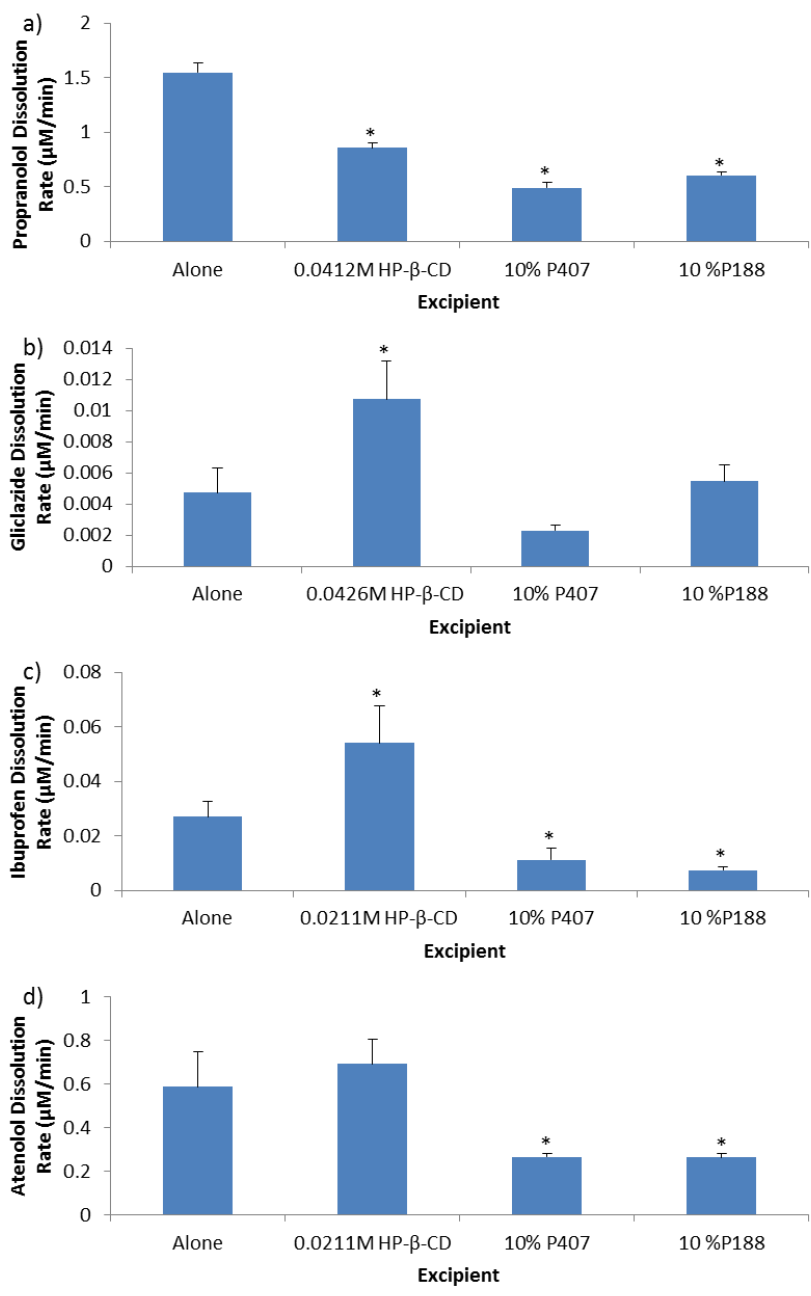


Figure 3.11. Mean dissolution rates of four drug compounds in different media \pm SD. * represents a statistically significant difference when compared to the control group (alone). a) propranolol, calculated from first 31 points assay, b) gliclazide, calculated from all points in assay, c) ibuprofen, calculated from all points in assay, d) atenolol, calculated from first 31 points in assay. Error bars are standard deviation, with $n \geq 3$.

3.6.4 Excipient Gain Factor

In the case of propranolol, the EGF for all three excipients is statistically greater than 1 at the highest concentrations used (Figure 3.12a). This is in contrast to the EGF for each excipient with atenolol where none of the three excipients were shown to affect the EGF (Figure 3.12b). For gliclazide neither P407 nor P188 affected the EGF. Only HP- β -CD, at the three highest molar ratios used, was shown to affect the EGF of gliclazide (Figure 3.13a). For ibuprofen, the only excipient and concentration which was shown to increase EGF above 1 was P407 at the 5% ^{w/v} concentration (Figure 3.13b).

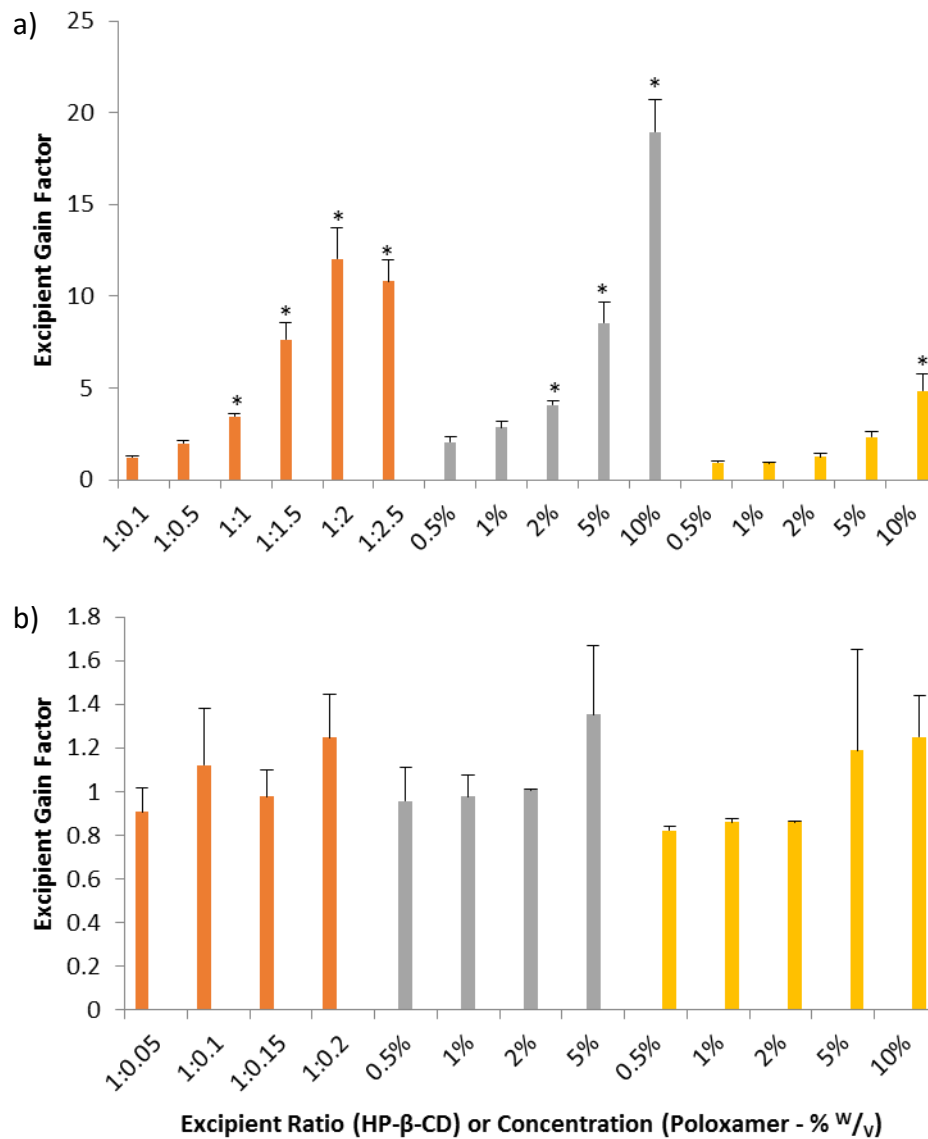


Figure 3.12. The EGF of a) propranolol and b) atenolol in HP-β-CD (orange bars), P407 (grey bars) and P188 (yellow bars). * represents statistical difference from EGF of 1, where p-value < 0.05. Error bars are standard deviation, with n ≥ 3.

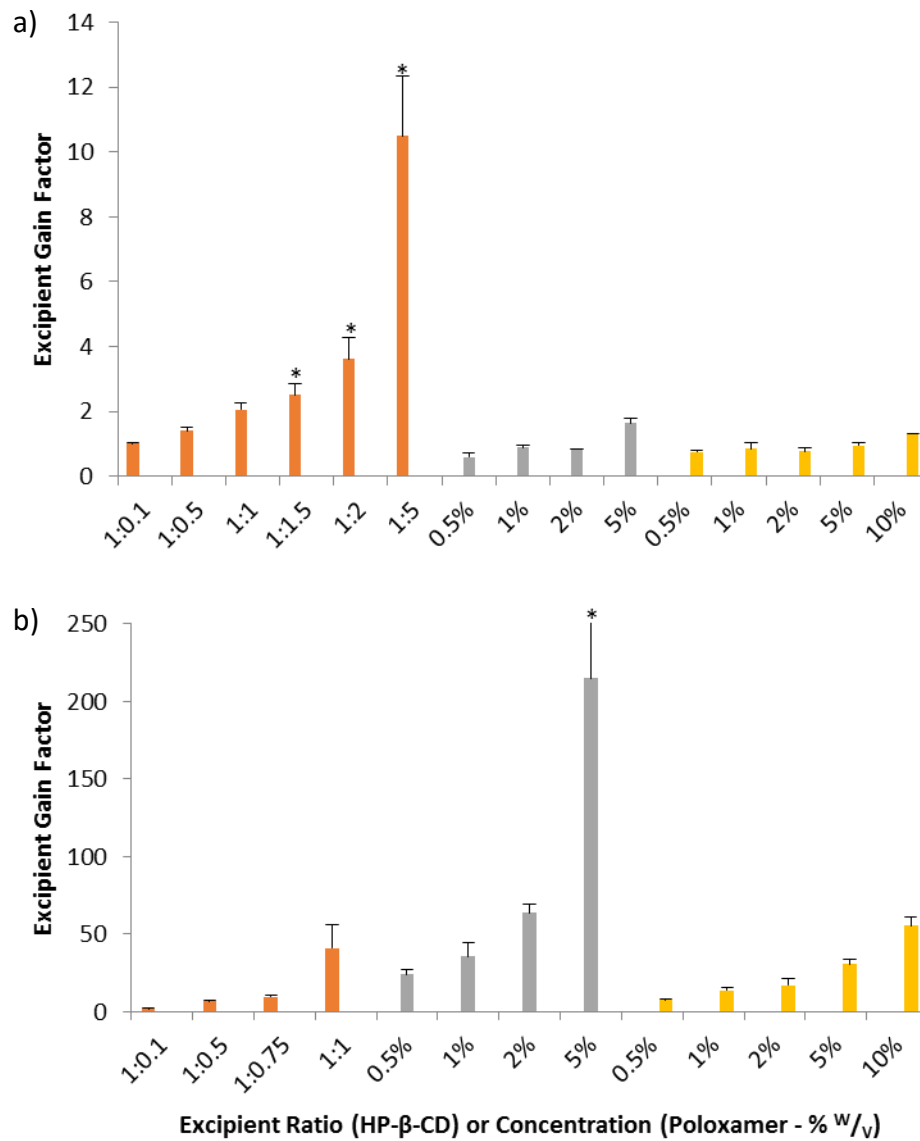


Figure 3.13. The EGF of a) gliclazide and b) ibuprofen in HP-β-CD (orange bars), P407 (grey bars) and P188 (yellow bars). * represents statistical difference from EGF of 1, where p-value < 0.05. Error bars are standard deviation, with n ≥ 3. Ibuprofen and 5% w/v P407 standard deviation is 187 (error bar cut-off for clarity).

3.6.5 Excipient Solution Viscosity

All excipient solutions had a statistically higher viscosity than acetate phosphate used in the disc dissolution assays (Table 3.1). The viscosity of P407 was greatest at 6.4 mPa.s; this was followed by P188 with a viscosity of 4.7 mPa.s. HP- β -CD had a viscosity only slightly greater than acetate phosphate (1.2 mPa.s and 0.95 mPa.s respectively).

Table 3.1. Viscosity of excipient solutions used during disc dissolution assays.

Excipient Solution	Viscosity (mPa.s)
Acetate Phosphate	0.9470 \pm 0.00888 ^a
0.0426 M HP- β -CD	1.204 \pm 0.0194 ^{a,*}
10% ^{w/v} P407	6.416 \pm 0.160 ^{a,*}
10% ^{w/v} P188	0.0270 ^{a,*}

^a – \pm is the standard deviation, n = 3

* – represents statistically significant difference from control following ANOVA

Solution flow behaviour index (n) was determined from fitting data to Ostwald de Waele equation (Figure 3.14). Acetate phosphate buffer, 10% ^{w/v} P407 and 10% ^{w/v} P188 were found to be Newtonian fluids with mean n = 1 \pm 0.02 (allowing for 2% error in the rheometer). The solution of HP- β -CD was found to have an average n = 0.974,

suggesting shear thinning solution, however two out of three repeats had indexes of 1.000 and 1.003, with the third having $n = 0.919$ (Table 3.2).

Table 3.2. Flow behaviour index of excipient solutions used during disc dissolution assays.

Excipient Solution	Flow Behaviour Index (n)
Acetate Phosphate	1.002 ± 0.009^a
0.0426 M HP- β -CD	0.974 ± 0.048^a
10% w/v P407	1.001 ± 0.003^a
10% w/v P188	1.000 ± 0.003^a

^a – \pm is the standard deviation, $n = 3$

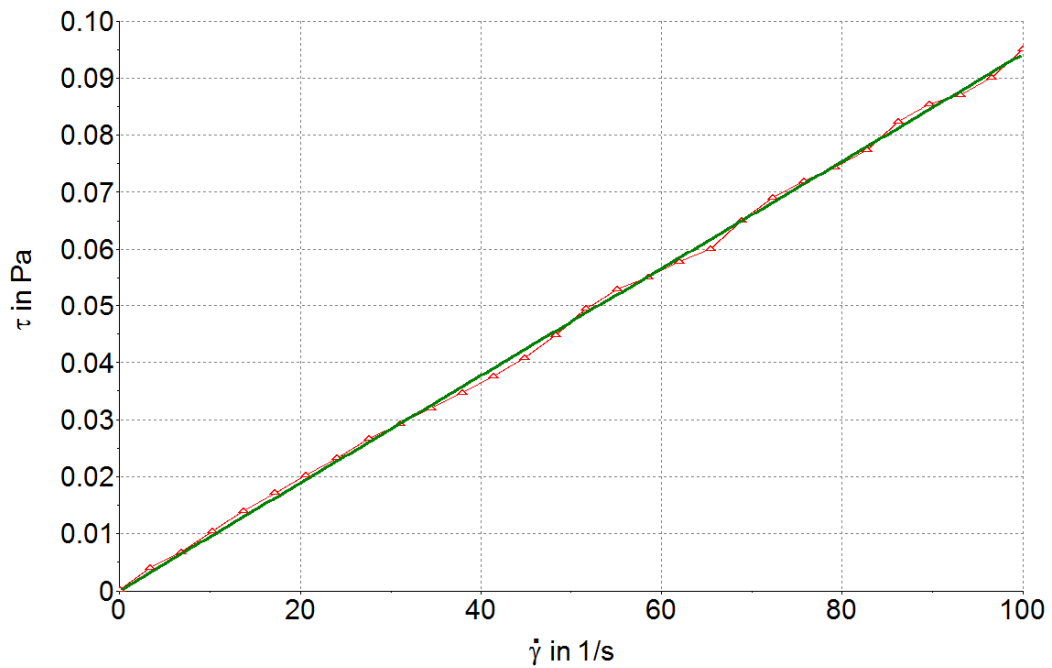


Figure 3.14. Example plot of τ (Pa) vs $\dot{\gamma}$ (s^{-1}), sample represents first acetate phosphate buffer run. Hollow red triangle with line behind is the data recorded by the software; solid green line is the Ostwald de Waele fitted line. The fitted results are: $K = 0.0009479$, $n = 0.9987$, $r^2 = 0.9996$.

Figure 3.15 represents the mean τ (Pa) vs $\dot{\gamma}$ (s^{-1}) for the acetate phosphate buffer and the three excipients examined. From the plot it can be observed that as the shear rate increases the shear stress for all four solutions increases. The effect is greatest for P407 followed by P188. The effect on acetate phosphate and HP- β -CD are similar, with shear rate resulting in a slight increase in shear stress for HP- β -CD when compared to acetate phosphate (Figure 3.15).

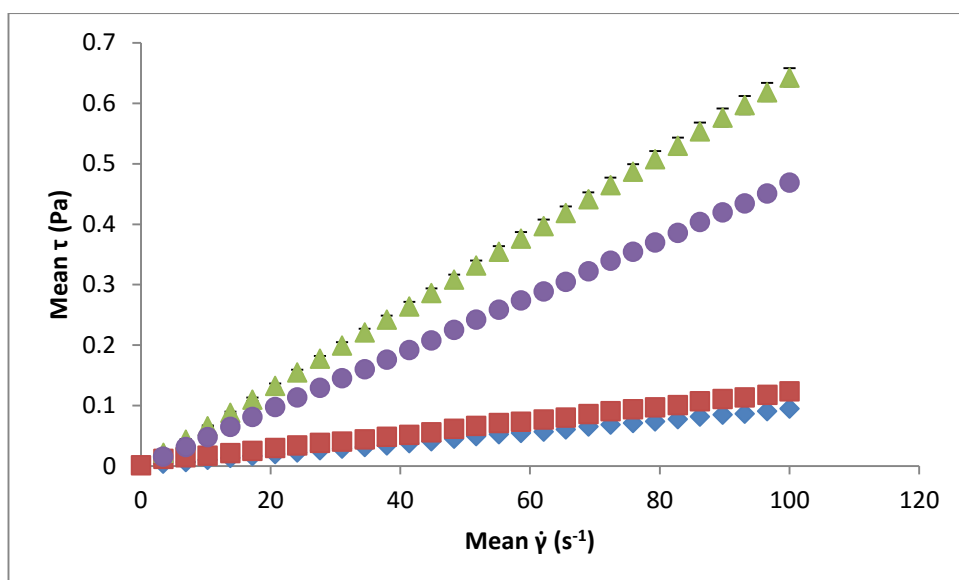


Figure 3.15. Scatterplot showing the mean τ (Pa) vs $\dot{\gamma}$ (s^{-1}) for all solvents investigated. (\blacklozenge) acetate phosphate buffer, (\blacksquare) HP- β -CD (0.0426 M), (\blacktriangle) P407 (10% w/v) and (\bullet) P188 (10% w/v). $n = 3$. Error bars represent standard deviation and where they are not visible their size does not exceed that of the symbol used.

3.7 Discussion

3.7.1 Precipitation Rates: CheqSol

HP- β -CD

Iervolino *et al.* have shown that ibuprofen precipitation can be delayed in the presence of between 1% w/v and 10% w/v HP- β -CD (160). They showed that nucleation was inhibited over 36 hours when a 6 mg/mL solution of ibuprofen was added to a 4:6 propylene glycol: water mix; when cyclodextrin was absent precipitation was observed at beginning of the experiment (160). Precipitation rates observed in these experiments agree with the results of Iervolino *et al.* at the highest ratios of drug to HP- β -CD (1:0.75 and 1:1) precipitation rate was reduced. When the

amounts used per experiment, at the highest ratios, were converted to the same units used by Iervolino *et al.* It was found that at least 1.5% w/v was present in the vials at the start of the assays. However, the concentration at the 1:0.5 molar ratio had an average concentration of 1.1% w/v and was found to have no effect on precipitation rate. The standard deviation of mean precipitation rates recorded for this group was large and could be related to the concentration differences used during the experiments, % w/v for HP- β -CD ranged from 0.6 to 1.7 for the 1:0.5 molar ratio. Precipitation reduction via nucleation inhibition was thought to be due to an alteration of the metastable zone and the increased solubility of ibuprofen in the presence of HP- β -CD (160). Cyclodextrins have been shown to decrease the precipitation of other drugs including itraconazole (156) and celecoxib (136), thus it can be concluded that cyclodextrins may reduce precipitation rate of compounds. No literature information could be found which studied the effect of HP- β -CD on propranolol, atenolol or gliclazide precipitation rates, and may be the first reporting of the HP- β -CD induced precipitation rate reduction for these drugs. It has been suggested that the modified cyclodextrins, such as HP- β -CD, can elicit effects via both complexation and non-complexation mechanisms (156).

Poloxamers

Crystal growth rate reduction has been observed for ibuprofen in the presence of increasing concentrations of P407 by Vetter *et al.* (161). The authors concluded that the crystal growth rate reduction was accounted for by adsorption of the poloxamer onto the surface of the crystal (161). This disagrees with the results seen here, as

both poloxamers were shown to increase precipitation rate at high concentrations. For ibuprofen and propranolol, both poloxamers increased precipitation rate at high concentrations, which is unexpected. This is not the first time that an increase in precipitation rate in the presence of excipient has been observed. Ilevbare *et al.* noted that the crystal growth rate of ritonavir in the presence of the novel cellulose polymer CAB Adp 0.25 was the same if not faster than the drug alone (162). A reduction in precipitation rate despite an increase in solubility could possibly be down to the interaction between drug and poloxamer. If the poloxamer does not adsorb onto the crystal structure then precipitation rate may be influenced by the number and size of particles or the width of the diffusion layer surrounding the crystals. This however cannot explain the results observed here for ibuprofen, as P407 adsorbs onto the crystal surface. The increase may be due to the method of obtaining the results, i.e. using CheqSol. The effect that P407 has on the nucleation rate of ibuprofen was not investigated by Vetter *et al.* as seed crystals were utilised during the experiments (161). No literature on the effects of P407 on ibuprofen nucleation could be found. The precipitation rate of atenolol was unaffected by large concentrations of poloxamer. Gliclazide precipitation rate decreased at high poloxamer concentrations, which was expected. The effect of poloxamers on the precipitation rates of the other drugs under investigation was not found in the literature.

Poloxamers have been found to have effects on the precipitation rate of other compounds in the literature. The crystal size of siramesine was reduced when

precipitated in the presence of P188 (0.025 %^{w/v}). The crystal size was reduced from 57 $\mu\text{m} \pm 4.7$ to 17 $\mu\text{m} \pm 7.2$ (163). Reduction in crystal size is thought to be the result of P188 adsorption onto the crystal surface preventing further growth (163). Every poloxamer may not have the same effect on precipitation for a specific drug. The results observed here show that for the drugs examined both poloxamers had a similar effect on precipitation inhibition. Guzmán *et al.* have shown that the different poloxamers are not all capable of inhibiting precipitation (136). They also demonstrated that at concentrations below the poloxamer CMC precipitation inhibition was not observed (136). This disagrees with results obtained by Dai *et al.* who found that P407 inhibited precipitation of the base under investigation whereas P188 did not (152). Dai *et al.*, however, conducted experiments with poloxamer concentrations below the CMC, although the method of precipitation involving a pH change was similar (152).

As detailed above, inhibition of crystal growth by poloxamers has been observed. The more hydrophobic block of the poloxamers can adsorb onto the crystal with the more hydrophilic POE blocks in the bulk media (94, 163). The layer of adsorbed poloxamers on the crystal structure has been shown to be non-homogenous (163) which could be due to areas of the crystal which have higher hydrogen bonding moieties (156). Hydrogen bonding has been suggested as the possible mechanism by which nucleation inhibition occurs (164). Raghavan *et al.* stated that the polymers with higher hydrogen bonding moieties are able to prevent crystal growth and alter crystal shape better than polymers with fewer moieties (164). An increase in viscosity may

also slow down crystal growth rate as diffusion of drug molecules to the crystal surface is delayed (152, 156).

During CheqSol assays conducted, precipitation was not observed in all experiments, despite the non-ionised form being present at a concentration greater than intrinsic solubility. These assays were repeated as no solubility results were obtained. The difference between assays where precipitation was observed is that the amount of drug used tended to be higher than assays where precipitation was absent. The free energy of the system with a lower concentration may not have been sufficient to overcome the maximum ΔG , as discussed by Nielsen, during the assay (147). This does not guarantee that the system would remain in its supersaturated state if left under the same conditions indefinitely; instead nucleation may occur at a delayed time point if localised breaches of the free energy barrier occur (147). Nielsen also demonstrates that n^* is reduced in more concentrated solutions (147).

3.7.2 Dissolution Rates: CheqSol versus Disc Dissolution Assays

According to the Noyes-Whitney equation, increases in solubility would be expected to result in an increased dissolution rate as the difference between bulk concentration and saturation solubility would be increased (Equation 3.3). This was not always observed, with the poloxamers during disc dissolution assays (chapter 3.6.3). A decrease in dissolution rate could be the result of an increase in the thickness of the saturated layer at the interface. It could also be the result of a decrease in diffusion coefficient and solute surface area. This will be discussed.

HP- β -CD

From the results it can be observed that dissolution rate is affected by the presence of the excipients under investigation. During CheqSol assays, HP- β -CD was found to decrease the dissolution rate of propranolol at molar ratios above 1:0.5. The dissolution rate was also observed to decrease during disc dissolution assays. Only one article examining the dissolution rate of propranolol in the presence of a cyclodextrin could be found in the literature. This paper looked at the differences between dissolution rates of different propranolol stereoisomers from a 1:1 complex with β -CD; however the dissolution rate of propranolol alone was not investigated for comparison (165). The complex in the paper was formed by freeze-drying a solution of racemic propranolol and β -CD; Duddu *et al.* found that there was no difference in dissolution rates of between the two stereoisomers when formed into a 1:1 complex with β -CD (165). The results from Duddu *et al.* are lower than the results for disc dissolution assays carried out here. The disc dissolution assays had a mean dissolution rate of 3.14 mg/min cm², compared to 1.42 and 1.45 mg/min cm² as reported in the paper (165). These results are however not comparable since the cyclodextrin and molar ratios differ between the two studies. In CheqSol assays, the observed decrease in dissolution rate could be due to changes in surface area, but cannot be evaluated at this point as this information is unknown. However, the surface area during disc dissolution assays was constant and known at the start of the assay, suggesting surface area is not the cause of the decrease. The thickness of the layer at the interface could be affected by the stirring rate. However, stirring

rates were constant for each assay type. Decreases in diffusion coefficient could be a factor, but the viscosity of the highest concentration of HP- β -CD was only slightly greater than the control buffer and the effect was observed at lower concentrations. The dissolution rate results could also be down to solubility; at pH 8.5 where the dissolution rates were determined the majority of molecules are in the ionised state. The ionised molecules, as seen in chapter 2.6.4, have a lower affinity for HP- β -CD and the solubility of ionised propranolol decreased as the concentration of HP- β -CD increased (chapter 2.5.4).

Disc dissolution assays carried out on gliclazide produce results which agree with literature findings that HP- β -CD increases the dissolution rate of gliclazide. The work carried out by Sharma *et al.* show that increasing the amount of HP- β -CD in a solid complex (1:0.5 to 1:1 gliclazide:HP- β -CD molar ratios) increases the dissolution rate (128). The experiments conducted by Sharma *et al.* were in pH 7.4 buffer and at 37°C, whereas work carried out here was in buffer at pH 6.5 and at room temperature. Other work has shown the effect the parent β -CD has on gliclazide dissolution. Özkan *et al.* have shown that gliclazide dissolution rate at pH 1.2 and 37°C is increased when gliclazide: β -CD complexes are dissolved in 0.1 M HCl (81). β -CD was also been also shown to increase the dissolution of gliclazide in artificial gastric juice at pH 1.2 by Moyano *et al.*, with experiments conducted at 37°C (166). These results are not comparable to the work carried out in the disc dissolution experiments as the complexes were not prepared in advance of assays. Instead solid drug was dissolved into a solution of the cyclodextrin. The ability of cyclodextrins to increase the

dissolution rate of gliclazide is evident in the literature and the results found here, an effect which may be non-discriminatory with regards to ionised state. In disagreement with the above, dissolution rates observed during CheqSol assays display a decrease in dissolution rate at the highest molar ratio (1:5) and unaffected at lower molar ratios. Özkan *et al.* have shown that the dissolution rate enhancement is affected by the method of complex preparation used. Increases in dissolution rate for physical mixtures has been associated with increased wetting of the compound (81).

HP- β -CD has previously been shown to increase the dissolution rate of ibuprofen. Mura *et al.* demonstrated that in unbuffered water, with a pH \approx 6, β -CD, methyl- β -CD, hydroxyethyl- β -CD and HP- β -CD increase the dissolution rate of ibuprofen at 37°C (130). These results agree with the dissolution rates obtained during disc dissolution assays but disagree with the dissolution rates observed during CheqSol assays (see below and chapter 3.7.3). The results from literature and the disc dissolution experiments carried out here suggest that the dissolution rate of both forms of ibuprofen molecules may be increased in the presence of HP- β -CD (130). As with gliclazide, dissolution rate reduction was observed during CheqSol assays.

The dissolution rate of atenolol has been shown to be increased by the presence of HP- β -CD in the formulation by Jalindar *et al.* (167). Although details of the conditions used for dissolution are not fully given, both distilled water and phosphate buffer at pH 1.5 were used. At both pHs the dissolution rate of atenolol was increased

compared to atenolol alone (167). These disagree with the results obtained here. It may be due to the state of the molecule. At pH 1.2 and in distilled water, atenolol would be mostly ionised, whereas at pH 10.5 unionised molecules would dominate. This is one explanation, however HP- β -CD has a greater affinity for unionised molecules (65, 85), and thus the increase in dissolution rate of atenolol at pH 10.5 would be expected to be greater in the presence of HP- β -CD than at pHs below 7.5.

It was noted that dissolution rates calculated from CheqSol assays usually decreased or remained the same in the presence of HP- β -CD. During CheqSol assays the system is under near equilibrium conditions. In the presence of HP- β -CD there are four states in which the compound may be found (Scheme 4.2). These are unionised, ionised, and in complexation with the cyclodextrin (both unionised and ionised, although as previously stated the amount of ionised drug complexed may be low). For an acid, if the pH increases more drug will need to dissolve as the equilibrium shifts to replace the depleted H^+ from the system. In the presence of HP- β -CD the depleted H^+ ions can be replaced from more than one equilibrium. This could be the reason that dissolution rate appears to be reduced. As the system re-equilibrates itself the amount of drug required to dissolve may be reduced thus decreasing dissolution rate.

Poloxamers

Propranolol release from P407 has previously been found to decrease as the concentration of P407 increases (168) agreeing with the results found. This release however, is from higher concentrations (between 20% w/v and 30% w/v) which form

gels at room temperature and the dissolution could therefore be reduced due to the resistance from the gel structure. The dissolution rate of propranolol in 10% ^{w/v} P188 increased during CheqSol assays, although this increase was associated with large standard deviation. No information on the effect of lower concentrations of poloxamers on propranolol dissolution rate could be found in the literature.

Gliclazide dissolution rates have previously been shown to be increased by the presence of poloxamers, in disagreement with the findings here. Islam *et al.* reported an increase in dissolution rate of gliclazide in varying molar ratios of gliclazide/P407 solid dispersions and physical mixtures at pH 7.4 (169). Both El-Maghraby and Alomrani, and Reddy *et al.* have shown that P188 increases the dissolution rate of unionised gliclazide (media at pH 1.2) in mass ratios ranging from 1:1 to 1:5 (170, 171) compared to the drug alone. Similarly to the case found in literature cyclodextrin dissolution studies, poloxamer was undissolved in the medium at the start of the assay, but was present in the formulation, which differs from the conditions seen in these experiments.

Dissolution rates of ibuprofen from solid dispersions and physical mixtures with P407 are increased compared to the drug on its own (172). This agrees with the dissolution rate at the highest poloxamer concentration during CheqSol assays but disagrees with lower concentrations and the dissolution rate observed during disc dissolution assays. Yong *et al.* have shown that in preparations containing P188 and ibuprofen, the dissolution rate of the drug is not significantly affected by the poloxamer (173).

It has also been shown that the method of preparation of an ibuprofen/P188 formulation can affect the dissolution rate improvement observed. Solid dispersions and melt granules increase ibuprofen dissolution rate whereas physical mixtures had no effect on the dissolution rate (174). The results observed in disc dissolution assays do not agree with the literature results, which instead show a decrease in dissolution rates. The dissolution rates determined during CheqSol assays do not show a clear pattern. At 0.5% w/v, 1% w/v, 2% w/v and 10% w/v P188 dissolution rates of ibuprofen are increased compared to drug alone, however the increase is not concentration dependent. At 5% w/v and 10% w/v P188 there is large variation in the determined rates.

Poloxamer 407 has been shown to affect atenolol dissolution rates differently. Microparticles prepared with atenolol and P407 showed no change in dissolution rate, as observed during CheqSol assays. However when these microparticles were compacted into tablets the dissolution rate decreased (135), similar to the results observed here during disc dissolution assays. As shown by Albertini *et al.* compaction of atenolol into tablets may reduce the dissolution rate compared to atenolol alone. This was observed when P407 was present in the tablet or present in the dissolution medium. The reduction in dissolution rate following compaction compared to powder could be linked to a reduced surface area. No literature on the effect of P188 on atenolol dissolution rate could be found.

One reason that the poloxamers may reduce the dissolution rates of compounds is by an effect related to their viscosity. Poloxamers may reduce the effect that stirring has on the medium with reduced movement, increasing the thickness of the layer in contact with the undissolved drug. This could also negatively affect the diffusion coefficient, decreasing diffusion away from the saturated layer. These effects would lead to a reduction in dissolution rate according to Noyes-Whitney (Equation 3.3). The method of formulation preparation can affect the dissolution rate enhancement offered by poloxamers as shown by Rouchotas *et al.* Phenylbutazone that has been surface modified with P407 has increased dissolution rate when compared to phenylbutazone/P407 solid dispersions (94).

General Discussion

For atenolol and propranolol, the dissolution rates measured during disc dissolution assays were calculated based on the first 31 data points, representing 15 and a half minutes. Data points nearing the end of the assay for these two compounds poorly fit the model, as a result of the more extensive dissolution observed, in some cases for atenolol, dissolution was complete by the end of the assay. Where the amount dissolved was greater, the surface area of the tablet is no longer equal to the starting surface area of 7.07 mm², leading to changes in Equation 3.3 not related to bulk concentration. For gliclazide and ibuprofen, where dissolution was less extensive, all data points were included.

The rates observed during CheqSol and dissolution assays cannot be quantitatively compared as the conditions under which dissolution rate is measured are not equivalent. In CheqSol assays dissolution rate is measured in near equilibrium conditions as the solution is flipped between sub- and supersaturated states. The CheqSol process also forms the complexes in a manner similar to neutralisation techniques described in the literature (81) as discussed in chapter 2.6.2. This differs from disc dissolution assays as the drug concentrations, and thus complex concentrations, are nil at the beginning of the assay and continuously increase until the assay is finished, solubility is reached, or complete dissolution of the tablet occurs. The concentrations therefore represent either end of the concentration gradient of the Noyes-Whitney equation. Another reason the rates are not comparable is the surface area of the drug. In disc dissolution assays the surface area of the tablet exposed to the dissolution media is 7.07 mm² whereas in CheqSol assays the surface area is unknown due to the presence of multiple nucleation points of unknown size. The surface area during CheqSol assays may change as the repeating cycles of precipitation and dissolution progress. The effect on dissolution rates was compared in a qualitative manner, to determine if the effect on dissolution rates was similar between both assay types. When investigating the effects of HP-β-CD, the molar ratios used between the two assays types were not the same with disc dissolution using greater amounts of cyclodextrin per mole of drug than CheqSol assays.

From the methods stated, dissolution assays are commonly determined when the excipient under investigation is present in the formulation and dissolves with the active ingredient. This was not carried out here, as for solubility studies using CheqSol, the excipients were fully dissolved at the point of dissolution and precipitation rate calculation. To allow for comparison of the effects between disc dissolution and CheqSol assays solutions of excipients were prepared. The use of excipients in the formulations may have also altered the absorbances measured as all three excipients absorb UV light (Figure 3.16). To obtain the spectra for Figure 3.16, three random reference spectra taken during disc dissolution assays were sampled and the mean calculated. The mean spectrum for the acetate phosphate buffer was subtracted from the mean spectra of the excipients. As the measurement process is carried out *in situ* without separation, the absorbances measured can be contributed to by all system components. If the excipients are not accounted for in the reference spectrum, absorbances during the dissolution stage cannot wholly be attributed to the drug under investigation. While, for some drugs the absorbance spectra may only be affected slightly by the dissolution of excipient, for some drugs with weak chromophores, such as ibuprofen, there would be a higher impact on the results.

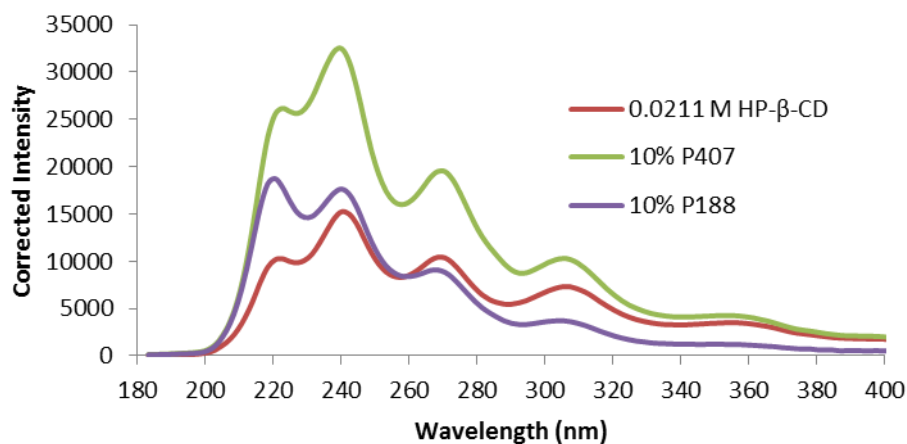


Figure 3.16. Corrected absorbance spectra of excipients. Mean spectra obtained by subtracting the reference spectra of dissolution media from the mean reference spectrum of acetate phosphate (n=3 for all groups).

3.7.3 CheqSol versus Disc Dissolution

An explanation to the differences between dissolution rates measured during CheqSol and Disc Dissolution could be due to excipients affecting crystal growth as discussed above. Thus during CheqSol assays dissolution rate could be further affected by the increased surface area during repeating cycles of dissolution and precipitation. If the excipient reduces crystal growth then the surface area available for dissolution may increase. This is not present during disc dissolution assays as it is a single stage dissolution process.

3.7.4 Excipient Gain Factor

Where EGF is significantly greater than 1, the supersaturated state of the drug is increased in the presence of the excipient. These results represent the first reporting of the effects of these excipients on the four drugs examined as no data on EGFs for the drugs and excipients could be found in the literature. From the results it is observed that all three excipients can increase the supersaturated state of propranolol at the highest concentrations. All three of the excipients were shown to increase kinetic solubility of propranolol at some concentrations during CheqSol studies (see chapter 2.5.4), which would agree with the results obtained here, as an increase in kinetic solubility would contribute to an increase in EGF. This would also be expected to require a reduced precipitation rate for stabilisation of the supersaturated state. For propranolol this was not observed with P407 and P188 (see chapter 3.6.1) with both poloxamers increasing precipitation rate at high concentrations. However, these precipitation results, were obtained from near equilibrium states which as described above (chapter 3.7.1) could have other factors affecting the rates.

The EGF results for gliclazide were also unexpected. Unlike propranolol all three excipients reduced the precipitation rate of gliclazide, but only HP- β -CD and P407 were shown to increase kinetic solubility (chapters 2.5.4 and 3.6.1). Both HP- β -CD and P407 would therefore be expected to show an increase in EGF, instead of just the cyclodextrin. P188 may have been expected to stabilise the supersaturated state,

and therefore increase the EGF, due to its effect on precipitation rate but this was not observed.

In the case of ibuprofen, P407 was the only excipient shown to increase EGF at 5% w/v (the size of which is large). The result however has a large standard deviation which may be affecting the ANOVA test carried out on the data. Further studies into the effect of the excipients could be carried out to determine if this is the case. When compared to the precipitation and kinetic solubility results obtained earlier, HP- β -CD would be expected to show an increase in EGF as ibuprofen precipitation rate was decreased and kinetic solubility was increased in its presence. Both P407 and P188 resulted in an increase ibuprofen precipitation rate and kinetic solubility, which could be expected to increase EGF (see chapters 2.5.4 and 3.6.1).

None of the excipients were shown to increase the EGF of atenolol, which agrees with the precipitation results obtained in chapter 3.6.1. However the results disagree with the atenolol kinetic solubility results – both poloxamers were shown to increase the kinetic solubility during CheqSol assays (chapter 2.5.4).

This technique for determining supersaturation in the presence of excipients, as described by Bevernage *et al.*, was used with the solvent-shift method of supersaturation with a specified and constant sampling period (158). The methods used here were not the solvent-shift method and the precipitation was induced by changing the pH to reduce the drug's solubility. The sampling time for each assay

also varies, due to the nature of the method. The AUC data did not have separate data for the intrinsic solubility like the work by Bevernage *et al.*, however the AUC does include the final intrinsic solubility in the AUC of each assay (158). Despite these differences, the EGF should provide information on the supersaturation taking place during each assay.

3.7.5 Measuring ‘Spring and Parachute’ Effects Using T3

As can be seen the T3 has the capabilities of detecting changes in dissolution and precipitation rates. However, the inconsistencies obtained between disc dissolution and CheqSol assays mean that further experiments would need to be carried out before any conclusions on the usefulness of using CheqSol data to investigate ‘spring and parachute’ effects could be drawn. Further research into the use of EGF data obtained from CheqSol assays should be carried out and compared to data from traditional methods to determine if the results are comparable.

The way in which dissolution and precipitation rates are calculated during CheqSol assays may affect the results. As the system is flipped between sub- and super-saturated states, and the drug dissolves and precipitates, the effects of the excipients on the growing crystals may be altered. For example, as detailed poloxamers have been shown to adsorb onto crystal surfaces reducing growth, if this crystal is then exposed to a sub-saturated solution dissolution may be reduced due to reduction in the diffusion of molecules away from the crystal and into the bulk solution. The adsorption onto the crystal surface may further affect precipitation/dissolution rates

as new nuclei may need to be formed for precipitation to take place. An increase in nuclei, and therefore an increase in surface area, could provide enough sites to overcome the dissolution rate reductions which may be observed.

3.8 Conclusions

While changes in dissolution and precipitation rates can be recorded during CheqSol assays, the process of repeated dissolution and precipitation may not be suitable for 'spring and parachute' measurements. The cycling between different states would not be found during transit through the GIT, nor during the normal reconstitution or formulation of drugs for other administration routes. The CheqSol method would also not be suitable in determining the time for precipitation to be observed as pH changes are utilised, which induces precipitation. Examination of precipitation and dissolution rates obtained during CheqSol reveals alterations of the rates during equilibrium chasing. If CheqSol precipitation and dissolution rates are to be examined they may be able to provide rough information on the possible effects induced by excipients, however further study would need to be conducted for more accurate data.

4 Chapter 4 – Association Constants

4.1 Introduction

As discussed formulations can be developed which affect the solubility, dissolution and/or precipitation of a drug. Knowledge of these effects induced by such excipients is important during drug formulation development, and any associations between excipients and the active ingredient in a formulation have to be considered. When there is association between the excipient and the drug compound, resulting in changes to the physicochemical properties, the strength of the association should also be considered. For immediate release drug delivery, the drug should be easily released from the complex or micelle. However this association should also be strong enough to allow the benefits of increased solubility and bioavailability to be achieved (175).

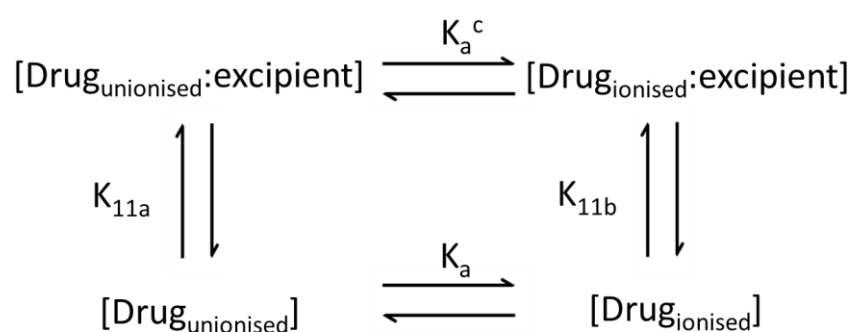
Simulations by Stella *et al.* have demonstrated the effects that dilution, protein binding and competitive binding can have on the amount of drug bound to cyclodextrin (176). Dilution was found to have a greater effect on the percentage bound for the theoretical compound with the lower association constant (610 M^{-1}) compared to the more highly associated compound (10000 M^{-1}), with a 1000-fold dilution reducing percentage bound from 98% to 5.7% and from 99.9% to 47.5% respectively (176). The authors also demonstrated that in the presence of a species which can compete for cyclodextrin binding, there was a further reduction in the amount of bound compound following dilution, with higher association constants for

the competitive agent having the more pronounced effect (176). A similar effect was produced in the presence of a protein with which the compound binds with increasing association constants having the greater effect (176). These effects have been observed *in vivo*, when cinnarizine is administered to beagle dogs, alone and in complex with β -CD there is no difference in AUC, however when DL-phenylalanine is co-administered at increasing doses with 1:2 cinnarizine: β -CD complex the AUC of cinnarizine increases (177). It was also shown that DL-phenylalanine did not increase the absorption of cinnarizine when not administered in complex with β -CD (178). This requirement for a competitive agent to release the drug from the complex was lost when either HP- β -CD or SBE- β -CD were used to increase the solubility of cinnarizine (179). The association constants for β -CD, HP- β -CD and SBE- β -CD were determined to be 6200 M^{-1} , 2242 M^{-1} and 4276 M^{-1} respectively (179, 180). Tokomura *et al.* suggested that the bioavailability of cinnarizine did not increase when complexed with β -CD due to the high association constant and required the presence of DL-phenylalanine to release the drug (178). However this trend was not followed with HP- β -CD and SBE- β -CD, as there was no difference in bioavailability between the two different cyclodextrins despite SBE- β -CD having a much larger association constant compared to HP- β -CD (179). The data cannot be directly compared however, as Järvinen *et al.* did not investigate cinnarizine:HP- β -CD capsules (only a solution), and so no conclusions about bioavailability differences between this and SBE- β -CD for this form can be drawn (179). The molar ratios of cinnarizine:SBE- β -CD were also greater than cinnarizine: β -CD, 1:4.6 compared to 1:2, which may be affecting the results (177, 179).

4.1.1 Determination of Association Constants

Association constants can be determined by different techniques, depending on the experimental procedure and the excipients used. For complexes with cyclodextrin the drug molecules will associate with either one or two HP- β -CD molecules (see chapter 2.6.5, whereas the interaction with poloxamer micelles may involve many more molecules (181).

For complexes with a 1:1 stoichiometry, in a single phase system (e.g. solution of complexing agent and compound in water), four equilibriums exist. Scheme 4.1 represents the four equilibriums in relation to each other.



Scheme 4.1

Where K_a and K_a^c are the dissociation constants of the drug in water and excipient respectively. The complex association constants for the unionised and ionised species are represented by K_{11a} and K_{11b} . For a monoprotic acid, the corresponding equations for the constants are (182):

$$K_a = \frac{[H^+][A^-]}{[HA]} \quad \text{Equation 4.1}$$

$$K_a^c = \frac{[H^+][AL^-]}{[HAL]} \quad \text{Equation 4.2}$$

$$K_{11a} = \frac{[HAL]}{[HA][L]} \quad \text{Equation 4.3}$$

$$K_{11b} = \frac{[AL^-]}{[A^-][L]} \quad \text{Equation 4.4}$$

Similar equations are used for monoprotic bases:

$$K_a = \frac{[H^+][B]}{[BH^+]} \quad \text{Equation 4.5}$$

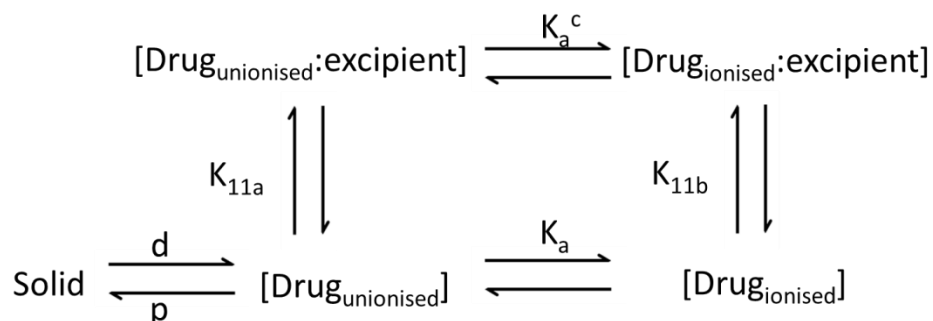
$$K_a^c = \frac{[H^+][BL]}{[BHL^+]} \quad \text{Equation 4.6}$$

$$K_{11a} = \frac{[BL]}{[B][L]} \quad \text{Equation 4.7}$$

$$K_{11b} = \frac{[BHL^+]}{[BH^+][L]} \quad \text{Equation 4.8}$$

Where [B], [BH⁺], [HA] and [A⁻] are the free unionised and ionised concentrations of bases and acids respectively. In the above equations [H⁺] and [L] are the concentrations of hydrogen ion and ligand in the system, and therefore [BL], [BHL⁺], [HAL] and [AL⁻] are the ligand bound unionised and ionised forms of bases and acids respectively. From the equations, it can be observed that higher association constants represent a stronger binding between the drug and complexing agent, represented by a larger proportion of bound to unbound molecules.

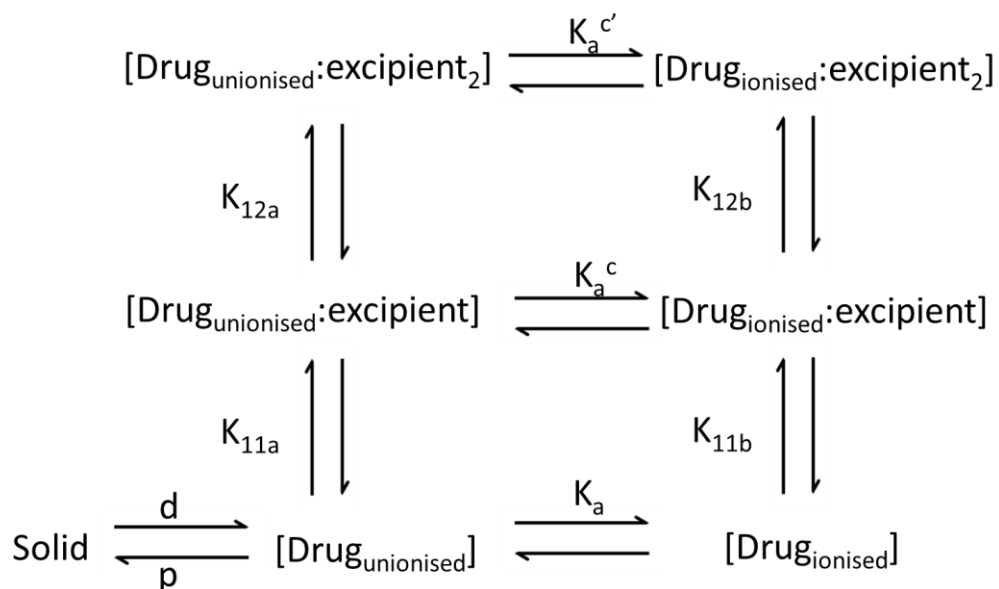
The scheme above however, is not observed during CheqSol or solubility assays as it is complicated by the presence of the solid phase in the system (Scheme 4.2).



Scheme 4.2

The additional constants are the dissolution and precipitation rates, represented by d and p in the above scheme respectively. The system in Scheme 4.2 is not at equilibrium during CheqSol assays, due to the kinetic nature of the measurements. The presence of solid in the system adds another equilibrium which can be accounted for by dissolution and precipitation rates. These equilibrium rates were investigated in chapter 3. Three of the drugs have been shown to form 1:1 complexes with HP- β -CD (122, 138, 140, 141) with gliclazide having been shown to form a 1:2 (gliclazide:HP- β -CD) complex with the cyclodextrin (139).

For the 1:2 complexation an extension to the above schemes is required with K_{12a} and K_{12b} representing the association constants of the unionised and ionised complexes respectively (Scheme 4.3).



Scheme 4.3

$$K_{12a} = \frac{[\text{HAL}_2]}{[\text{HAL}][\text{L}]} \text{ or } \frac{[\text{BL}_2]}{[\text{BL}][\text{L}]} \quad \text{Equation 4.9}$$

$$K_{12b} = \frac{[\text{AL}_2^-]}{[\text{AL}^-][\text{L}]} \text{ or } \frac{[\text{BHL}_2^+]}{[\text{BHL}^+][\text{L}]} \quad \text{Equation 4.10}$$

The overall binding constant for a drug, D, and ligand with the stoichiometry m:n, in either the unionised or ionised form, is given by (183):

$$K_{mn} = \frac{[\text{D}_m\text{L}_n]}{[\text{D}]^m[\text{L}]^n} \quad \text{Equation 4.11}$$

In the case of gliclazide which has been shown to form 1:2 complexes with cyclodextrins (139) the equation for the overall association constant would be:

$$K_{12} = \frac{[G:HP-\beta-CD_2]}{[G][HP-\beta-CD]^2}$$

Equation 4.12

As with complexation, the association with micelles can be examined. Scheme 4.1 and Scheme 4.2 still represent this association. The ligand part of the equations would represent the surfactant micelles, and may not follow 1:1 stoichiometry. The use of the equations described above may not be appropriate for the determination of association constants for micelle forming agents. The methods used are described below.

4.1.2 Complexation Association Constants Determination

A number of methods have been described to determine the association constant between drug and complexing excipient.

Potentiometry

Connors and Lipari described a method to determine association constants for acids using potentiometry. The method involves potentiometric pK_a determinations of the drug in the absence and presence of the excipient. The pK_a^c , measured in the presence of the complexing agent is an apparent pK_a^c (pK_a') due to the presence of solute in the system resulting in non-complexed species of the drug contributing to the pK_a measurement (182).

By ascertaining the pK_a and the pK_a' , the ΔpK_a can be calculated by subtracting the pK_a' in the presence of cyclodextrin from the pK_a of the drug alone (Equation 4.13) (182).

$$\Delta pK_a = pK_a' - pK_a \quad \text{Equation 4.13}$$

For acids, the ΔpK_a can be defined as $\log_{10}C$ and for 1:1 stoichiometry (184):

$$C = \frac{1 + K_{11a}[L]}{1 + K_{11b}[L]} = 10^{\Delta pK_a} \quad \text{Equation 4.14}$$

When the non-ionised form binds more strongly than the ionised form, C will be greater than one, and will be less than one if the ionised form binds more strongly (185). When the non-ionised form binds more strongly in the presence of the complexing agent then the pK_a of the acid will increase. K_{11a} and K_{11b} can then be estimated by assigning $[L]$ the value of $[L_t] - [A_t]$ and finding the best fit for the constants from Equation 4.15 (182):

$$[L_t] \text{ (M)} = [L] \left(1 + \frac{(K_{11a} + K_{11b} \cdot C)[A_t]}{1 + C + (K_{11a} + K_{11b} \cdot C)[L]} \right) \quad \text{Equation 4.15}$$

Where $[L_t]$ is the total ligand concentration and $[A_t]$ is the total acid concentration.

When a 1:2 complex is formed the value for C includes terms for the additional species which can be formed (182, 185).

$$C = \frac{1 + K_{11a}[L] + K_{11a}K_{12a}[L]^2}{1 + K_{11b}[L] + K_{11b}K_{12b}[L]^2} \quad \text{Equation 4.16}$$

Estimation of the association constants is carried out in a similar way as above by determining the best fit of the data to Equation 4.17 (182, 185).

$$[L_t] (M) = [L] + [S_t] \left[\frac{M}{2A} + \frac{N}{2B} \right] \quad \text{Equation 4.17}$$

Where:

- $[S_t]$ = total solubility
- $M = K_{11a}[L] + 2K_{11a}K_{12a}[L]^2$.
- $N = K_{11b}[L] + 2K_{11b}K_{12b}[L]^2$
- $A = 1 + K_{11a}[L] + K_{11a}K_{12a}[L]^2$.
- $B = 1 + K_{11b}[L] + K_{11b}K_{12b}[L]^2$.

Another method using potentiometric results to determine the K_{11a} and K_{11b} association constants has been described. By plotting the double reciprocal equation (Equation 4.18) of $\frac{K_a}{(K_a' - K_a)}$ versus $1/[L]$ (186).

$$\frac{K_a}{K_a' - K_a} = \frac{1}{(K_{11b} - K_{11a})[L]} + \frac{K_{11a}}{K_{11b} - K_{11a}} \quad \text{Equation 4.18}$$

Where [L] can be estimated as $[L_t] - [A_t]$. The association constants are then calculated from the intercept and slope as follows (186):

$$K_{11a} (M^{-1}) = \frac{\text{intercept}}{\text{slope}} \quad \text{Equation 4.19}$$

$$K_{11b} (M^{-1}) = \frac{1 + \text{intercept}}{\text{slope}} \quad \text{Equation 4.20}$$

As described above [L] is estimated from $[L_t] - [A_t]$, which assumes that all substrate molecules in the system have complexed with the ligand. However if the ligand is not present in a large excess compared to the drug under investigation, as is the case with the experimental conditions used here, this is a poor estimate of [L] due to the presence of the free drug molecules in the system. In this case another method for the determination of the association constants would be preferred.

In the case of the basic drugs investigated, the pK_a is calculated for the conjugate acid; however, the calculations above are based on the ionisation of a compound. The association constant of the base is required (pK_b). For the calculations above the pK_b is calculated from pK_a by the following:

$$pK_b = 14 - pK_a \quad \text{Equation 4.21}$$

This term is used in place of pK_a in Equations 4.13, 4.14, 4.16 and 4.18 for determining association constants of propranolol and atenolol.

Solubility

The results from the solubility studies carried out can be used to determine association constants. For complexes which have a 1:1 stoichiometry, the association constant, K_{11a} , can be calculated from the slope of the phase-solubility diagrams, and the solubility of drug alone (Equation 4.22) (78). The association constant can also be calculated from Equations 4.3 and 4.7, but rearranged to Equation 4.23.

$$K_{11a} (M^{-1}) = \frac{\text{slope}}{S_o(1 - \text{slope})} \quad \text{Equation 4.22}$$

$$K_{11a} (M^{-1}) = \frac{S_t - S_o}{S_o(L_t - S_t + S_o)} \quad \text{Equation 4.23}$$

Where slope = the slope of the phase-solubility diagram, S_o = the intrinsic solubility of the drug alone, S_t = the total solubility of the unionised drug in the presence of excipient, L_t = the total concentration of excipient in the system.

For compounds which form 1:2 complexes with the ligand, determination of the association constants K_{11a} and K_{12a} is through Equation 4.24 (187).

$$\frac{[S_t - S_o]}{[L]} = K_{11a}S_o + K_{11a}K_{12a}S_o[L] \quad \text{Equation 4.24}$$

By plotting $\frac{[S_t - S_o]}{[L]}$ versus $[L]$, the intercept of the line is $K_{11a}S_o$ and the slope of the line is $K_{11a}K_{12a}S_o$. The free ligand concentration, $[L]$ can be estimated by $[L_t] - [S_t - S_o]$. This method for estimating $[L]$ ignores the influence of $[DL_2]$ when calculating the free ligand concentration (187). Iga *et al.* developed a method which allows the determination of K_{11a} and K_{12a} from solubility data without estimating $[L]$ (188). By plotting the linear graph of Equation 4.25, the 1:1 and 1:2 association constants can be calculated.

$$\frac{[S_t - S_o]}{[L_t] - 2[S_t - S_o]} = \alpha + \beta([L_t] - 2[S_t - S_o]) \quad \text{Equation 4.25}$$

$$\alpha = \frac{K_{11a}S_o}{1 - K_{11a}S_o} \quad \text{Equation 4.26}$$

$$\beta = \frac{K_{11a}K_{12a}S_o}{(1 - K_{11a}S_o)^2} \quad \text{Equation 4.27}$$

4.1.3 Other Methods for Complexation Constant Determination

Potentiometry and solubility studies are not the only methods which allow the determination of association constants. Some of these techniques will be discussed below.

Fluorescence spectroscopy can be used to determine the association constant between a drug and complexing agent by measuring the difference between the intensity of fluorescent light in the absence and presence of ligand and fitting the data to Equation 4.28 (189). The measurements can be carried out using different excitation and emission wavelengths (175).

$$\frac{F}{F_o} = \frac{1 + \left(\frac{K_{11a}}{k_s}\right)K_{11a}[L]}{1 + K_{11a}[L]} + \frac{k_L}{k_S} [L]$$

Equation 4.28

Where, F_o and F are the fluorescence intensity in the absence and presence of the ligand respectively. The proportionality constant, k_i , represents the relationship between concentration and fluorescence intensity of the species. If the proportionality constant of the ligand is zero, i.e. the fluorescence intensity of the ligand is not affected by its concentration, then the last term of the equation can be ignored and the equation can be written as (175, 189):

$$\frac{F}{F_o} = \frac{1 + \left(\frac{K_{11a}}{k_s}\right)K_{11a}[L]}{1 + K_{11a}[L]}$$

Equation 4.29

If complexation with cyclodextrin results in chemical shift changes following nuclear magnetic resonance (NMR), then association constant determination can be carried out. A way in which NMR data can be used to calculate K_{11a} values is when the concentration of ligand is present in solution in a large excess compared to the concentration of drug. The change in chemical shift can be used to determine the association constant (190, 191).

$$\frac{1}{\Delta\delta} = \frac{1}{K_{11a} \Delta\delta_{\max}[H]_o} + \frac{1}{\Delta\delta_{\max}}$$

Equation 4.30

Where $\Delta\delta$ is the chemical shift of a nucleus in the drug (measured alone) minus the observed chemical shift in the presence of ligand, and $\Delta\delta_{\max}$ is the difference in chemical shift between the drug and the drug:ligand complex. A plot of $1/\Delta\delta$ versus $1/[H]_0$ can be used to determine the association constant and the $\Delta\delta_{\max}$ (190, 191).

Isothermal titration calorimetry is another useful method for association constant determination. It involves the enthalpy released when a reaction occurs, such as the complexation between cyclodextrin and drug molecules (192). The association constant is related to Gibbs Free energy, temperature and enthalpy and entropy changes according to the van't Hoff equation (Equation 4.31) (192, 193):

$$\Delta G \text{ (kJ/mol)} = -RT \ln K = \Delta H - T\Delta S \quad \text{Equation 4.31}$$

Where R is the gas constant.

Two cells are set up for each assay (reference and sample) and kept at a constant temperature. In the sample assay, compound is added to ligand, or vice versa. The energy required to bring the sample cell back to temperature is recorded and this data is used to calculate the enthalpy of binding per mole of compound (ΔH_b), the association constant, K, and the stoichiometry of the association, n (192, 194). By using the Marquardt method to fit the data to Equation 4.32 the above parameters can be determined (194). The below equation is when drug is added to a cell containing ligand.

$$Q \text{ (J/mol)} = \frac{n[L_t]\Delta H_b V_o}{2} \left(1 + \frac{[D_t]}{n[L_t]} + \frac{1}{nK_{11}[L_t]} - \left(\left(1 + \frac{[D_t]}{n[L_t]} + \frac{1}{nK_{11}[L_t]} \right)^2 - \frac{4[D_t]}{n[L_t]} \right)^{\frac{1}{2}} \right) \quad \text{Equation 4.32}$$

Where Q is the amount of heat evolved on addition of drug into the cell, V_o is the volume of the cell, $[L_t]$ and $[D_t]$ are the total concentrations (M) of ligand and drug in the cell (194).

4.1.4 Micelle Association Constant Determination

Morisue and colleagues described a method to determine the association constant of compounds with micelle forming surfactants (195). Knowledge of the CMC of the surfactants is required for this method.

$$\frac{[S_t] - [S_w]}{[S_w]} = \frac{K_{11a}}{N} ([C_t] - \text{CMC}) \quad \text{Equation 4.33}$$

Where $[S_t]$ is the compound solubility in the presence of surfactant at concentration t , $[S_w]$ is the intrinsic solubility of the drug, $[C_t]$ is the total concentration of surfactant used, and N is the aggregation number of the surfactant into micelles. Concentrations used in this method are moles/L. By plotting Equation 4.33, the slope of the line is therefore K_{11a}/N (195). This method has been used by others including Dar *et al.* and Kabir-ud-Din *et al.* (181, 196).

As explained by Dar *et al.*, from the association constant it is possible to determine the number of drug molecules per micelle (S^M) using the equation (181):

$$S^M = \frac{[S_t] - [S_w]}{[M_t]} = K_{11a}[S_w] \quad \text{Equation 4.34}$$

Where $[M_t]$ is the micelle concentration. This would give additional information on the association between drug and poloxamer. Knowledge of the aggregation number is required for determination of the association constant.

4.1.5 Calculating K_a^c

As described above, some of the methods allow the determination of both K_{11a} and K_{11b} . The relationship between the four constants described in Scheme 4.1 is represented by Equation 4.35. Therefore, if three of the four constants are known the fourth can be calculated by using this relationship (182).

$$\frac{K_a}{K_a^c} = \frac{K_{11a}}{K_{11b}} \quad \text{Equation 4.35}$$

4.2 Aims

The aims of this chapter are to try to determine the association constants of the unionised and, where possible/appropriate, the ionised species between all four drugs and each of the three excipients. Where possible, the association constant will be calculated using the techniques described above. Where more than one method

is utilised the results for each calculation will be compared. For propranolol, the constants from the CheqSol assays will be compared to the constants calculated from shake-flask solubility method.

4.3 Methods

4.3.1 Complexation Association Constants

The association constants for cyclodextrins will be calculated using different equations. The K_{11a} using Equation 4.22 and the regression equations (with molar concentrations for S_0 and HP- β -CD concentration) from chapter 2.5.3. For Equation 4.23, the mean K_{11a} for each cyclodextrin ratio was used; the mean of these K_{11a} s was calculated for comparison.

As the literature has shown that gliclazide has a 1:2 stoichiometry with cyclodextrins, the method described by Iga *et al.* and solubility data was used to determine K_{11a} and K_{12a} values. As ibuprofen, in the presence of HP- β -CD displayed an A_p -type phase-solubility graph, despite literature suggesting the formation of only 1:1 complexes, the above procedure was carried out to determine if 1:2 complexes might have been formed during the kinetic solubility assays.

The use of the pH-metric pK_a assays and a double reciprocal plot to calculate K_{11a} and K_{11b} was examined by plotting $K_a / (K_a' - K_a)$ versus $1/[HP-\beta-CD]$. Some equations used K_a or K_a^c for the determination of association constants. For acids, these values were used, however, for bases K_a and K_a^c were converted to K_b and K_b^c .

4.3.2 Micelle Association Constants

The association constant for poloxamers and the drug compounds was calculated by plotting $\frac{([S_t] - [S_w])}{[S_w]}$ versus $([C_t] - \text{CMC})$, the x- and y- intercepts for this data was set as the origin. The poloxamer concentrations were converted to molar concentrations (for molecular weights and CMC see Table 2.2) before plotting to allow comparison between association constants for HP- β -CD and any found in the literature. Association constant determination was calculated by multiplying the slope by the aggregation number of the poloxamer micelles according to slope = K_{11a}/N . The number of drug molecules per micelle was also determined using Equation 4.34, assuming an aggregation number of 9 for P407 and 15 for P188 (97, 98).

Statistical analysis was carried out using Minitab™ 16, and involved regression analysis. Graphs were plotted using Microsoft® Excel 2010.

4.4 Results

4.4.1 Complexation Association Constants

Using the solubility results (see chapter 2.5.3 for S_0 and slope values) and Equations 4.22 and 4.23 the K_{11a} of the drugs were determined (Table 4.1). It was observed that all four drugs complex with HP- β -CD with varying strengths of association. According to both equations for K_{11a} , ibuprofen complexes most strongly with HP- β -CD, the order of association is ibuprofen > propranolol > gliclazide > atenolol. Equation 4.23, gives association constants lower than Equation 4.22 for all four drugs. The Higuchi

and Connors method using Equation 4.22 appears to be most widely used in the literature. The method utilising Equation 4.23 requires the calculation of a mean association constant, and could be affected by outliers in the data.

Table 4.1. K_{11a} values from CheqSol studies of the four compounds with HP- β -CD

Drug	K_{11a} (Equation 4.22)	K_{11a} (Equation 4.23)
Propranolol	238 M ⁻¹	184 M ⁻¹
Atenolol	11.9 M ⁻¹	21.1 M ⁻¹
Ibuprofen	6920 M ⁻¹	1380 M ⁻¹
Gliclazide	176 M ⁻¹	118 M ⁻¹

The solubility results for gliclazide plotting using Equation 4.25 can be found in Figure 4.1. It can be observed that the results do not form a linear relationship, with an R^2 value of 5.73% and p-value of 0.648. As there is no linear relationship, this method did not provide information on the 1:1 or 1:2 association constants of gliclazide with HP- β -CD.

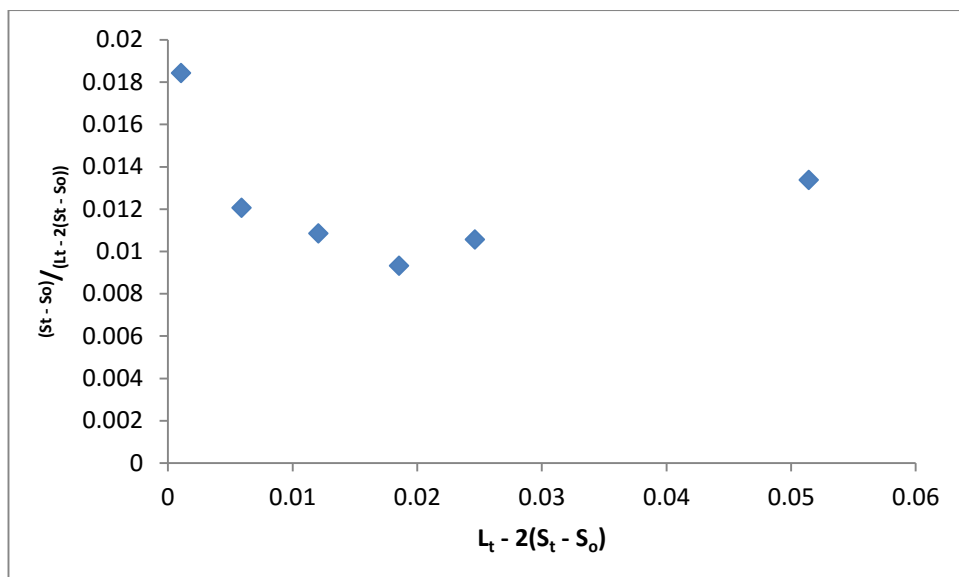


Figure 4.1. Scatterplot of Iga *et al.* method to determine K_{11a} and K_{12a} of gliclazide following phase-solubility results.

Ibuprofen did not produce a linear phase-solubility curve, suggesting the possibility of more than one HP- β -CD molecule involved in the complex (see chapter 2.6.5). Ibuprofen also did not form a linear relationship using the method described by Iga *et al.*, with a p-value of 0.736 and R^2 value of 6.97% (Figure 4.2). This method was also not useful for the determination of association constants between ibuprofen and HP- β -CD.

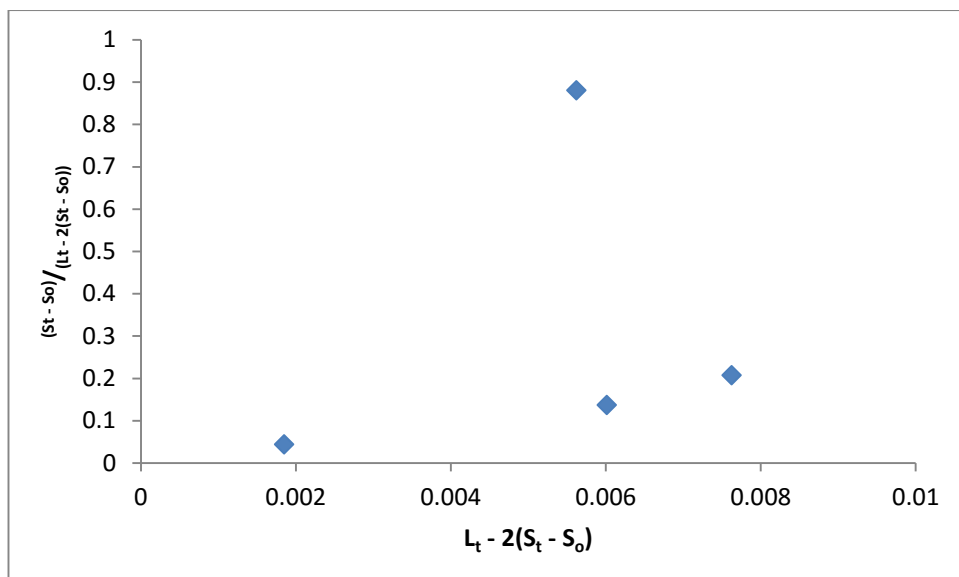


Figure 4.2. Scatterplot of Iga *et al.* method to determine K_{11a} and K_{12a} of ibuprofen following phase-solubility results.

A shake-flask solubility study was carried out with propranolol in the presence of HP- β -CD for both ionised and unionised forms, see chapter 2.6.5 for solubility and slope values. The association constants for both forms using Equations 4.22 and 4.23 can be found in Table 4.2.

Table 4.2. K_{11} values from shake-flask solubility studies of propranolol in the presence of HP- β -CD at the two wavelengths studied and both forms. Unionised was measured at pH 12.0 and ionised at pH 5.5. Values are K_{11a} and K_{11b} for unionised and ionised forms respectively.

Species	Wavelength	K_{11} (Equation 4.22)	K_{11} (Equation 4.23)
Unionised	254 nm	259 M ⁻¹	182 M ⁻¹
	280 nm	354 M ⁻¹	254 M ⁻¹
Ionised	254 nm	-0.744 M ⁻¹	-0.752 M ⁻¹
	280 nm	-0.717 M ⁻¹	-0.726 M ⁻¹

The association constants for the ionised species of the compounds with HP- β -CD (K_{11b} values) were determined from shake-flask solubility results in pH 5.5 buffer. As seen earlier in chapter 2.4.5, the solubility of the ionised species appears to decrease in the presence of HP- β -CD, which reflects the negative association constants.

The double reciprocal plots of $\frac{K_a}{(K_a' - K_a)}$ versus $\frac{1}{[HP-\beta-CD]}$ (Equation 4.18) show no linear pattern for the acidic compounds (Figure 4.3). For propranolol and atenolol (using K_b values) there is a linear relationship present, although at the lower HP- β -CD concentrations a grouping of the data can be observed so the linear relationship may not hold at these concentrations (Figure 4.4). At the lowest ratios used the concentration of HP- β -CD is negative when the amount of drug present is subtracted.

The K_{11a} and K_{11b} were calculated for propranolol and atenolol as they were shown to follow linear regression with p-values less than 0.05.

- Propranolol: $K_{11a} = 67.7 \text{ M}^{-1}$, $K_{11b} = -76.4 \text{ M}^{-1}$.
- Atenolol: $K_{11a} = -1480 \text{ M}^{-1}$, $K_{11b} = -1240 \text{ M}^{-1}$.

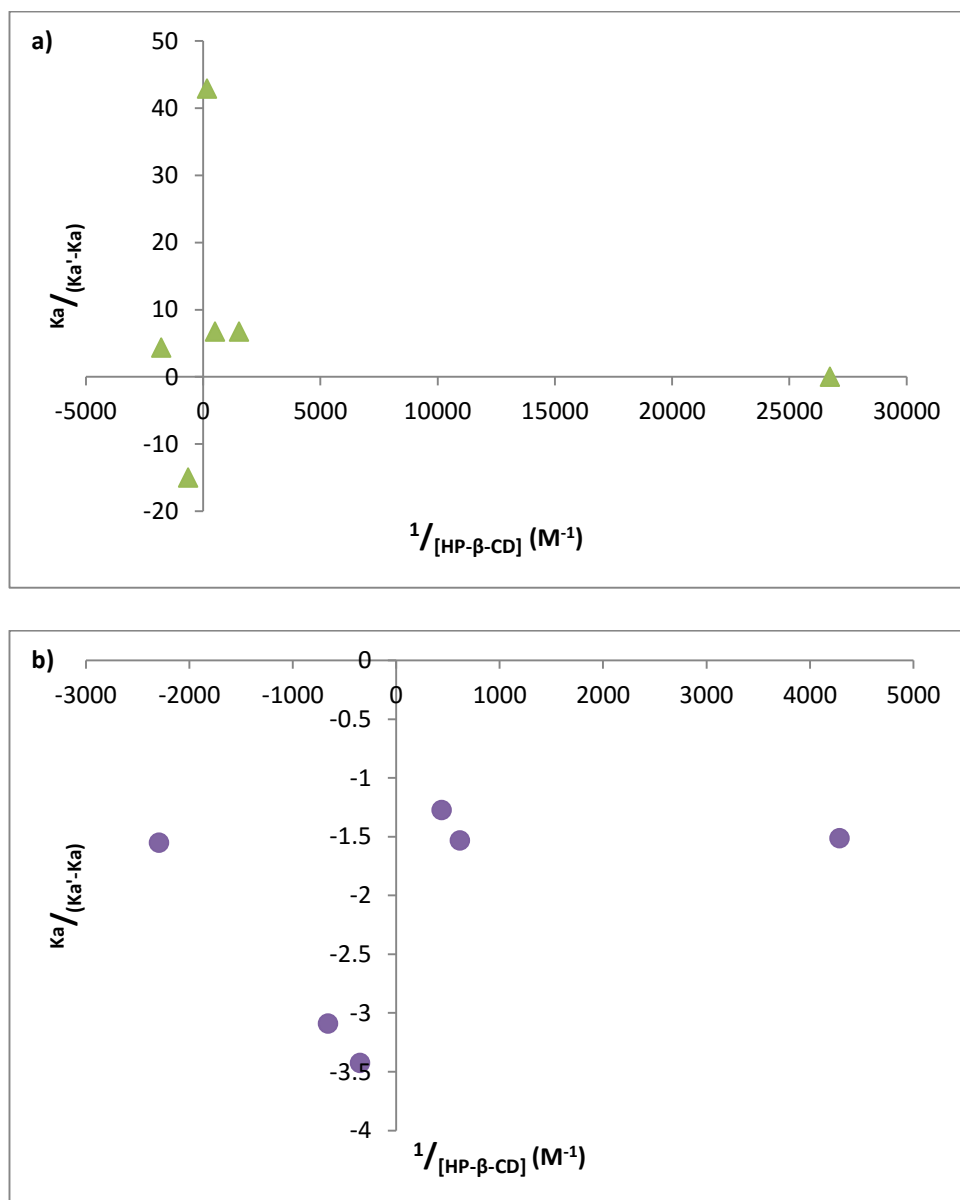


Figure 4.3. Double reciprocal plots of acidic drugs. a) gliclazide and b) ibuprofen.

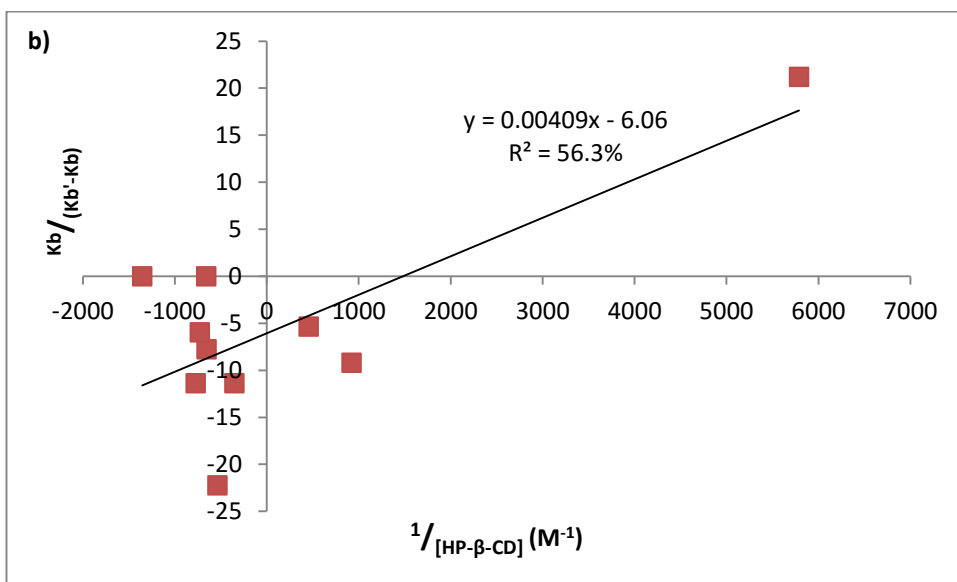
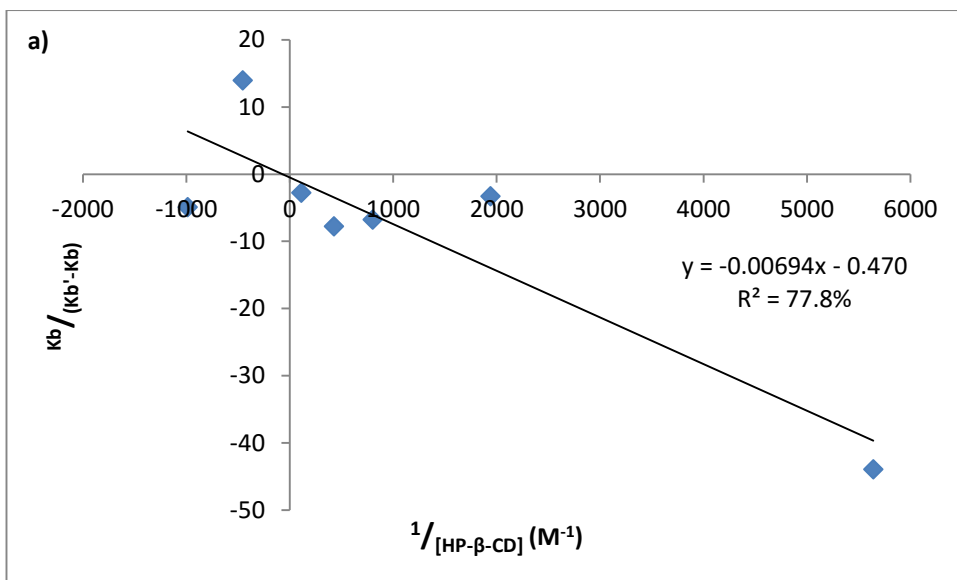


Figure 4.4. Double reciprocal plots of basic drugs. a) propranolol and b) atenolol.

4.4.2 Micelle Association Constants

P407

Regression analysis for the scatterplots of $\frac{([St] - [Sw])}{[Sw]}$ versus $([C_t] - CMC)$ was carried out and the slope of regression line, or K^{11a}/N , recorded (Figures 4.5 and 4.6), as detailed in Table 2.3, the CMC of P407 is 0.0000794 M (83, 101). The K^{11a}/N for

propranolol, atenolol, gliclazide and ibuprofen were determined to be 2120 M^{-1} , 47.0 M^{-1} , 651 M^{-1} and 33000 M^{-1} respectively. To quote the K_{11a} , the aggregation number needs to be known. As there are reported to be nine molecules per micelle for P407 (97), the association constants for P407 and the four drugs can be found Table 4.3. The order for association is ibuprofen > propranolol > gliclazide > atenolol.

Table 4.3. Association constants, as K_{11a}/N and adjusted to K_{11a} when $N = 9$, of the four drugs in the presence of P407.

Drug	K_{11a}/N	$K_{11a}, N = 9$
Propranolol	2120 M^{-1}	19100 M^{-1}
Atenolol	47.0 M^{-1}	423 M^{-1}
Gliclazide	651 M^{-1}	5860 M^{-1}
Ibuprofen	33000 M^{-1}	297000 M^{-1}

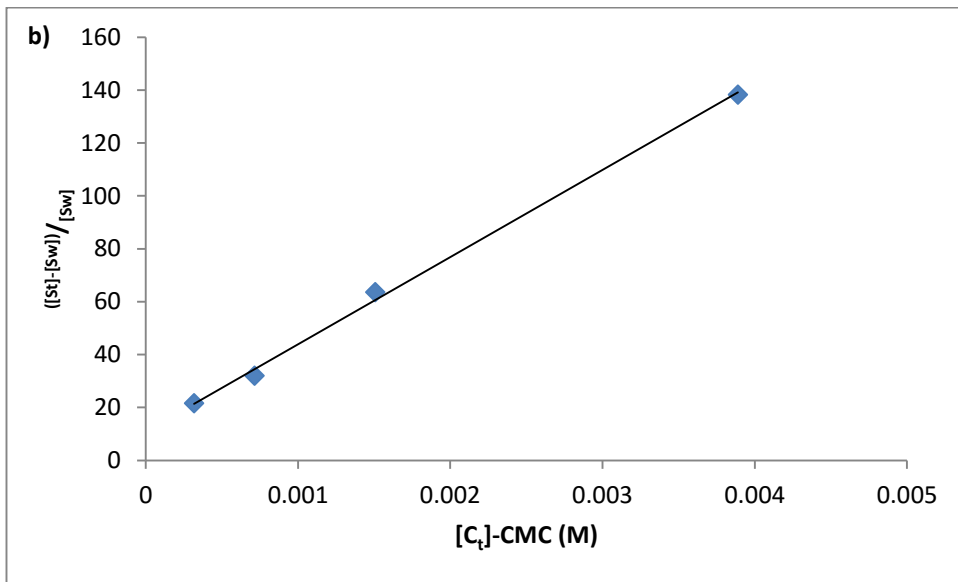
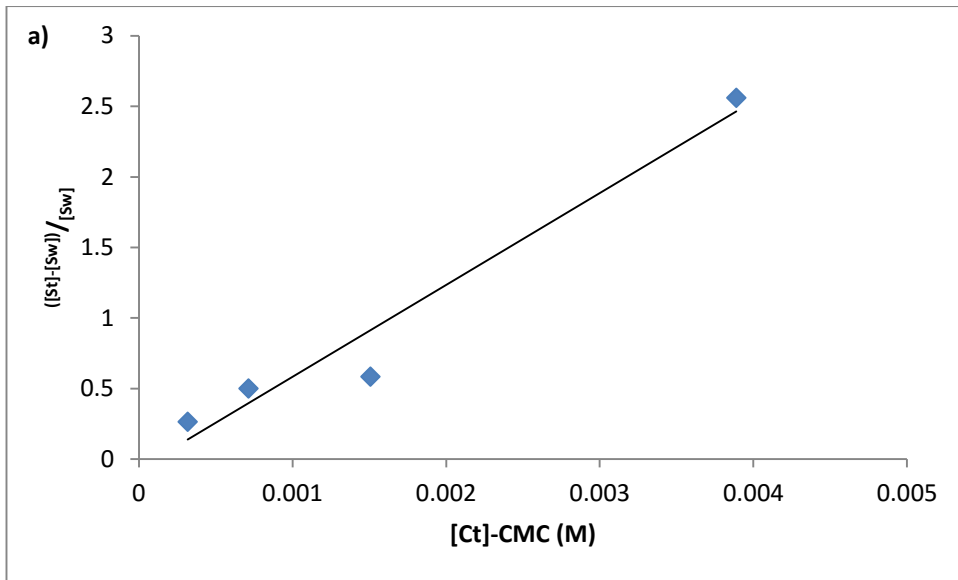


Figure 4.5. Scatterplots of $\frac{([St] - [Sw])}{[Sw]}$ versus $([C_t] - CMC)$ for a) gliclazide and b) ibuprofen in the presence of P407.

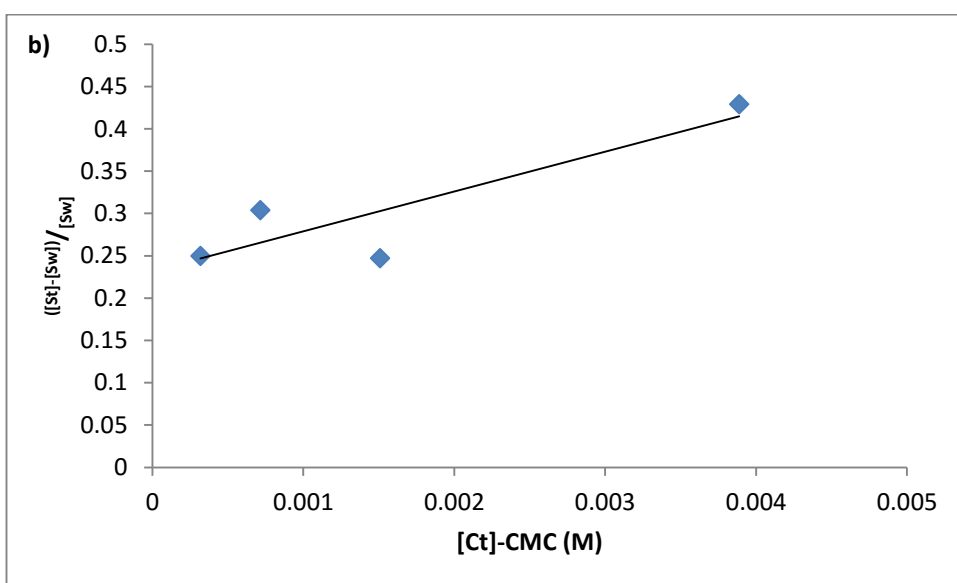
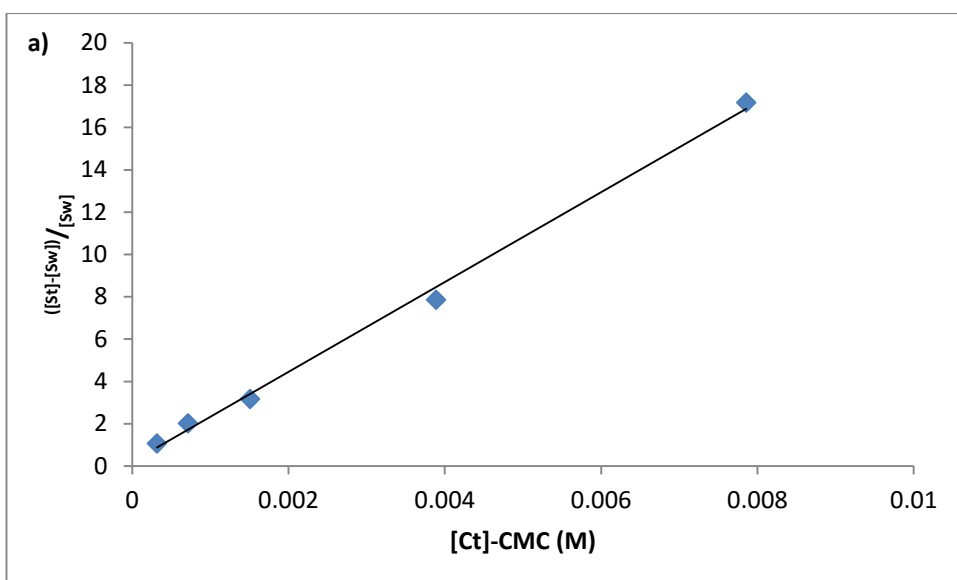


Figure 4.6. Scatterplots of $\frac{([St] - [Sw])}{[Sw]}$ versus $([C_t] - CMC)$ for a) propranolol and b) atenolol in the presence of P407.

P188

Association constants were determined from the slopes of $\frac{([St] - [Sw])}{[Sw]}$ versus $([C_t] - CMC)$, where the CMC for P188 is 0.00004 M (Figures 4.7 and 4.8) (84, 99). Table 4.4 details the association constants. The association constants of the four compounds

with P188 were found to be 366 M⁻¹, 29.1 M⁻¹, 153 M⁻¹ and 3580 M⁻¹ for propranolol, atenolol, gliclazide and ibuprofen respectively. The K_{11a} ranges for the four compounds with aggregation number of 15 (98) can also be found in Table 4.4. Similarly to P407, ibuprofen associates most strongly with P188 followed by propranolol then gliclazide, with atenolol having the weakest association.

Table 4.4. Association constants, as K_{11a}/N and adjusted to K_{11a} when $N = 15$, of the four drugs in the presence of P188.

Drug	K_{11a}/N	$K_{11a}, N = 15$
Propranolol	366 M ⁻¹	5490 M ⁻¹
Atenolol	29.1 M ⁻¹	437 M ⁻¹
Gliclazide	153 M ⁻¹	2230 M ⁻¹
Ibuprofen	3580 M ⁻¹	53700 M ⁻¹

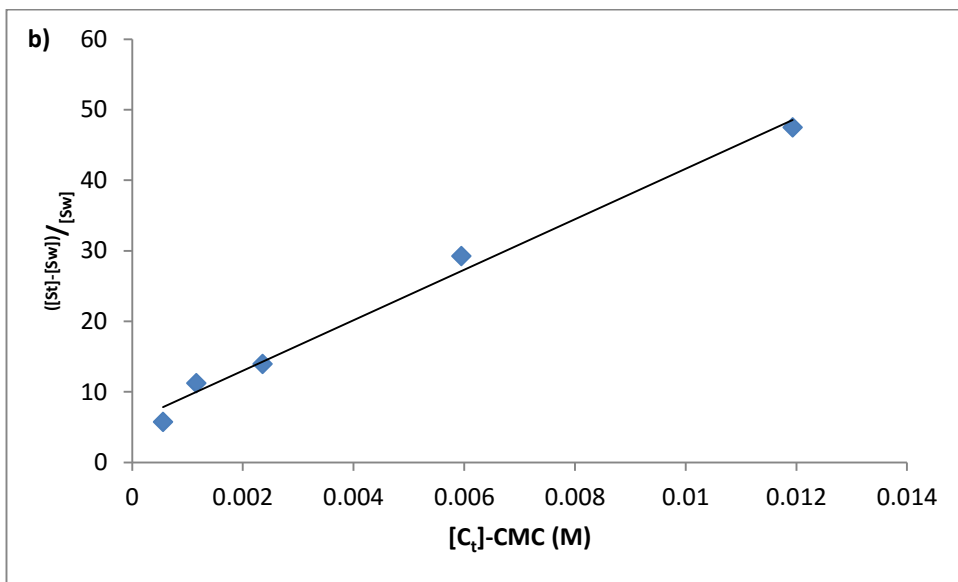
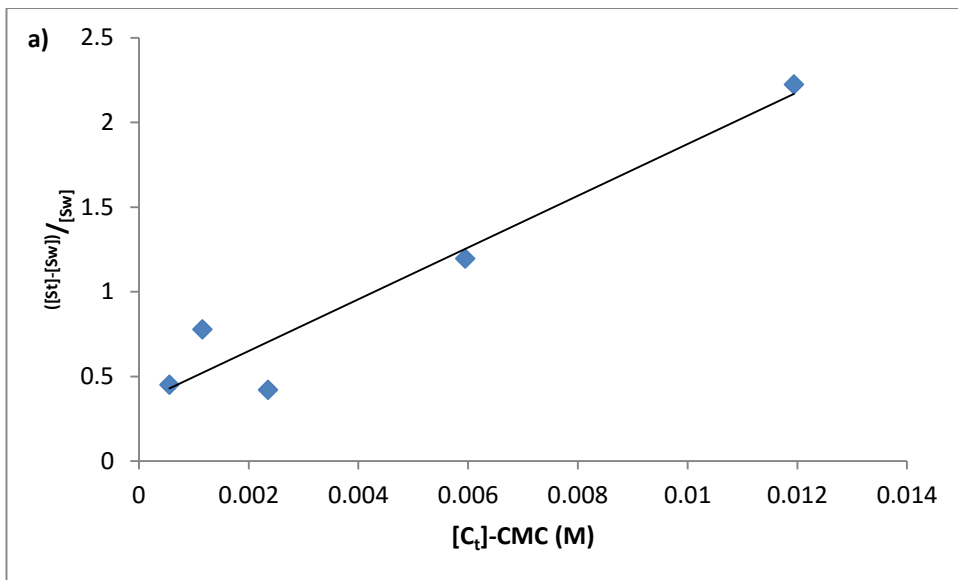


Figure 4.7. Scatterplots of $\frac{([St] - [Sw])}{[Sw]}$ versus $([C_t] - CMC)$ for a) gliclazide and b) ibuprofen in the presence of P188.

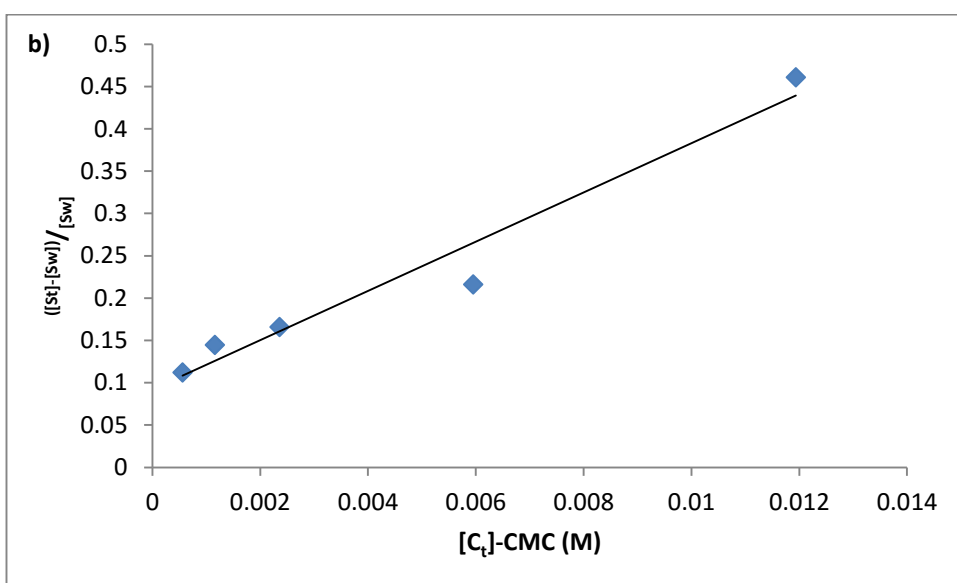
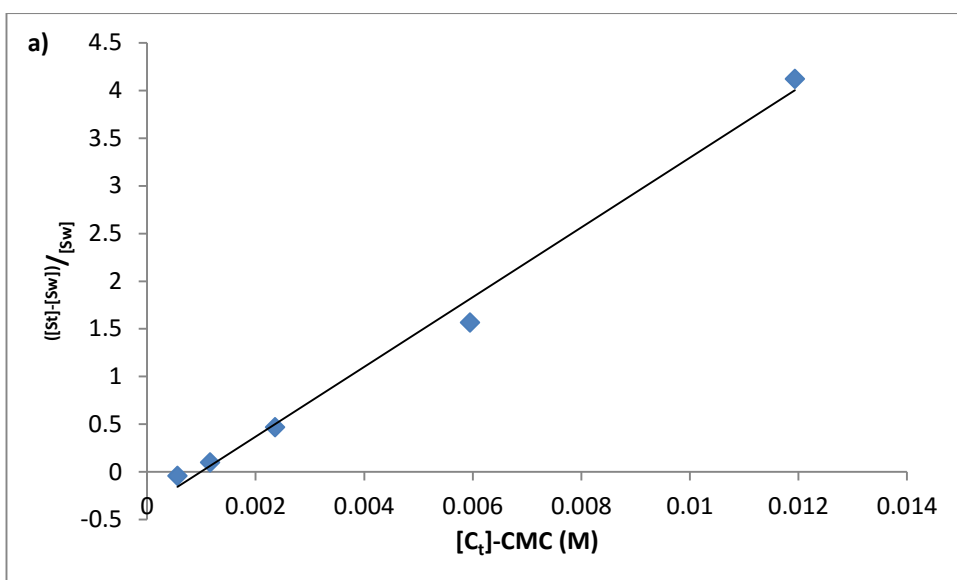


Figure 4.8. Scatterplots of $\frac{([St] - [Sw])}{[Sw]}$ versus $([C_t] - \text{CMC})$ for a) propranolol and b) atenolol in the presence of P188.

For propranolol, the average number of drug molecules per micelle of P407 and P188, calculated from previously quoted aggregation numbers, were 7.51 and 2.16 respectively, with mean intrinsic solubility of 0.000393 M. The average number of atenolol molecules in P407 micelles was 22.2, and for P188 was 23.0 from a S_0 value

of 0.0526 M. In the P407 micelle there were 43.1 molecules of ibuprofen and 0.5244 molecules of gliclazide. For P188 these values were 0.207 and 7.79 for gliclazide and ibuprofen respectively (Table 4.5). The mean solubility values for ibuprofen and gliclazide were 0.000145 M and 0.0000928 M respectively.

Table 4.5. Table showing the average number of molecules per micelle, mean intrinsic solubility values of drugs alone from chapter 2.5.3. Propranolol 0.000393M, atenolol 0.0526 M, gliclazide 0.0000928 and ibuprofen 0.000145 M.

Drug	Average Number of Molecules per Micelle	
	P407	P188
Propranolol	7.51	2.16
Atenolol	22.2	23.0
Gliclazide	0.544	0.207
Ibuprofen	43.1	7.79

4.5 Discussion

4.5.1 Complexation Association Constants

From the association constants calculated using phase-solubility studies, it can be seen that ibuprofen interacts most strongly with HP- β -CD, followed by propranolol, then gliclazide with atenolol showing the least amount of association with the

cyclodextrin. Association constants for the complex between ibuprofen and HP- β -CD vary in the literature. K_{11a} values range from 50 M^{-1} to 5400 M^{-1} following phase-solubility studies (130, 197-199). Using the methods described for solubility studies the K_{11a} for ibuprofen was found to be higher than the literature range. Differences in experimental conditions could affect the values observed. Both Mura *et al.* and Song *et al.* carried out solubility studies in unbuffered conditions. Mura *et al.* conducted the experiments at approximately pH 6 and Song *et al.* used aqueous solutions for phase-solubility studies, the association constants will therefore have contributions from mostly ionised species with some contribution from unionised ibuprofen species (130, 197). While the solubilities determined during CheqSol studies were not carried out at static pH, and both ionised and unionised species were present, the final solubility results used were for the unionised species. Temperature can also affect the constant. Mura *et al.* investigated the effect of temperature and reported that as the temperature was increased from 25°C to 45°C the K_{11a} decreased (130). For example, the association constant of ibuprofen with HP- β -CD increased from 5.4 M^{-1} at 25°C to 3.8 M^{-1} at 45°C (130). Song *et al.* did not mention the experimental temperature conditions (197). Oh *et al.* reported a K_{11a} value of 533 M^{-1} , determined using fluorescence spectroscopy which is less than the association constants calculated here (140). As expected, Loftsson *et al.* have demonstrated that as the pH of the system is increased, and the proportion of ionised ibuprofen species increases, the association constant decreases from 1740 M^{-1} at pH 4.6 to 50 M^{-1} at pH 7.5 (199). The lower association constant measured at pH 4.6 than the constant determined here could be down to the higher ionisation at pH 4.6, which is close to

the pK_a of ibuprofen, whereas the constant calculated here is from unionised data, which would have a stronger association. None of the literature for ibuprofen closely matches the experimental conditions carried out here, and so direct comparison of the results is not applicable. No data on the association constants of HP- β -CD with the other three drugs could be found in the literature.

Using the method described by Iga *et al.* did not appear to be a suitable method in this instance as neither gliclazide nor ibuprofen showed a linear relationship. As ibuprofen has not been shown to form 1:2 complexes with HP- β -CD, the formation of these is unlikely to be the reason for the A_p type phase-solubility curve seen earlier. Gliclazide, however, has been shown to form 1:2 complexes with cyclodextrins. From the results, the K_{11a} and K_{12a} were 141 M^{-1} and -3.20 M^{-1} respectively. The results from experiments conducted here suggest that only 1:1 complexes are formed. This may be due to the type of solubility experiment conducted, which is a kinetic study and therefore the system is not at equilibrium. The studies which demonstrated 1:2 stoichiometry were conducted using β -CD, and there may be some form of steric hindrance to the entry of either the aromatic or aliphatic ring groups in the molecule. The K_{11a} for gliclazide here is similar to the K_{11aS} calculated earlier, using Equations 4.22 and 4.23.

The association constant of propranolol calculated from the shake-flask solubility data is similar to the constants from CheqSol assays. The constants at the 254 nm wavelength were closer to the CheqSol results with both equations. The negative

association constants of ionised propranolol suggest that there is no association between the propranolol ion and HP- β -CD. It was expected that the ionised form of propranolol would have a lower association with the cyclodextrin as it is more hydrophilic and less attracted to the more hydrophobic core of HP- β -CD. The similarities between the shake-flask and CheqSol phase solubility studies of propranolol with HP- β -CD provide more evidence that the CheqSol method can be used for phase-solubility studies and association constant determination for 1:1 stoichiometries. With further work the literature evidence for this technique can be expanded.

The double reciprocal plots show poor linear correlation between the data points for both gliclazide and ibuprofen. It can be seen that at the lowest ratios, using the method described by Connor and Lipari (182) and again by Kahle and Holzgrabe (186), the value for [HP- β -CD] is negative. When these data points are excluded the R^2 values for all four drugs improves (Figures 4.9 and 4.10). However, data for ibuprofen and gliclazide still show poor fit with R^2 values less than 27%. The results for atenolol now also show a non-linear relationship with the negative values excluded. For propranolol the K_{11a} and K_{11b} values with the excluded data using Equations 4.19 and 4.20 (Table 4.6) show the results are not the same when the low concentrations are excluded. Excluding ibuprofen, HP- β -CD was found not to affect the pK_a of the drugs investigated, thus it would be expected that this method would be suitable for determining the association constants of ibuprofen only. However, from this data it can be concluded that for the four drugs investigated, with the HP- β -CD ratios used,

this method is not suitable for determining association constants between drug and HP- β -CD. As HP- β -CD concentration is estimated by subtracting the drug concentration from the ligand concentration ($[L_t] - [A_t]$), as discussed, the value for $[L]$ is inaccurate as there is not a large excess of $[L_t]$ compared to $[A_t]$ in all instances and not all of the drug is likely to be bound to the cyclodextrin. Another method for free ligand concentration estimation in the system would be preferable. However, without prior knowledge of the level of association, this would be difficult. The other method using the phase-solubility studies is therefore more appropriate.

Due to the large influence that the highest x-coordinate has on the regression equation, the results should be interpreted with caution. It is noted that if these values are excluded then there is no observable linear relationship.

Table 4.6. Comparison of association constants with excluded data.

Drug	Constant	All Points	Excluded Data
Propranolol	K_{11a}	67.7 M^{-1}	-4.8 M^{-1}
	K_{11b}	-76.4 M^{-1}	-14.3 M^{-1}

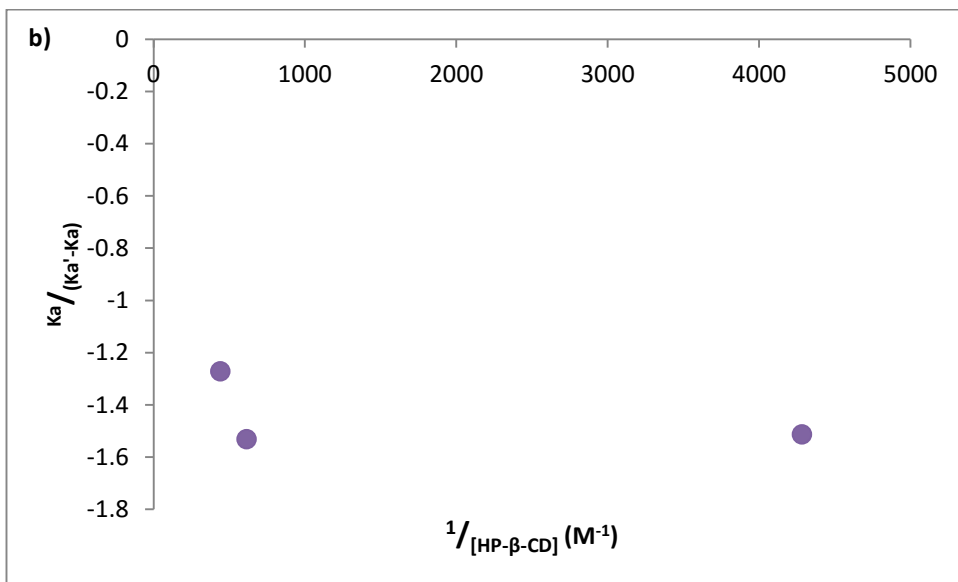
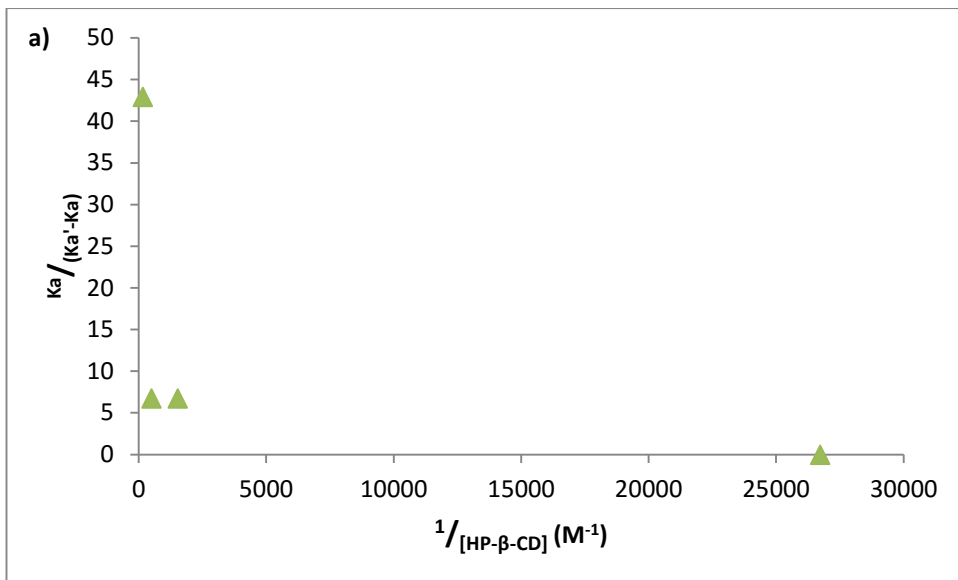


Figure 4.9. Double reciprocal plots of acidic drugs with negative HP- β -CD concentrations excluded. a) gliclazide and b) ibuprofen.

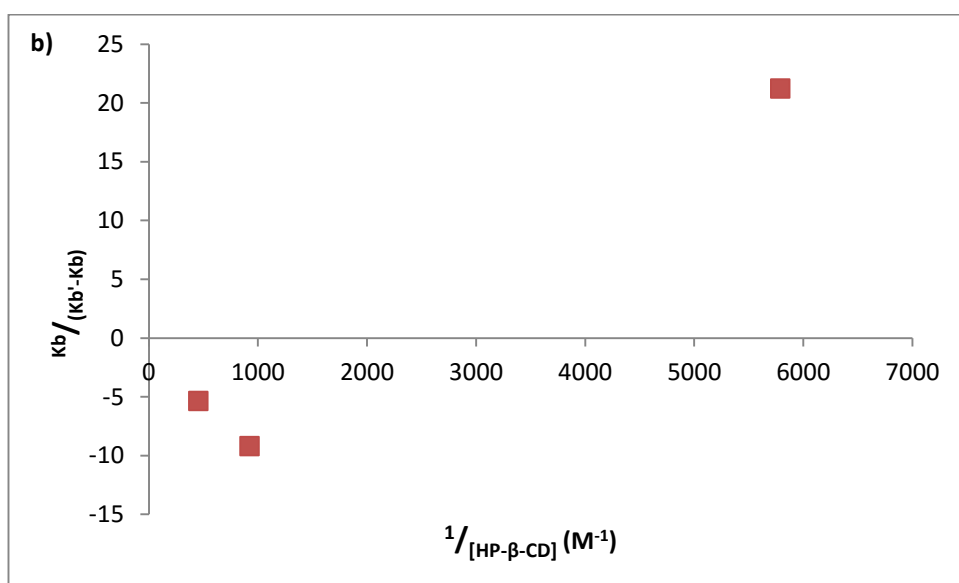
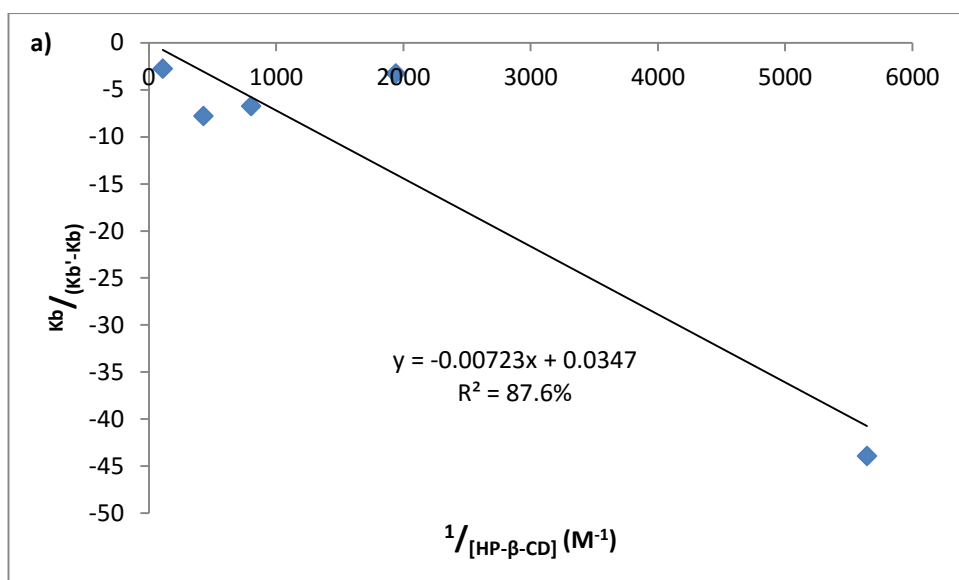


Figure 4.10. Double reciprocal plots of basic drugs with negative HP- β -CD concentrations excluded. a) propranolol and b) atenolol.

It was considered if calculation of K_{11} values using Equation 4.13 followed by Equation 4.14 (for 1:1 stoichiometry) or Equation 4.16 (for 1:2 stoichiometry) from the K_{11a} values determined from solubility data could be carried out. However, as described for ibuprofen there are variations in K_{11a} in the literature; and here for all drugs

depending on the method used to calculate K_{11a} , so the calculated K_{11b} using this information may not be accurate for the experiment conducted. It would also not be useful when no effect on pK_a was observed during pH-metric pK_a analysis as Equation 4.13 uses changes in pK_a to determine association constants values.

4.5.2 Micelle Association Constants

As no literature could be found on the association constants between poloxamers and the four drugs examined this thesis represents the first presentation of this data. The association constants are determined from poloxamer concentration above the CMC as below this concentration there should be no changes in drug solubility (181). From Tables 4.3 and 4.4 it can be seen that propranolol, gliclazide and ibuprofen associate more strongly with P407 than P188. The association constant for atenolol with P188 is slightly greater than that for P407, despite a higher K_{11a}/N , which is due to the higher number of molecules per 188 micelle. As all four drugs had a lower increase in solubility per % w/v P188 than for P407 it would be expected that the association constants would be greater for P407, as observed with all except atenolol. The K_{11a} results for atenolol are unexpected as the P407 gave a higher solubilisation at the concentrations examined and the solubility results suggest that P407 is the better solubiliser for the four compounds. The results for atenolol do not appear to have a linear relationship with an intercept through the origin, which could be a result of atenolol associating with poloxamer molecules present as monomer units in the system. The higher association between propranolol, gliclazide and ibuprofen with P407 may be due to the higher percentage of the hydrophobic POP per molecule

compared to P188, approximately 30% versus 20%. Atenolol is more hydrophilic (the solubility of atenolol is at least 130 times greater than the other three drugs) than propranolol, ibuprofen and glimepiride and may be expected to have a higher association with the more hydrophilic P188, and hence an increased K_{11a} . The increased effect on the solubility of atenolol with P407 may be due to the number of micelles present in the system. As the concentration of monomer subunits in the system remains constant (45), the number of micelles present in solution was calculated from the concentration of poloxamer present (minus the CMC) and the aggregation number. The number of micelles present in solutions of P407 was found to be greater than the number of micelles present in P188 solutions at concentrations of 1% w/v and above. As the association constants are similar, the number of micelles into which atenolol can enter may have affected the solubilisation of the compound by P407.

The aggregation numbers used here may not be the aggregation number of the system. Previous work has shown that the aggregation number can be affected by temperature and the presence of other molecules such as drugs. Sharma and Bhatia have shown that the aggregation number of P407 is reduced by the presence of the anti-inflammatory agents naproxen and indomethacin from 88.6 to 51.9 and 50.6 respectively (200). The authors also noted that the aggregation number determined during their study for P407 was higher than expected (200). Another study has shown that the aggregation number for P407 is 73.4, again quoted as being higher than expected (201). As the temperature of the system increases the aggregation

numbers for poloxamers have been shown to increase (202, 203). As the temperature was kept constant during experiments carried out for CheqSol assays, there would be no effect due to changes in temperature in these studies. The presence of salt in the system has been shown to affect the aggregation number of Pluronic L64 or poloxamer 184 (204, 205), therefore the effect of ISA water on the aggregation numbers of P407 and P188 cannot be ruled out; this would not have a large effect on the results here, as salt concentration was constant, but could affect literature comparisons. The aggregation numbers quoted should therefore be used with caution to give an estimate of the K_{11a} if the aggregations behaviour under the experimental conditions has not been investigated. If the aggregation numbers are unknown then K_{11a}/N may still provide information on the relative strength of association of the compounds investigated compared to each other.

From the number of molecules per micelle it can be observed that fewer molecules for each drug are present in the micelle of P188 than P407. As before this pattern could be due to the difference between the hydrophilicity of both poloxamers. The drugs would be more attracted to the more hydrophobic P407 than P188.

4.5.3 General Discussion

For all three excipients, the order of association was the same. Ibuprofen associates most strongly, followed by propranolol, gliclazide and atenolol. The order does not appear to be inversely related to the intrinsic solubility of the drugs (atenolol > propranolol > ibuprofen > gliclazide). One explanation into the order could be the

affect that ionisation has on the association. Although the quoted solubilities used are intrinsic, the solubility determination was carried out at pHs within two units of each drug's pK_a and it is unclear from the results whether this affects the results. To investigate if percentage ionisation may have an effect on association constants, the percentage ionised at each crossing point during CheqSol assays was calculated for each excipient at all concentrations and the mean taken. The percentage ionised was calculated from the pK_a and mean pH of the crossing point. ANOVA with Tukey's analysis was carried out for each excipient independently, this analysis showed that for each excipient the percentage ionised for each drug was statistically different from the other. From Figure 4.11, it can be seen that in the presence of all excipients and absence of solubilising excipients that atenolol is the least ionised of all drugs, followed by propranolol. In the absence of excipient and in the presence of P188 ibuprofen was the most ionised. Gliclazide was therefore the most ionised in the presence of HP- β -CD and P407. As the unionised forms of the drug is more lipophilic, it may be expected that lower ionisation would result in a stronger association with the excipient. This however was not observed when percentage ionised was examined. The association between drug and excipient also needs to consider the hydrophilicity/lipophilicity of individual molecules both in their unionised and ionised states. The partition coefficient was not determined during this study however the logP for the drugs are reported to be 3.97, 3.48, 2.6 and 0.16 for ibuprofen, propranolol, gliclazide and atenolol respectively (206). From this it can be observed, that for the drugs investigated, the lipophilicity appears to affect the strength of the association between the compound and each of the excipients.

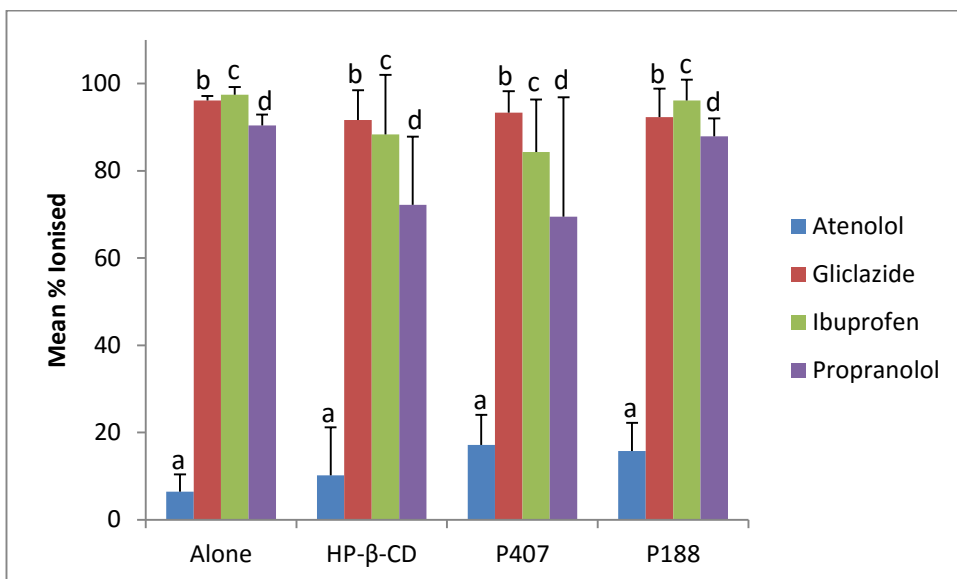


Figure 4.11. Mean % ionised of all drugs in the presence and absence of excipients during CheqSol crossing points. ANOVA analysis for each excipient was carried out independently; for each excipient all drugs were statistically different from each other as represented by different letters.

4.6 Conclusions

Calculation of K_{11a} values using Higuchi and Connors Equation 4.22 for HP-β-CD complexation appears to be the most appropriate for the CheqSol method as presented in this thesis, including for gliclazide despite previous studies showing the presence of 1:2 complexes with cyclodextrin. Calculation of the association constants using potentiometry did not give reasonable results for any of the drugs, despite the cyclodextrin having effects on the pK_a of ibuprofen. For the other three drugs, this method using potentiometric data would not have been expected to produce accurate association constant results as experiments did not show an effect on pK_a .

by HP- β -CD. The association constants for the charged species of the drugs were not able to be determined with the available data. Further work would have to be carried out for this determination. All drugs associated more strongly with P407 than P188, and bound least strongly with HP- β -CD.

5 Chapter 5 – Molecule Design

5.1 Introduction

Part of the aims of this PhD was to investigate the possibility of the development of a new pharmaceutical excipient which can be used to improve the solubility of a number of poorly water soluble drugs. The aim was to develop a compound which could self-assemble around an active ingredient to improve its solubility.

Molecular self-assembly is the ability of a molecule to form ordered complex structures spontaneously (207). In the synthesis of large molecules or structures Whitesides *et al.* described self-assembly as involving:

- Synthesis of subunits (molecules).
- Many copies of the subunit molecule(s).
- Self-assembly with non-covalent bonding (208).

The bonds which form between molecules in the self-assembled structure include hydrogen bonds, van der Waal forces, hydrophobic interactions and electrostatic attractions (207). For molecules to self-assemble spontaneously there must be a reduction in Gibb's free energy. As discussed earlier, two main driving forces for a change in free energy are enthalpy and entropy, see Equation 3.4. The entropy change associated with self-assembly can be calculated according to Equation 5.1 where ϕ_{free} and ϕ_{N} are the volume fraction of the free solute and the self-assembled

interfaces respectively, N is the number of free solute molecules and k is Boltzmann constant (209).

$$\Delta S \text{ (J/K)} = -k(\ln\phi_N - N\ln\phi_{\text{free}}) \quad \text{Equation 5.1}$$

The arrangement of molecules into self-assembled structures would result in a reduction in disorder (208) and a decrease in entropy. Therefore the process would need to be exothermic with a magnitude greater than the $T\Delta S$ term for self-assembly to be thermodynamically viable.

Different types of self-assembly have been described. These include static and dynamic self-assembly, with further variations including templated and biological (207). Static self-assembly involves the formation of structures that are in equilibrium. In contrast to this dynamic self-assembly (sometimes referred to as self-organisation) produces structures which are not in equilibrium but are releasing energy (210). Templated self-assembly aims to produce structures in a “bottom-up” manner with, as the name suggests, the use of templates (211).

5.1.1 Common self-assemblies

Self-assembling molecules are common and examples are numerous. Common self-assemblies of molecules include crystals, micelles, liposomes and gels. Crystals are examples of solid self-assemblies (212). The molecules or ions are arranged in lattice structures with intermolecular forces holding them together. As discussed earlier,

surfactants and phospholipids self-assemble into micelles and liposomes respectively. The driving forces for this self-assembly is the hydrophobic effect, with steric and electrostatic (for polar head groups) forces opposing the formation of micelles (213). As discussed and observed earlier, these self-assembled structures can improve the solubility of poorly soluble drugs by protecting the whole or part of the compound from water molecules in the system.

5.1.2 Nature's self-assembly

Biology and nature provides a large number of examples of self-assembly. The nucleic acids, viruses, phospholipid bilayers and clathrin are just a few of the examples.

Nucleic acids (deoxyribonucleic acid (DNA) and ribonucleic acid (RNA)) are capable of self-assembly. The two strands are held together by hydrogen bonds between the complementary base pairs. Viruses are composed of nucleic acid surrounded by a self-assembled protein coat. The subunits of the protein coat of the tobacco mosaic virus can self-assemble into various forms such as a 20S aggregate disk and helix around the RNA (214). The subunits are held together by hydrophobic, electrostatic and intersubunit carboxylate interactions (215). Clathrin is a triskelion (a molecule which has three identical legs from a central point), containing three heavy and three light chains in its structure (216). Clathrin triskelia have the ability to self-assemble into cages or coats (if adaptor molecules are present) (216). Clathrin also has the ability to form different vesicles with different sizes and shapes. This allows the

encapsulation of various substances (217). Phospholipids are another example of natural self-assembly. The phospholipid molecules have a hydrophilic polar head group and hydrophobic aliphatic tails. The bilayer is formed when the molecules arrange themselves so that the hydrophobic tails are surrounded on either side by the polar head groups. The phospholipids can also interact with other compounds which make up membranes such as oligosaccharides and proteins. The same type of interactions are involved with these associations as before (218).

5.1.3 Polymers

There are numerous examples of self-assembling polymers in the literature including the poloxamers seen in earlier chapters. Other examples of polymers which can self-assemble include the triblock copolymer of poly(L-lysine) dendrimer-PEG-poly(L-lysine) dendrimer (219). The positively charged L-lysine at the chain termini of the triblock copolymer interact with the negatively charged phosphates of plasmid DNA. The DNA is found within the hydrophobic core (along with the dendritic sections of the copolymer and the linear PEG forms the hydrophilic shell in spherical structures at a charge ratio of 4.0 (219).

5.1.4 Small molecules

Trimesic acid (1,3,5-Benzenetricarboxylic acid) is a small molecule which self-assembles into chicken wire type structures, see Figure 5.1a (220). Another example of trigonal small molecule self-assembly are trigonal rigid triphenols (Figure 5.1b), which are composed of three triphenols bound to a benzene ring (221). These

molecules form intermolecular hydrogen bonds similar to the ones found in trimesic acid and form chicken wire or honeycomb type structures (221). The bile acids have also been shown to self-assemble into structures with a hydrophobic core and hydrophilic shell (110). Another example is the self-assembly of Trigonal(FKFE)₂ into nanometre sized spherical structures by the formation of hydrogen bonds between the antiparallel β -sheets of the polypeptide arms (222). This is not the only example of peptides in triskelion structures being used for self-assembly. FTAEA is formed from the addition of peptides to 9-fluorenylmethoxycarbonyl (Fmoc), with additional stabilisation from Fmoc-FY (223). This two component system can assemble into spheres with a diameter of approximately 70 nm (223).

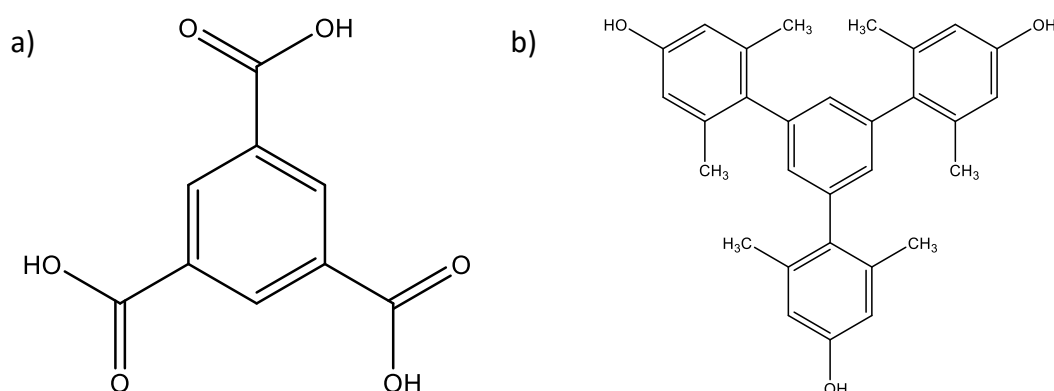


Figure 5.1. Structure of a) trimesic acid and b) and example of a trigonal rigid triphenol.

5.1.5 Molecular Field Point Descriptors

Field points were used during the molecule design phase to allow the likelihood of interactions between other molecules of the same substance or a different

substance. Cheeseright *et al.* described how molecules with similar fields should bind to the same active site, independently of the structure of the molecules (224). The field points are mapped around the molecule and coded different colours depending on the type of field. The size of the field point displayed represents the depth of the energy potential of the functional group (224).

The field points used by the software are:

- Blue - nucleophilic field points or hydrogen bond acceptors.
- Red – electrophilic field points or hydrogen bond donors.
- Yellow – van der Waals surface field points.
- Gold – hydrophobic field points (224, 225).

5.2 Aims

The aims of this section are to design molecules which can be put forward for molecular dynamics. The molecules will be designed so that there are functional groups present which may allow for self-assembly and improve the solubility of poorly soluble compounds. The full ideal characteristics for the molecules can be found in the overall project aims in chapter 1.10.

5.3 Methods

5.3.1 Literature Review

As a starting point for molecule design a review of the literature was carried out. The review focussed on looking at the structure of molecules reported to self-assemble into larger structures.

5.3.2 Molecule design

FieldView 2.0.2 Revision 14848 (Cresset Group, Hertfordshire, UK) was used for drawing the molecules based on design ideas. Field points were added to the structures and examined. If the field points suggested that the molecule would self-assemble, with a hydrophobic core then it was accepted for further investigation.

Molecules with apparent acceptable field points were then input into I-Lab 2.0 (ACD/Labs, <https://ilab.acdlabs.com/iLab2/>) for prediction of physicochemical properties (pK_a , solubility, Log P) and IUPAC naming.

5.4 Results

5.4.1 Literature Review

After reviewing the literature it was observed that a number of self-assembling molecules are triskelion structures including FTAEA (requires stabilisation) (223), trimesic acid (220) and trigonal rigid triphenols (221). Other small molecules which can self-assemble included bile acids such as cholic acid (110). Hydrogen bonding appeared to be important in molecules which self-assemble. Although larger

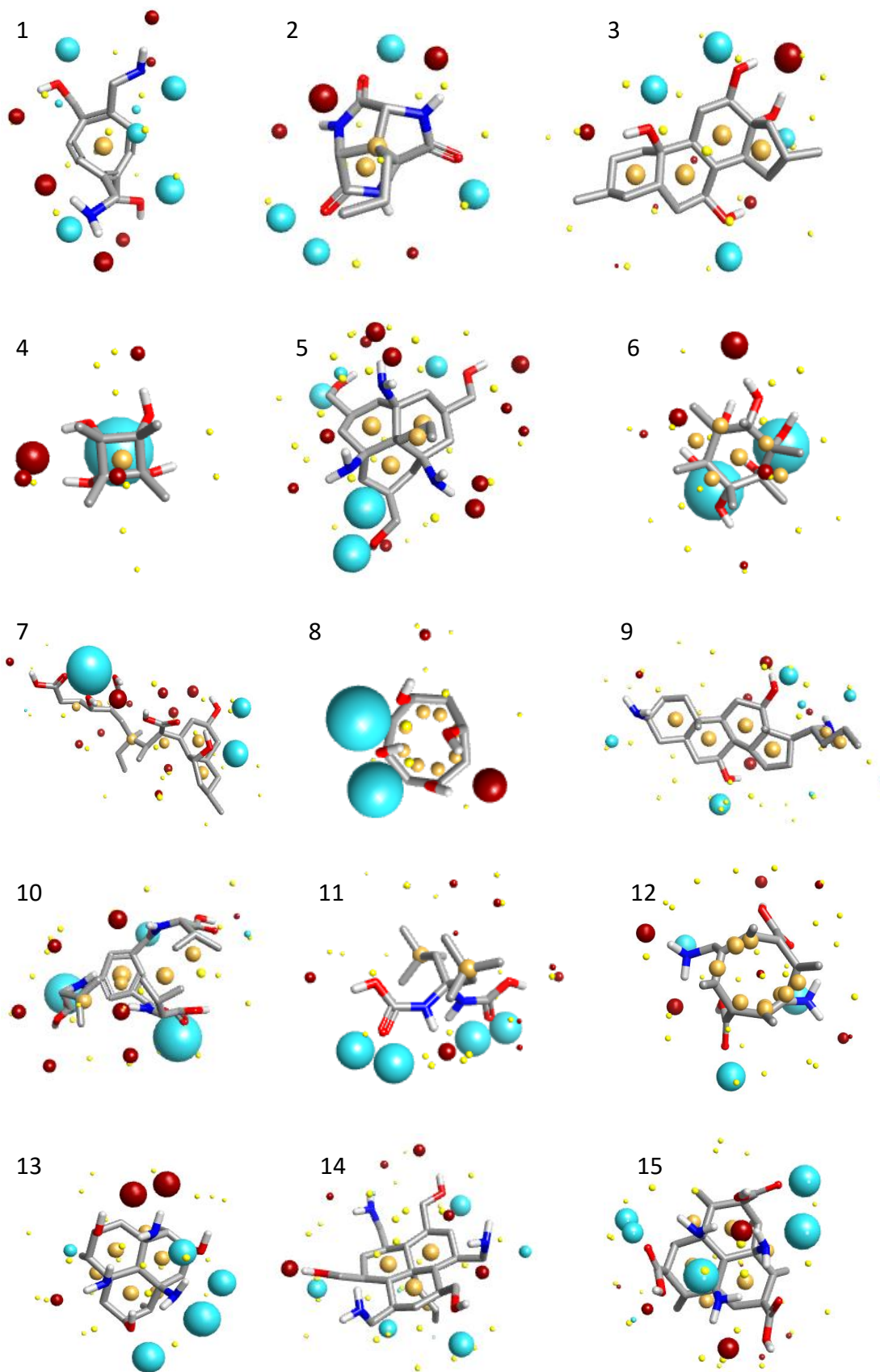
molecules have been shown to self-assemble, their properties do not fit with the desired molecule design in the aims.

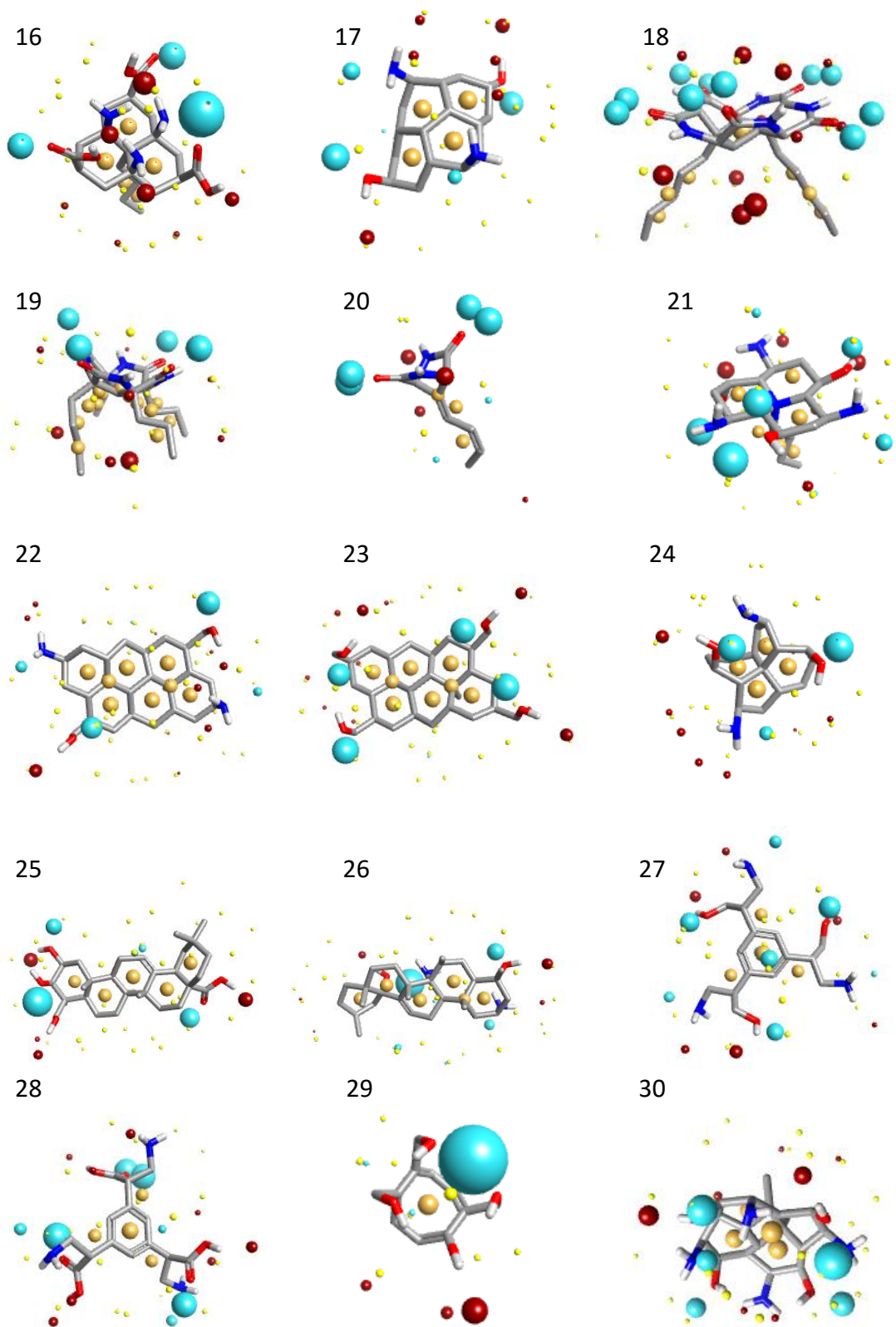
5.4.2 Molecule Design

A number of molecules were designed. Their field points are displayed.

The designed molecules should have a side which has hydrophobic field points and another side with electrophilic and nucleophilic field points to interact with poorly soluble drug and water/hydrophilic molecules respectively.

Molecules designed can be found in Figure 5.2. The 2D structure and the IUPAC names for each of the molecules can be found in appendix 3.





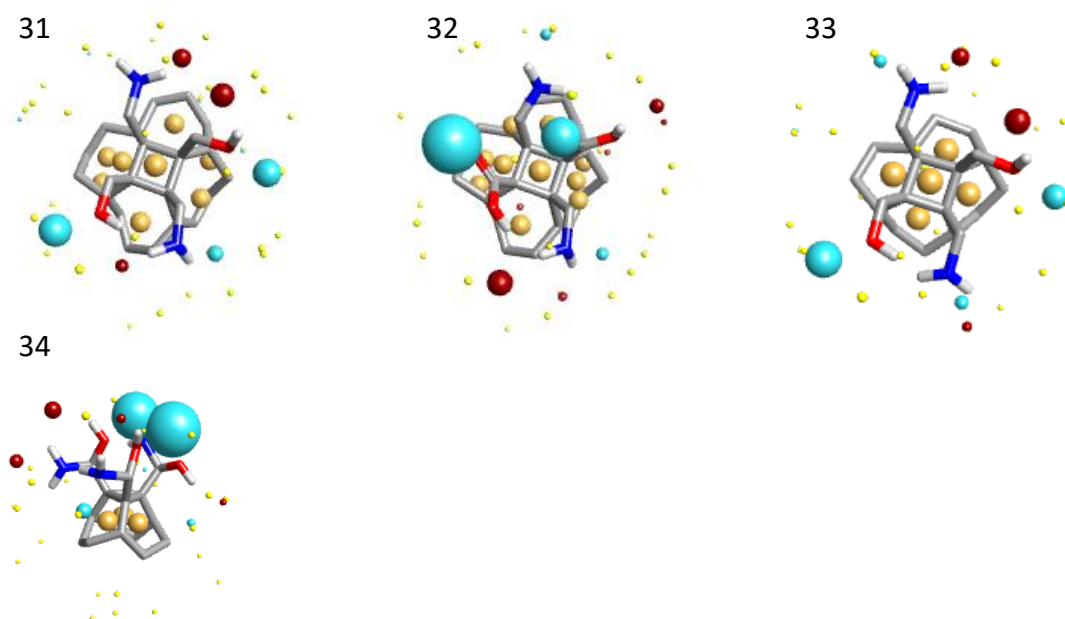


Figure 5.2. Molecule designs (1-34) which were drawn using FieldView 2.0.2

Revision 14848. Atoms are represented by colour: carbon is represented by grey atoms; hydrogen by white; oxygen by red; and nitrogen by blue. The field points as described above are nucleophilic points are blue spheres, electrophilic points are red spheres, van der Waals surfaces are yellow spheres and hydrophobic points are gold spheres.

5.5 Discussion

5.5.1 Molecule Design

The structure of the molecules designed had some common features and can therefore be grouped. Six molecules (numbers 1, 4, 6, 8, 12 and 29) are single ring compounds. These were designed with hydrophilic groups on one side of the molecule, with a hydrophobic side. The hydrophobic strength was increased in two of the molecules (6 and 12) by the addition of methyl groups to one side of the ring.

It was hypothesised that the hydrophilic functional groups would allow for the self-assembly of the molecules and the hydrophobic side would allow for the interaction with poorly soluble compounds to increase their solubility.

Another group of molecules was designed based on two to six ring structures joined around a central point. Around the outside of the structure was placed hydrophilic groups capable of hydrogen bonding. From the below the central point one or more aliphatic chains are found, to improve hydrophobic interactions. There were 11 molecules in this group (2, 5, 13, 14, 15, 16, 18, 19, 20, 21 and 30).

The third group of molecules were based on a steroid structure. The steroid cholic acid has been found to self-assemble with a hydrophobic core (110). However, the convex surface of the molecule is hydrophobic and the concave surface hydrophilic (110). These molecules were designed to flip the surfaces to allow the self-assembly with a hydrophobic core. Six molecules were designed in this manner (3, 9, 22, 23, 25 and 26).

Molecule 7 was designed to have a similar shape to the above molecules based on steroids, with fewer ring structures allowing for more bond rotation within the molecule which may help in self-assembly and association with other molecules.

Molecules 10, 27 and 28 were designed based on the ability of trimesic acid to self-assemble (226). The aromatic ring in the centre of the molecule has three identical

substitutions on the ring. It was hypothesised that as other molecules with three side chains such as clathrin and trigonal rigid triphenols can self-assemble and allow inclusion of other molecules within the core (217, 221), then these would also self-assemble in a similar way.

Molecule 11 is a small molecule that was designed to investigate whether this type of molecule would be suitable for self-assembly and solubilisation.

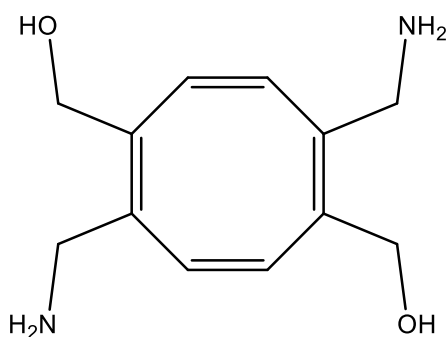
The basis for the design of the other six molecules shown in Figure 5.2 (17, 24, 31, 32, 33 and 34) was similar to the second group of molecules described above. The structures had four or five rings in their structure which allowed the formation of a concave hydrophobic surface, suited to association with other hydrophobic molecules. Depending on the structure hydrophilic groups capable of hydrogen bonding were placed around the outside or protruding from the convex side of the molecule.

5.5.2 Selected Molecules

From the above molecules, five were selected for further *in silico* investigation using Materials Studio. The molecules were selected based upon their structure, and predictions on the physicochemical properties were carried out using ACD I-Lab 2.0.

[4,8-bis(aminomethyl)cycloocta-1,3,5,7-tetraene-1,5-diyl]dimethanol or 'Molecule 1' is an eight membered ring with alternating single and double bonds. It was chosen

as a suitable candidate due to the oxygen and nitrogen atoms being placed in positions which should allow hydrogen bonding between molecules. In addition, the core of the ring structure is hydrophobic which should allow the interaction with hydrophobic compounds. The physicochemical properties for the molecule can be found in Table 5.1. The pK_as suggest that physiological pH the molecule will be ionised at both amine groups in the structure. Solubility prediction for Molecule 1 has been classed as having borderline reliability.

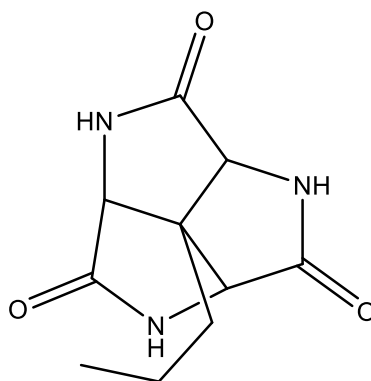


Molecule 1

Table 5.1. Predicted physicochemical properties of Molecule 1.

Property	ACD I-Lab Result
Molecular Weight	222.28
Predicted pK _a (s)	10.08 (amine group) 9.48 (amine group)
Predicted Solubility	67.8 mg/mL

Molecule 2, or 6b-propylhexahydro-1,3,5-triazacyclopenta[cd]pentalene-2,4,6(1H)-trione, has a hydrophobic region extending out from the three ring structure. The oxygen and nitrogen atoms should contribute to the ability of self-assembly. Physicochemical predictions show that there are no groups with pK_as that would be ionised within the physiological range. The solubility prediction is greater than for Molecule 1 however also has borderline reliability (Table 5.2).

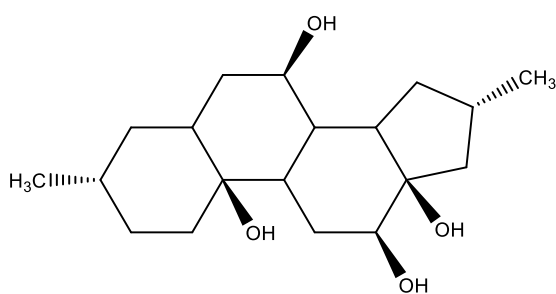


Molecule 2

Table 5.2. Predicted physicochemical properties of Molecule 2.

Property	ACD I-Lab Result
Molecular Weight	223.23
Predicted pK _a (s)	N/A
Predicted Solubility	97.7 mg/mL

Molecule 3 was designed based on cholic acid which has self-assembling properties (110). The hydrophilic and hydrophobic groups of the molecule were switched so that the concave section of the molecule would be hydrophobic and in self-assembled structures be in the centre. Its IUPAC name is 3,16-dimethylgonane-7,10,12,13-tetrol. The physicochemical properties predicted by the software can be found in Table 5.3. The molecule, according to the pK_a predictions would be non-ionisable in physiological pH. The molecule is predicted to have a low solubility with moderate reliability; however it may have the ability to self-assemble in a manner similar to cholic acid.

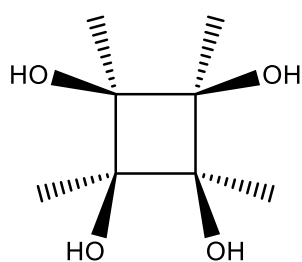


Molecule 3

Table 5.3. Predicted physicochemical properties of Molecule 3.

Property	ACD I-Lab Result
Molecular Weight	324.45
Predicted $pK_a(s)$	N/A
Predicted Solubility	0.59 mg/mL

Molecule 4 is a small molecule with four hydroxyl groups on one side of the ring structure and four methyl groups on the other, giving the molecule a hydrophobic and hydrophilic face. The low solubility is not reliable, and there are no pK_as affecting the ionisation within the physiological pH ranges (Table 5.4). The IUPAC name is (1R,2r,3S,4s)-1,2,3,4-tetramethylcyclobutane-1,2,3,4-tetrolate.



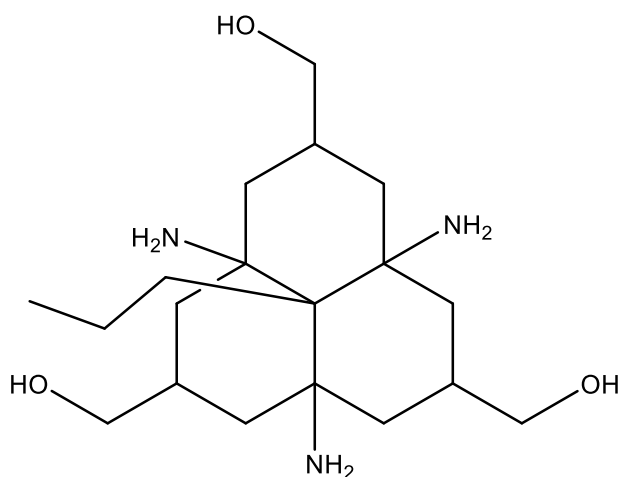
Molecule 4

Table 5.4. Predicted physicochemical properties of Molecule 4.

Property	ACD I-Lab Result
Molecular Weight	176.21
Predicted pK _a (s)	N/A
Predicted Solubility	3.9 mg/mL

The final molecule selected for further *in silico* investigation was (3a,6a,9a-triamino-9b-propyldodecahydro-1H-phenalene-2,5,8-triyl)trimethanol or Molecule 5. The overall shape of this molecule is similar to that of Molecule 2. The hydrophilic region

is however larger than that for Molecule 2 which may provide a greater surface area for self-assembly. Molecules are predicted to have a charge of 2⁺ or 3⁺ in physiological conditions with three primary amine groups in its structure (Table 5.5). The solubility is predicted to be low, however the results are not reliable.



Molecule 5

Table 5.5. Predicted physicochemical properties of Molecule 5.

Property	ACD I-Lab Result
Molecular Weight	355.51
Predicted pK _a (s)	10.59 (amine group) 9.10 (amine group) 7.61 (amine group)
Predicted Solubility	0.44 mg/mL

5.5.3 Other Molecules

Of the other molecules designed (Figure 5.2), some would also have been suitable candidates for further investigation if time had permitted. Molecules 6, 8, 11, 12, 14, 17, 21, 24, 26, 29, 30, 31, 32 and 33 had a structure would have been considered for further investigation.

Of the other molecules, which were not suitable for further *in silico* investigation, the decision was made based upon the likelihood of either electrophilic or nucleophilic fields being present on both sides of the molecule, and therefore affecting the ability to interact with the less hydrophilic compounds for which they are intended to increase solubility. This was the reason for rejecting Molecules 7, 9, 10, 13, 15, 16, 18, 19, 25, 27 and 28. Another reason for not selecting a molecule for further investigation was due to the shape of the molecule. Due to the flat shape of Molecules 22 and 23, there may be a limit to the type of molecule with which it can interact. These two molecules may only undergo planar stacking. For the other two molecules not covered (20 and 34), while both appear to have a shape which may self-assemble with a hydrophobic core, there is only a relatively small area where hydrogen bonding can occur, which may be too small if there are other molecules present.

6 Chapter 6 – Molecular Dynamics Simulations

6.1 Introduction

The previous chapter described the design of molecules which would then be put through further *in silico* investigation with the use of molecular dynamics.

6.1.1 Force Fields

During atomistic molecular dynamics, which will be used here, the behaviour of molecules at the atomic level requires to be simulated. A number of force fields have been developed which carry out this function. Developed force fields include: Condensed-phase Optimized Molecular Potentials for Atomistic Simulation Studies (COMPASS); Polymer Consistent Force Field (pcff); Chemistry at HARvard Macromolecular Mechanics (CHARMM); Assisted Model Building with Energy Refinement (AMBER); and DREIDING. The force field used during a dynamics simulation may depend on the type of molecule being investigated or the environment which is being represented. The force fields use different parameters to describe different atoms, bonds and interactions (227). DREIDING is a generic force field and atoms are allocated to an atom type, with atoms of the same type treated equally (227). This force field may be useful for novel compounds including biological and inorganic substances (227). Other force fields have been developed for the analysis of specific types of molecules such as CHARMM for biological macromolecules such as proteins and DNA (228). The group of AMBER force fields were designed originally for the study of proteins and nucleic acids (229), however

further developments have extended its use to include smaller organic molecules such as pharmaceutical compounds (229). Both the COMPASS force field and pcff are part of the same family of *ab initio* consistent force fields (230). Force fields which do not use *ab initio* data derived the parameters from experimentally observed data (231, 232). The use of *ab initio* force fields allows the prediction of atom or molecule behaviour where this data is missing or incomplete (231).

6.1.2 Cohesive energy density

Molecular dynamics can be used to predict if a substance will be soluble in another by determination of the solubility parameter (δ). The solubility parameter is equal to the square root of the cohesive energy density (CED) (Equation 6.1). CED is defined as the amount of energy required to remove one unit volume of molecules from their neighbours to infinite separation. CED can be determined by Equation 6.2 where ΔH is the heat of vaporisation, R is the gas constant, T is the temperature in Kelvin and V_m is the molar volume (233).

$$\delta \text{ ((cal/cc)}^{1/2}) = \sqrt{\text{CED}} \quad \text{Equation 6.1}$$

$$\text{CED (cal/cc)} = \frac{\Delta H - RT}{V_m} \quad \text{Equation 6.2}$$

The solubility parameter can be used for predicting the likelihood that a compound is soluble in a solvent. Compounds with similar δ are likely to have similar solubility characteristics (233). However this is not always true. Two compounds can have similar values for CED and δ but be immiscible. Miscibility depends on the type of

intermolecular interactions that the compounds form, for example the presence of strongly polar groups or hydrogen bonding groups versus the absence of similar groups (233, 234) and so CED and δ should be used as an indication of whether substances are miscible if they are likely to associate with each other.

When predicting if one molecule will be soluble in another the solubility parameters for the compound and solvent can be examined. The difference between these two values ($\Delta\delta$) indicates whether the compound will be soluble in the solvent, the lower the value of $\Delta\delta$ the higher the likely solubility of the compound in the solvent (234).

6.2 Aims

This chapter aims to investigate whether the molecules identified in the previous chapter are likely to increase the solubility of poorly soluble molecules with the use of molecular dynamics.

6.3 Methods

Molecular simulations were carried out using the Forcite module on Materials Studio 5.5. The force field used was COMPASS27. This force field was used as it uses *ab initio* data and due to the fact that novel molecules were to be used there would likely be a lack of experimental data for the bonds. The first step in the process was to create the amorphous cell using the AC construct tool. Following amorphous cell creation, the energy of the system was minimised using the Geometry Optimization tool in the module, the system was allowed to carry out up to 5,000,000 iterations to

calculate the minimum energy. This process took around 45 minutes to complete for each amorphous cell. Before the solubility parameter can be calculated, the dynamics of the system have to be determined using the Dynamics tool. Dynamics was conducted under constant temperature at 298K, set using the Andersen thermostat option, and volume. Dynamics was run for 500,000 steps, with each step equalling one femtosecond giving a total simulation time of 500 picoseconds. One frame was output every 500 steps, giving a total of 1001 frames per run. Cohesive energy density calculations were then run to determine the solubility parameter. Mean solubility parameters were calculated from the 1001 frames of dynamics data. The solubility parameters were used to determine if an excipient might increase the solubility of ibuprofen and gliclazide. Control simulations with water and either excipient or drug alone, with the same quantity of molecules, were used to allow quantification of the effect. Ibuprofen and gliclazide were chosen due to the low solubility results observed during experimental solubility studies. Excipients used were chosen from the molecules designed earlier (see chapter 5). HP- β -CD was used as a comparison on the ability of the selected novel compounds to increase solubility, the molecule was built with seven substitutions as the batches used had between five and eight substitutions per molecule. The ratios used were 1:1 and 1:2 (drug:excipient) for both drugs and all excipients. The simulations were conducted in 1000 molecules of water. For the 1:1 ratio, one molecule each of drug and excipient was used, and for the 1:2 ratio, one molecule of drug was used with two molecules of excipient.

Investigation of whether the excipient compounds may self-assemble was carried out with five molecules in 1000 molecules of water and the described procedure above was followed for molecular dynamics calculations.

Statistical analysis of the data was carried out using Minitab 16[®]. Analysis of variance was carried out with Tukey's test to determine solubility parameters were statistically different from each other.

6.4 Results

To investigate whether the five novel molecules might increase the solubility of ibuprofen and gliclazide, molecular dynamics simulations were carried out. Following the simulations the solubility parameters were recorded. Control simulations were conducted with 1000 molecules of water, one drug molecule in water (1000 molecules) and the excipients (either one or two molecules) in the presence of 1000 water molecules. The solubility parameters for all simulations can be found in Tables 6.1 and 6.2.

6.4.1 Ibuprofen and Gliclazide Solubility

Water alone had a solubility parameter (δ) of 47.905 ± 0.250 (cal/cc)^{1/2} when 1000 molecules of water were investigated. The solubility parameter of ibuprofen in 1000 molecules of water was 47.667 ± 0.257 (cal/cc)^{1/2}. The difference between the two solubility parameters ($\Delta\delta$) is 0.238 (cal/cc)^{1/2}, this value is used to determine if the excipients may increase the solubility of ibuprofen. If $\Delta\delta$ is smaller when an excipient

is included in the simulations then the solubility of the drug is expected to increase. When HP- β -CD is present in a 1:1 ratio (ibuprofen:HP- β -CD) δ drops to 46.045 ± 0.253 (cal/cc)^{1/2} and at a 1:2 ratio 44.591 ± 0.245 (cal/cc)^{1/2} the $\Delta\delta$ are 0.189 and 0.178 respectively (Table 6.1). The difference in solubility parameters for each of the five novel molecules can also be found in Table 6.1. From the table it can be observed that at the 1:1 ratio the order for increasing ibuprofen solubility is Molecule 1 > Molecule 3 > Molecule 5 > Molecule 2 > Molecule 4. This pattern is not maintained at the 1:2 ratio, Molecule 3 > Molecule 5 > Molecule 1 = Molecule 4 > Molecule 2. The $\Delta\delta$ for the 1:2 ratio was lower than the 1:1 ratio for all excipients.

The results for gliclazide vary from the results obtained for ibuprofen. The solubility parameter for gliclazide in 1000 water molecules was 47.541 ± 0.261 (cal/cc)^{1/2}. When investigating the effects of HP- β -CD *in silico*. At the 1:1 ratio (gliclazide:HP- β -CD) δ is 45.900 ± 0.251 (cal/cc)^{1/2} and at a 1:2 ratio 44.454 ± 0.243 (cal/cc)^{1/2} the $\Delta\delta$ are 0.334 and 0.315 respectively (Table 6.2). Investigation of the five novel compounds can be observed to produce the key differences between gliclazide (Table 6.2) and ibuprofen. Not all of the molecules reduced the solubility parameter with gliclazide compared to the excipient in water. Molecule 2 did not decrease the solubility parameter at either ratio. Molecule 1 decreased the solubility parameter only at the 1:1 ratio while Molecule 4 showed a $\Delta\delta$ decrease at the 1:2 ratio. A decrease of solubility parameter was observed at both ratios for both Molecules 3 and 5. From the table it can be observed that at the 1:1 ratio the order for increasing gliclazide solubility is Molecule 1 > Molecule 5 > Molecule 3 > Molecule 4 > Molecule

2. Similarly to ibuprofen this order is not maintained at the 1:2 ratio, Molecule 5 > Molecule 3 > Molecule 4 > Molecule 1 > Molecule 2. The $\Delta\delta$ for the 1:2 ratio was lower than the 1:1 ratio for Molecules 3, 4 and 5 but higher than the 1:1 ratio for Molecules 1 and 2.

The difference between the $\Delta\delta$ of the drug control versus the $\Delta\delta$ of drug in the presence of excipient was examined. It can be observed from Tables 6.1 and 6.2 that all excipients reduce the solubility parameter of ibuprofen greater than gliclazide, represented by a larger difference between $\Delta\delta$ in water and $\Delta\delta$ in water and excipient. For both drugs the lowest change in solubility parameter was observed with HP- β -CD at the 1:2 ratio, followed by the 1:1 ratio of HP- β -CD (Figure 6.1).

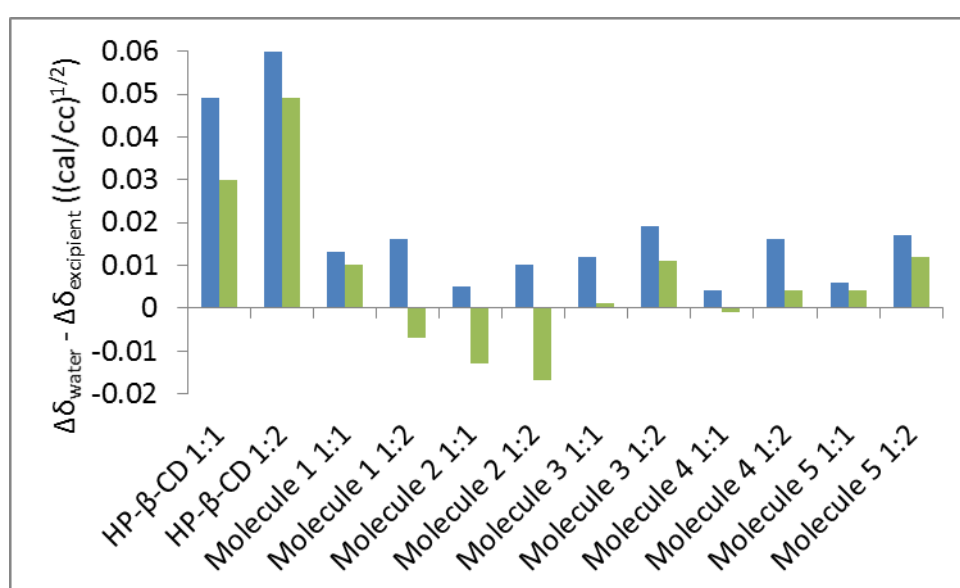


Figure 6.1. Bar chart of the difference between $\Delta\delta_{\text{water}}$ and $\Delta\delta_{\text{excipient}}$. Blue represents ibuprofen and green represents gliclazide. Negative changes represent an expected decrease in solubility of the compound.

Table 6.1. Mean (standard deviation) solubility parameters (cal/cc)^{1/2} for ibuprofen.

All simulations run in 1000 water Molecules, n = 1001.

	No Drug	Ibuprofen x 1	Δδ
No Excipient	47.905 (0.250)	47.667 (0.257)	0.238
HP-β-CD x 1	46.234 (0.245)	46.045 (0.253)	0.189
HP-β-CD x 2	44.769 (0.240)	44.591 (0.245)	0.178
Molecule 1 x 1	47.684 (0.259)	47.459 (0.257)	0.225
Molecule 1 x 2	47.479 (0.254)	47.257 (0.255)	0.222
Molecule 2 x 1	47.658 (0.257)	47.425 (0.258)	0.233
Molecule 2 x 2	47.421 (0.247)	47.193 (0.262)	0.228
Molecule 3 x 1	47.549 (0.263)	47.323 (0.258)	0.226
Molecule 3 x 2	47.207 (0.257)	46.988 (0.248)	0.219
Molecule 4 x 1	47.724 (0.274)	47.490 (0.267)	0.234
Molecule 4 x 2	47.547 (0.267)	47.325 (0.259)	0.222
Molecule 5 x 1	47.538 (0.254)	47.306 (0.251)	0.232
Molecule 5 x 2	47.167 (0.259)	46.946 (0.251)	0.221

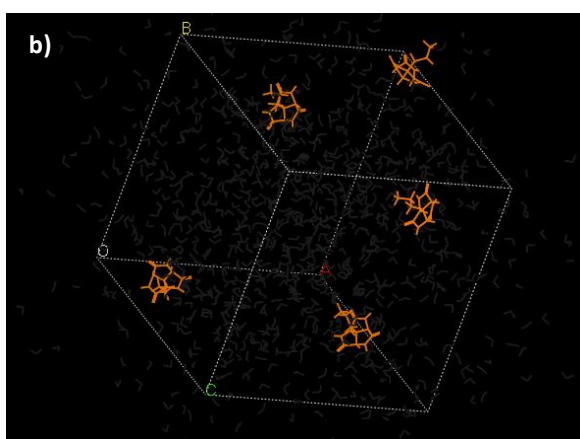
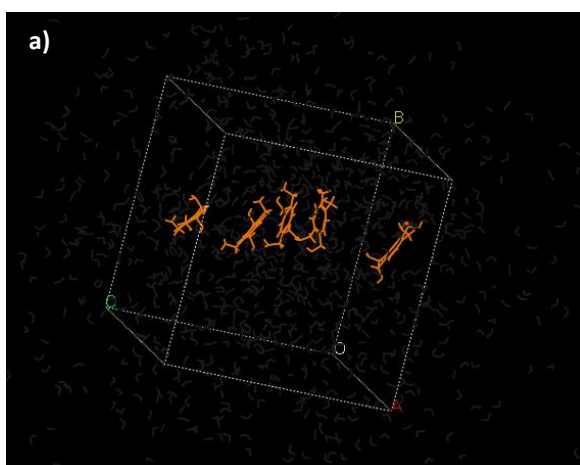
Table 6.2. Mean (standard deviation) solubility parameters (cal/cc)^{1/2} for gliclazide.

All simulations run in 1000 water Molecules, n = 1001.

	No Drug	Gliclazide x 1	Δδ
No Excipient	47.905 (0.250)	47.541 (0.261)	0.364
HP-β-CD x 1	46.234 (0.245)	45.900 (0.251)	0.334
HP-β-CD x 2	44.769 (0.240)	44.454 (0.243)	0.315
Molecule 1 x 1	47.684 (0.259)	47.330 (0.267)	0.354
Molecule 1 x 2	47.479 (0.254)	47.108 (0.254)	0.371
Molecule 2 x 1	47.658 (0.257)	47.281 (0.263)	0.377
Molecule 2 x 2	47.421 (0.247)	47.040 (0.261)	0.381
Molecule 3 x 1	47.549 (0.263)	47.186 (0.260)	0.363
Molecule 3 x 2	47.207 (0.257)	46.854 (0.254)	0.353
Molecule 4 x 1	47.724 (0.274)	47.359 (0.259)	0.365
Molecule 4 x 2	47.547 (0.267)	47.187 (0.256)	0.360
Molecule 5 x 1	47.538 (0.254)	47.178 (0.260)	0.360
Molecule 5 x 2	47.167 (0.259)	46.815 (0.258)	0.352

6.4.2 Excipient Self-Assembly

To determine if the five novel excipients might self-assemble molecular dynamics was run on five excipient molecules in 1000 molecules of water. Molecule 1 appears to show stacking of the ring moieties of the molecules (Figure 6.2a). Molecules 2 and 3 did not appear to show signs of self-assembly (Figure 6.2b and c). Two of the molecules appeared to be closely associated during the dynamics simulation for Molecule 4 (Figure 6.2d). During the simulation for Molecule 5, all excipient molecules showed signs of self-assembly (Figure 6.2e).



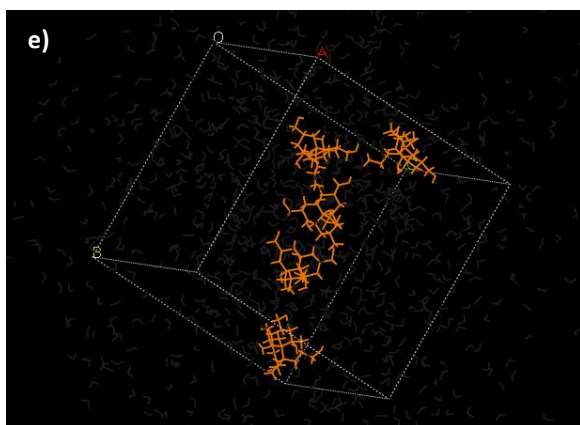
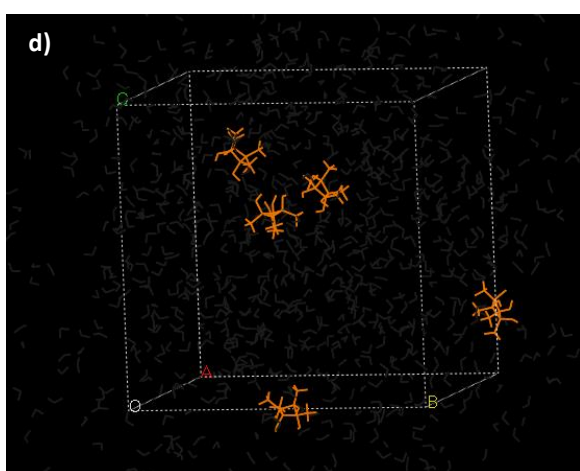
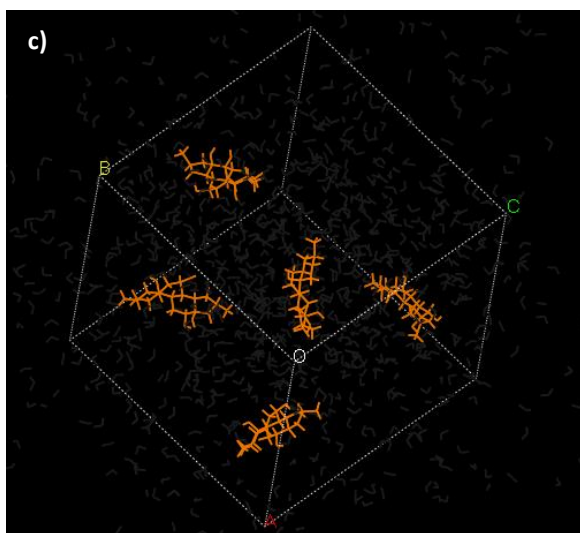


Figure 6.2. Screenshots of dynamics simulations of five novel excipients in water. a) Molecule 1, b) Molecule 2, c) Molecule 3, d) Molecule 4, e) Molecule 5. Water not shown.

6.5 Discussion

6.5.1 Ibuprofen and Gliclazide Solubility

As the change in solubility parameter for ibuprofen was smaller than the solubility parameter for gliclazide in water, this suggests that the solubility of ibuprofen is greater than gliclazide solubility. This agrees with the results obtained in (chapter 2.5.3). As discussed earlier the mean solubility of gliclazide was 0.0928 mM in water whereas the mean solubility of ibuprofen in water was 0.145 mM. It was therefore expected that ibuprofen would have a smaller solubility parameter than gliclazide. As a control ibuprofen and gliclazide were investigated with HP- β -CD to determine if solubility results observed experimentally could be replicated *in silico*. HP- β -CD increased the solubility of both ibuprofen and gliclazide. The solubility parameter of ibuprofen was affected to a smaller extent than gliclazide indicating that HP- β -CD increased the solubility of ibuprofen to a greater degree than gliclazide. This agrees with the results in chapter 2.5.3. The simulations were not able to show the entry of either ibuprofen or gliclazide into the cavity of the cyclodextrin molecule (Figure 6.3), as described in the literature (139, 140). From the figure, it can be seen that there is little interaction between ibuprofen and HP- β -CD, but an association between gliclazide and the side chains of HP- β -CD may be present.

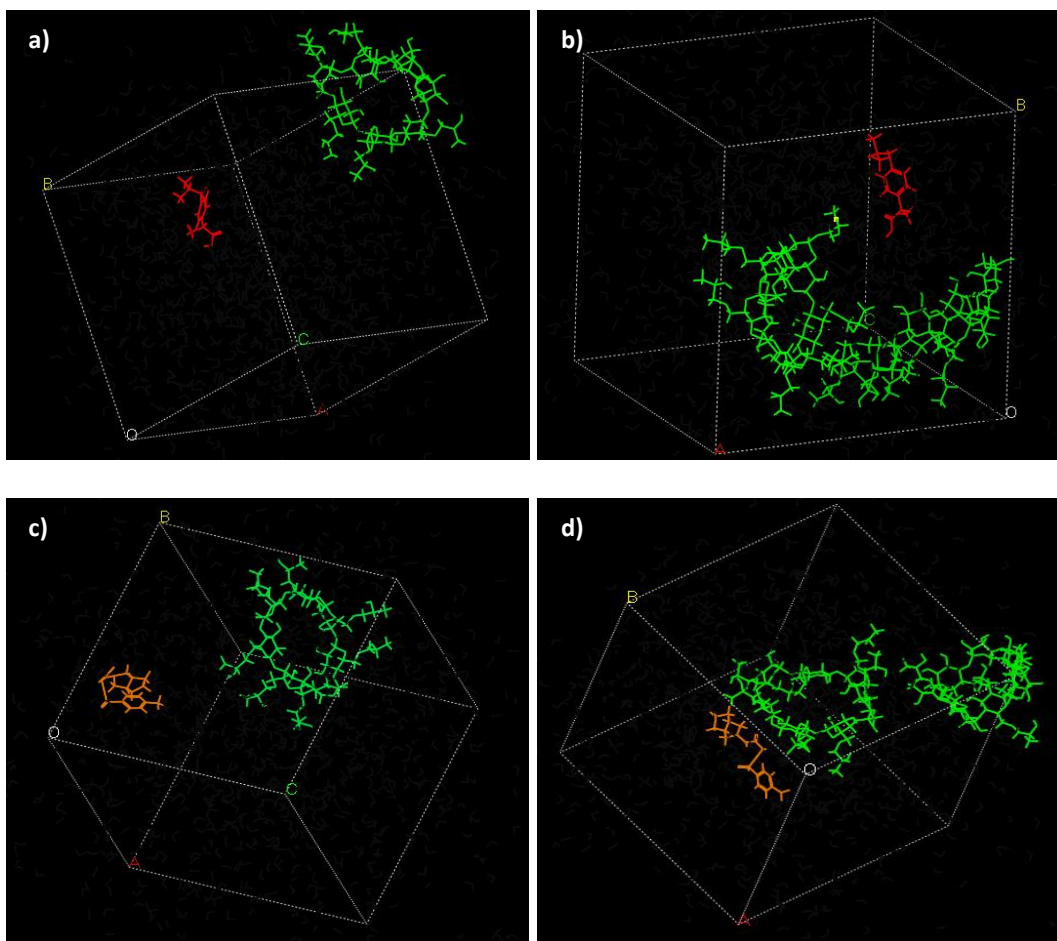


Figure 6.3. Screenshots of the dynamics simulations between a) ibuprofen and HP- β -CD at 1:1 ratio, b) ibuprofen and HP- β -CD at 1:2 ratio, c) gliclazide and HP- β -CD at 1:1 ratio, d) gliclazide and HP- β -CD at 1:2 ratio. HP- β -CD is represented in green, ibuprofen in red and gliclazide in orange, water not shown.

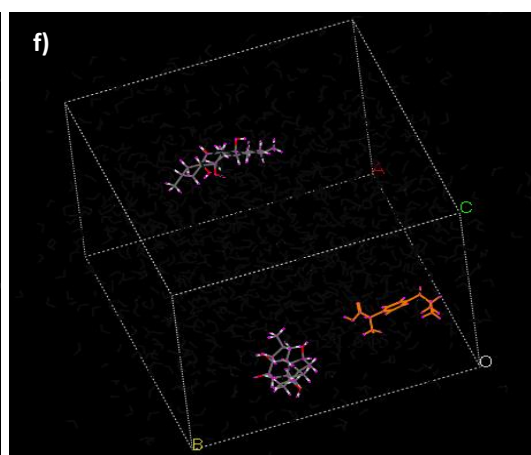
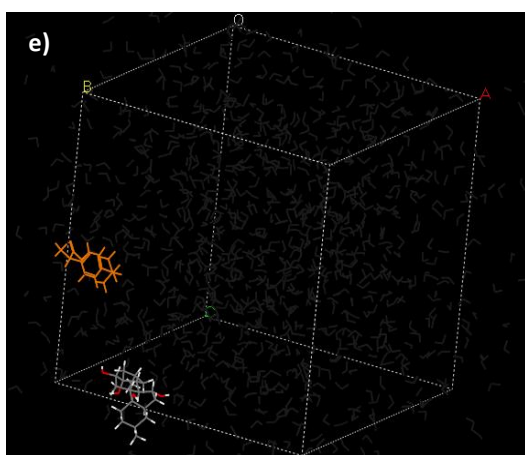
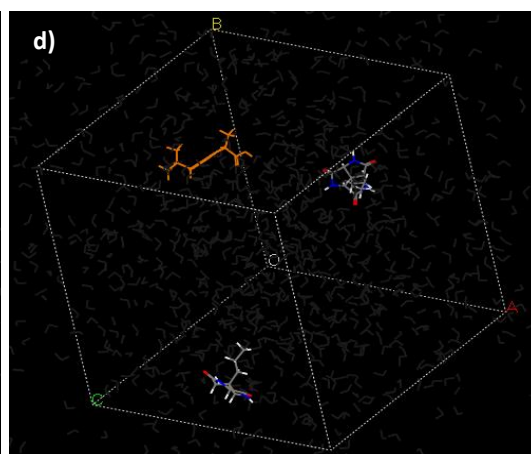
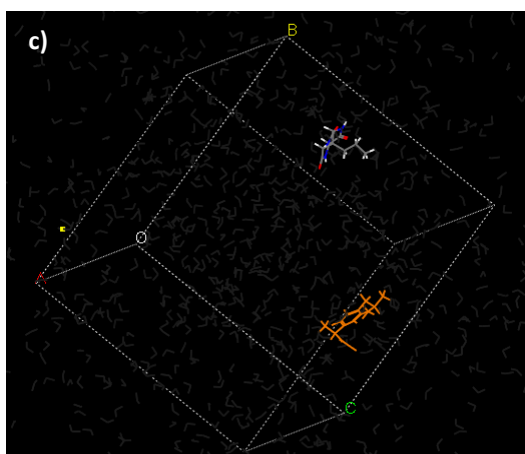
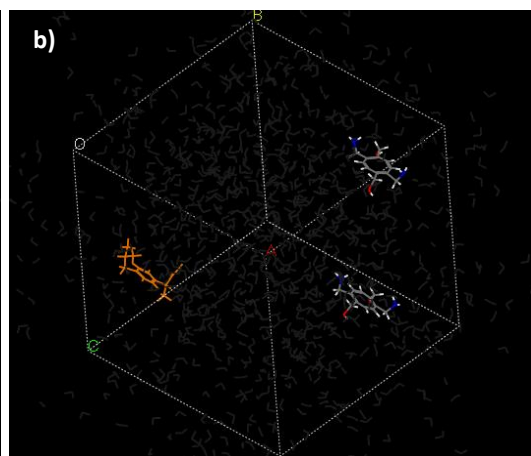
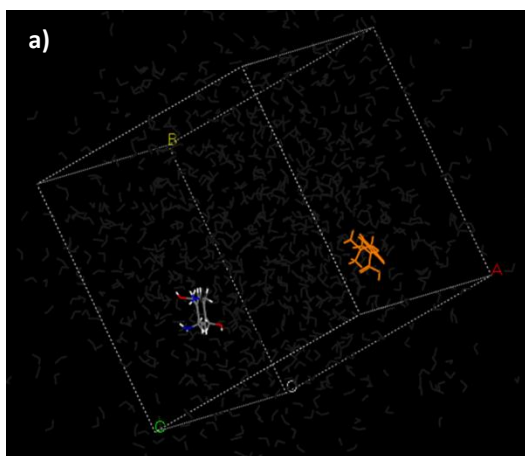
For ibuprofen the change in solubility parameters for all excipients suggest that all may increase the solubility of ibuprofen. However, all five novel excipients had higher $\Delta\delta$ than HP- β -CD suggesting that all five did not increase the solubility of ibuprofen to the same extent as the cyclodextrin. At the 1:2 ratio the solubility of ibuprofen is expected to increase as $\Delta\delta$ decreased for all excipients tested. Some of the molecules

appeared to show a greater than expected solubility improvement as the ratio of excipient to ibuprofen increased; suggesting that for maximal solubility enhancement more than one molecule of the excipient is required. This could suggest that self-assembly around the drug molecule is occurring. For ibuprofen at the 1:1 ratio, Molecule 1 offers the greatest increase in solubility, for the 1:2 ratio it is Molecule 3 which offers the greatest increase in solubility.

Not all of the novel excipients increase the solubility of gliclazide. Molecule 2 appears to reduce the solubility of gliclazide when compared to gliclazide alone (Figure 6.1 and Table 6.2) suggesting that Molecule 2 would not be suitable for further investigation. Neither Molecule 1 nor Molecule 4 would be suitable for further investigation due to the apparent decrease in gliclazide solubility with the 1:1 and 1:2 molar ratios respectively. Similar to the effect observed for ibuprofen both the 1:2 ratios of Molecules 3 and 5 increased the solubility of gliclazide to a greater extent than the 1:1 ratio. It was also observed that the solubility increases for gliclazide were all lower than the respective solubility increases for ibuprofen in the presence of each excipient, this included HP- β -CD. Further investigation may uncover a molecule which has good solubility enhancing properties for both of the compounds investigated here. It would also be useful to include other poorly soluble molecules in the simulations run here, using the same excipients to provide more information on the molecules.

There does not appear to be an observable association between Molecules 1, 2, 3 and 5 and ibuprofen (Figure 6.4). There does appear to be an interaction between Molecule 4 and ibuprofen (Figure 6.4g and h). Therefore this molecule may be expected to show the greatest increase in solubility for ibuprofen; however Molecule 4 results in the lowest $\Delta\delta$ at the 1:1 ratio and second lowest $\Delta\delta$ at the 1:2 ratio. When gliclazide simulations were examined (Figure 6.5) there may be an interaction between the drug and Molecules 3, 4 and 5 at the 1:2 ratio, other excipients and ratios show no apparent association. The disagreement between interaction and solubility increase may be down to the lack of protection against water molecule contact or an issue with the computational processing. As neither drug can be seen to enter the HP- β -CD cavity, which would be expected; the use of the graphical representation of the dynamics simulations to determine interaction may require more processing power than that allowed with the system used. More processing power would have allowed more molecules to be included in the cells for more iterations and overall time frame.

No data in the literature could be found which had methods which could be compared to the work carried out here, so further work is required. It has been shown that the software can be used for solubility prediction. Lüder *et al.* have demonstrated that predicted solubility results using Materials Studio 3.1 are close to the experimentally determined solubilities of 47 molecules using Monte Carlo simulations (235).



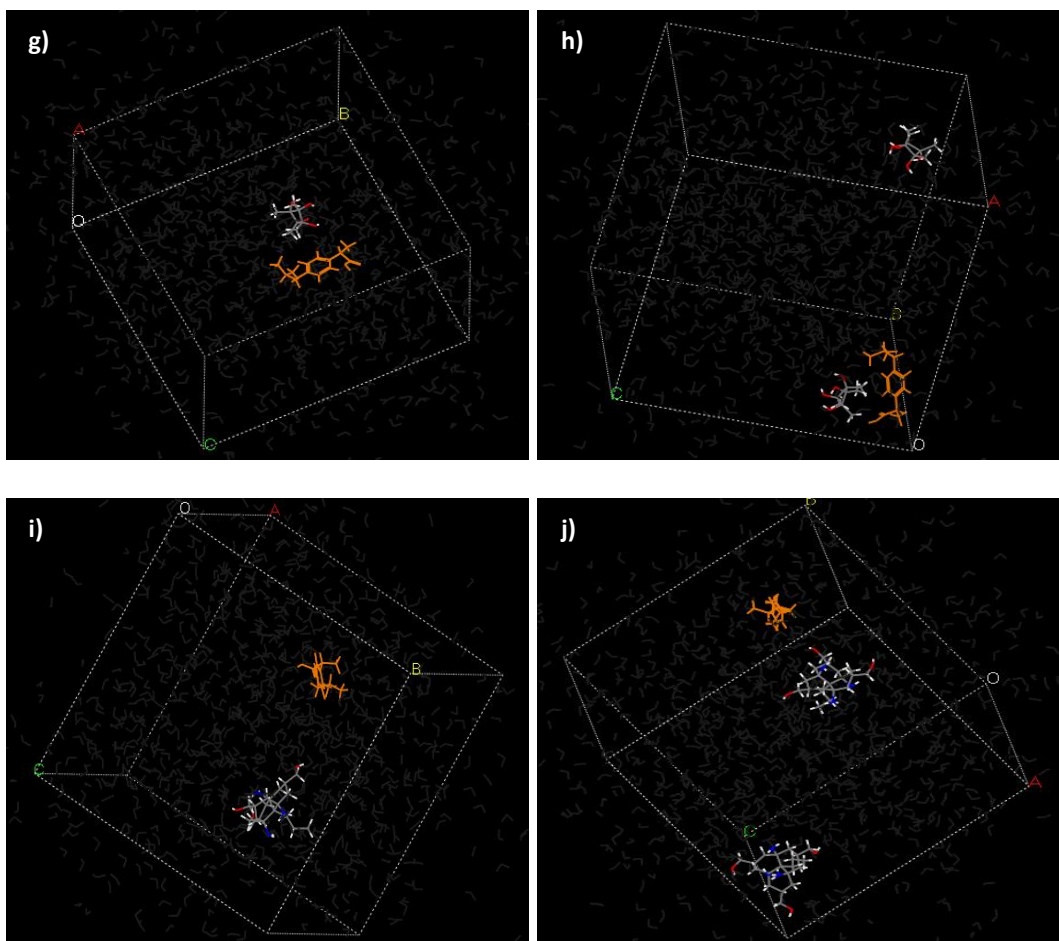
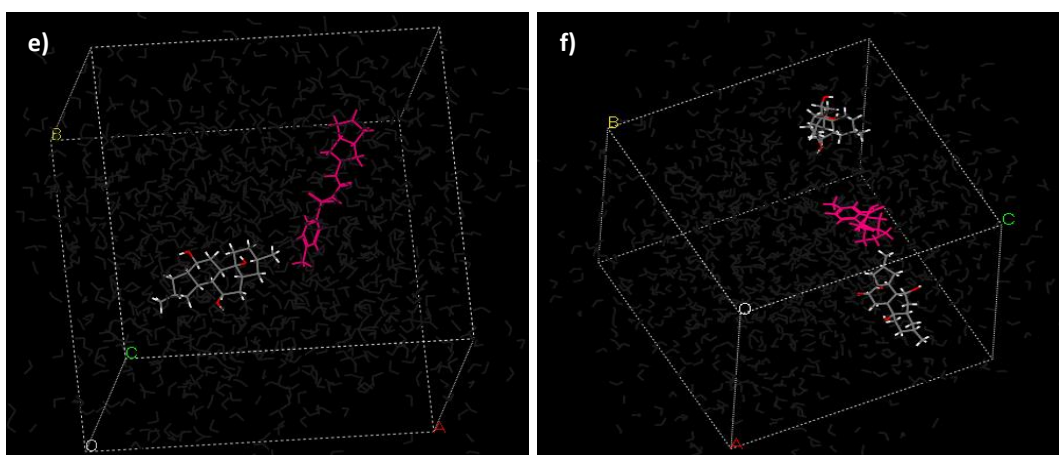
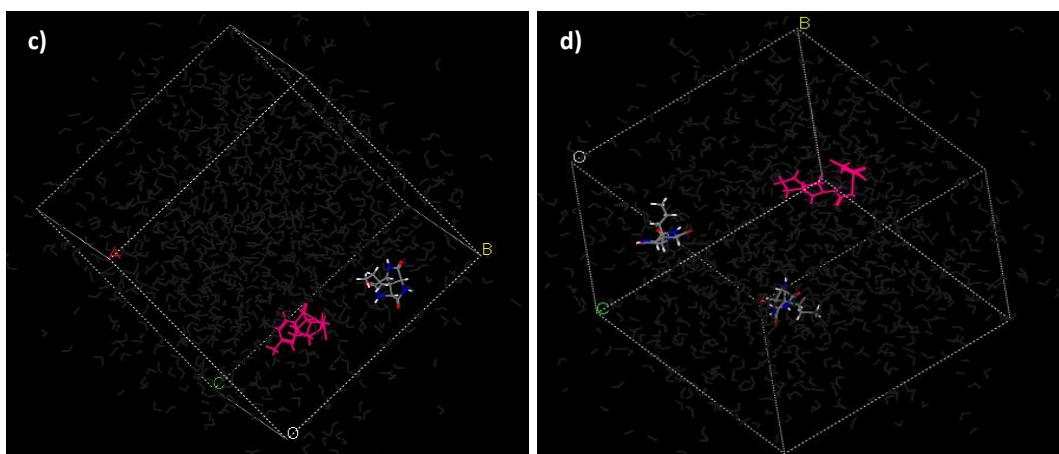
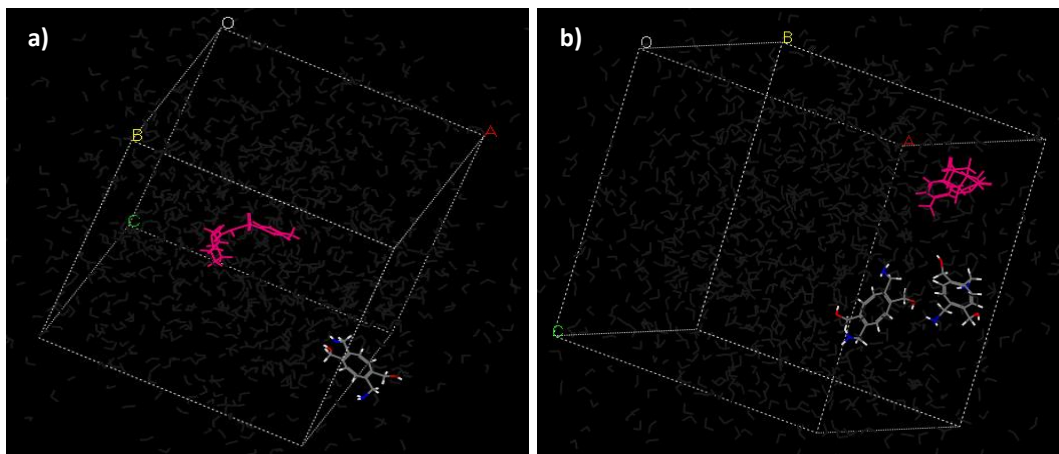


Figure 6.4. Screenshots of dynamics simulations of ibuprofen (represented in orange) with the five novel excipients. a) Molecule 1 (1:1 ratio), b) Molecule 1 (1:2 ratio), c) Molecule 2 (1:1 ratio), d) Molecule 2 (1:2 ratio), e) Molecule 3 (1:1 ratio), f) Molecule 3 (1:2 ratio), g) Molecule 4 (1:1 ratio), h) Molecule 4 (1:2 ratio), i) Molecule 5 (1:1 ratio), j) Molecule 5 (1:2 ratio). Water not shown.



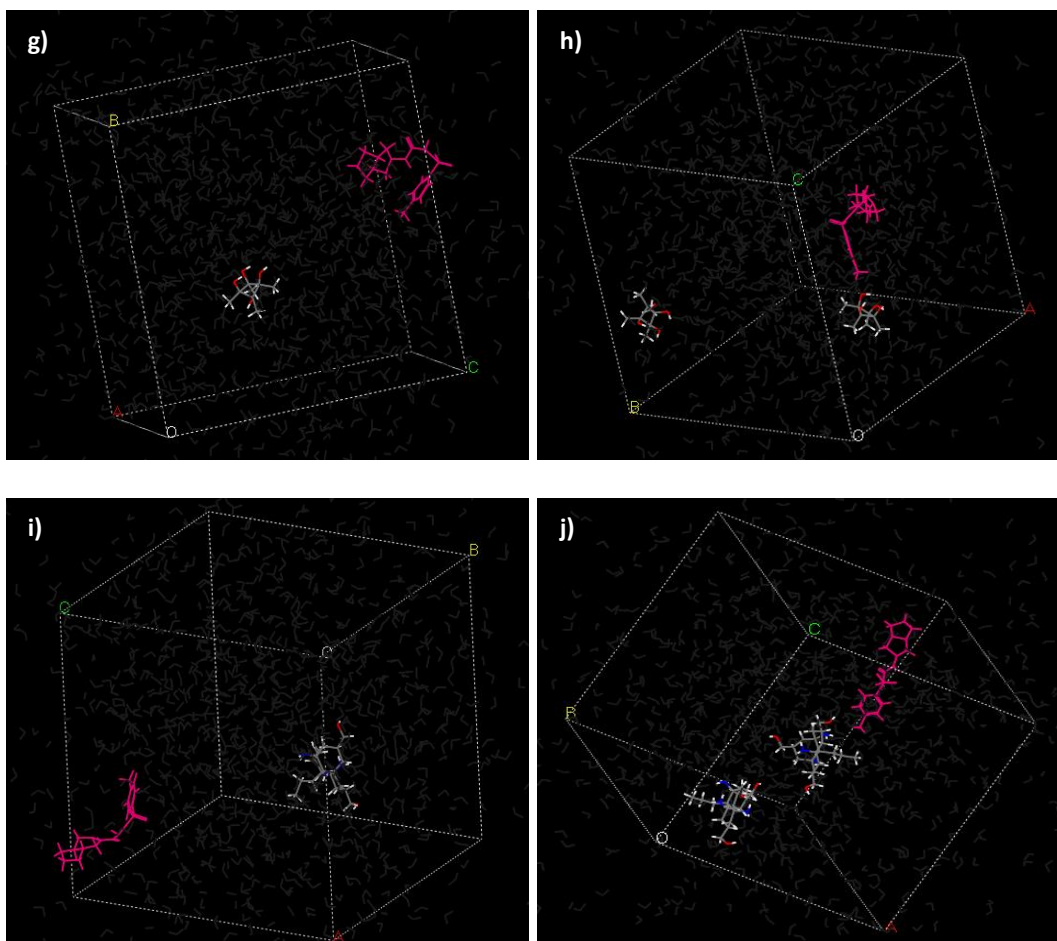


Figure 6.5. Screenshots of dynamics simulations of gliclazide (represented in pink) with the five novel excipients. a) Molecule 1 (1:1 ratio), b) Molecule 1 (1:2 ratio), c) Molecule 2 (1:1 ratio), d) Molecule 2 (1:2 ratio), e) Molecule 3 (1:1 ratio), f) Molecule 3 (1:2 ratio), g) Molecule 4 (1:1 ratio), h) Molecule 4 (1:2 ratio), i) Molecule 5 (1:1 ratio), j) Molecule 5 (1:2 ratio). Water not shown.

6.5.2 Excipient Self-Assembly

From the results, it can be seen that Molecules 2 and 3 are unlikely to spontaneously self-assemble in water alone. This may not be the case however if other molecules are also present in the system. No self-assembly between the two molecules of

Molecules 2 and 3 was observed in the presence of ibuprofen and gliclazide (Figure 6.4d and f and Figure 6.5d and f). The ability of Molecules 1, 4 and 5 to self-assemble means that, in agreement with the aims of the project, these would be chosen in preference to the two which do not self-assemble.

6.5.3 Simulation Conditions Choice

In an ideal situation, the number of water molecules used for the simulations would have been increased. However, increasing the number of water molecules in the cell to 5000 resulted in an increased run time for all calculations. For Forcite Dynamics, the simulation run time increased from approximately 57 hours to approximately 425 hours. Due to time constraints the number of water molecules was limited to 1000 per simulation. This was also the reason why the number of iterations was kept at 500,000. The temperature of 298K was chosen to maintain consistency between the experimental and computational results.

The concentrations of ibuprofen and gliclazide used during the simulations was 55.5 mM. This is higher than the solubility of both drugs determined during the CheqSol studies conducted in chapter 2. For the excipients used the concentration was either 55.5 mM or 111 mM for the 1:1 and 1:2 ratios respectively. This concentration is below the solubility of the cyclodextrin and below the predicted solubility of Molecules 1 and 2. The concentration is however higher than the predicted solubility of Molecules 3, 4 and 5. It would be preferable to use a concentration below the predicted solubility of the drugs and excipients, however computational power

described above limited this. The molecular weight of HP- β -CD (with seven substitutions) used during simulations was greater than the average molecular weight of the cyclodextrin used during experimental sections, but is within the range of the number of substitutions and the range of molecular weights of the product.

6.6 Conclusions

Analysis of the results shows that none of the five novel excipients investigated are predicted to increase the solubility of either ibuprofen or gliclazide to a greater extent than HP- β -CD. Of the five that were investigated, Molecules 3 and 5 at the 1:2 ratio provided the greatest increase in solubility for both ibuprofen and gliclazide. As Molecule 5 was also shown to self-assemble *in silico* then Molecule 5 would be the most preferential novel excipient for further investigation of the five examined.

7 Chapter 7 - Conclusions and Future Work

7.1 Conclusions

7.1.1 Experimental Results

As discussed, the CheqSol technique appears to be useful for phase-solubility studies when non-ionisable excipients are used. At the commencement of this research the CheqSol method described was used mainly for solubility determination of compounds in aqueous conditions, with most literature references using ISA water as the only solvent investigated. This thesis provides data which show that this technique is suitable for phase-solubility studies with HP- β -CD, P407 and P188. From these results it was concluded that other non-ionisable excipients could be investigated in this way. Use of the method may therefore have a place in the pharmaceutical industry during the formulation development stage. It can provide solubility results in a shorter time frame than the traditional shake-flask method, which may speed up formulation development. The technique provides information on the dissolution and precipitation rates during the chasing phase of the CheqSol method. Following examination of these rates in reference to the 'spring and parachute' effect it was found that the data produced by the equipment did not give consistent results and could not provide information on this effect for formulation purposes. The CheqSol method could be used to screen if an effect on precipitation and dissolution rates could be expected, but further work would be required for more reliable results. The technique, however, could be used to allow the calculation of the 1:1 association constant using Equation 4.22 described by Higuchi and Connors

(78). This method for determining the association constant was the most appropriate for the experimental procedure from the different techniques investigated.

7.1.2 Computational Results

The computational work carried out in this thesis was conducted as a starting point for future studies and was exploratory in nature. It may be possible to use this technique to investigate the solubility enhancements offered by novel excipients. However, the five molecules investigated here were predicted to have lower effects on solubility increases for ibuprofen and gliclazide when compared to HP- β -CD. In some cases the predicted solubility of gliclazide in the presence of the excipient was lower than the solubility of gliclazide alone. The results are limited by the concentrations of the drug and excipient molecules in water which were for some of the molecules above the actual/predicted solubility.

7.2 Future Work

7.2.1 Experimental

The work discussed in this thesis gives some information on the use of the CheqSol technique for the determination of excipient induced solubility increases. As the work concentrated on the use of non-ionisable excipients, it would be preferable to further investigate ionisable excipients. The use of cholic acid as an ionisable, micelle forming excipient was carried out during preliminary work, it was found however, that this compound may not be suitable for CheqSol studies due to its low aqueous solubility and likelihood of precipitation. Further studies using other charged or

ionisable excipients which have higher water solubility such as sodium laurel sulphate or L- α -dimyristoylphosphatidylcholine could be investigated (9, 236).

Following the CheqSol investigation, the analysis of the crystals formed during dissolution would provide more information on the way the excipient and drug interact during the cycling to examine if the technique had any effect on the crystal structure. Comparing the crystals at the point of precipitation and at the end of the assay may also provide useful information. Studies including scanning electron microscopy, X-ray diffraction, nuclear magnetic resonance, infrared spectroscopy and differential scanning calorimetry can be carried out for characterisation of the crystals formed during the process (128, 141, 166). It would also be useful to alter the CheqSol settings to allow the system to come to equilibrium at various stages throughout a run. This could provide information in changes in dissolution and precipitation rate following repeated cycling of the system.

7.2.2 Computational

Before any definite conclusions can be drawn about the usefulness of this method, further studies would have to be conducted. The results from further computational studies would need to be compared to experimental data before its effectiveness can be determined. The molecular dynamics simulations should therefore be carried out using excipient/drug combinations which have already been investigated, or carry out the required combinations experimentally. It would be preferable if the simulations could be carried out with more water molecules, so that all molecules are

present below their solubility values. If the method is determined to be useful then further studies with novel excipients could be carried out.

8 References

1. Schneider G. Prediction of Drug-Like Properties. Adaptive Systems in Drug Design: Eureka.Com Inc; 2002.
2. Healey N. A Solution for Poor Solubility: World Pharma; 2014 [08/12/2015]. Interview with Professor Colin Pouton, Dr Hywel Williams and Professor Martin Kuentz]. Available from: <http://www.worldpharmaceuticals.net/features/featurea-solution-for-poor-water-solubility-4214373/>.
3. Li S, He H, Parthiban LJ, Yin H, Serajuddin AT. IV-IVC Considerations in the Development of Immediate-Release Oral Dosage Form. Journal of pharmaceutical sciences. 2005;94(7):1396-417.
4. British Pharmacopoeia 2015 [cited 2014]. Available from: <http://www.pharmacopoeia.co.uk/bp2015/ixbin/bp.cgi>.
5. Liu R. Introduction. Water-Insoluble Drug Formulation Second Edition Second Edition ed: CRC Press; 2008. p. 1-4.
6. Lipinski CA, Lombardo F, Dominy BW, Feeney PJ. Experimental and computational approaches to estimate solubility and permeability in drug discovery and development settings. Advanced drug delivery reviews. 2001;46(1-3):3-26.
7. Yeh MK, Chang LC, Chiou AH. Improving tenoxicam solubility and bioavailability by cosolvent system. AAPS PharmSciTech. 2009;10(1):166-71.
8. Duma RJ, Akers MJ, Turco SJ. Parenteral Drug Administration: Routes, Precautions, Problems, Complications and Drug Delivery Systems. Pharmaceutical

Dosage Forms: Parenteral Medications Volume 1 Second Edition Second Edition ed:
Marcel Dekker Inc; 1992.

9. Strickley RG. Solubilizing Excipients in Oral and Injectable Formulations. *Pharmaceutical research*. 2004;21(2):201-30.
10. Brazeau GA, Fung H-L. Effect of organic cosolvent-induced skeletal muscle damage on the bioavailability of intramuscular [14C]diazepam. *Journal of pharmaceutical sciences*. 1990;79(9):773-7.
11. *Handbook of Pharmaceutical Excipients*. 7th Edition ed. London: Pharmaceutical Press; 2012.
12. Amidon GL, Lennernäs H, Shah VP, Crison JR. A Theoretical Basis for a Biopharmaceutic Drug Classification: The Correlation of in Vitro Drug Product Dissolution and in Vivo Bioavailability. *Pharmaceutical research*. 1995;12(3):413-20.
13. Chen ML, Amidon GL, Benet LZ, Lennernas H, Yu LX. The BCS, BDDCS, and regulatory guidances. *Pharmaceutical research*. 2011;28(7):1774-8.
14. The Biopharmaceutics Classification System (BCS) Guidance: U.S. Food and Drug Administration; [24/07/2013]. Available from: <http://www.fda.gov/AboutFDA/CentersOffices/OfficeofMedicalProductsandTobacco/CDER/ucm128219.htm>.
15. Box K, Comer JE, Gravestock T, Stuart M. New ideas about the solubility of drugs. *Chem Biodivers*. 2009;6(11):1767-88.
16. Chevillard F, Lagorce D, Reynes C, Villoutreix BO, Vayer P, Miteva MA. In silico prediction of aqueous solubility: a multimodel protocol based on chemical similarity. *Molecular pharmaceutics*. 2012;9(11):3127-35.

17. Klopman G, Wang S, Balthasar DM. Estimation of aqueous solubility of organic molecules by the group contribution approach. Application to the study of biodegradation. *J Chem Inf Comput Sci*. 1992;32(5):474-82.
18. Ruelle P, Rey-Mermet C, Buchmann M, Kesselring UW, Huyskens PL. A New Predictive Equation for the Solubility of Drugs Based on the Thermodynamics of Mobile Disorder. *Pharmaceutical research*. 1991;8(7):840-50.
19. Chen Y, Qi X, Liu R. Prediction of Solubility. *Water-Insoluble Drug Formulation Second Edition* CRC Press; 2008.
20. Huuskonen J. Estimation of Aqueous Solubility for a Diverse Set of Organic Compounds Based on Molecular Topology. *J Chem Inf Comput Sci*. 2000;40(3):773-7.
21. Salahinejad M, Le TC, Winkler DA. Aqueous solubility prediction: do crystal lattice interactions help? *Molecular pharmaceutics*. 2013;10(7):2757-66.
22. Yalkowsky SH, Banerjee S. Measurement, Evaluation and Sources of Solubility. *Aqueous Solubility: Methods of Estimation for Organic Compounds*. New York: Marcel Dekker, Inc; 1992. p. 149-55.
23. Miyako Y, Zhao Y, Takeshima K, Kataoka T, Handa T, Pinal R. Solubility of hydrophobic compounds in water-cosolvent mixtures: relation of solubility with water-cosolvent interactions. *Journal of pharmaceutical sciences*. 2010;99(1):293-302.
24. Serajuddin AT. Salt formation to improve drug solubility. *Advanced drug delivery reviews*. 2007;59(7):603-16.

25. Baka E, Comer JEA, Takács-Novák K. Study of equilibrium solubility measurement by saturation shake-flask method using hydrochlorothiazide as model compound. *Journal of pharmaceutical and biomedical analysis*. 2008;46(2):335-41.
26. Stuart M, Box K. Chasing Equilibrium: Measuring the Intrinsic Solubility of Weak Acids and Bases. *Anal Chem*. 2005;77:983-90.
27. Narasimham L, Barhate VD. Kinetic and intrinsic solubility determination of some β -blockers and antidiabetics by potentiometry. *J Pharm Res*. 2011;4(2):532-6.
28. Box KJ, Völgyi G, Baka E, Stuart M, Takács-Novák K, Comer JEA. Equilibrium versus kinetic measurements of aqueous solubility, and the ability of compounds to supersaturate in solution—a validation study. *Journal of pharmaceutical sciences*. 2006;95(6):1298-307.
29. Sibley RJ, Alberty RA, Bawendi MG. Fundamental Equations of Thermodynamics. *Physical Chemistry Fourth Edition* John Wiley and Sons, Inc.; 2005.
30. Bindu MB, Kusum B, Banji D. Novel Strategies for Poorly Water Soluble Drugs. *Int J Pharm Sci Rev Res*. 2010;4(3):76-84.
31. Berge SM, Bighley LD, Monkhouse DC. Pharmaceutical salts. *Journal of pharmaceutical sciences*. 1977;66(1):1-19.
32. Verbeeck RK, Kanfer I, Walker RB. Generic substitution: the use of medicinal products containing different salts and implications for safety and efficacy. *European journal of pharmaceutical sciences : official journal of the European Federation for Pharmaceutical Sciences*. 2006;28(1-2):1-6.

33. Morris KR, Fakes MG, Thakur AB, Newman AW, Singh AK, Venit JJ, et al. An integrated approach to the selection of optimal salt form for a new drug candidate. *International journal of pharmaceutics*. 1994;105(3):209-17.
34. Neau SH. *Pharmaceutical Salts. Water-Insoluble Drug Formulation Second Edition* CRC Press; 2008. p. 417-36.
35. Kumar L, Amin A, Bansal AK. Salt Selection in Drug Development. *Pharm Technol*. 2008;3(32).
36. Neau SH. Prodrugs for Improved Aqueous Solubility. *Water-Insoluble Drug Formulation Second Edition* CRC Press; 2008. p. 437-66.
37. Rautio J, Kumpulainen H, Heimbach T, Oliyai R, Oh D, Jarvinen T, et al. Prodrugs: design and clinical applications. *Nature reviews Drug discovery*. 2008;7(3):255-70.
38. Leu Y-L, Roffler SR, Chern J-W. Design and Synthesis of Water-Soluble Glucuronide Derivatives of Camptothecin for Cancer Prodrug Monotherapy and Antibody-Directed Enzyme Prodrug Therapy (ADEPT). *J Med Chem*. 1999;42(18):3623-8.
39. Summary of Product Characteristics, Telzir film-coated tablets ViiV Healthcare UK Ltd; [09/01/12]. Available from: <http://www.medicines.org.uk/EMC/default.aspx>.
40. Flamholc L, Gisslén M. Once-daily fosamprenavir with ritonavir in the treatment of HIV infection in therapy-naïve patients. *Ther Clin Risk Manag*. 2008;4(6):1281-4.

41. Chaudhari P, Sharma P, Barhate N, Kulkarni P, Mistry C. Solubility enhancement of hydrophobic drugs using synergistically interacting cyclodextrins and cosolvent. *Curr Sci.* 2007;92(11):1586-91.
42. Rubino JT, Yalkowsky SH. Cosolvency and Deviations from Log-Linear Solubilization. *Pharmaceutical research.* 1987;4(3):231-6.
43. Summary of Product Characteristics, Rocaltrol Capsules: Roche; [11/11/11]. Available from: <http://www.medicines.org.uk/EMC/default.aspx>.
44. Summary of Product Characteristics, Zemplar 5 microgram/mL solution: Abbott Laboratories; [14/11/11]. Available from: <http://www.medicines.org.uk/EMC/default.aspx>.
45. Liu R, Dannenfelser R-M, Li S. Micellization and Drug Solubility Enhancement. *Water-Insoluble Drug Formulation Second Edition* CRC Press; 2008. p. 255-306.
46. Shi Y, Porter W, Merdan T, Li LC. Recent advances in intravenous delivery of poorly water-soluble compounds. *Expert Opin Drug Deliv.* 2009;6(12):1261-82.
47. Mendonca CR, Silva YP, Bockel WJ, Simo-Alfonso EF, Ramis-Ramos G, Piatnicki CM, et al. Role of the co-surfactant nature in soybean w/o microemulsions. *Journal of colloid and interface science.* 2009;337(2):579-85.
48. Gursoy RN, Benita S. Self-emulsifying drug delivery systems (SEDDS) for improved oral delivery of lipophilic drugs. *Biomedicine & pharmacotherapy = Biomedecine & pharmacotherapie.* 2004;58(3):173-82.
49. Cannon JB, Shi Y, Gupta P. Emulsions, Microemulsions, and Lipid-Based Drug Delivery for Drug Solubilization and Delivery – Part I: Parenteral Applications. *Water-Insoluble Drug Formulation Second Edition* CRC Press; 2008.

50. Nyman DW, Campbell KJ, Hersh E, Long K, Richardson K, Trieu V, et al. Phase I and pharmacokinetics trial of ABI-007, a novel nanoparticle formulation of paclitaxel in patients with advanced nonhematologic malignancies. *Journal of clinical oncology : official journal of the American Society of Clinical Oncology*. 2005;23(31):7785-93.
51. Summary of Product Characteristics, Neoral Soft Gelatin Capsules, Neoral Oral Solution: Novartis Pharmaceuticals UK Ltd; [16/12/11]. Available from: <http://www.medicines.org.uk/EMC/default.aspx>.
52. Summary of Product Characteristics, Konakion MM: Roche Products Ltd; [16/12/11]. Available from: <http://www.medicines.org.uk/EMC/default.aspx>.
53. Liu R, Cannon JB, Paspal YL. Liposomes in Solubilization. *Water-Insoluble Drug Formulation Second Edition* CRC Press; 2008. p. 375-416.
54. Kirby C, Clarke J, Gregoriadis G. Effect of the Cholesterol Content of Small Unilamellar Liposomes on their Stability in vivo and in vitro. *Biochem J*. 1980;186(2):591-8.
55. Hanusova V, Bousova I, Skalova L. Possibilities to increase the effectiveness of doxorubicin in cancer cells killing. *Drug metabolism reviews*. 2011;43(4):540-57.
56. Tippayamontri T, Kotb R, Paquette B, Sanche L. Cellular uptake and cytoplasm / DNA distribution of cisplatin and oxaliplatin and their liposomal formulation in human colorectal cancer cell HCT116. *Investigational new drugs*. 2011;29(6):1321-7.
57. Lakshmi P, Kumar GA. Nano-Suspension Technology: A Review. *Int J Pharm Pharm Sci*. 2010;2(4):35-40.
58. Patel VR, Agrawal YK. Nanosuspension: An approach to enhance solubility of drugs. *J Adv Pharm Tech Res*. 2011;2(2):81-7.

59. Summary of Product Characteristics, Abraxane Powder for Suspension for Infusion: Celgene Ltd; [28/11/11]. Available from: <http://www.medicines.org.uk/EMC/default.aspx>.
60. Merisko-Liversidge EM, Liversidge GG. Drug nanoparticles: formulating poorly water-soluble compounds. *Toxicologic pathology*. 2008;36(1):43-8.
61. Saenger W. Cyclodextrin Inclusion Compounds in Research and Industry. *Angew Chem Int Ed Engl*. 1980;19(5):344-62.
62. Vyas A, Saraf S, Saraf S. Cyclodextrin based novel drug delivery systems. *J Incl Phenom Macrocycl Chem*. 2008;62(1-2):23-42.
63. Tong W-Q, Wen H. Applications of Complexation in the Formulation of Insoluble Compounds. *Water-Insoluble Drug Formulation Second Edition* CRC Press; 2008. p. 133-60.
64. Lagona J, Mukhopadhyay P, Chakrabarti S, Isaacs L. The cucurbit[n]uril family. *Angew Chem Int Ed Engl*. 2005;44(31):4844-70.
65. Shaikh M, Mohanty J, Singh PK, Nau WM, Pal H. Complexation of acridine orange by cucurbit[7]uril and beta-cyclodextrin: photophysical effects and pKa shifts. *Photochemical & photobiological sciences : Official journal of the European Photochemistry Association and the European Society for Photobiology*. 2008;7(4):408-14.
66. Sanghvi R, Evans D, Yalkowsky SH. Stacking complexation by nicotinamide: a useful way of enhancing drug solubility. *International journal of pharmaceutics*. 2007;336(1):35-41.

67. Uekama K, Hirayama F, Irie T. Cyclodextrin Drug Carrier Systems. Chem Rev. 1998;98:2045-76.
68. Summary of Product Characteristics, Sporanox 10 mg/mL Oral Solution: Janssen-Cilag Ltd; [07/12/11]. Available from: <http://www.medicines.org.uk/EMC/default.aspx>.
69. Summary of Product Characteristics, Abilify 7.5 mg/mL solution for injection (IM): Bristol-Myers Squibb Pharmaceuticals Ltd; [07/12/11]. Available from: <http://www.medicines.org.uk/EMC/default.aspx>.
70. Summary of Product Characteristics, VFEND 200 mg powder for solution for infusion: Pfizer Ltd; [07/12/11]. Available from: <http://www.medicines.org.uk/EMC/default.aspx>.
71. Torrado JJ, Espada R, Ballesteros MP, Torrado-Santiago S. Amphotericin B formulations and drug targeting. Journal of pharmaceutical sciences. 2008;97(7):2405-25.
72. Singh S. Phase transitions in liquid crystals. Phys Rep. 2000;324(2-4):107-269.
73. Balasubramanian D, Srinivas V, Gaikar VG, Sharma MM. Aggregation behavior of hydrotropic compounds in aqueous solution. J Phys Chem. 1989;93(9):3865-70.
74. Coffman RE, Kildsig DO. Hydrotropic Solubilization - Mechanistic Studies. Pharmaceutical research. 1996;13(10):1460-3.
75. Sistla A, Kertelj A, Shenoy N. Development of an Intravenous Formulation of SU010382 (Prodrug of SU5416, an Anti-Angiogenesis Agent). J Pharm Sci Technol. 2008;62(3):200-10.

76. British Pharmacopoeia 2012 [cited 2012]. Available from: <http://pharmacopoeia.co.uk/bp2012/ixbin/bp.cgi?n=1&id=8156&tab=browse&a=display&r=C6pLwNyb3nR>.
77. Davis J, Schmidt WC. Benzathine Penicillin G. N Engl J Med. 1957;256(8):339-42.
78. Higuchi T, Connors KA. Phase-Solubility Techniques. In: Reilley CN, editor. Advances in Analytical Chemistry and Instrumentation. 4. New York: Interscience; 1965. p. 117-212.
79. Benet LZ, Goyan JE. Potentiometric determination of dissociation constants. Journal of pharmaceutical sciences. 1967;56(6):665-80.
80. Sirius T3 Instruction Manual. Revision 1.: Sirius Analytical Ltd.; 2009.
81. Özkan Y, Atay T, Dikmen N, İşimer A, Aboul-Enein HY. Improvement of water solubility and in vitro dissolution rate of gliclazide by complexation with β -cyclodextrin. Pharm Acta Helv. 2000;74(4):365-70.
82. Singh-Joy SD, McLain VC. Safety assessment of poloxamers 101, 105, 108, 122, 123, 124, 181, 182, 183, 184, 185, 188, 212, 215, 217, 231, 234, 235, 237, 238, 282, 284, 288, 331, 333, 334, 335, 338, 401, 402, 403, and 407, poloxamer 105 benzoate, and poloxamer 182 dibenzoate as used in cosmetics. Int J Toxicol. 2008;27 Suppl 2:93-128.
83. Safety Data Sheet - Pluronic F127: BASF; [19/08/2014]. Available from: <http://candmz04.brenntag.ca/MSDS/Fr/00066950.pdf>.
84. Pluronic® F-68: Sigma-Aldrich; [19/08/2014]. Available from: <http://www.sigmaaldrich.com/catalog/product/sigma/p7061?lang=en®ion=GB>.

85. Rekharsky MV, Inoue Y. Complexation Thermodynamics of Cyclodextrins. *Chem Rev.* 1998;98(5):1875-917.
86. Loftsson T, Jarho P, Másson M, Järvinen T. Cyclodextrins in drug delivery. *Expert Opin Drug Deliv.* 2005;2(2):335-51.
87. Li S, Purdy WC. Cyclodextrins and their Applications in Analytical Chemistry. *Chem Rev.* 1992;92(6):1457-70.
88. Ghosh I, Nau WM. The strategic use of supramolecular pK(a) shifts to enhance the bioavailability of drugs. *Advanced drug delivery reviews.* 2012;64(9):764-83.
89. Weisz PB, Kumor K, Macarak EJ. Protection of erythrocytes against hemolytic agents by cyclodextrin polysulfate. *Biochem Pharmacol.* 1993;45(5):1011-6.
90. Santucci L, Fiorucci S, Chiucchiù S, Sicilia A, Bufalino L, Morelli A. Placebo-controlled comparison of piroxicam- β -cyclodextrin, piroxicam, and indomethacin on gastric potential difference and mucosal injury in humans. *Dig Dis Sci.* 1992;37(12):1825-32.
91. Irie T, Uekama K. Pharmaceutical applications of cyclodextrins. III. Toxicological issues and safety evaluation. *Journal of pharmaceutical sciences.* 1997;86(2):147-62.
92. Davies B, Morris T. Physiological Parameters in Laboratory Animals and Humans. *Pharmaceutical research.* 1993;10(7):1093-5.
93. Gould S, Scott RC. 2-Hydroxypropyl-beta-cyclodextrin (HP-beta-CD): a toxicology review. *Food and chemical toxicology : an international journal published for the British Industrial Biological Research Association.* 2005;43(10):1451-9.

94. Rouchotas C, Cassidy OE, Rowley G. Comparison of surface modification and solid dispersion techniques for drug dissolution. *International journal of pharmaceutics*. 2000;195(1-2):1-6.
95. Shin S-C, Cho C-W. Physicochemical Characterizations of Piroxicam-Poloxamer Solid Dispersion. *Pharm Dev Technol*. 1997;2(4):403-7.
96. Schmolka IR. A review of block polymer surfactants. *J Am Oil Chem Soc*. 1977;54(3):110-6.
97. Cespi M, Bonacucina G, Mencarelli G, Pucciarelli S, Giorgioni G, Palmieri GF. Monitoring the aggregation behaviour of self-assembling polymers through high-resolution ultrasonic spectroscopy. *International journal of pharmaceutics*. 2010;388(1-2):274-9.
98. Wulff-Pérez M, Torcello-Gómez A, Gálvez-Ruíz MJ, Martín-Rodríguez A. Stability of emulsions for parenteral feeding: Preparation and characterization of o/w nanoemulsions with natural oils and Pluronic f68 as surfactant. *Food Hydrocoll*. 2009;23(4):1096-102.
99. Sasaki W, Shah SG. Availability of drugs in the presence of surface-active agents I. Critical micelle concentrations of some oxyethylene oxypropylene polymers. *Journal of pharmaceutical sciences*. 1965;54(1):71-4.
100. Rassing J, Attwood D. Ultrasonic velocity and light-scattering studies on the polyoxyethylene-polyoxypropylene copolymer Pluronic F127 in aqueous solution. *International journal of pharmaceutics*. 1983;13(1):47-55.
101. Pluronic® F-127: Sigma-ALdrich; [19/08/2014]. Available from: <http://www.sigmaaldrich.com/catalog/product/sigma/p2443?lang=en®ion=GB>.

102. Schmolka IR. A review of block polymer surfactants. *Journal of The American Oil Chemists' Society*. 1977;54(3):110-6.
103. Zhang Y, Tang L, Sun L, Bao J, Song C, Huang L, et al. A novel paclitaxel-loaded poly(epsilon-caprolactone)/Poloxamer 188 blend nanoparticle overcoming multidrug resistance for cancer treatment. *Acta biomaterialia*. 2010;6(6):2045-52.
104. Korolenko TA, Johnston TP, Dubrovina NI, Kisarova YA, Zhanaeva SY, Cherkanova MS, et al. Effect of poloxamer 407 administration on the serum lipids profile, anxiety level and protease activity in the heart and liver of mice. *Interdisciplinary toxicology*. 2013;6(1):18-25.
105. Hunter RL, Luo AZ, Zhang R, Kozar RA, Moore FA. Poloxamer 188 Inhibition of Ischemia/Reperfusion Injury: Evidence for a Novel Anti-adhesive Mechanism. *Ann Clin Lab Sci*. 2010;40(2):115-25.
106. Jewell RC, Khor SP, Kisor DF, Lacroix KAK, Wargin WA. Pharmacokinetics of rheothrx injection in healthy male volunteers. *Journal of pharmaceutical sciences*. 1997;86(7):808-12.
107. Grindel JM, Jaworski T, Emanuele RM, Culbreth P. Pharmacokinetics of a novel surface-active agent, purified poloxamer 188, in rat, rabbit, dog and man. *Biopharmaceutics & drug disposition*. 2002;23(3):87-103.
108. Li C, Palmer WK, Johnston TP. Disposition of poloxamer 407 in rats following a single intraperitoneal injection assessed using a simplified colorimetric assay. *Journal of pharmaceutical and biomedical analysis*. 1996;14(5):659-65.

109. Posa M, Kevresan S, Mikov M, Cirin-Novta V, Sarbu C, Kuhajda K. Determination of critical micellar concentrations of cholic acid and its keto derivatives. *Colloids Surf B Biointerfaces*. 2007;59(2):179-83.
110. Madenci D, Egelhaaf SU. Self-assembly in aqueous bile salt solutions. *Curr Opin Colloid Interface Sci*. 2010;15(1-2):109-15.
111. Ekwall P, Rosendahl T, Löfman N. Studies on Bile Acid Salt Solutions. I. The Dissociation Constants of the Cholic and Deoxycholic Acids. *Acta Chem Scand*. 1957;11(4):590-8.
112. Choi H-G, Lee M-K, Kim M-H, Kim C-K. Effect of additives on the physicochemical properties of liquid suppository bases. *International journal of pharmaceutics*. 1999;190(1):13-9.
113. Yong CS, Choi JS, Quan Q-Z, Rhee J-D, Kim C-K, Lim S-J, et al. Effect of sodium chloride on the gelation temperature, gel strength and bioadhesive force of poloxamer gels containing diclofenac sodium. *International journal of pharmaceutics*. 2001;226(1-2):195-205.
114. Ryu J-M, Chung S-J, Lee M-H, Kim C-K, Shim C-K. Increased bioavailability of propranolol in rats by retaining thermally gelling liquid suppositories in the rectum. *J Control Release*. 1999;59(2):163-72.
115. Yasuda M. Dissociation Constants of Some Carboxylic Acids in Mixed Aqueous Solvents *Bull Chem Soc Jpn*. 1959;32(5):429-32.
116. Shedlovsky T. The Behaviour of Carboxylic Acids in Mixed Solvents. In: Pesce B, editor. *Electrolytes ; proceedings of an international symposium held in Trieste June, 1959*. New York: Pergamon; 1962. p. 146-51.

117. Preparation of pH buffer solutions [27/06/2013]. Available from: <http://delloyd.50megs.com/moreinfo/buffers2.html>.
118. Basci NE, Temizer A, Bozkurt A, Isimer A. Optimization of mobile phase in the separation of β -blockers by HPLC. *Journal of pharmaceutical and biomedical analysis*. 1998;18(4-5):745-50.
119. Profiles of Drug Substances, Excipients, and Related Methodology: Academic Press; 2007.
120. Winters CS, Shields L, Timmins P, York P. Solid-State Properties and Crystal Structure of Gliclazide. *Journal of pharmaceutical sciences*. 1994;83(3):300-4.
121. Redenti E, Szente L, Szejtli J. Cyclodextrin Complexes of Salts of Acidic Drugs. Thermodynamic Properties, Structural Features, and Pharmaceutical Applications. *Journal of pharmaceutical sciences*. 2001;90(8):979-86.
122. Hergert LA, Escandar GM. Spectrofluorimetric study of the β -cyclodextrin-ibuprofen complex and determination of ibuprofen in pharmaceutical preparations and serum. *Talanta*. 2003;60(2-3):235-46.
123. Silchenko S, Lau L, Dhareshwar S, Hidalgo I. Potentiometric Study of the Effect of HP-b-Cyclodextrin (HP-b-CD) on the Acid-Base Equilibria and Octanol-Water Distribution of Some Model Drugs 2006 [15/05/2012]. Available from: <http://abstracts.aapspharmaceutica.com/expoaaps06/cc/forms/attendee/index.aspx?content=sessionInfo&sessionId=599>.
124. Singh MK, Pal H, Koti ASR, Sapre AV. Photophysical Properties and Rotational Relaxation Dynamics of Neutral Red Bound to β -Cyclodextrin. *J Phys Chem*. 2004;108(9):1465-74.

125. Schmidt E, Dooley N, Ford SJ, Elliott M, Halbert GW. Physicochemical investigation of the influence of saccharide-based parenteral formulation excipients on L-p-boronphenylalanine solubilisation for boron neutron capture therapy. *Journal of pharmaceutical sciences*. 2012;101(1):223-32.
126. Meindersma GW, van Schoonhoven T, Kuzmanovic B, de Haan AB. Extraction of toluene, o-xylene from heptane and benzyl alcohol from toluene with aqueous cyclodextrins. *Chem Eng Process Process Intensif*. 2006;45(3):175-83.
127. Product Information - (2-Hydroxypropyl)- β -Cyclodextrin Solution: Sigma-Aldrich; [10/04/2012]. Available from: http://www.sigmaaldrich.com/etc/medialib/docs/Sigma/Product_Information_Sheet/2/h5784pis.Par.0001.File.tmp/h5784pis.pdf.
128. Sharma GS, Srikanth MV, Sunil SA, Rao NS, Murthy KVR. Dissolution Rate Enhancement of Poorly Soluble Gliclazide by Complexation with Hydroxy Propyl beta Cyclodextrin. *Res J Pharm Biol Chem Sci*. 2011;2(3):814-23.
129. Loftsson T, Magnúsdóttir A, Másson M, Sigurjónsdóttir JF. Self-association and cyclodextrin solubilization of drugs. *Journal of pharmaceutical sciences*. 2002;91(11):2307-16.
130. Mura P, Bettinetti GP, Manderioli A, Faucci MT, Bramanti G, Sorrenti M. Interactions of ketoprofen and ibuprofen with β -cyclodextrins in solution and in the solid state. *International journal of pharmaceutics*. 1998;166(2):189-203.
131. Liu L, Zhu S. Preparation and characterization of inclusion complexes of prazosin hydrochloride with β -cyclodextrin and hydroxypropyl- β -cyclodextrin. *Journal of pharmaceutical and biomedical analysis*. 2006;40(1):122-7.

132. Ghodke DS, Chaulang GM, Patil KS, Nakhat PD, Yeole PG, Naikwade NS, et al. Solid State Characterization of Domperidone: Hydroxypropyl- β -Cyclodextrin Inclusion Complex. *Indian J Pharm Sci.* 2010;72(2):245-9.
133. Vandelli MA, Salvioli G, Mucci A, Panini R, Malmusi L, Forni F. 2-Hydroxypropyl- β -cyclodextrin complexation with ursodeoxycholic acid. *International journal of pharmaceutics.* 1995;118(1):77-83.
134. Newa M, Bhandari KH, Oh DH, Kim YR, Sung JH, Kim JO, et al. Enhanced dissolution of ibuprofen using solid dispersion with poloxamer 407. *Archives of pharmacal research.* 2008;31(11):1497-507.
135. Albertini B, Passerini N, Di Sabatino M, Monti D, Burgalassi S, Chetoni P, et al. Poloxamer 407 microspheres for orotransmucosal drug delivery. Part I: formulation, manufacturing and characterization. *International journal of pharmaceutics.* 2010;399(1-2):71-9.
136. Guzman HR, Tawa M, Zhang Z, Ratanabanangkoon P, Shaw P, Gardner CR, et al. Combined use of crystalline salt forms and precipitation inhibitors to improve oral absorption of celecoxib from solid oral formulations. *Journal of pharmaceutical sciences.* 2007;96(10):2686-702.
137. Brewster ME, Vandecruys R, Verreck G, Peeters J. Supersaturating drug delivery systems: effect of hydrophilic cyclodextrins and other excipients on the formation and stabilization of supersaturated drug solutions. *Pharmazie.* 2008;63(3):217-20.

138. Castronuovo G, Niccoli M. Thermodynamics of inclusion complexes of natural and modified cyclodextrins with propranolol in aqueous solution at 298 K. *Bioorganic & medicinal chemistry*. 2006;14(11):3883-7.
139. Moyano JR, Arias-Blanco MJ, Gines JM, Rabasco AM, Pérez-Martínez JI, Mor M, et al. Nuclear Magnetic Resonance Investigations of the Inclusion Complexation of Gliclazide with β -Cyclodextrin. *Journal of pharmaceutical sciences*. 1997;86(1):72-5.
140. Oh I, Lee M-Y, Lee Y-B, Shin S-C, Park I. Spectroscopic characterization of ibuprofen/2-hydroxypropyl- β -cyclodextrin inclusion complex. *International journal of pharmaceutics*. 1998;175(2):215-23.
141. Nikolic V, Nikolic L, Stankovic M, Kapor A, Popsavin M, Cvetkovic D. A molecular inclusion complex of atenolol with 2-hydroxypropyl- β -cyclodextrin: The production and characterization thereof. *J Serb Chem Soc*. 2007;72(8-9):737-46.
142. Sirius T3 Brochure. Sirius Analytical.
143. Brouwers J, Brewster ME, Augustijns P. Supersaturating drug delivery systems: the answer to solubility-limited oral bioavailability? *Journal of pharmaceutical sciences*. 2009;98(8):2549-72.
144. Noyes AA, Whitney WR. The Rate of Solution of Solid Substances in Their Own Solutions. *J Am Chem Soc*. 1897;19(12):930-4.
145. Dokoumetzidis A, Macheras P. A century of dissolution research: from Noyes and Whitney to the biopharmaceutics classification system. *International journal of pharmaceutics*. 2006;321(1-2):1-11.

146. Neau SH. Solubility Theories. Water-Insoluble Drug Formulation Second Edition CRC Press; 2008. p. 5-22.
147. Nielsen AE. Energies of Nucleation. Kinetics of precipitation. New York: Pergamon Press Ltd; 1964. p. 1-10.
148. Lindfors L, Forssen S, Westergren J, Olsson U. Nucleation and crystal growth in supersaturated solutions of a model drug. Journal of colloid and interface science. 2008;325(2):404-13.
149. Erdemir D, Lee AY, Myerson AS. Nucleation of Crystals from Solution: Classical and Two-Step Models. Acc Chem Res. 2009;42(5):621-9.
150. Kashchiev D, van Rosmalen GM. Review: Nucleation in solutions revisited. Cryst Res Technol. 2003;38(78):555-74.
151. Nielsen AE. Kinetics of Nucleation. Kinetics of precipitation. New York: Macmillan; 1964. p. 11-28.
152. Dai WG, Dong LC, Li S, Deng Z. Combination of Pluronic/Vitamin E TPGS as a potential inhibitor of drug precipitation. International journal of pharmaceutics. 2008;355(1-2):31-7.
153. Ozaki S, Kushida I, Yamashita T, Hasebe T, Shirai O, Kano K. Inhibition of crystal nucleation and growth by water-soluble polymers and its impact on the supersaturation profiles of amorphous drugs. Journal of pharmaceutical sciences. 2013;102(7):2273-81.
154. Bevernage J, Forier T, Brouwers J, Tack J, Annaert P, Augustijns P. Excipient-mediated supersaturation stabilization in human intestinal fluids. Molecular pharmaceutics. 2011;8(2):564-70.

155. Xu S, Dai WG. Drug precipitation inhibitors in supersaturable formulations. *International journal of pharmaceutics*. 2013;453(1):36-43.
156. Brewster ME, Vandecruys R, Peeters J, Neeskens P, Verreck G, Loftsson T. Comparative interaction of 2-hydroxypropyl-beta-cyclodextrin and sulfobutylether-beta-cyclodextrin with itraconazole: phase-solubility behavior and stabilization of supersaturated drug solutions. *European journal of pharmaceutical sciences : official journal of the European Federation for Pharmaceutical Sciences*. 2008;34(2-3):94-103.
157. Mole J, Box K, Comer J, Stuart M. A novel experiment for assessing precipitation rates for ionizable drugs in supersaturated aqueous solutions. AAPS Annual Meeting. San Diego 2007.
158. Bevernage J, Hens B, Brouwers J, Tack J, Annaert P, Augustijns P. Supersaturation in human gastric fluids. *Eur J Pharm Biopharm*. 2012;81(1):184-9.
159. Sirius Instruction Manual - GI Dissolution. Sirius Analytical Ltd.; 2011.
160. Iervolino M, Raghavan SL, Hadgraft J. Membrane penetration enhancement of ibuprofen using supersaturation. *International journal of pharmaceutics*. 2000;198(2):229-38.
161. Vetter T, Mazzotti M, Brozio Jr. Slowing the Growth Rate of Ibuprofen Crystals Using the Polymeric Additive Pluronic F127. *Cryst Growth Des*. 2011;11(9):3813-21.
162. Ilevbare GA, Liu H, Edgar KJ, Taylor LS. Understanding Polymer Properties Important for Crystal Growth Inhibition—Impact of Chemically Diverse Polymers on Solution Crystal Growth of Ritonavir. *Cryst Growth Des*. 2012;12(6):3133-43.

163. Zimmermann A, Millqvist-Fureby A, Elema MR, Hansen T, Mullertz A, Hovgaard L. Adsorption of pharmaceutical excipients onto microcrystals of siramesine hydrochloride: effects on physicochemical properties. *Eur J Pharm Biopharm.* 2009;71(1):109-16.
164. Raghavan SL, Trividic A, Davis AF, Hadgraft J. Crystallization of hydrocortisone acetate: influence of polymers. *International journal of pharmaceutics.* 2001;212(2):213-21.
165. Duddu SP, Vakilynejad M, Jamali F, Grant DJW. Stereoselective Dissolution of Propranolol Hydrochloride from Hydroxypropyl Methylcellulose Matrices. *Pharmaceutical research.* 1993;10(11):1648-53.
166. Moyano JR, Arias-Blanco MJ, Ginés JM, Giordano F. Solid-state characterization and dissolution characteristics of gliclazide- β -cyclodextrin inclusion complexes. *International journal of pharmaceutics.* 1997;148(2):211-7.
167. Jalindar GP, Saumya D, Daulat KG. Studies in dissolution enhancement of atenolol using HP- β CD. *Int Res Pharm.* 2011;2(8):142-7.
168. Moore T, Croy S, Mallapragada S, Pandit N. Experimental investigation and mathematical modeling of Pluronic® F127 gel dissolution: drug release in stirred systems. *J Control Release.* 2000;67(2-3):191-202.
169. Islam S, Dey LR, Shahriar M, Dewan I, Islam SA. Enhancement of Dissolution Rate of Gliclazide Using Solid Dispersions: Characterization and Dissolution Rate Comparison. *Bangladesh Pharm J.* 2013;16(1):45-52.

170. El-Maghraby GM, Alomrani AH. Effect of binary and ternary solid dispersions on the in vitro dissolution and in-situ rabbit intestinal absorption of gliclazide. *Pak J Pharm Sci.* 2011;24(4):459-68.
171. Reddy V, Panda KC, Panda N. Solubility enhancement of Gliclazide with Poloxamer188 by lyophilization technique. *J Pharm Chem.* 2013;7(3):21-7.
172. Ali W, Williams AC, Rawlinson CF. Stoichiometrically governed molecular interactions in drug: poloxamer solid dispersions. *International journal of pharmaceutics.* 2010;391(1-2):162-8.
173. Yong CS, Lee MK, Park YJ, Kong KH, Xuan JJ, Kim JH, et al. Enhanced oral bioavailability of ibuprofen in rats by poloxamer gel using poloxamer 188 and menthol. *Drug development and industrial pharmacy.* 2005;31(7):615-22.
174. Passerini N, Albertini B, González-Rodríguez ML, Cavallari C, Rodriguez L. Preparation and characterisation of ibuprofen–poloxamer 188 granules obtained by melt granulation. *European journal of pharmaceutical sciences : official journal of the European Federation for Pharmaceutical Sciences.* 2002;15(1):71-8.
175. Junquera E, Aicart E. A fluorimetric, potentiometric and conductimetric study of the aqueous solutions of naproxen and its association with hydroxypropyl- β -cyclodextrin. *International journal of pharmaceutics.* 1999;176(2):169-78.
176. Stella VJ, Rao VM, Zannou EA, Zia V. Mechanisms of drug release from cyclodextrin complexes. *Advanced drug delivery reviews.* 1999;36(1):3-16.
177. Tokumura T, Nanbas M, Tsushima Y, Tatsuishi K, Kayano M, Machida Y, et al. Enhancement of bioavailability of cinnarizine from its β -cyclodextrin complex on oral

administration with dl-phenylalanine as a competing agent. Journal of pharmaceutical sciences. 1986;75(4):391-4.

178. Tokumura T, Tsushima Y, Kayano M, Machida Y, Nagai T. Enhancement of bioavailability of cinnarizine from its β -cyclodextrin complex on oral administration with DL-phenylalanine as a competing agent. Journal of pharmaceutical sciences. 1985;74(4):496-7.

179. Järvinen T, Järvinen K, Schwarting N, Stella VJ. β -cyclodextrin derivatives, SBE4- β -CD and HP- β -CD, increase the oral bioavailability of cinnarizine in beagle dogs. Journal of pharmaceutical sciences. 1995;84(3):295-9.

180. Tokumura T, Ueda H, Tsushima Y, Kasai M, Kayano M, Amada I, et al. Inclusion Complexes of Cinnarizine with β -Cyclodextrin in Aqueous Solution and in the Solid State. Chem Pharm Bull. 1984;32(10):4179-84.

181. Dar AA, Rather GM, Das AR. Mixed Micelle Formation and Solubilization Behavior toward Polycyclic Aromatic Hydrocarbons of Binary and Ternary Cationic–Nonionic Surfactant Mixtures. J Phys Chem B. 2007;111(12):3122-32.

182. Connors KA, Lipari JM. Effect of cycloamyloses on apparent dissociation constants of carboxylic acids and phenols: Equilibrium analytical selectivity induced by complex formation. Journal of pharmaceutical sciences. 1976;65(3):379-83.

183. Connors KA. The Stability of Cyclodextrin Complexes in Solution. Chem Rev. 1997;97(5):1325-58.

184. Connors KA, Lin S-F, Wong AB. Potentiometric Study of Molecular Complexes of Weak Acids and Bases Applied to Complexes of α -Cyclodextrin with para-Substituted Benzoic Acids. Journal of pharmaceutical sciences. 1982;71(2):217-22.

185. Connors KA. Potentiometry. Binding Constants: The Measurement of Molecular Complex Stability: Wiley Interscience; 1987. p. 241-60.
186. Kahle C, Holzgrabe U. Determination of binding constants of cyclodextrin inclusion complexes with amino acids and dipeptides by potentiometric titration. Chirality. 2004;16(8):509-15.
187. Connors KA. Solubility Measurement. Binding Constants: The Measurement of Molecular Complex Stability: Wiley Interscience; 1987. p. 261-81.
188. Iga K, Hussain A, Kashihara T. New direct calculation of K1:1 and K1:2 complexation constants using solubility method. Journal of pharmaceutical sciences. 1981;70(1):108-9.
189. Connors KA. Additional Methods. Binding Constants: The Measurement of Molecular Complex Stability: Wiley Interscience; 1987. p. 339-62.
190. Fielding L. Determination of Association Constants (K_a) from Solution NMR Data. Tetrahedron. 2000;56(34):6151-70.
191. Hanna MW, Ashbaugh AL. Nuclear Magnetic Resonance Study of Molecular Complexes of 7,7,8,8-Tetracyanoquinodimethane and Aromatic Donors^{1,2}. J Phys Chem. 1964;68(4):811-6.
192. Deshpande T. Isothermal Titration Calorimetry: Application in Drug Discovery: PharmaXChange.info; 2012 [15/09/2014]. Available from: <http://pharmaxchange.info/press/2012/08/isothermal-titration-calorimetry-application-in-drug-discovery/>.

193. Waters LJ, Bedford S, Parkes GMB, Mitchell JC. Influence of lipophilicity on drug–cyclodextrin interactions: A calorimetric study. *Thermochim Acta*. 2010;511(1-2):102-6.
194. Pierce MM, Raman CS, Nall BT. Isothermal Titration Calorimetry of Protein–Protein Interactions. *Methods*. 1999;19(2):213-21.
195. Morisue T, Moroi Y, Shibata O. Solubilization of Benzene, Naphthalene, Anthracene, and Pyrene in Dodecylammonium Trifluoroacetate Micelles. *J Phys Chem*. 1994;98(49):12995-3000.
196. Kabir-ud-Din, Shafi M, Bhat PA, Dar AA. Solubilization capabilities of mixtures of cationic Gemini surfactant with conventional cationic, nonionic and anionic surfactants towards polycyclic aromatic hydrocarbons. *Journal of hazardous materials*. 2009;167(1-3):575-81.
197. Song LT, Jiang XY, Tang KW, Miao JB. Study on Inclusion Interaction of Ibuprofen with β -Cyclodextrin Derivatives. *Latin Am Appl Res*. 2011;41(2):147-51.
198. Loftsson T, Másson M, Brewster ME. Self-association of cyclodextrins and cyclodextrin complexes. *Journal of pharmaceutical sciences*. 2004;93(5):1091-9.
199. Loftsson T, Ólafsdóttir BJ, Friðriksdóttir H, Jónsdóttir S. Cyclodextrin complexation of NSAIDs: physicochemical characteristics. *European journal of pharmaceutical sciences : official journal of the European Federation for Pharmaceutical Sciences*. 1993;1(2):95-101.
200. Sharma PK, Bhatia SR. Effect of anti-inflammatories on Pluronic F127: micellar assembly, gelation and partitioning. *International journal of pharmaceutics*. 2004;278(2):361-77.

201. Sharma PK, Reilly MJ, Jones DN, Robinson PM, Bhatia SR. The effect of pharmaceuticals on the nanoscale structure of PEO-PPO-PEO micelles. *Colloids Surf B Biointerfaces*. 2008;61(1):53-60.
202. Linse P, Malmsten M. Temperature-dependent micellization in aqueous block copolymer solutions. *Macromolecules*. 1992;25(20):5434-9.
203. Zhou Z, Chu B. Light-scattering study on the association behavior of triblock polymers of ethylene oxide and propylene oxide in aqueous solution. *Journal of colloid and interface science*. 1988;126(1):171-80.
204. Mata JP, Majhi PR, Guo C, Liu HZ, Bahadur P. Concentration, temperature, and salt-induced micellization of a triblock copolymer Pluronic L64 in aqueous media. *Journal of colloid and interface science*. 2005;292(2):548-56.
205. Cappel MJ, Kreuter J. Effect of nonionic surfactants on transdermal drug delivery: II. Poloxamer and poloxamine surfactants. *International journal of pharmaceutics*. 1991;69(2):155-67.
206. Drug Bank: Open Data Drug and Drug Target Database [17/09/2014]. Available from: <http://www.drugbank.ca/>.
207. Whitesides GM, Grzybowski B. Self-assembly at all scales. *Science*. 2002;295(5564):2418-21.
208. Whitesides GM, Mathias JP, Seto CT. Molecular Self-Assembly and Nanochemistry: A Chemical Strategy for the Synthesis of Nanostructures. *Science*. 1991;254(5036):1312-9.
209. Bergström LM. Thermodynamics of Self-Assembly. In: Tadashi M, editor. *Application of Thermodynamics to Biological and Materials Science*: InTech; 2011.

210. Voise J, Schindler M, Casas J, Raphael E. Capillary-based static self-assembly in higher organisms. *Journal of the Royal Society, Interface / the Royal Society*. 2011;8(62):1357-66.
211. Cheng JY, Ross CA, Smith HI, Thomas EL. Templated Self-Assembly of Block Copolymers: Top-Down Helps Bottom-Up. *Adv Mater*. 2006;18(19):2505-21.
212. Whitesides GM, Boncheva M. Beyond molecules: Self-assembly of mesoscopic and macroscopic components. *Proc Natl Acad Sci U S A*. 2002;99(8):4769-74.
213. Rangel-Yagui CO, Junior AP, Tavares LC. Micellar solubilization of drugs. *J Pharm Pharmaceut Sci*. 2005;8(2):147-63.
214. Klug A. The tobacco mosaic virus particle: structure and assembly. *Philos Trans R Soc Lond B Biol Sci*. 1999;354(1383):531-5.
215. Kegel WK, van der Schoot P. Physical regulation of the self-assembly of tobacco mosaic virus coat protein. *Biophys J*. 2006;91(4):1501-12.
216. Edeling MA, Smith C, Owen D. Life of a clathrin coat: insights from clathrin and AP structures. *Nat Rev Mol Cell Biol*. 2006;7(1):32-44.
217. Fotin A, Cheng Y, Sliz P, Grigorieff N, Harrison SC, Kirchhausen T, et al. Molecular model for a complete clathrin lattice from electron cryomicroscopy. *Nature*. 2004;432(7017):573-9.
218. Singer SJ, Nicolson GL. The fluid mosaic model of the structure of cell membranes. *Science*. 1972;175(4023):720-31.
219. Choi JS, Joo DK, Kim CH, Kim K, Park JS. Synthesis of a Barbell-like Triblock Copolymer, Poly(l-lysine) Dendrimer-block-Poly(ethylene glycol)-block-Poly(l-lysine)

- Dendrimer, and Its Self-Assembly with Plasmid DNA. *J Am Chem Soc.* 2000;122(3):474-80.
220. Kolotuchin SV, Thiessen PA, Fenlon EE, Wilson SR, Loweth CJ, Zimmerman SC. Self-Assembly of 1,3,5-Benzenetricarboxylic (Trimesic) Acid and Its Analogues. *Chem Eur J.* 1999;5(9):2537-47.
221. Moorthy JN, Natarajan P, Bajpai A, Venugopalan P. Trigonal Rigid Triphenols: Self-Assembly and Multicomponent Lattice Inclusion. *Cryst Growth Des.* 2011;11(8):3406-17.
222. Matsuura K, Murasato K, Kimizuka N. Artificial Peptide-Nanospheres Self-Assembled from Three-Way Junctions of β -Sheet-Forming Peptides. *J Am Chem Soc.* 2005;127(29):10148-9.
223. Wang W, Chau Y. Efficient and facile formation of two-component nanoparticles via aromatic moiety directed self-assembly. *Chem Commun.* 2011;47(37):10224-6.
224. Cheeseright T, Mackey M, Rose S, Vinter A. Molecular Field Extrema as Descriptors of Biological Activity: Definition and Validation. *J Chem Inf Model.* 2006;46(2):665-76.
225. TorchV10 10.2 Manual. Cresset; 2013.
226. Korolkov VV, Allen S, Roberts CJ, Tendler SJB. Green Chemistry Approach to Surface Decoration: Trimesic Acid Self-Assembly on HOPG. *J Phys Chem C.* 2012;116(21):11519-25.
227. Mayo SL, Olafson BD, Goddard WA. DREIDING: a generic force field for molecular simulations. *J Phys Chem.* 1990;94(26):8897-909.

228. Brooks BR, Brooks CL, 3rd, Mackerell AD, Jr., Nilsson L, Petrella RJ, Roux B, et al. CHARMM: the biomolecular simulation program. *Journal of computational chemistry*. 2009;30(10):1545-614.
229. Wang J, Wolf RM, Caldwell JW, Kollman PA, Case DA. Development and testing of a general amber force field. *Journal of computational chemistry*. 2004;25(9):1157-74.
230. Chang KS, Yoshioka T, Kanezashi M, Tsuru T, Tung KL. A molecular dynamics simulation of a homogeneous organic–inorganic hybrid silica membrane - Supplementary Information. *Chem Commun (Camb)*. 2010;46(48).
231. Hill J-R, Sauer J. Molecular Mechanics Potential for Silica and Zeolite Catalysts Based on ab Initio Calculations. 2. Aluminosilicates. *J Phys Chem*. 1995;99(23):9536-50.
232. Sun H. COMPASS: An ab Initio Force-Field Optimized for Condensed-Phase Applications-Overview with Details on Alkane and Benzene Compounds. *J Phys Chem B*. 1998;102(38):7338-64.
233. Burke J. Solubility Parameters: Theory and Application. In: Jensen CW, editor. *The Book and Paper Group Annual*. 3: The American Institute for Conservation; 1984. p. 13-58.
234. Huynh LK. *Rational Design of Drug Formulations Using Computational Approaches*. Toronto: University of Toronto; 2011.
235. Luder K, Lindfors L, Westergren J, Nordholm S, Persson R, Pedersen M. In silico prediction of drug solubility: 4. Will simple potentials suffice? *Journal of computational chemistry*. 2009;30(12):1859-71.

236. Rahaman T, Fardous J, Perveen FF, Sultana S. Capacity of Non Ionic and Ionic Surfactants for Solubilisation of Paracetamol. Bangladesh Pharm J. 2013;16(1):77-80.

Appendix 1 – Abbreviations

AMBER	Assisted Model Building with Energy Refinement
ANOVA	Analysis of Variance
AUC	Area Under the Curve
β -CD	β -cyclodextrin
BCS	Biopharmaceutics Classification System
CED	Cohesive Energy Density
CHARMM	Chemistry at HARvard Macromolecular Mechanics
CheqSol	Chasing Equilibrium Solubility
CMC	Critical Micelle Concentration
COMPASS	Condensed-Phase Optimized Molecular Potentials for Atomistic Simulation Studies
CTAB	Cetyltrimethylammonium Bromide
DMA	Dimethylacetamide

DMSO	Dimethylsulfoxide
DNA	Deoxyribonucleic acid
EGF	Excipient Gain Factor
GIT	Gastrointestinal Tract
HCl	Hydrochloric Acid
HPLC	High-Performance Liquid Chromatography
HPMC	Hydroxypropyl Methylcellulose
HP- β -CD	Hydroxypropyl- β -cyclodextrin
ISA	Ionic Strength Adjusted
IUPAC	International Union of Pure and Applied Chemistry
KOH	Potassium Hydroxide
MEC	Molar Extinction Coefficient
MSR	Molar Solubilisation Ratio
NMR	Nuclear Magnetic Resonance
pcff	Polymer Consistent Force Field

PEG	Polyethylene Glycol
POE	Polyoxyethylene
POP	Polyoxypropylene
PVP	Polyvinylpyrrolidone
SBE- β -CD	Sulfobutylether- β -cyclodextrin
SDDS	Supersaturating Drug Delivery Systems
SEDDS	Self-Emulsifying Drug Delivery Systems
δ	Solubility Parameter

Appendix 2 – Table of the total volumes and pH recordings for each vial for Shake-Flask Solubility Studies.

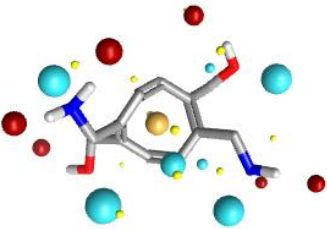
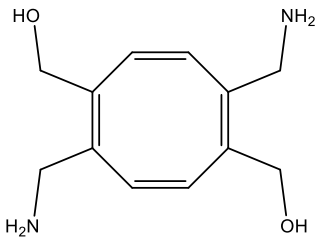
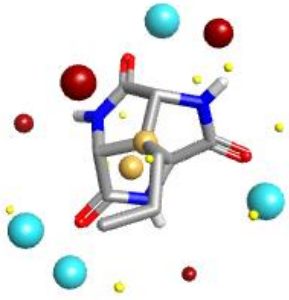
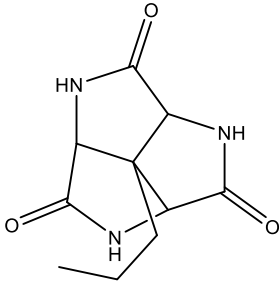
Vial	Propranolol HCl Weight (mg)	Buffer Volume (mL)	HP- β -CD Stock Volume (mL)	Titrant Volume (mL)	pH before shaking	pH after shaking
1	3-4	1.5	0	0.031090	11.91	11.81
2	3-4	1.5	0	0.028363	11.91	11.78
3	3-4	1.425	0.075	0.018603	11.91	11.80
4	3-4	1.425	0.075	0.022977	11.91	11.80
5	3-4	1.125	0.375	0.037230	11.92	11.82
6	3-4	1.125	0.375	0.024647	11.91	11.82
7	3-4	0.75	0.75	0.043439	11.91	11.88
8	3-4	0.75	0.75	0.043286	11.91	11.86

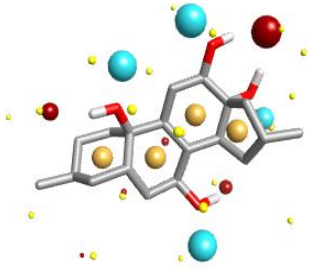
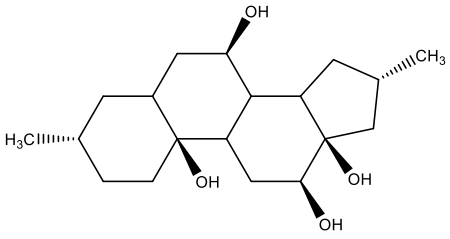
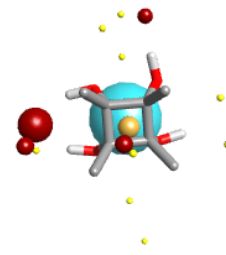
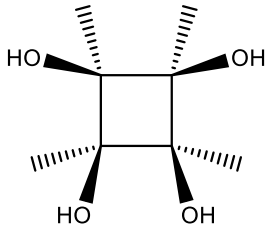
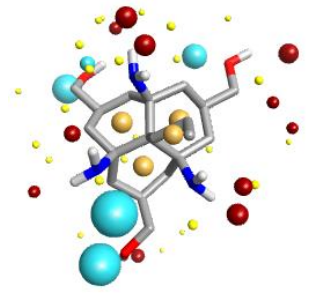
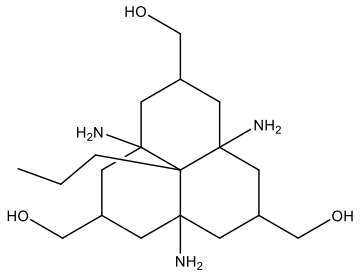
9	3-4	0.375	1.125	0.031833	11.91	11.86
10	3-4	0.375	1.125	0.036900	11.91	11.87
11	3-4	0	1.5	0.034337	11.90	11.87
12	3-4	0	1.5	0.037935	11.91	11.89
13	300	1.5	0	0.000282	5.21	5.19
14	300	1.5	0	0.001635	5.22	5.60
15	300	1.425	0.075	0.000753	5.21	5.60
16	300	1.425	0.075	0.000964	5.21	5.16
17	300	1.125	0.375	0.000729	5.21	5.06
18	300	1.125	0.375	0.000588	5.21	5.15

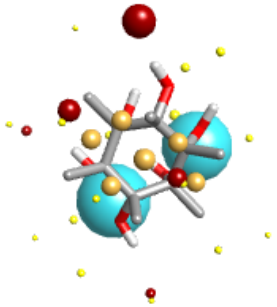
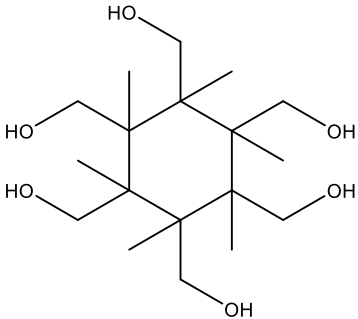
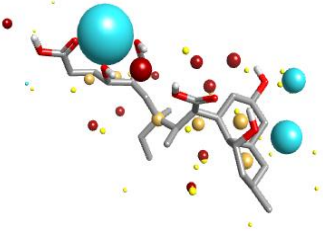
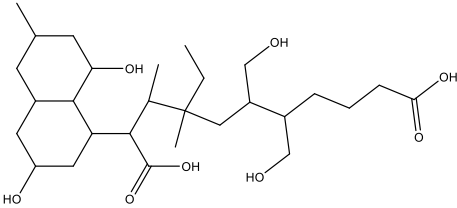
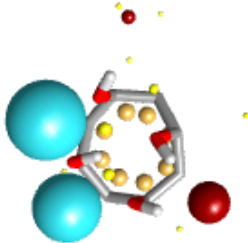
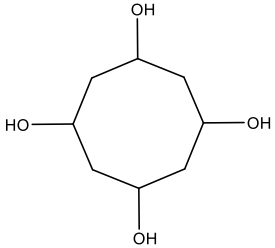
19	300	0.75	0.75	0.000564	5.21	5.16
20	300	0.75	0.75	0.000541	5.21	5.16
21	300	0.375	1.125	0.000541	5.22	5.17
22	300	0.375	1.125	0	5.21	5.16
23	300	0	1.5	0	5.21	5.16
24	300	0	1.5	0	5.21	5.16
25	0	1.5	0	0.014276	11.91	11.89
26	0	1.5	0	0.015143	11.91	11.88
27	0	0	1.5	0.018227	11.90	11.91
28	0	0	1.5	0.009196	11.90	11.94

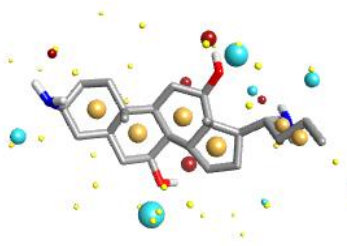
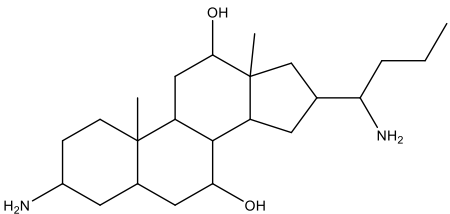
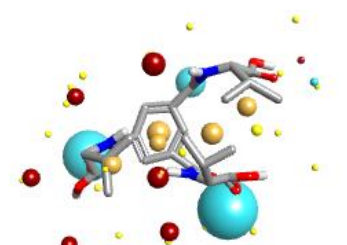
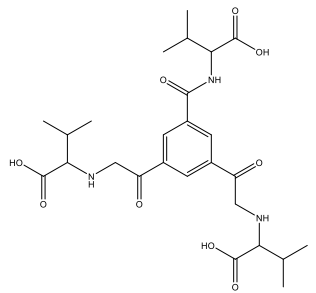
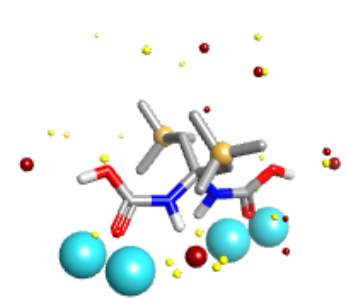
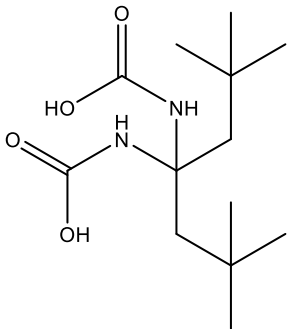
29	0	1.5	0	0	5.47	5.46
30	0	1.5	0	0	5.48	5.49
31	0	0	1.5	0	5.49	5.51
32	0	0	1.5	0	5.49	5.51

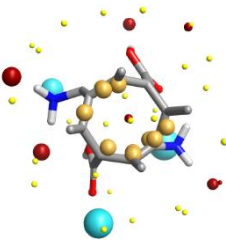
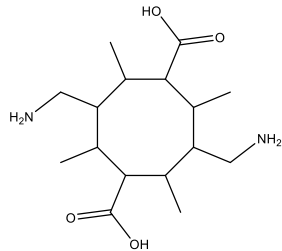
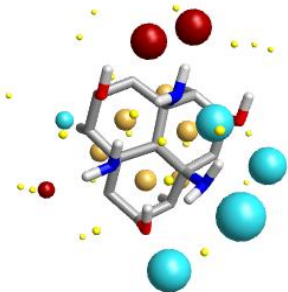
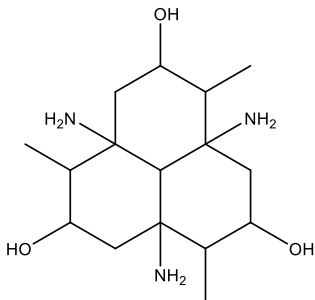
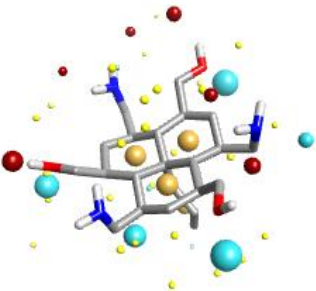
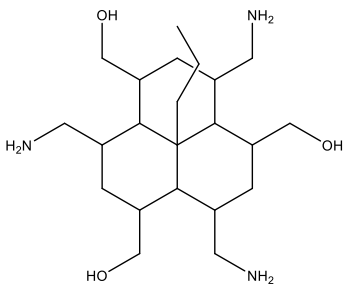
Appendix 3 – Table detailing the 3D- and 2D- structures of the designed molecules. The IUPAC names for each of the molecules has been included.

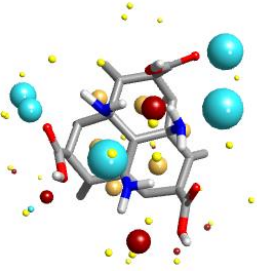
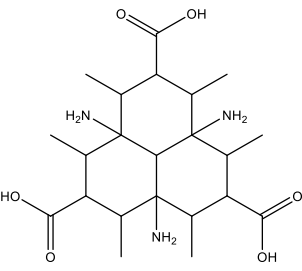
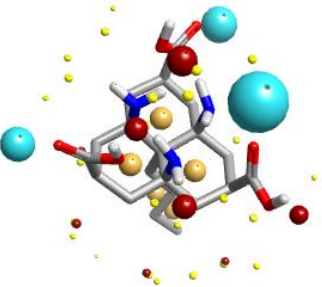
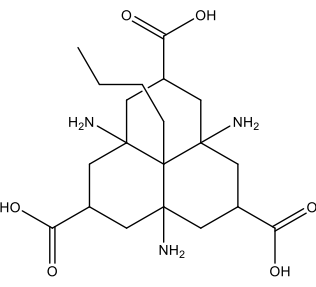
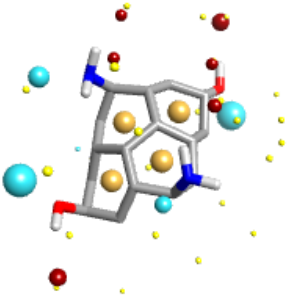
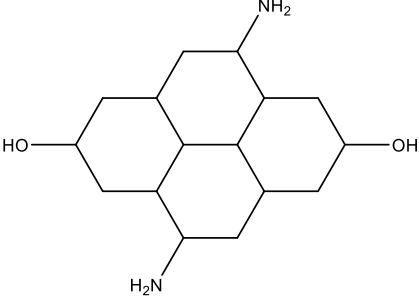
Molecule Number	3D Structure	2D Structure	IUPAC Name
1			<p>[4,8-bis(aminomethyl)cycloocta-1,3,5,7-tetraene-1,5-diyl]dimethanol</p>
2			<p>6b-propylhexahydro-1,3,5-triazacyclopenta[cd]pentalene-2,4,6(1<i>H</i>)-trione</p>

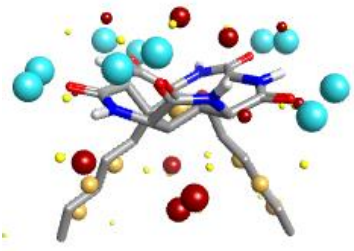
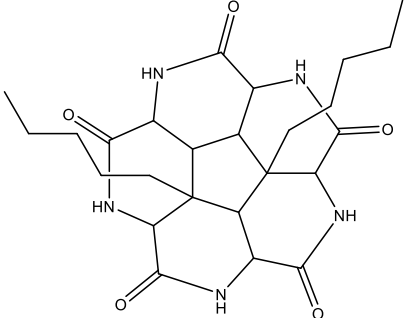
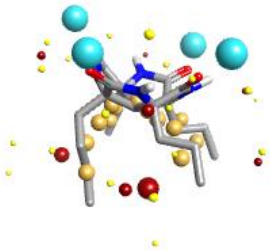
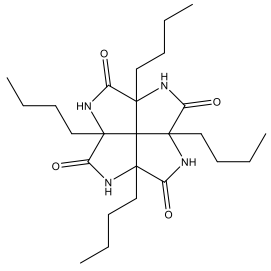
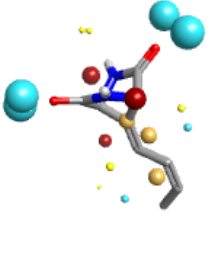
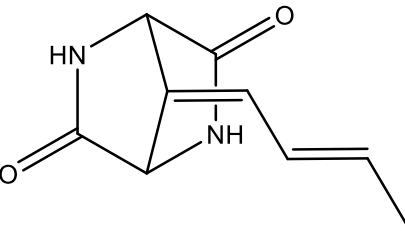
3			3,16-dimethylgonane-7,10,12,13-tetrol
4			(1 <i>R</i> ,2 <i>r</i> ,3 <i>S</i> ,4 <i>s</i>)-1,2,3,4-tetramethylcyclobutane-1,2,3,4-tetrolate
5			(3 <i>a</i> ,6 <i>a</i> ,9 <i>a</i> -triamino-9 <i>b</i> -propyldodecahydro-1 <i>H</i> -phenalene-2,5,8-triyl)trimethanol

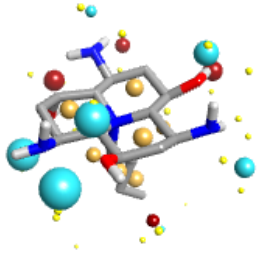
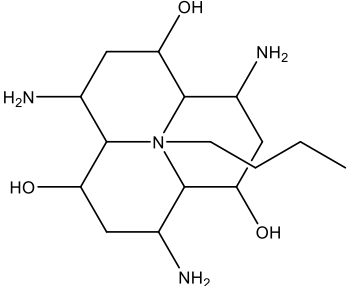
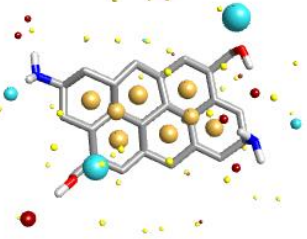
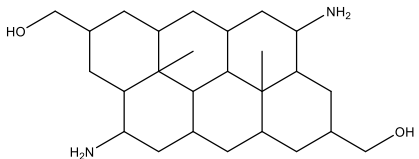
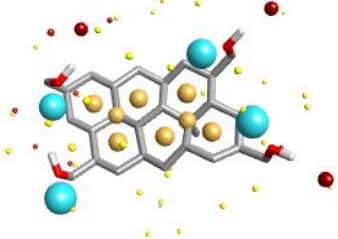
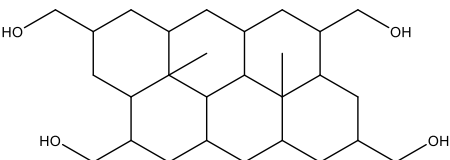
6			<p>(1,2,3,4,5,6-hexamethylcyclohexane-1,2,3,4,5,6-hexyl)hexamethanol</p>
7			<p>2-(3,8-dihydroxy-6-methyldecahydronaphthalen-1-yl)-4-ethyl-6,7-bis(hydroxymethyl)-3,4-dimethylundecanedioic acid</p>
8			<p>cyclooctane-1,3,5,7-tetrol</p>

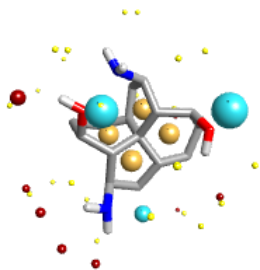
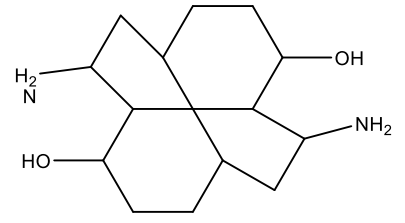
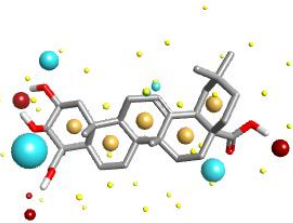
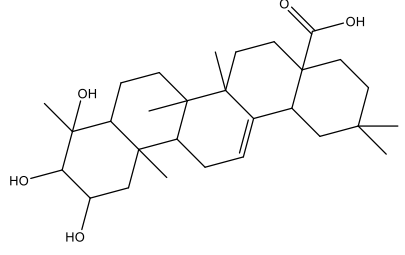
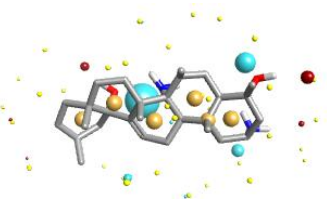
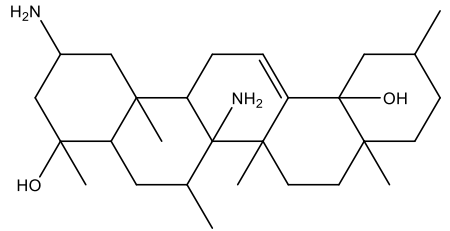
9			3-amino-16-(1-aminobutyl)androstane-7,12-diol
10			2-[(3,5-bis<[(1-carboxy-2-methylpropyl)amino]acetyl>benzoyl)amino]-3-methylbutanoic acid
11			(2,2,6,6-tetramethylheptane-4,4-diyl)dicarbamic acid

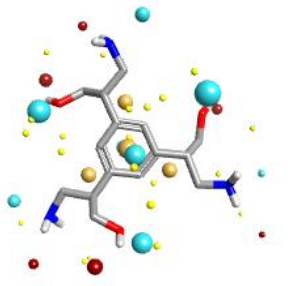
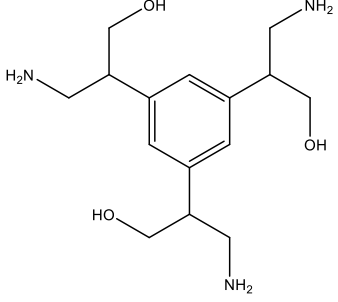
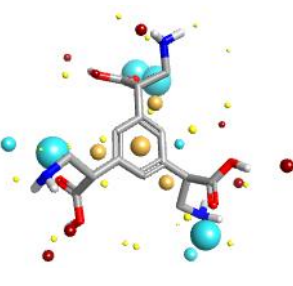
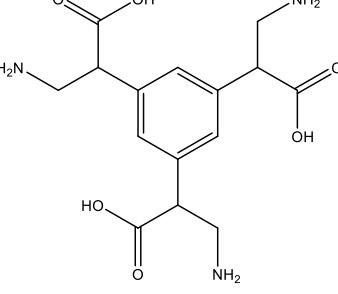
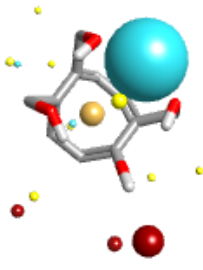
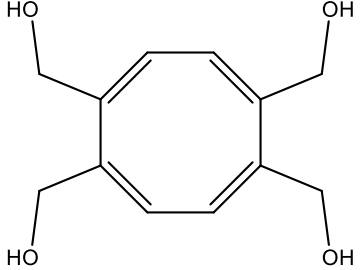
12			<p>3,7-bis(aminomethyl)-2,4,6,8-tetramethylcyclooctane-1,5-dicarboxylic acid</p>
13			<p>3a,6a,9a-triamino-1,4,7-trimethyldodecahydro-1H-phenalene-2,5,8-triol</p>
14			<p>[3,6,9-tris(aminomethyl)-9b-propyldodecahydro-1H-phenalene-1,4,7-triyl]trimethanol</p>

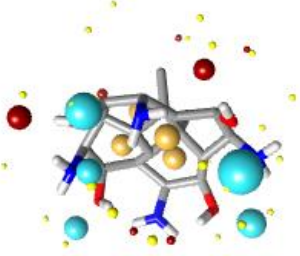
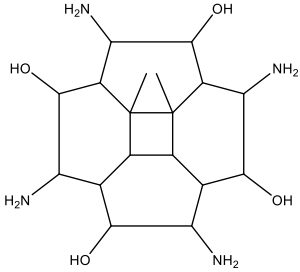
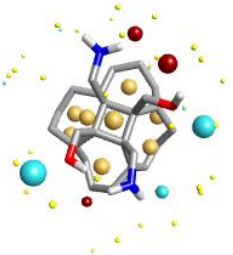
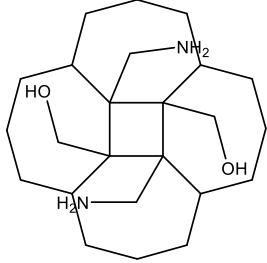
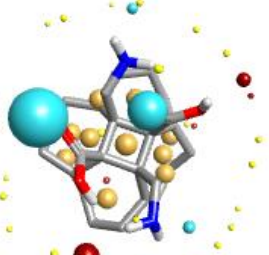
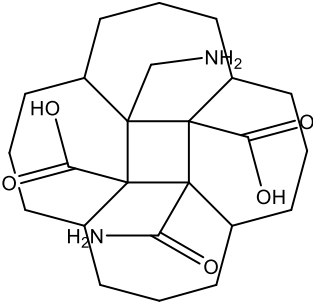
15			<p>3a,6a,9a-triamino-1,3,4,6,7,9-hexamethyldodecahydro-1H-phenalene-2,5,8-tricarboxylic acid</p>
16			<p>3a,6a,9a-triamino-9b-butyl-dodecahydro-1H-phenalene-2,5,8-tricarboxylic acid</p>
17			<p>4,9-diaminohexadecahydro-2,7-diol</p>

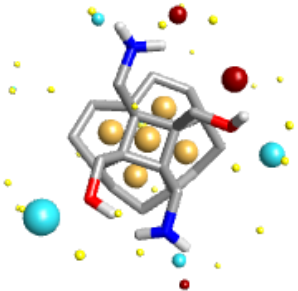
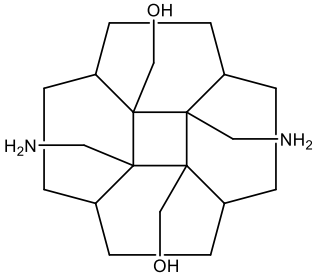
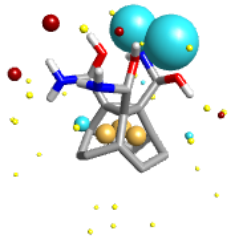
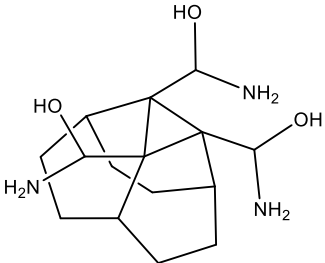
18			<p>10b,10d-dipentyltetradecahydro-1,3,5,7,9-pentaazadibenzo[ghi,mno]fluoranthene-2,4,6,8,10(1H)-pentone</p>
19			<p>2a,4a,6a,8a-tetrabutylloctahydro-1,3,5,7-tetraazapentaleno[1,6-<i>cd</i>]pentalene-2,4,6,8-tetrone</p>
20			<p>7-[(2<i>E</i>)-but-2-en-1-ylidene]-2,5-diazabicyclo[2.2.1]heptane-3,6-dione</p>

21			<p>3,6,9-Triamino-9b-butyl-9b-aza- 1,2,3,3a,4,5,6,6a,7,8,9,9a-didecahydrophenalene- 1,4,7-triol</p>
22			<p>(4,10-diamino-12b,12e- dimethyldocosahydronaphtho[7,8,1,2,3- <i>nopqr</i>]tetraphene-2,8-diyl)dimethano</p>
23			<p>(12b,12e-dimethyldocosahydronaphtho[7,8,1,2,3- <i>nopqr</i>]tetraphene-2,4,8,10-tetrayl)tetramethanol</p>

24			<p>2,7-diaminotetradecahydroindeno[7,1-<i>cd</i>]indene-3,8-diol</p>
25			<p>9,10,11-trihydroxy-2,2,6a,6b,9,12a-hexamethyl-1,3,4,5,6,6a,6b,7,8,8a,9,10,11,12,12a,12b,13,14b-octadecahdropicene-4a(2<i>H</i>)-carboxylic acid</p>
26			<p>2,6a-diamino-4,6,6b,8a,11,14b-hexamethyl-1,3,4,4a,5,6,6a,6b,7,8,8a,9,10,11,12,14,14a,14b-octadecahdropicene-4,12a(2<i>H</i>)-diol</p>

27			2,2',2''-benzene-1,3,5-triyltris(3-aminopropan-1-ol)
28			2,2',2''-benzene-1,3,5-triyltris(3-aminopropanoic acid)
29			cycloocta-2,4,6,8-tetraene-1,2,5,6-tetraol

30			<p>2,4,6,8-tetraamino-8b,8c- dimethylhexadecahydrodibenzo[<i>def,jkl</i>]biphenylene -1,3,5,7-tetrol</p>
31			<p>[5b,10b-bis(aminomethyl)dodecahydro-1,10:5,6- dipropanocyclobuta[1,2-α:3,4-α']di[7]annulene- 5a,10a-diyl]dimethanol</p>
32			<p>5b-(aminomethyl)-10b-carbamoyldodecahydro- 1,10:5,6-dipropanocyclobuta[1,2-α:3,4- α']di[7]annulene-5a,10a-dicarboxylic acid</p>

33			<p>[8c,8e- bis(aminomethyl)dodecahydrodibenzo[<i>def,jkl</i>]biphe- nylene-8b,8d(2<i>H</i>,3<i>H</i>)-diyl]dimethanol</p>
34			<p>hexahydro-3,4-ethanocyclopropa[<i>de</i>]naphthalene- 3a,3b,6b(1<i>H</i>)-triyiltris(aminomethanol)</p>

Appendix 4 – Abstracts for Publications and Posters

Determination of excipient based solubility increases using the CheqSol method.

Kelly Etherson*, Gavin Halbert, Moira Elliott

Int J Pharm, 2014; 465(1-2):202 – 209

Aqueous solubility is an essential characteristic assessed during drug development to determine a compound's drug-likeness since solubility plays an important pharmaceutical role. However, nearly half of the drug candidates discovered today display poor water solubility; therefore methods have to be applied to increase solubility. Solubility determination using the CheqSol method is a novel rapid solubility screening technique for ionisable compounds. The aim of this study is to determine if the CheqSol method can be employed to determine solubility increases of four test drugs (ibuprofen, gliclazide, atenolol and propranolol) induced by non-ionising excipients such as hydroxypropyl- β -cyclodextrin and poloxamers 407 and 188. CheqSol assays were performed for the drugs alone or in combination with varying solubiliser concentrations. The measured intrinsic solubility of all four drugs increased with all the excipients tested in an excipient concentration dependent manner providing results consistent with previous literature. The results demonstrate that it may be possible to use this method to determine the solubility increases induced by non-ionic solubilising excipients with results that are comparable to standard equilibrium based solubility techniques. Since the technique is automated and requires only small drug quantities it may serve as a useful solubility or formulation screening tool providing more detailed physicochemical information than multiwell plate or similar visual systems.

Using CheqSol to Determine Propranolol and Ibuprofen Solubility Improvement with Hydroxypropyl- β -Cyclodextrin

K. A. Etherson, M. Elliott, G. W. Halbert

Presented at APS PharmSci Conference 2013, Edinburgh, UK

Abstract - Hydroxypropyl- β -cyclodextrin (HP- β -CD) has the ability to increase drug solubility. Here the effect on propranolol hydrochloride and ibuprofen solubility, using CheqSol studies, is investigated. CheqSol is useful for assessing excipient bound solubility changes.

Introduction

Aqueous solubility is an important characteristic affecting drug delivery methods. The excipient HP- β -CD, a complexing agent, can increase drug solubility. The solubility of ionisable compounds can be determined using the CheqSol method [1] and from this data association constants ($K_{1:1}$) can be determined. The aims of these experiments are to determine the solubility improvement of propranolol and ibuprofen by HP- β -CD using CheqSol, and their association constants.

Materials and Methods

Phase-solubility studies were carried out with the drugs on their own and in the presence of HP- β -CD using CheqSol assays. The assays were run on a Sirius T3 instrument. Drug:HP- β -CD molar ratios used were in the range 1:0.1 to 1:2. For complexation reactions the association constant can be determined if there is knowledge of the complex stoichiometry. Both ibuprofen and propranolol have been found to form 1:1 complexes with cyclodextrins, therefore the Higuchi and Connors method can be used for $K_{1:1}$ determination [2].

Results and Discussion

HP- β -CD increased the solubility of propranolol HCl in a linear, concentration dependent manner (Figure 1a). At ratios of ibuprofen:HP- β -CD up to 1:0.75, solubility increased linearly (Figure 1b), with a positive deviation from linearity at 1:1 ratios. Propranolol:HP- β -CD complex formation constant was found to be 298 M^{-1} , and the $K_{1:1}$ for ibuprofen is 1511 M^{-1} , from the linear portion of the graph.

No data on the effect that HP- β -CD has on propranolol solubility could be found in the literature. The cyclodextrin has previously been shown to increase ibuprofen solubility [3]. Loftsson *et al.* found the slope of the phase solubility diagram to be 1.17 ± 0.01 [3] which is in disagreement with our figure of 0.129 ± 0.02 , this could be due to the different methods used. The A_p type curve observed for ibuprofen may indicate that other stoichiometries between ibuprofen and HP- β -CD were formed, in disagreement with literature. Association constants between drugs and cyclodextrins may be affected by pH, assay type and temperature and thus literature values can vary. Examination of the association constants shows that ibuprofen associates with HP- β -CD more strongly than propranolol. This could be due to the lower solubility of ibuprofen in water, which may be more likely to associate with excipients.

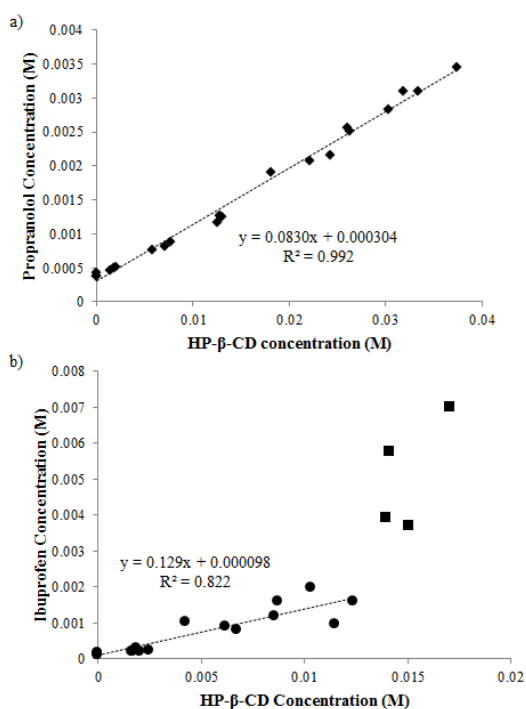


Figure 1. Phase solubility studies of the effect of HP-β-CD concentration on the solubility of a) propranolol and b) ibuprofen. ♦ propranolol (all ratios), ● ibuprofen (ratios up to 1:0.75), ■ ibuprofen (1:1 ratio)

Conclusions

The cyclodextrin, HP-β-CD, can increase the solubility of propranolol and ibuprofen in a concentration dependent manner. The results indicate a stronger association between ibuprofen with the solubilising agent than for propranolol. The results demonstrate that CheqSol can be used to determine the solubility changes offered by excipients used in a pharmaceutical formulation.

Acknowledgements

The authors gratefully acknowledge funding from Cancer Research UK for this research.

Using CheqSol to Determine Propranolol and Ibuprofen Solubility Improvement with Hydroxypropyl- β -Cyclodextrin.

Kelly Etherson, Gavin Halbert, Moira Elliott

Presented at the AAPS 2013 Annual Meeting and Exposition in San Antonio, Texas.

Purpose

The excipient HP- β -CD, a complexing agent, can increase drug solubility. The solubility of ionisable compounds can be determined using the CheqSol method and from this data association constants (K1:1) can be determined. The aims of these experiments are to determine the solubility improvement of propranolol and ibuprofen by HP- β -CD using CheqSol, and their association constants.

Methods

Phase-solubility studies were carried out with the drugs on their own and in the presence of HP- β -CD using CheqSol assays. The assays were run on a Sirius T3 instrument. Drug:HP- β -CD molar ratios used were in the range 1:0.1 to 1:2. Both ibuprofen and propranolol have been found to form 1:1 complexes with cyclodextrins, therefore the Higuchi and Connors method for K1:1 determination was used.

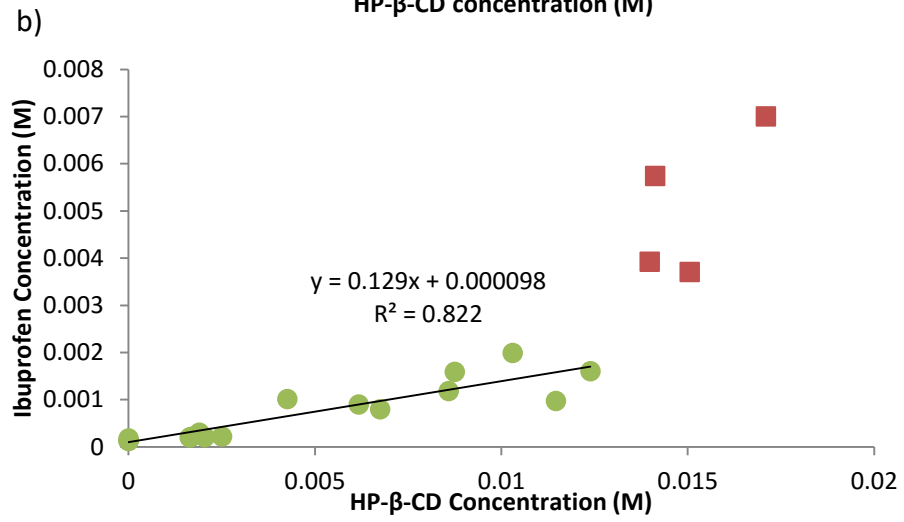
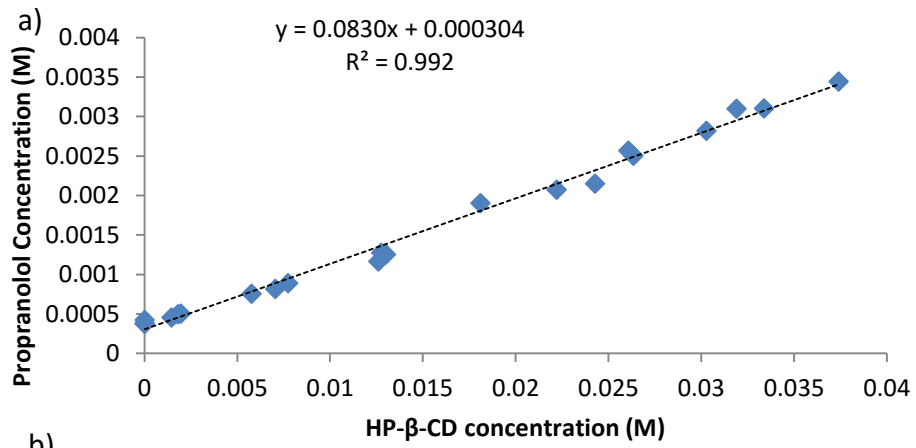
Results

HP- β -CD increased the solubility of propranolol HCl in a linear, concentration dependent manner (Figure 1a). At ratios of ibuprofen:HP- β -CD up to 1:0.75, solubility increased linearly, with a positive deviation from linearity at 1:1 ratios (Figure 1b). Propranolol:HP- β -CD complex formation constant was found to be 298 M^{-1} , and the K1:1 for ibuprofen is 1511 M^{-1} , from the linear portion of the graph. No data on the

effect that HP- β -CD has on propranolol solubility could be found in the literature. The cyclodextrin has previously been shown to increase ibuprofen solubility. The A_p type curve observed for ibuprofen may indicate that other stoichiometries between ibuprofen and HP- β -CD were formed, in disagreement with literature. Association constants between drugs and cyclodextrins may be affected by pH, assay type and temperature and thus literature values can vary.

Conclusion

The cyclodextrin, HP- β -CD, can increase the solubility of propranolol and ibuprofen in a concentration dependent manner. The results indicate a stronger association between ibuprofen with the solubilising agent than for propranolol. This could be due to the lower solubility of ibuprofen in water, which may be more likely to associate with excipients. The results demonstrate that CheqSol can be used to determine the solubility changes offered by excipients used in a pharmaceutical formulation.



Effect of excipients on the pH induced precipitation rate of drugs.

Gavin Halbert, Kelly Etherson, Moira Elliott

Presented at the AAPS 2015 Annual Meeting and Exposition in Orlando, Florida.

Purpose

Drug precipitation from saturated aqueous systems is an important biopharmaceutical issue during parenteral and enteral administration causing either phlebitis or reduced absorption. Since precipitation is dynamic investigation requires the creation of a saturated solution using either amorphous solids, co-solvents or pH shifts followed by determination of solubility relaxation back to the equilibrium value. For oral drugs this has led to the spring and parachute theory and categorisation of excipients by calculation of the excipient gain factor. In this study we have employed the CheqSol analysis to measure precipitation rates in order to investigate the “parachute” properties of cyclodextrin (hydroxypropyl-beta-cyclodextrin HPβCD) and surfactants (poloxamer 127 or 188) with ibuprofen and propranolol.

Methods

CheqSol experiments were conducted with a Sirius T3 titrator (Sirius Analytical Instruments Ltd, UK), in ionic strength adjusted (ISA) HPLC grade water containing 0.15M potassium chloride (VWR, Leuven, Belgium), at 25°C ± 0.5°C under an argon atmosphere, with a Ag/AgCl pH electrode and a MMS UV–VIS Carl Zeiss Microimaging spectrophotometer with an ultra-mini immersion probe. Drug was weighed into the analysis vial and HP-β-CD or surfactant in 1.5 mL ISA water added with the mass of drug varied depending on expected solubility. After dissolution the sample was titrated from ionisation to non-ionisation through addition of acid or base until

precipitation was detected and the measured precipitation rate was employed in the analysis.

Results

HPβCD at low concentrations increases the precipitation rate of both drugs but decreases this in a concentration dependent manner to a constant rate once the molar ratio of HPβCD to drug reaches 1:1 (ibuprofen at 16mM, propranolol at 20mM). The final precipitation rates are reduced to around one half to one quarter of drug alone. Both poloxamers exhibit a general trend of increasing precipitation rate with increasing concentration although some curves exhibit an inflexion at low concentrations. The precipitation rates measured at high concentrations are up to ten times greater than those measured with drug alone.

Conclusion

These results indicate that the effect on pH shift induced precipitation rates of HPβCD and the poloxamers is different. HPβCD reduces the precipitation rate probably due to its ability to form inclusion complexes, which bind to the drug. Poloxamers increase precipitation rate indicating quick release of drug solubilised in micelles. All the excipients are known to increase the intrinsic and kinetic solubility of both drugs and to be able to act as a “parachutes” inhibiting precipitation of other drugs from supersaturated solutions. However, in this dynamic system precipitation rate differences are evident which may be important for in vivo systems where conditions are not static. Further study of this phenomenon is therefore warranted with a broader selection of drugs and excipients and dynamic systems, which mimic in vivo challenges to supersaturated solutions.

